MUNI
MED

Habilitation thesis

# Human intracranial high-frequency oscillations – both physiological and pathological phenomena

MUDr. Martin Pail, Ph.D.

[1st] Department of Neurology

Faculty of Medicine, Masaryk University

Brno 2021

# Summary

High-frequency oscillations (HFOs) of the electrical brain activity have attracted considerable attention. By the term HFOs, as we know them today, we mean frequencies of brain activity over > 80 Hz. HFOs represent not only the electrical manifestation of neuronal events but, above all, the very effective mechanisms of brain function. HFOs play a pivotal role in synchronizing local and distributed neuronal networks, as is critical for normal brain function. These oscillations can be detected by both non-invasive and invasive electroencephalography (EEG). However, most published papers have presented HFOs results from invasive EEG due to a significantly better signal-to-noise ratio using this approach.

HFOs represent a heterogeneous group of (patho)physiological phenomena, including different oscillations classified by many criteria, most often frequency. Furthermore, oscillations can be classified according to the mechanisms of origin, pathogenicity or physiological function, location, morphology, duration, amplitude, entropy, and other characteristics.

In clinical medicine, HFOs have been predominantly studied in epileptology due to the need to detect HFOs by invasive EEG monitoring, used to evaluate intractable focal epilepsies. At first, HFOs were considered to be mainly pathological events occurring primarily in the area responsible for seizure generation. Thus, the first substantial application of HFOs took place in the context of epilepsy surgery in order to find out and remove this pathological area. This is now followed by other applications such as assessment of epilepsy severity and antiepileptic therapy monitoring. Over the past years, HFOs were also found in vast areas of the human brain distant from the epileptic network, having a physiological role. HFOs and the mechanisms of their formation are currently attracting considerable attention to research in identifying the epileptogenic region of the brain on the one hand, and on the other hand, in studying their physiological function within cognitive functions, memory, movement control, and others.

This submitted habilitation thesis represents a summary of current knowledge regarding HFOs and a collection of the author's previously published research (as the principal author or co-author) relevant to the topic. The author significantly contributed to all the presented papers, whether in elaborating on the methodology, the analysis of the included subjects' clinical data, the description of the exact anatomical localization of the intracerebral electrodes contacts, interpretation of the research results, and last but not least, the writing of the manuscripts.

In the following text, it will be discussed the phenomena of both pathological and physiological HFOs. Following the introduction, the second and third chapters will focus on HFO detection and genesis. Further, two basic subgroups of HFOs, ripples and fast ripples, will be described. In detail, their role in both epileptogenesis and physiological processes will be discussed. Finally, very high-frequency oscillations will be introduced, the latest discovery in this field.

# Acknowledgment

I would like to thank all my colleagues, I have had the opportunity to work with and still work on high-frequency oscillations research under both physiological and pathological conditions. First of all, I would like to thank Jan Cimbálník, MSc., Ph.D., and Associate professor Robert Roman, M.D., Ph.D., for our joint research, which has led to some discoveries that I present in this habilitation thesis.

I would also like to thank my colleague from neurosurgery Associate professor Jan Chrastina, M.D., Ph.D., without whom it would not be possible to research in the field of invasive EEG monitoring.

I also thank Professor Gregory A. Worrell, M.D., Ph.D., for an opportunity to spend some time in the excellent science laboratory, Mayo Systems Electrophysiology Laboratory, at MAYO Clinic in Rochester, USA, and gain new knowledge and experience.

In particular, I would like to thank my postgraduate supervisor, Professor Milan Brázdil, M.D., Ph.D., who introduced me to the field of science and epilepsy research. Without his influence and supervision, this work and my study results would have never been created.

# CONTENTS

**CHAPTER 1** Introduction to high-frequency oscillations ..... 1

**CHAPTER 2** Detection of high-frequency oscillations ..... 5

Commentary on published paper: Intracerebrally recorded high-frequency oscillations: simple visual assessment versus automated detection ..... 15

**CHAPTER 3** Mechanisms of high-frequency oscillations genesis ..... 26

**CHAPTER 4** Ripples ..... 32

**CHAPTER 5** Fast ripples ..... 36

**CHAPTER 6** High-frequency oscillations and medically intractable epilepsy ..... 40

Commentary on published paper: Hippocampal high-frequency oscillations in unilateral and bilateral mesial temporal lobe epilepsy ..... 44

Commentary on published paper: Multi-feature localization of epileptic foci from interictal, intracranial EEG ..... 56

**CHAPTER 7** Characteristics of high-frequency oscillations ..... 68

Commentary on published paper: Frequency-independent characteristics of high-frequency oscillations in epileptic and non-epileptic regions ..... 70

**CHAPTER 8** Physiological vs. pathological high-frequency oscillations ..... 83

Commentary on published paper: High-frequency oscillations in epileptic and non-epileptic human hippocampus during a cognitive task ..... 87

Commentary on published paper: Cognitive processing impacts high-frequency intracranial EEG activity of human hippocampus in patients with pharmacoresistant focal epilepsy ..... 103

**CHAPTER 9** Very high-frequency oscillations ..... 115

Commentary on published paper: Very high-frequency oscillations: Novel biomarkers of the epileptogenic zone ..... 117

**CHAPTER 10** Conclusion and future directions ..... 131

**REFERENCES** ..... 135

# List of Abbreviations

| | |
|---|---|
| **EEG** | electroencephalography |
| **iEEG** | invasive electroencephalography |
| **SEEG** | stereo-electroencephalography |
| **HFOs** | high-frequency oscillations |
| **GFOs** | gamma-frequency oscillations |
| **pHFOs** | pathological high-frequency oscillations |
| **nHFOs** | non-pathological (physiological) high-frequency oscillations |
| **VHFOs** | very high-frequency oscillations |
| **R** | ripples |
| **FR** | fast ripples |
| **SOZ** | seizure onset zone |
| **IZ** | irritative zone |
| **MTLE** | mesial temporal lobe epilepsy |
| **EH** | epileptic hippocampus |
| **NEH** | non-epileptic hippocampus |
| **HS** | hippocampal sclerosis |
| **FCD** | focal cortical dysplasia |

# CHAPTER 1

# Introduction to high-frequency oscillations

A neuron's ability to generate an action potential with millisecond accuracy depends on the rapid fluctuation of its membrane potential. Field potential oscillations reflect synchronized rhythmic synaptic potentials and/or repetitive firing by neuronal ensembles and populations in specific brain areas. From the very beginning of the development of neurophysiology and electroencephalography (EEG), low, and especially in recent years, high-frequency oscillations of the electrical activity of the brain have attracted considerable attention. These oscillations represent not only the electrical manifestation of neuronal events but, above all, the very effective mechanisms of brain function, e.g., the processing of information in various cognitive processes and consciousness (Buzsáki, 1992). Neuronal oscillations span a wide range of spatial and temporal scales that extend beyond traditional clinical EEG (Worrell et al., 2008). It was actually one of the ideas originally proposed by Hans Berger (1929) that fast brain activity changes as recorded in the human EEG may be related to specific mental activities. However, according to Berger, the high-frequency range includes 20 Hz and higher frequencies, nowadays usually called the high beta or the gamma band. The conventional range of EEG analysis usually involves frequencies below 40 Hz. By the term high-frequency oscillations (HFOs), as we know them today, we mean frequencies much higher (> 80 Hz), as will be mentioned below. The discovery that EEG contains useful information at higher frequencies (above the traditional 80Hz limit) has profoundly impacted our understanding of brain function (Zijlmans et al., 2012). The study of the mechanisms underlying the origin of oscillations brings not only new knowledge of the physiological functions of the brain but also makes it possible to understand the pathophysiology of a number of diseases, including epilepsy.

In the introduction, it should be noted and emphasized that brain neuronal oscillations represent a very heterogeneous group of (patho)physiological phenomena, which includes different oscillations that can be classified by many criteria, most often frequency. Furthermore, oscillations can be classified according to the mechanisms of origin, pathogenicity or physiological function, location, morphology, duration, amplitude, entropy, and other characteristics (Jiruska & Bragin, 2011; Jefferys et al., 2012; Matsumoto et al., 2013; Pail et al., 2017, 2020; Cimbalnik et al., 2019, 2020). However, a necessary attributes of HFOs are rhythmicity, repetitive character, and at least four waves within one oscillation (Worrell et al., 2012).

For a very long time, neurophysiology has focused on the study of brain activity and oscillations whose frequencies were only up to 30 Hz and were empirically divided into four basic frequency bands. These bands are traditionally referred to as Greek letters: delta (up to 3.5Hz), theta (4-7.5Hz), alpha (8-13Hz), and beta (14-30Hz) (Schomer & Lopes da Silva, 2017). However, the situation changed after

discovering an activity whose frequency was above the upper limit of these traditional frequencies, which was a breakthrough in brain research. The HFOs discovery was made possible mainly by using intracranial electrodes implanted for presurgical diagnostics in epileptic patients, which offer the unique opportunity to study neural activity from also deep brain structures. Hence, HFOs have first been studied concerning epileptic diseases. Nevertheless, studies over the past decades suggested that high-frequency oscillations might have an essential role in both normal and pathological brain function (Engel et al., 2009).

The main representatives of these higher oscillations are gamma oscillations (30-80 Hz), high-frequency oscillations (HFOs, 80-600 Hz) (Buzsáki, 1992; Bragin et al., 1999a,b; Worrell et al., 2008; Engel Jr. et al., 2009), and very high-frequency oscillations (VHFOs, above 600 Hz), which have been discovered lately (Usui et al., 2010; Brázdil et al., 2017). However, it is important to note that the classification of higher oscillations by frequency is currently very variable, and the boundaries between different types of oscillations are not clearly defined and differ in individual publications. Some authors consider gamma brain activity as a high-frequency activity. The majority of works, contrariwise, set a lower limit for high-frequency activity from 80 Hz and 100 Hz, respectively. Therefore, we will talk about high-frequency oscillations as a higher activity than 80 Hz in this work.

Higher oscillations, especially HFOs, and mechanisms of their origin, are currently attracting much attention to research focused on studying cognitive functions, memory, movement control, and others. Gamma frequency oscillations (GFOs, ~30-80 Hz), the first studied type of oscillations, play a dominant role in these physiological functions, especially learning and memory. The published studies implicate GFOs and synchrony as a fundamental mechanism of percept binding, and as such, they play a critical role in brain function (Buzsáki & Chrobak, 1995; Buzsáki & Wang, 2012; Kucewicz et al., 2017). Gamma oscillations are the mechanism that allows modulation of neuronal activity, synchronization of neuronal activity both locally and between distant areas of the cortex, and phase coding of information. These processes represent a highly efficient, metabolically undemanding mechanism for combining multisensory stimuli in their processing (Buzsáki & Chrobak, 1995; Buzsáki & Wang, 2012; Jiruška, 2013; Kucewicz et al., 2017).

High-frequency oscillations (80-600 Hz) have been firstly recorded in rat hippocampus and parahippocampal gyrus (Buzsáki et al., 1992; Chrobak & Buzsáki, 1996). Since the end of the last century, also human HFOs in frequencies over 80 Hz have been repeatedly identified in recordings from invasive EEG monitoring (employing microwires, depth macro electrodes, or subdural strips/grids) in epileptic patients (Bragin et al., 1999a,b; Staba et al., 2002; Worrell et al., 2004, 2008; Urrestarazu et al., 2007; Jacobs et al., 2008, 2009; Bagshaw et al., 2009; Brázdil et al., 2010; Crépon et al., 2010; Usui et al., 2010; Brázdil et al., 2017). These short-lasting phenomena (20-100 ms) are above all a result of the synchronization of neuronal populations, are generally split into two categories according to their frequency: ripples (R), ranging between 80-250 Hz, and fast ripples (FR), in the range of 250-600 Hz

(Bragin et al., 1999a, Worrell et al., 2008). Similar to HFOs, VHFOs are further divided into subgroups (Brázdil et al., 2017): very fast ripples; up to 1000 Hz, and ultra fast ripples; over 1000 Hz (Fig.1).

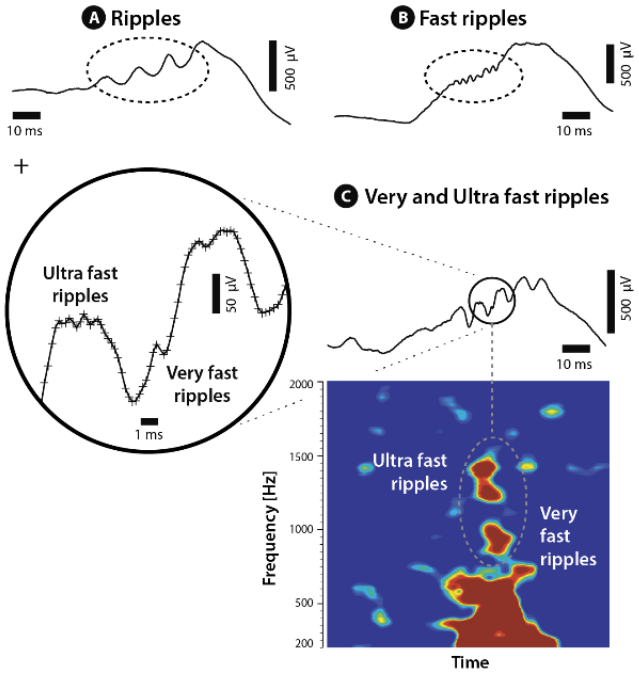


*Figure 1: Demonstration of individual HFOs (ripples and fast ripples), very and ultra fast ripples in time-frequency analysis (Brázdil et al., 2017)*

These human HFOs were first recorded with microwires (diameter = 40 µm, that extended beyond the tip of clinical depth electrodes) from mesiotemporal structures (hippocampus and entorhinal cortex) in patients with mesiotemporal lobe epilepsy (MTLE) during interictal periods by the group of Bragin and Engel at the University of California (Bragin et al., 1999a; Staba et al., 2002). Lately, the breakthrough in clinical HFO research was made by Gotman's group, Montreal Neurological Institute (MNI), who observed interictal HFOs in the seizure onset zone using small broadband depth electrodes (contact area 0.8 $mm^2$) (Jirsch et al., 2006). These observations were later confirmed by Worrell et al. (2008) using standard subdural macro electrodes (contact area 9.4 $mm^2$) and recording from a more extended brain area. Until now, there has been an increasing number of papers demonstrating the relationship between HFOs and epileptogenic brain tissue. Research from multiple groups reported increased rates of interictal HFOs in the seizure onset zone (SOZ), including high-gamma (Worrell et al., 2004), ripples (Urrestarazu et al., 2007; Worrell et al., 2008; Jacobs et al., 2008, 2009, 2010), and fast ripples (Bragin et al., 1999a,b; Bragin et al., 2002a,b; Staba et al., 2002). HFOs were often observed at the time of epileptic spikes (approximately up to 80 %); less of them occurred entirely independently on spikes in timing and localization (Urrestarazu et al., 2007; Frauscher et al., 2017). HFOs were also found using standard macroelectrodes not only interictally but also during the ictal period and occur predominantly in the region of primary epileptogenesis and SOZ (Jirsch et al., 2006). Ictal HFOs

spanning ripple and fast ripple frequency (and high gamma) bands have been repeatedly implicated in seizure generation in human focal epilepsy (Fisher et al., 1992; Traub et al., 2001; Grenier et al., 2003; Worrell et al., 2004; Jirsch et al. 2006). HFOs appear to be a good indicator of disease activity (Zijlmans et al., 2009) and possibly predict outcome after epilepsy surgery (Jacobs et al., 2010).

HFOs play a pivotal role in synchronizing local and distributed neuronal networks, as is critical for normal brain function. These functional couplings are transient (with a duration in the order of hundreds of milliseconds), dynamic (the strength of association between two cortical regions has a time-varying nature) and frequency-specific, neuronal groups oscillate in specific bands according to a precise phase relationship (Le Van Quyen & Bragin, 2007; Worrell et al., 2012).

HFOs were predominantly studied in epileptology because of the need of HFO detection by invasive EEG monitoring (used in evaluating intractable focal epilepsies). Thus, the first substantial application of HFOs took place in the context of epilepsy surgery. This is now followed by other applications such as assessment of epilepsy severity and antiepileptic therapy monitoring (Frauscher et al., 2017).

Over the past years, HFOs were also found in vast areas of the human brain distant from the epileptic network (the seizure onset or irritative zone), having a physiological role as it will be shown further (Axmacher et al., 2008; Carr et al., 2011; Girardeau & Zugaro, 2011; Lachaux et al., 2012; Buzsáki & Lopes da Silva, 2012; Nagasawa et al., 2012; Matsumoto et al., 2013; Alkawadri et al., 2014; Kucewicz et al., 2014, Pail et al., 2017, 2020).

HFOs and the mechanisms of their formation are currently attracting considerable attention to research in identifying the epileptogenic region of the brain on the one hand, and on the other hand, in studying their physiological function within cognitive functions, memory, movement control, and others.

# CHAPTER 2

# Detection of high-frequency oscillations

Electroencephalography (EEG) plays a principal role in the non-invasive evaluation of the brain's functional state and invasive presurgical evaluation of patients with intractable focal epilepsy. Localization of focal epileptic brain is critical for successful epilepsy surgery. While ripples are considered to be a signature of both normal and pathological brain processes, fast ripples are believed to primarily reflect the neuronal substrates of epileptogenesis and epileptogenicity (Engel et al., 2009). Both are detectable most often and in the best manner invasively, as it will be discussed in more detail. Based on this fact, there is an intense interest in HFOs recorded with invasive electroencephalography as potential biomarkers to improve epileptogenic brain localization and resective surgery (to be discussed in the chapter on pathological HFOs).

There are several types of labelings; HFOs, high-frequency activity (HFA), and high-frequency power (HFP), in the literature, describing different frequency ranges and types of high-frequency brain electrical activity (Buzsáki & Silva, 2012). The term HFA was recently suggested to encompass both HFOs and HFP (Burke et al., 2015). However, the concept of HFOs and high-frequency power is unfortunately confused in individual studies; the terms are often conflated, or their distinction is ignored in the literature (Cimbalnik et al., 2016); see further.

Neuronal oscillations of functional networks in the human brain occur over a wide range of spatial and temporal scales (Worrell et al., 2012). HFOs can be recorded using extracellular microwire electrodes (~10 to 50 μm), which are widely used to record the neural activity spanning single neuron to collective oscillations of large neuronal assemblies (Buzsáki, 2004). HFOs can be highly localized within a radius of ~150 μm surrounding to more spatially extended activity; up to 10 mm (Kajikawa & Schroeder, 2011). Intracranial studies using microelectrodes showed that HFOs are transient (ripples: 19-360 ms and fast ripples: 6-53 ms) local field potentials oscillations (ripples: 120-1050 μV and fast ripples: 100-1250 μV), which are localized to small tissue volumes (<1 mm) (Bragin et al., 2002a,b). Also, standard clinical subdural or intracerebral macro electrodes (surface area: 1–10 $mm^2$) can be used to record HFOs, recording from a more extended brain area (Urrestarazu et al., 2007; Worrell et al., 2008; Brázdil et al., 2010; Crépon et al., 2010). These studies reported that the HFO generator is very small below 1 $mm^3$ using microelectrodes, compared to that in the range of 1 or a few $cm^3$ using macro electrodes (Bragin et al., 2002a,b; Andrade-Valenca et al., 2011). Nevertheless, using these types of macro electrodes, the recorded signal consists of a spatial average of locally generated local field potentials and volume conducted activity (Kajikawa & Schroeder, 2011) and not of single-neuron action potentials or multi-unit activity (Worrell et al., 2012). There is also a combination of these two systems,

hybrid electrode systems that combine clinical macro electrodes with additional experimental microelectrodes (Bragin et al., 2002a,b; Worrell et al., 2008). Although studies have previously demonstrated that especially fast ripples are often localized to sub-millimeter scales (Bragin et al., 2002a,b), a correlation between electrode size and HFO detections was not observed (Châtillon et al., 2011). However, it is still unclear whether HFOs assessed with microelectrodes represent the same phenomena as HFOs detected with macro electrodes (Frauscher et al., 2017), as the patterns of the HFOs detected by EEG are quantitatively different from those detected by microwires (Worrell et al., 2008). According to Worrell's study, a larger surface area of macroelectrodes leads to spatially undersampling HFO activity (especially FR) compared to microwires. Sufficient detection of FR might be explained by the subtle and discrete clusters of abnormally bursting neuronal cell assemblies, not homogeneously distributed over the whole epileptogenic tissue. These neuronal populations could generate FR not visible in standard stereo-electroencephalography (SEEG) (Bragin et al., 2003). One must always keep in mind the possible low signal-to-noise ratio and the limited sampling frequency that reduces FR's successful detection.

For clinical application, it would be preferable to record fast oscillations noninvasively. Noteworthy, in recent studies, the evidence of HFOs recorded from scalp electrodes has appeared (Kobayashi et al., 2010; Andrade-Valenca et al., 2011; Melani et al., 2013). This was an unexpected and surprising result, given the small HFO generator size of 100-200 μm and a much larger area of the synchronized cortex (at least 6 to 9 $cm^2$), which is required for the corresponding activity to appear on the scalp (Tao et al., 2005). It is unlikely that the HFOs described in intracranial studies could be visible on the scalp in this context. Nevertheless, it is essential to note that the skull does not filter high frequencies; only because of the skull's distance and resistivity, which attenuates an already small activity, it makes their recording less likely (Frauscher et al., 2017). A recent simulation study, showed that HFOs could be detected within the lower noise level of the ripple band (80-200 Hz), even though their median amplitude on scalp EEG recordings is > 10 times smaller than interictal epileptiform discharges and is consistent with cortical generators of approximately 1 cm (Frauscher et al., 2017).
This finding was confirmed by a study using data from simultaneous scalp EEG and intracranial recording, which confirmed that scalp HFOs derive from cortical HFOs (Zelmann et al., 2014). In the SOZ, the rates and proportion of channels with gamma and ripple oscillations were found higher, suggesting that they could be used for the SOZ identification as interictal EEG scalp markers (Andrade-Valenca et al., 2011). These oscillations (mostly co-occurred with spikes) are less sensitive but much more specific and accurate than alone spikes to delineate the SOZ (Andrade-Valenca et al., 2011; Melani et al., 2013). Nevertheless, as the authors themselves state, this correlation is particularly high for neocortical epilepsy, not for seizures originated in deep mesial structures. In a recent study, it was shown that it might be feasible to record even frequencies > 250 Hz using subdermal electrodes (Pizzo et al., 2016). Moreover, great caution should be taken when evaluating these oscillations as blinks, saccadic eye movements, and various muscle activities typically result in notable increases in gamma power (>25 Hz) and contaminate the recorded signal in the HFO spectrum (Worrell et al., 2012; Xiang et

al., 2014). However, gradually, there is increasing evidence that HFOs are useful for measuring disease activity and assessing treatment response using non-invasive EEG. The contribution of non-invasive methods for measuring epileptogenicity is particularly promising in children because they show high scalp HFO rates (Frauscher et al., 2017).

Another possibility of non-invasive methods is to use magnetoencephalography to detect high-frequency activity and HFOs (Xiang et al., 2009; van Klink et al., 2016). The results demonstrated high concordance of detected events with lesions as identified by MRI in 70 % of subjects and with the SOZ as identified by invasive EEG (Xiang et al., 2009; Frauscher et al., 2017). In one published work, magnetoencephalogram recordings of likely physiological ripple and fast ripples oscillations in the human somatosensory cortex have been reported (Curio et al., 1994).

Nevertheless, invasive EEG recordings performed in the sense of presurgical epilepsy evaluation in people with drug-resistant epilepsy provide us with excellent data for examining high-frequency oscillations in the EEG, as they have a high signal-to-noise ratio and are less sensitive to artifacts compared to non-invasive recording techniques (Thomschewski et al., 2019). Invasive EEG in humans is only obtained in clinical situations where direct recording from the brain is required, as it is commonly performed only in epileptic patients requiring diagnostic localization for surgical treatment. Studies investigating HFOs in the human epileptic brain have primarily utilized standard clinical subdural or depth macro electrodes. The electrode cross-sectional area determines the scale of spatial sampling, and at this time, however, the optimal electrode cross-section and spacing for mapping epileptic brain is unknown (Worrell et al., 2012).

The technical aspects of HFO detection have been examined by different research groups (see reviews e.g., Worrell et al., 2012; Zijlmans et al., 2017). The detection of HFOs is a challenging task, primarily due to their usual low signal-to-noise ratio, their association with epileptic activity, and the still open questions regarding their nature and definition (Thomschewski et al., 2019). These issues will be discussed further. New recording technologies (digital electronics and computing) have advanced so that, at high temporal and spatial resolutions, HFOs can be registered in human focal epilepsy (Worrell et al., 2012). When recording, for an appropriate temporal sampling, we need a recording with a low noise level for high frequencies (Worrell et al., 2012; Schomer & Lopes da Silva, 2017; Zijlmans et al., 2017). The limiting factor for detecting higher frequency activities and oscillations, in particular, is the sampling frequency of registered EEG. The higher the used sampling frequency is, the higher activity can be detected in the EEG. To adequately sample the temporal dynamics of HFOs, a reasonable approach is sampling at about 4-5 times higher than the upper frequency of interest since several samples are needed to form the wave shape (Schomer & Lopes da Silva, 2017; Zijlmans et al., 2012). Preferentially, a sampling frequency of 2,000 Hz or above should be used for studying HFOs (Zijlmans et al., 2012). Only the technological progress made it possible to use a higher sampling frequency, which made signal processing complicated due to the amount of data analyzed. Also, because of the deluge of multichannel data generated by these experiments, the development of modern data mining

techniques was required to extract meaningful information relating to time, frequency, and space (Worrell et al., 2012). Fortunately, the technical challenges of data transfer, storage, and analysis of large terabyte data sets are now possible (Worrell et al., 2012). Regarding spatial sampling, the literature suggests that clinical SEEG electrodes have several advantages (robust HFO measurements, their sampling scale, and surgical safety record), which represents a good compromise between micro- and macro-scales (Bragin et al., 1999b; Urrestarazu et a, 2007; Worrell et al., 2008; Worrell et al., 2012; Zijlmans et al., 2017; Thomschewski et al., 2019).

The detection and labeling of interictal and ictal HFOs can be broadly categorized into three groups: a) expert manual review (time-consuming, not feasible for large data sets, considered the gold standard, but subjective, associated with low inter-reviewer reliability); b) supervised detection (high sensitivity and low specificity automated detection combined with expert review); c) unsupervised detection (fully automated detection and data labeling, requires high specificity and sensitivity detectors) (Gardner et al., 2007; Worrell et al., 2012; Zelmann et al., 2012; von Ellenrieder et al., 2016). A common approach to account for inter-reviewer reliability is to consider more than one reviewer, checking for consistency in the markings (Gardner et al., 2007; Worrell et al., 2012; Zelmann et al., 2012; von Ellenrieder et al., 2016).

Visual analysis and expert reviewers are the gold standards for evaluating invasive EEG signals and HFOs. Even though it is not a perfect solution (very time-consuming, requires expertise, and might be subjective), it is a reasonable approach given that these experts are the clinical users of EEG and that they are considered as the gold standard when identifying other electrophysiological signals (spikes, seizures,…). Considering the mentioned HFO criteria (Jacobs et al., 2012; Worrell et al., 2012), visual inspection requires enlarging the signal both in time scale and amplitude in order to discern these discrete events from the background EEG (Thomschewski et al., 2020). In HFO rating, it is crucial to control for inter-reviewer reliability and consistency in the markings (Zelmann et al., 2012). Visual analysis, however, entails serious obstacles, making HFO assessment impossible for clinical routine (Frauscher et al., 2017).

To overcome these issues, various detectors have been developed and validated over the last few years (see review Zijlmans et al., 2017). Regarding using automated detectors, there are used two basic approaches. One possibility is that the supervised training algorithm is used for optimizing the parameters of the detector; it means that all detected events are validated by an expert reviewer (Worrell et al., 2012). Conversely, some of the researchers consider the output of the detector as the "true" HFOs. However, this approach requires high specificity and sensitivity detectors by setting strict and precise parameters (e.g., restricting the number of oscillations above certain energy levels) (Staba et al., 2002).

The objective of the mentioned approaches is to detect HFO events that can be distinguished from ongoing background activity (Jacobs et al., 2012). Thus, a logical approach is to compare the energy of the signal with an energy threshold. The oscillatory events can be visualized by applying a band-pass filter to restrict the range of frequencies under consideration and to increase the time and

amplitude scales. Many detectors use forward and backward filtering to eliminate phase distortion (Gardner et al., 2007). Another possibility is an EEG time-frequency map, which can show the amount of high-frequency activity (Fig.2; Zijlmans et al., 2012). It is important to consider that automatic detector design is based on a definition and description of HFOs, usually on at least four waves within one oscillation in a frequency range from 80 to 600 Hz that "distinctively" stand out from the background signal (Zijlmans et al. 2017).

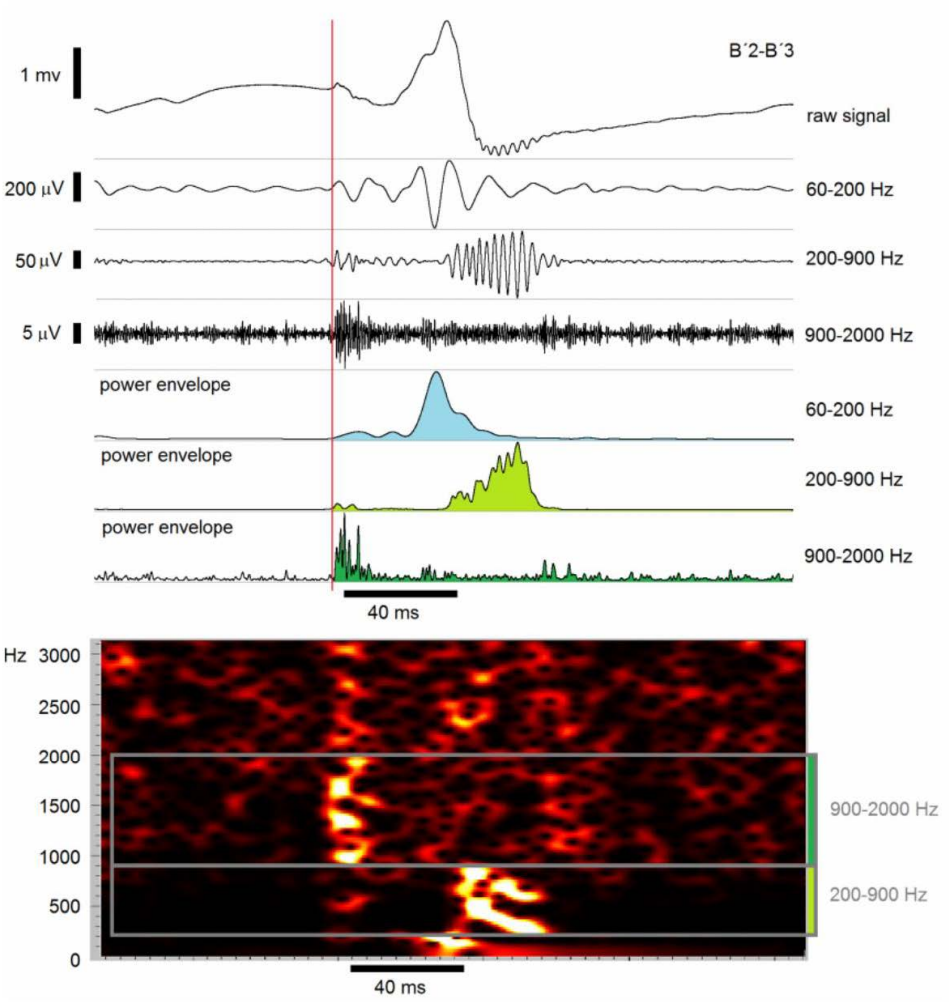


*Figure 2: Visualization of HFOs by applying a band-pass filter and power envelope analysis to restrict the range of frequencies, and time-frequency map*

When the energy of the filtered local field potential (LFP) is statistically larger than the threshold during a specific interval, the segment is considered as a possible HFOs (Staba et al., 2002; Gardner et al., 2007; Crépon et al., 2010; Worrell et al., 2012; Zelmann et al., 2012). Finally, in order to designate high-frequency activity as an oscillation, it should have a rhythmic and repetitive character in addition to high frequency (Worrell et al., 2012). Unfortunately, there is no unity in this classification, and the

individual papers differ among themselves in the number of a minimum number of repetitions of individual waves within one oscillation. Furthermore, there is no consensus in individual studies whether HFOs should be a band-limited event, or as we can say an isolated event in the time-frequency map (as in Crépon et al., 2010) or it can be a broadband event, and it could contain a variety of frequencies within a range (e.g., Staba et al., 2002; Worrell et al. 2008).

Several mathematical approaches were established to improve ictal and interictal EEG analysis (Staba et al., 2002; Gardner et al., 2007; Worrell et al., 2008; Tito et al., 2009; Ayala et al., 2011; Blanco et al., 2011; Nikulin et al., 2011; Zijlmans et al., 2017). Algorithms for detection of spontaneous or induced HFOs commonly require at least four waves within one oscillation of sinusoidal like morphology in the filtered signal (above 80 Hz) that stand out from the ongoing background activity (with energy more abundant than the 95 percentile), and at least 25 ms inter-event interval settings the range of HFO amplitude (10-1000 μV) and duration (30-100 ms) reported spans a wide range (Worrell et al., 2012). The emphasis must always be on differentiating true HFOs from the high-frequency power changes associated with increased neuronal firing (Ray et al., 2008; Schomburg et al., 2012; Waldert et al., 2013) and band-pass filtering of interictal epileptiform sharp waves and nonspecific transients (Bénar et al., 2010; Worrell et al., 2012; Cimbalnik et al., 2016), will be discussed below.

Most HFOs are found within sharp EEG components (Urrestarazu et al., 2007; Jacobs et al., 2008; Crépon et al., 2010). Nevertheless, artifactual high-frequency activities can also be caused by Fourier spectral decomposition of a rapidly changing intracerebral EEG signal by high-pass filtering these sharp components of epileptiform discharges (spikes or sharp waves). Therefore, they include a wide range of high-frequency components that usually induce a broadband increase in the high-frequency power but without actual HFOs in the non-filtered local field potential (Urrestarazu et al., 2007; Bénar et al., 2010; Worrell et al., 2012). The transient being the result of all those harmonics' additive superposition, a narrow band filter will generate spurious oscillations in the transient vicinity. That is why these inauthentic oscillations might cause bias in the data (Worrell et al., 2012). These phenomena are well known, firstly reported over a century ago by Gibbs (Gibbs, 1899) and referred to as "Gibbs' phenomena". Therefore, defining the frequency range of interest, for example (~80–600 Hz), and what type of high-frequency activity is being analyzed is critical when reporting results (Cimbalnik et al., 2016), to avoid the detection of these false oscillations (Bénar et al., 2010).

One aspect that is very important when using automatic HFO detection is artifact removal (Frauscher et al., 2017). Furthermore, recent studies showed that filtered extracellular action potentials (e.g., muscle activity, eye-movements) 'contaminate' high-frequency activity (Ray et al., 2008; Schomburg et al., 2012; Waldert et al., 2013; Thomschewski et al., 2020). The high-frequency power from these sources is due to the high-frequency Fourier components required to represent the raw data and should not be confused with actual data oscillations or true HFOs. In the extreme case of data discontinuity (e.g., a square wave signal), the Fourier component sums at the discontinuity do not die out as higher frequency terms are added, a phenomenon referred to as "Gibbs' artifact" (Gibs, 1899;

Cimbalnik et al., 2016). Further, the impact of the external reference electrodes (e.g., linked mastoids) have already been described, as this approach used may contribute to the artifact contamination of invasive EEG (iEEG) data. To this end, a bipolar montage might have resulted in less artifactual events (Thomschewski et al., 2020). Moreover, future automated detection algorithms should implement artifact matching in additional EMG and EOG channels in order to improve detected event specificity (Thomschewski et al., 2020).

For this reason, assessing HFOs during sleep is advisable, as artifacts are lowest then (Frauscher et al., 2017). Nevertheless, in our published studies, we had to compare data from wakefulness, as we did not have data from sleep in the included subjects. Even so, our results are in line with the published data. In our studies that began later but which are not part of this habilitation, we have already analyzed data also in sleep and monitored the behavior of HFOs and their characteristics concerning sleep and wakefulness (both rest and performing task).

The detectors that efficiently eliminate false HFO markings by phase correlation of band-pass filtered signal with a low pass filtered signal, which leads to a clear distinction of pure ("true") oscillations, are needed (Cimbálník et al., 2018).

The raw EEG signal (Fig.3) analysis process used in our studies was as follows. In the first step, the signal is band-pass filtered by a sequence of overlapping frequency bands. Each filtered band is processed separately in the subsequent steps.

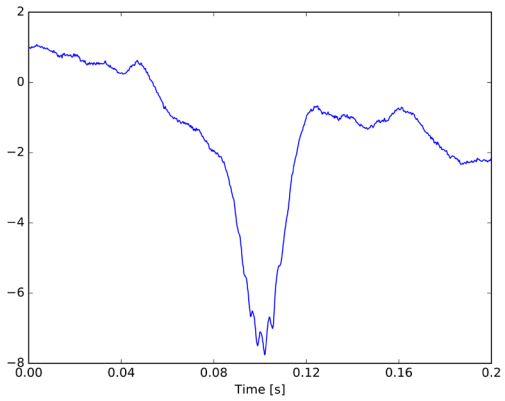


*Figure 3: Raw signal - spike with HFO.*

First, the amplitude envelope of the filtered signal is calculated using a Hilbert transform (Fig.4).

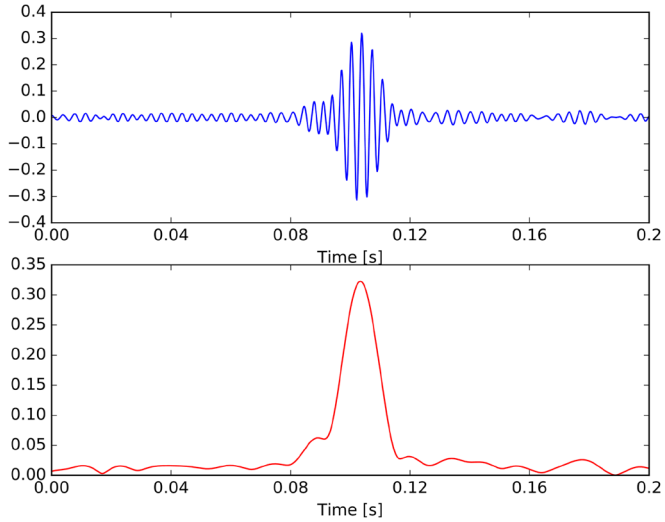


*Figure 4: Top - Band pass filtered signal. Bottom - Amplitude envelope of the filtered signal.*

Second, the band passed signal and the band passed signal with lower frequency cut off are converted to cosine representation of the signal cycles, and the correlation between them is calculated in the sliding window (Fig. 5). The metric serves to eliminate higher amplitude in filtered signal related to Gibb's phenomenon, such as spikes and other sharp transients.

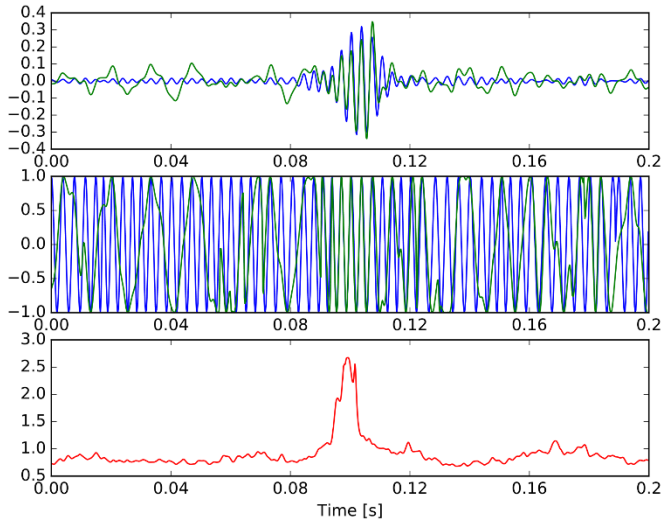


*Figure 5: The band passed signal (top), the band passed signal with lower frequency cut off are converted to cosine representation of the signal cycles (middle), and the correlation between them is calculated in the sliding window (bottom).*

The third step of metric calculation consists of calculating the dot product of the normalized signal amplitude envelopes and frequency stability metric, thus obtaining a signal that takes into account

both amplitude and frequency features of the analyzed signal (Fig. 6).

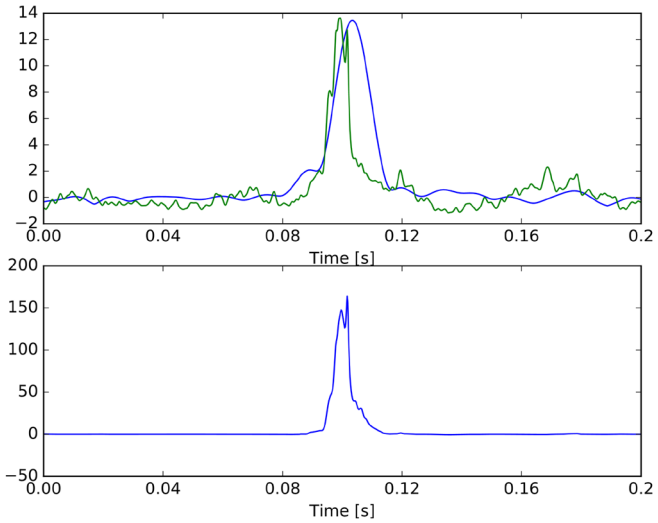


*Figure 6: Top - Dot product of the normalized signal amplitude envelopes. Bottom - Frequency stability metric.*

HFO detection is performed by applying a threshold to the product metric and a cascade of min/max thresholds based on previous HFO detections done by expert reviewers.

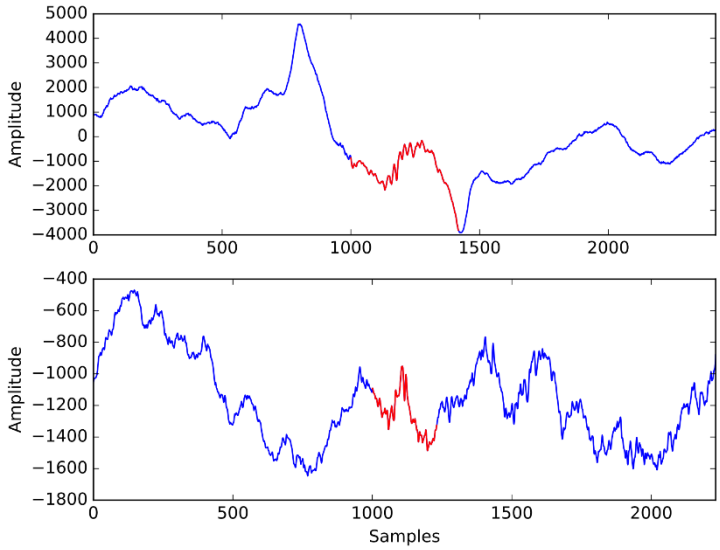


*Figure 7: Examples of correct positive detection (top) and false-positive detection (bottom).*

In individual studies, when investigating electrophysiological brain recordings, it is necessary to distinguish HFP and HFOs terms. The term HFOs should be reserved only to describe true high-frequency local field potential oscillations in the intracerebral EEG, which are oscillations visible in the

raw recording and not the high-frequency Fourier components from a band-pass filter. This HFP has a low correlation with the raw signal in the frequency band of interest (Worrell et al., 2012). The confusion of these terms can lead to different results, as both terms designate and express something else. In focal epilepsy with multiple spikes and sharp waves, HFP is more widely distributed than the occurrence of HFOs (Cimbalnik et al., 2016). As Jacobs et al. (2016) demonstrated, the HF power increase during spikes is less specific for the SOZ than visually identified individual HFO events.

There is a critical need for data and computer code sharing to create reproducible research and advance the use of HFOs biomarkers in brain mapping (Cimbalnik et al., 2016). So far, it has not been possible to compare the results from different laboratories, which differ in particular in the methodology of HFO detection (definition of HFOs, expert visual review vs. proprietary detectors; long vs. short datasets; a number of patients). Comparing detectors on a single dataset is essential to analyze their performance and to emphasize the issues involved in validation. Furthermore, the detectors are optimized for the dataset for which they were designed. Therefore, it is advisable to train and validate the detector on a dataset with similar characteristics to the one of interest because what is valid in one center would probably not be valid for another place (Worrell et al., 2012; Zelmann et al., 2012; Thomschewski et al., 2019). When comparing results from different centers, it is crucial to take into account not only the difference in the optimization of the detectors but also the electrode size, the number and distribution of the contacts, the sampling rate and filters, and the quality of the data (Worrell et al., 2012). All these aspects affect the generating reproducible results. To this date, a multicentre prospective study has not been conducted to validate the used detectors and determine the clinical utility of HFO biomarkers, which is needed for the translation of HFO electrophysiological biomarkers to clinical practice (Cimbalnik et al., 2016).

As intracerebral EEG recordings are primarily limited to patients with focal epilepsy thus, the specificity of intracranial recorded spikes, sharp waves, and HFOs as biomarkers of the epileptogenic brain remains challenging (Worrell et al., 2012).

If we summarize it all, objective, consistent, accurate labeling of epileptiform activity in large-scale recordings requires automated detectors. Automated detectors help significantly decrease the time required to detect HFOs and reduce the bias that human raters cause. Nonetheless, the definition of a gold standard for HFO detection is needed (Zelmann et al., 2012; Worrell et al., 2012; Zijlmans et al., 2017). Several HFO studies have been published concerning the visual quantification or automated detection of ripples and fast ripples. Nevertheless, the optimal algorithm for HFO study in macro and micro EEG recordings has not yet been determined.

**Published research**

# Intracerebrally recorded high frequency oscillations: simple visual assessment versus automated detection

Martin Pail

Josef Halámek

Pavel Daniel

Robert Kuba

Ivana Tyrlíková

Jan Chrastina

Pavel Jurák

Ivan Rektor

Milan Brázdil

**Clin Neurophysiol. 2013 Oct;124(10):1935-42. doi: 10.1016/j.clinph.2013.03.032.**

## Commentary on published paper

Electroencephalography (EEG) plays a principal role in the non-invasive and invasive evaluation of the brain's functional state. Invasive EEG recordings performed in subjects with drug-resistant epilepsy in the context of presurgical epilepsy evaluation provide us with excellent data for investigating high-frequency oscillations in the EEG.

High-frequency oscillations are a type of brain activity that represents the electrical manifestation of neuronal events, but above all, the very effective brain function mechanisms in both physiological and pathological conditions. Based on this fact, there is intense interest in HFOs recorded by electroencephalography, particularly within epileptology. In epilepsy, detected HFOs are used mainly to identify the area responsible for seizure generation (epileptogenic zone), the seizure onset zone (SOZ), respectively (Worrell et al., 2004; Jacobs et al., 2008). As it was mentioned, there are several options for detecting HFOs; automatic, visual, and a combination of both (Worrell et al., 2012).

Although it seems possible to identify the SOZ with high specificity by looking at only 5-10 min of interictal HFO activity (Urrestarazu et al., 2007; Jacobs et al., 2008; Andrade-Valença et al., 2011), it is still a lot of data that an expert reviewer has to go through and evaluate. In addition to that, we should mention that more repeated measurements eliminate accidental interferences and refine the measurement. Efforts should still be made to analyze more extended periods of EEG. Therefore, automatic detection has been developed to reduce a neurophysiologist's work and time evaluating EEG data. This approach also enables more objective marking of HFOs and more easily identifies HFOs on all channels.

In the presented study, we compared the possible contribution, in SOZ detection, of simple visual assessment of intracerebrally recorded HFOs with standard automated detection. The SOZ was defined in the contacts, which showed the first electroencephalographic ictal activity. We decided to compare the fully automated version because most clinicians will probably use this method.

We analyzed SEEG recordings from patients with medically intractable focal epilepsies, both temporal and extratemporal. Independently using simple visual assessment and automated detection of HFOs, we identified the depth electrode contacts with maximum occurrences of ripples and fast ripples. The SOZ was determined by independent visual identification in standard SEEG recordings, and the congruence of results from visual versus automated HFO detection was compared.

Our study confirmed that conventional intracranial EEG macro electrodes (sampling rate 1 kHz) can be used for HFO detection in both temporal and extratemporal lobe epilepsies. However, based on our current knowledge, the sampling frequency used in this study for fast ripple analysis was insufficient. Simple visual assessment of SEEG traces and standard automated detection of HFOs seemed to

contribute comparably to the identification of the SOZ in patients with focal epilepsies. Nevertheless, automated detection has the considerable advantage of saving time.

The significant disadvantages of visual inspection are that it is much work to assess all of the channels in all of the patients, and it requires experienced reviewers. The widespread clinical use of HFOs will only be possible if some kind of reliable automated or semiautomated method for their identification is implemented (Worrell et al., 2008; Crépon et al., 2010). A semiautomated method allows the removal of artifacts and the possible modification of the duration of the detected HFOs, and it could be used for all types of recordings. Nevertheless, most clinicians probably would use the fully automated version. Automatic detection (objective, a consistent method with accurate labeling of epileptiform activity in large-scale recordings) is crucial for the HFO investigation as biomarkers of epileptogenic tissue and is likely necessary to propel future clinical applications (Zelmann et al., 2012; Worrell et al., 2012). The time-consuming visual assessment of HFOs, which prevented their clinical application in the past, might now be overcome by validated computer-assisted algorithms (Frauscher et al., 2017).

Furthermore, according to this study, it seemed that when using macro electrodes in neocortical extratemporal epilepsies, the SOZ might be better determined (higher specificity) by the ripple range than by fast ripples. This bias was probably related to the lower sensitivity of macroEEG for fast ripple detection (Worrell et al., 2008) and the lower sampling frequency used. Nevertheless, Crépon et al. (2010) implied that neocortical epileptic networks do not have to generate fast ripples if the hippocampus is not involved in this network. Actually, pathological HFOs are generated by remote pathologically interconnected neuron clusters (Bragin et al., 2002a). These findings contradict other recent studies (Jacobs et al., 2008, 2009; Brázdil et al., 2010) in which fast ripples were detected in the pathological neocortex (focal cortical dysplasia), although fast ripples were observed with a lower rate or were a less specific marker for SOZ than in the mesiotemporal regions.

In summary, we proved standard automated detection of HFOs, in comparison with visual analysis of HFOs, achieves comparable results, and enables the evaluation of HFO characteristics (several frequency bands, changes in time, changes concerning seizures) in whole data. Automated and visual detection of HFOs yields comparable identification of the SOZ. This detection allows general purpose and objective evaluation without any bias from the neurophysiologist's experiences and practice.

Due to the detection of HFOs in pathological and non-pathological areas, this study highlights the importance of establishing methods to distinguish pathologic HFOs from physiologic HFOs to their further use in clinical epileptology.

Clinical Neurophysiology 124 (2013) 1935–1942

Contents lists available at SciVerse ScienceDirect

Clinical Neurophysiology

journal homepage: www.elsevier.com/locate/clinph

# Intracerebrally recorded high frequency oscillations: Simple visual assessment versus automated detection

Martin Pail [a,b], Josef Halámek [c], Pavel Daniel [d], Robert Kuba [a,b], Ivana Tyrlíková [a], Jan Chrastina [d,e], Pavel Jurák [c], Ivan Rektor [a,d], Milan Brázdil [a,b,*]

[a] Brno Epilepsy Center, Department of Neurology, St. Anne's University Hospital and Faculty of Medicine, Masaryk University, Brno, Czech Republic
[b] Behavioral and Social Neuroscience Research Group, CEITEC – Central European Institute of Technology, Masaryk University, Brno, Czech Republic
[c] Institute of Scientific Instruments, Academy of Sciences of the Czech Republic, Brno, Czech Republic
[d] Molecular and Functional Neuroimaging Research Group, CEITEC – Central European Institute of Technology, Masaryk University, Brno, Czech Republic
[e] Brno Epilepsy Center, Department of Neurosurgery, St. Anne's University Hospital and Faculty of Medicine, Masaryk University, Brno, Czech Republic

ARTICLE INFO

*Article history:*
Accepted 15 March 2013
Available online 21 May 2013

*Keywords:*
High frequency oscillations
Spikes
Ripples
Fast ripples
Temporal lobe epilepsy
Extratemporal lobe epilepsy
Seizure onset zone
Epileptogenic zone

## HIGHLIGHTS

- Simple visual assessment of SEEG traces (filtered in frequency ranges 80–200 Hz and 200–450 Hz) and standard automated detection of HFO contribute comparably (similar sensitivity) to the identification of the SOZ in subjects with focal epilepsies.
- Fully automated detection of HFO enables the objective evaluation of whole data without any bias from the neurophysiologist's experience.
- When using macroelectrodes in neocortical extratemporal epilepsies, the SOZ might be better determined (higher specificity) by the ripple range than by fast ripples.

## ABSTRACT

*Objective:* We compared the possible contribution (in the detection of seizure onset zone – SOZ) of simple visual assessment of intracerebrally recorded high-frequency oscillations (HFO) with standard automated detection.
*Methods:* We analyzed stereo-EEG (SEEG) recordings from 20 patients with medically intractable partial seizures (10 temporal/10 extratemporal). Independently using simple visual assessment and automated detection of HFO, we identified the depth electrode contacts with maximum occurrences of ripples (R) and fast ripples (FR). The SOZ was determined by independent visual identification in standard SEEG recordings, and the congruence of results from visual versus automated HFO detection was compared.
*Results:* Automated detection of HFO correctly identified the SOZ in 14 (R)/10 (FR) out of 20 subjects; a simple visual assessment of SEEG recordings in the appropriate frequency ranges correctly identified the SOZ in 13 (R)/9 (FR) subjects.
*Conclusions:* Simple visual assessment of SEEG traces and standard automated detection of HFO seem to contribute comparably to the identification of the SOZ in patients with focal epilepsies. When using macroelectrodes in neocortical extratemporal epilepsies, the SOZ might be better determined by the ripple range.
*Significance:* Standard automated detection of HFO enables the evaluation of HFO characteristics in whole data. This detection allows general purpose and objective evaluation, without any bias from the neurophysiologist's experiences and practice.


* Corresponding author. Address: Department of Neurology, St. Anne's University Hospital and Faculty of Medicine, Pekařská 53, 656 91 Brno, Czech Republic. Tel.: +420 543 182 649; fax: +420 543 182 624.
*E-mail address:* mbrazd@med.muni.cz (M. Brázdil).

1388-2457/$36.00 © 2013 Published by Elsevier Ireland Ltd. on behalf of International Federation of Clinical Neurophysiology.
http://dx.doi.org/10.1016/j.clinph.2013.03.032

## 1. Introduction

Electroencephalography (EEG) plays a principal role in the non-invasive and invasive presurgical evaluation of patients with intractable epilepsy. EEG is used mainly to identify the area responsible for seizure generation, the seizure onset zone (SOZ). Several mathematical approaches were recently established to improve ictal and interictal (especially invasive) EEG analysis (Staba et al., 2002; Gardner et al., 2007; Worrell et al., 2008; Tito et al., 2009; Ayala et al., 2011; Nikulin et al., 2011).

Interictal high-frequency oscillations (HFO) in frequencies over 80 Hz have been recently identified in recordings from invasive EEG monitoring (employing microwires, depth macroelectrodes, or subdural strips/grids) in epileptic patients (Bragin et al., 1999; Staba et al., 2002; Worrell et al., 2004, 2008; Urrestarazu et al., 2007; Jacobs et al., 2008, 2009; Bagshaw et al., 2009; Brázdil et al., 2010; Crépon et al., 2010). These HFO were first recorded with microwires from mesiotemporal structures in patients with mesiotemporal lobe epilepsy (MTLE) during interictal periods (Bragin et al., 1999; Staba et al., 2002). Urrestarazu et al. (2007) observed interictal HFO in the SOZ using small broadband depth electrodes (contact area 0.8 $mm^2$); these observations were later confirmed by Worrell et al. (2008) using standard subdural macroelectrodes (contact area 9.4 $mm^2$) and recording from a more extended brain area.

These short-lasting phenomena (20–100 ms), a result of the synchronization of neuronal populations, are generally split into two categories according to their frequency: ripples (R), ranging between 80–200 Hz, and fast ripples (FR), in the range of 200–500 Hz (Bragin et al., 1999). Their occurrence increases during non-REM sleep (Staba et al., 2004; Bagshaw et al., 2009). Very high frequency oscillations (VHFO), ranging from 1000–2500 Hz, were recently observed (Usui et al., 2010) using subdural electrodes.

Ripples are considered to be a signature of both normal and pathological brain processes; fast ripples are believed to reflect primarily the neuronal substrates of epileptogenesis and epileptogenicity (Engel et al., 2009). In humans, ripple oscillations were observed in the processes important for memory consolidation in the hippocampus and parahippocampal structures (Bragin et al., 1999; Axmacher et al., 2010). Physiological HFO at about 600 Hz were noticed in the neocortex during somatosensory stimulation (Curio et al., 1997).

Interictal HFO are to a high degree spatially localized to the SOZ; this was confirmed in observations with both microwires and macroelectrodes (Worrell et al., 2004; Jacobs et al., 2008), and less are linked to lesions (Jacobs et al., 2009). Ictal HFO occur predominantly in the region of primary epileptogenesis (SOZ), and less are found in areas of secondary seizure spread (Jirsch et al., 2006). Based on the results of previously published papers, it seems that the SOZ can be determined with high specificity through the evaluation of 10 min of HFO activity (Jacobs et al., 2008; Zelmann et al., 2009; Andrade-Valença et al., 2012).

Most HFO are seen predominantly at the same time as spikes (Engel et al., 2003; Urrestarazu et al., 2007; Worrell et al., 2008). Although the SOZ is characterized by concomitant spiking activity (high sensitivity), spikes are often seen outside the SOZ as well (low specificity) (Jacobs et al., 2008). For this reason, many studies have focused on interictal HFO and their role in both identifying the SOZ and differentiating it from surrounding remote areas, which is critical for successful resective epilepsy surgery. HFO occurrence (both interictal and ictal) within the SOZ seems to be more sensitive and specific than spikes (Jacobs et al., 2008; Zijlmans et al., 2011). Thus, interictal HFO could be a better marker of epileptogenicity than interictal spikes. HFO (particularly FR) seem to occur especially within pathological mesial temporal structures as the area responsible for seizure generation and in neocortical epileptogenic structures as well, although less often (Jacobs et al., 2008). In our recent study, the combination of HFO detection rates with power spectral analysis clearly demonstrated the capacity of HFO to detect the SOZ in patients with extratemporal focal cortical dysplasia (Brázdil et al., 2010).

A large amount of data is generated during long-term invasive video EEG monitoring, and for that reason a widespread clinical use of HFO will only be possible if some kind of reliable automated or semiautomated method for their identification is implemented. The advantage of simple visual assessment is in the simplicity. However, the major disadvantages of visual inspection are that it is a lot of work to assess all channels in all patients, it is inevitably subjective, and it requires experienced reviewers.

The automatic detection which was developed to reduce work for the neurophysiologist also enables more objective marking of HFO and more easily identifies HFO on all channels. Several HFO studies have been published concerning the visual quantification or automated detection of ripples and fast ripples. Nevertheless, the optimal algorithm for HFO study in macroEEG recordings has not yet been determined.

The aim of the study was to compare the probability of detecting the SOZ with HFO by simple visual assessment and intracerebrally recorded HFO with standard automated detection. We decided to compare the fully automated version because this method is probably what most clinicians would use.

## 2. Methods

### 2.1. Subjects

The main demographic and clinical characteristics of all subjects are shown in Table 1. We studied 20 consecutive patients (including all of the patients from our center who underwent resection; we knew the histology results and the EEG sampling frequency we used enables HFO evaluation) with medically intractable focal epilepsies (12 females; 8 males) and a mean age of 31 years (SD = 10.3; range 12–47 years). All of the subjects had been referred to the Brno Epilepsy Center, Department of Neurology. All the subjects fulfilled the diagnostic criteria for medically intractable temporal lobe epilepsy (TLE) or extratemporal lobe epilepsy (ETLE); 10 subjects had TLE and 10 subjects had ETLE. The diagnosis was made according the ILAE criteria (Commission on Classification and Terminology of ILAE, 1989). The majority of subjects had no history of precipitating events. Five subjects with TLE had meningoencephalitis, perinatal asphyxia, mushroom poisoning, prematurity, and prolonged delivery before the first seizure; one subject with ETLE suffered from commotio cerebri. Two subjects had a history of febrile convulsions. The majority of subjects had a history of complex partial seizures, in 8 subjects with sporadic seizure generalization (GTCS). The mean age at seizure onset was 13.3 (SD = 8.7; range 0.75–36 years) (Table 1).

All of the subjects had been routinely investigated, including long-term continuous noninvasive and invasive video EEG monitoring, MRI, and neuropsychological testing. The diagnosis of unilateral TLE/ETLE in our subjects was based on a concordance of history data, ictal and interictal EEG findings, ictal semiology, neuropsychology, and neuroimaging findings. Some of the subjects revealed structural lesions on MRI scans (see Table 1). Most of the subjects had not undergone previous intracranial surgery. One subject had *extirpation* of pilocytar astrocytoma within the parieto–occipital region 2 years before SEEG and re-operation; a partial anterior corpus callosotomy had been performed in one subject due to atonic seizures that afterward disappeared. Prior to invasive

**Table 1**
Demographic and clinical data.

| Subject | Gender | Age at SEEG | Febrile seizures | Age at seizure onset | Seizure frequency/ monthly | MRI (signs of) | Type and side of epilepsy | Brain lobes explored and number of implanted electrodes | Region SOZ | Intervention/ histopathology | Outcome (Engel) |
|---|---|---|---|---|---|---|---|---|---|---|---|
| 1 | F | 35 | – | 15 | CPS 100 | FCD parietal operculum | E/R | F (3), I (1), P (5), T (1) | Right parietal operculum | Lesionectomy/ FCD IIA | IIIA (3.5 years) |
| 2 | M | 39 | – | 11 | CPS 100 | Negative | E/R | F (7) | Right inferior frontal gyrus | Cortical resection/FCD IIA | IA (3 years) |
| 3 | M | 47 | – | 3 | CPS 60, + | Negative | E/R | F (4), T (3), I (1), P (1) | Right frontoorbital cortex, mesial frontopolar and lateral prefrontal cortex | Cortical resection/FCD IIA | IIIA (3 years) |
| 4 | M | 18 | + | 3 | CPS 10 | Negative | E/R | F (9), P (2), O (1) | Right precentral sulcus | Pericentral topectomy/FCD IIA | IIA (3 years) |
| 5 | F | 24 | – | 20 | SPS 500 | Asymmetric gyrification within right SMA | E/R | F (4), P (3) | Right precentral gyrus | Partial lesionectomy | IV B (2.5 years) |
| 6 | F | 12 | – | 2.5 | CPS 80 | Lesion of right orbitofrontal cortex | E/R | F (5), T (3) | Right orbitofrontal cortex | Lesionectomy | IIIA (1 year) |
| 7 | M | 23 | – | 15 | CPS 10 + | Right frontopolar tuberous sclerosis | E/R | F (4), F′ (3), P′ (1), T (1), T′ (1), O′ (1) | Right fronto-polar region | Lesionectomy/ FCD IIB | IV A (2 years) |
| 8 | M | 29 | – | 17 | CPS 15 + | Negative | E/L | T′ (4), T (1), P (1), P′ (1), O′ (2) | Left occipital pole | Cortical resection | IV A (2 years) |
| 9 | F | 35 | – | 11 | CPS 23 | FCD in right superior frontal gyrus, postoperative changes after partial anterior callosotomy | E/R | F (6), P (1), F′ (3) | Right mesial and lateral prefrontal cortex | Lesionectomy/ FCD IA | IIIA (2 years) |
| 10 | F | 23 | – | 13 | SPS 2 + | Local atrophy and gliosis in trigone of left lateral ventricle after extirpation of pilocytar astrocytoma within parieto–occipital region | E/L | T′ (2), P′ (1) O′ (2) | Left parietooccipital bounder and occipital lobe | Reoperation, lesionectomy/ reparative changes after extirpation of pilocytar astrocytoma | IA (1 year) |
| 11 | F | 29 | – | 24 | CPS 10 | DNET or ganglioglioma within right amygdala | T/R | T (3), T′ (3) | Right hippocampus | AMTR/DNET grade I | IB (1.5 years) |
| 12 | F | 41 | – | 9 months | CPS 80 | Bilateral hippocampal sclerosis, blurring of the gray-white matter junction in right temporal pole | T/R | F (5), T (5) | Right hippocampus | AMTR | IA (1.5 years) |
| 13 | F | 26 | – | 3 | CPS 3 + | Blurring of the gray-white matter junction in left temporal pole | T/L | F′ (5) T′ (3), P′ (1) | Left temporopolar region | AMTR | IA (1.5 years) |
| 14 | M | 23 | – | 14 | CPS 80 | Chorioidal fissure cyst | T/L | T (2)/F′ (3), T′ (5) | Left temporopolar region | AMTR/FCD IA | IV B (1 year) |
| 15 | F | 28 | – | 13 | CPS 10 | Meningoencephalocele and hypotrophy of left temporal pole | T/L | T′ (6) | Left temporopolar region | AMTR and plastic surgery of skull base | IB (2 months) |
| 16 | F | 46 | – | 36 | CPS 10 | Negative | T/L | F′ (2), T′ (6) | Left hippocampus | AMTR | IA (1 year) |
| 17 | F | 47 | – | 17 | CPS 18 | Postischemic gliotic changes within left parieto–occipital and right occipital area | T/R | F (1), T (5), T′ (2) | Right hippocampus | AMTR/FCD IA | IIIA (1.5 years) |
| 18 | M | 35 | – | 23 | CPS 5 + | Abnormal gyrification of the base of right temporal lobe | T/R | T (5), F (1), T′ (2) | Right hippocampus | AMTR | IA (1 year) |
| 19 | M | 40 | + | 8 | CPS 20 + | Left hippocampal sclerosis | T/L | F (3), T (3)/ F′ (3), T′ (3) | Left hippocampus | AMTR/HS gradus IV l.sin. | III (2 years) |

(*continued on next page*)

**Table 1** (*continued*)

| Subject | Gender | Age at SEEG | Febrile seizures | Age at seizure onset | Seizure frequency/ monthly | MRI (signs of) | Type and side of epilepsy | Brain lobes explored and number of implanted electrodes | Region SOZ | Intervention/ histopathology | Outcome (Engel) |
|---|---|---|---|---|---|---|---|---|---|---|---|
| 20 | F | 19 | – | 16 | CPS 2 + | Negative | T/L | T′ (7) | Left temporopolar region | AMTR | IV B (1 year) |

CPS – complex partial seizure; + – sporadic ictal generalization; SOZ – seizure onset zone; SMA – supplementary motor area; DNET – dysembryoplastic neuroepithelial tumor; FCD – focal cortical dysplasia; AMTR – anteromedial temporal resection; E – extratemporal; T – temporal; R – right; L – left; FCD – focal cortical dysplasia; F – frontal; P – parietal; T – temporal; O – occipital, I – insular; ′ – left.

EEG, two subjects underwent the implantation of a vagus nerve stimulation system with unfavorable seizure frequency outcome. Informed consent was obtained from each participant after all of the procedures were fully explained. The study received the approval of the local ethics committee.

### 2.2. SEEG

Preoperative invasive SEEG were obtained from all of the subjects. The sites of electrode placements were individualized according to seizure semiology, clinical history, noninvasive EEG investigations, and neuroimaging results. Several standard multicontact depth electrodes (ALCIS with a diameter of 0.8 mm, a contact length of 2 mm, and intercontact intervals of 1.5 mm; the surface area of each contact 5 $mm^2$) were orthogonally implanted in each subject to localize the seizure origin (see Table 1). The exact positions of the electrode contacts in the brain were verified using postplacement MRI with electrodes in situ. In each subject, the SOZ was determined by a standard visual analysis of ictal SEEG recordings. The SOZ was defined as the contacts that showed the first electroencephalographic ictal activity.

A total of 10 min of artifact-free interictal SEEG data (recorded during wakefulness) was analyzed for each subject. The EEGs were low-pass filtered at 450 Hz and sampled at 1024 Hz. A reference montage with linked earlobes as a reference was used for the analysis.

### 2.3. Selection of subsequently analyzed contacts

In each subject, 6–12 recording contacts with the maximum of interictal spikes were visually selected for further HFO analysis (by co-authors RK and IT). The contacts with spikes were chosen since non-spiking channels are not usually seen in the SOZ (Jacobs et al., 2008). The SOZ was always included and at least 2 probes were involved. Only these contacts were analyzed in the visual assessment and automated detection of HFO. The number of analyzed contacts was limited by the possibilities of visual analysis. The visual analysis is time consuming and the same contacts should be analyzed with both detections. The SOZ selection was blinded to the other co-authors. The only information given was that one contact should be in the SOZ. The selection of this contact was the aim in the next blind analysis.

### 2.4. Visual assessment of HFOs in resting awake SEEG

A simple visual inspection (analogous to an "EEG reading") of 10-min resting awake SEEG recordings from the 6–12 chosen contacts was performed independently by two co-authors (MB and PD) blinded to the results of SOZ detection by a standard analysis of ictal SEEG (a minimal number of oscillations – 4 waves). The contacts with detected HFOs by both reviewers were included in the analysis and the remaining detected oscillations were excluded from the study. HFO detection was performed independently in

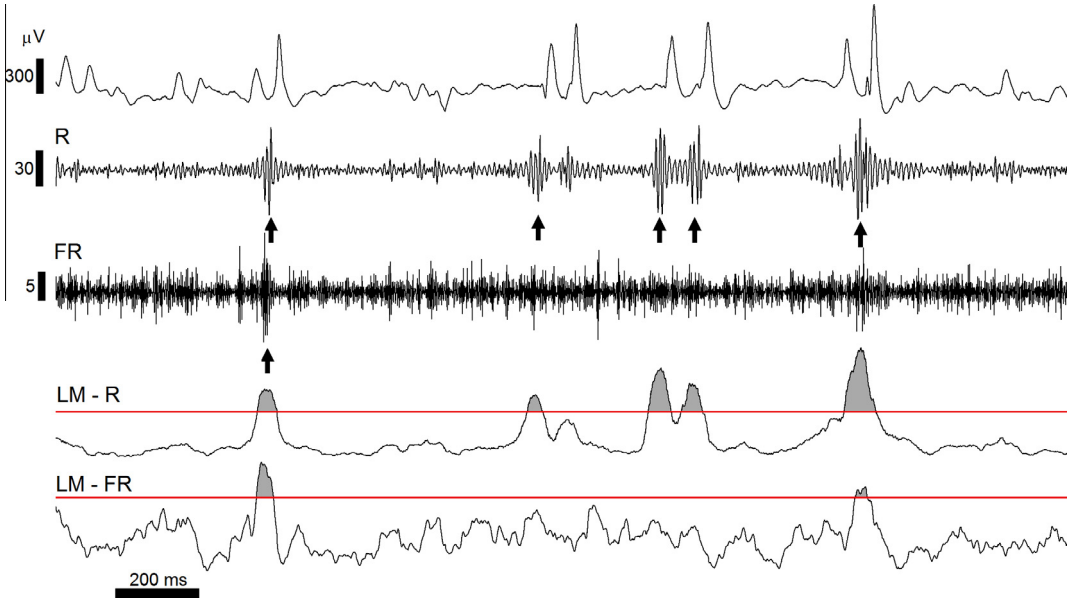


**Fig. 1.** The demonstration of detection of HFO by simple visual assessment and standard automated detection. There are presented raw data, visual HFO detection in two frequency ranges, R (80–200 Hz) and FR (200–450 Hz) and automated detection of HFO (according to the algorithm by Gardner et al. (2007)) based on line length.

**Table 2**
Contacts within the identified SOZ and with the maximum occurrence of ripples and fast ripples.

| Subject | SOZ according to SEEG | Visual analysis | | Automated detection | | Outcome |
|---|---|---|---|---|---|---|
| | | Ripples | Fast ripples | Ripples | Fast ripples | |
| 1 | Po7 – inferior parietal lobulus | Po7 | Po7 | Po7 | Po7 | IIIA (3.5 years) |
| 2 | L8 – inferior frontal gyrus | L8 | – | L8 | – | IA (3 years) |
| 3 | O4,5 – orbital gyri | O5 | O5 | O5 | O9 – orbital gyri | IIIA (3 years) |
| 4 | L7 – precentral sulcus | L7 | L7 | L7 | L7 | IIA (3 years) |
| 5 | X13,14 – precentral gyrus | X13,14 | – | – | – | IV B (2.5 years) |
| 6 | O7-13 – orbital gyri | O13 | O13 | O13 | O13 | IIIA (1 year) |
| 7 | P7-13 frontopolar area | P9 | – | P9 | O1 – anterior cingulate gyrus | IV A (2 years) |
| 8 | K′5 - occipital gyrus | K′5 | K′5 | K′5 | D′5 – medial temporal gyrus | IV A (2 years) |
| 9 | P2 – superior frontal gyrus | P2 | P2 | P2 | – | IIIA (2 years) |
| 10 | S′8 – middle orbital gyrus | H′3 – lingual gyrus | H′3 | S′8 | H′4 – lingual gyrus | IA (1 year) |
| 11 | B1-4 - middle hippocampus | B′2 – middle hippocampus | B′2 | B2 | B2 | IB (1.5 years) |
| 12 | B1-2 - middle hippocampus | B1 | C′1 – posterior hippocampus | B1 | B1 | IA (1.5 years) |
| 13 | P′1-2 temporal pole | B′2 – middle hippocampus | B′2 | P′1 | B′2 | IA (1.5 years) |
| 14 | Tp′4-10 – temporal pole | Tp′8 | B′1 – middle hippocampus | Tp′8 | Tp′8 | IV B (1 year) |
| 15 | B′9 – temporal cortex | B′1 – middle hippocampus | B′9 | B′1 | – | IB (2 months) |
| 16 | B′1-5 - middle hippocampus | – | – | – | – | IA (1 year) |
| 17 | B3 – middle hippocampus | B3 | B3 | D4 – posterior hippocampus | B3 | IIIA (1.5 years) |
| 18 | B1-3 – middle hippocampus, C1-3 – posterior hippocampus | C1 | C1 | C1 | C1 | IA (1 year) |
| 19 | C′1-3 – middle hippocampus | B1 – anterior hippocampus | B1 | B1 | B1 | III (2 years) |
| 20 | Tp′ temporal pole | B′3 middle hippocampus | B′4 | C′2 – posterior hippocampus | Tp′3 | IV B (1 year) |

Electrodes on the left side are indicated by primes; SOZ – seizure onset zone.

two frequency ranges, R (80–200 Hz) and FR (200–450 Hz). In each subject, the contacts with maximum occurrence of HFO in each subgroup (R and FR) were identified. (See for an example Fig. 1.)

### 2.5. Automated detection of HFOs in resting awake SEEG

Automated detection of HFO (according to the algorithm by Gardner et al. (2007)) based on line length was performed by our program co-authors (JH and PJ). As the first step, the signal was filtered in the given pass band (R <80;200 Hz> and FR <200;450 Hz>, after that the line length was computed in the moving window (length of window R 50 ms, FR 10 ms) as the sum of absolute differences in signal. The threshold level was given as the 97.5 percentile of line length amplitude. The distribution function was given by analysis over all epoch. Only the peaks, that were longer than 40 ms at R or 15 ms at FR were counted.

The number of detected events significantly depends on the parameters used. If finding the exact number of ripples and fast ripples is the main aim, the parameters must be optimized. We wanted to define the SOZ contact only; this contact should be dominant with a wider area of parameters. Small changes of parameters were tested, and if the SOZ contact selection was changed by a minor change in parameters, the data was marked as nondetectable (See for an example Fig. 1).

### 2.6. Statistical analysis

The results of different approaches (in the detection of the SOZ by means of HFO in 10-min resting awake SEEG) were compared. The concordance between simple visual assessment and automatic detected electrodes (with the predominant occurrence of HFO – the highest rate) with the detection of the SOZ by visual analysis of ictal recordings were determined.

We used a binomial cumulative distribution function to assess the significance of the number of agreements between the two methods (visual analysis of R × SOZ; visual analysis of FR × SOZ; automated detection of R × SOZ; automated detection of FR × SOZ; visual analysis of R × automated detection of R; visual analysis of FR × automated detection of FR).

## 3. Results

The results of HFO detection by different diagnostic approaches are shown in Tables 2 and 3.

The contacts with R were found in 18 subjects [90%] and FR in 15 [75%] (Table 3). The correctness of detection and comparison of visual and automated detection may be verified by two points – according to the SOZ definition from SEEG and good outcome.

**Table 3**
The results of different diagnostic approaches.

| Outcome | Visual analysis | | Automated detection | |
|---|---|---|---|---|
| | Ripples | Fast ripples | Ripples | Fast ripples |
| I-IV | 13/6/1 | 9/7/4 | 14/4/2 | 10/5/5 |
| I-II | 4/4/1 | 3/4/2 | 7/1/1 | 4/2/3 |
| III-IV | 9/2/0 | 6/3/2/ | 7/3/1 | 6/3/2 |

Numbers: proper detection/false detection/nondetection of SOZ.

Only 9 patients (47.4%) in whom the presumed SOZ was removed had good outcomes (Engel I and II). One patient underwent only limited resection, and his outcome was Engel IVB. Ten patients had poor outcome or partial improvement (Engel III or IV).

### 3.1. Ripples

The contact with the maximum R rate as defined by automated detection correctly identified the SOZ in 14 out of 20 subjects [70%]. A simple visual assessment of SEEG records in the appropriate frequency range correctly identified the SOZ in 13 out of 20 subjects [65%] (Table 3). In terms of the epilepsy type, the contacts with highest R rate were defined within the SOZ in 9 cases of ETLE (both for visual and automated detection), but in only 4/10 (visually) and 5/10 (automated detection) cases of TLE.

According to the postsurgical outcome, the removal of identified contacts with the highest rate of automatically detected ripples resulted in Engel I for 6 patients, in Engel II for 1 patient, in Engel III for 4 patients, and in Engel IV for 3 patients; visually identified R resulted in Engel I for 3 patients, in 1 patient Engel II, in Engel III for 5 patients, and in Engel IV for 4 patients (Tables 2 and 3).

### 3.2. Fast ripples

The specificity of both approaches was lower for FR detection. The contact with the maximum FR rate obtained from automated analysis correctly identified the SOZ in 10/20 [50%]; visual analysis correctly identified the SOZ in 9/20 subjects [45%] (Table 3).

The SOZ was revealed by means of FR in ETLE in 6/10 subjects visually and 4/10 subjects by automated detection. In 10 subjects with TLE, the contacts with the highest FR rate were seen within the identified SOZ only in 3/10 subjects visually or 6/10 subjects by automated detection.

According to the postsurgical outcome, the removal of identified contacts with the highest rate of automatically detected fast ripples resulted in Engel I for 3 patients, in Engel II for 1 patient, in Engel III for 4 patients, and in Engel IV for 2 patients; visually identified FR resulted in Engel I for 2 patients, in Engel II for 1 patient, in Engel III for 5 patients and in Engel IV for 1 patient.

The concordance between the obtained results (for both R and FR) and the identified SOZ was not significant for either used methods. The highest agreement between the results and the SOZ was in automated detection in the R range in 14/20 subjects ($p = 0.058$ uncorrected, 0.348 corrected for multiple comparison). An important discrepancy between both approaches was surprisingly frequent: in the R range this was present in 5 subjects and in the FR range in 7 subjects. The significance of the number of agreements between visual analysis and automated detection was not statistically significant in either R or FR ranges.

## 4. Discussion

The diagnostic value and the usefulness of interictal HFO, and especially of fast ripples, were suggested by Bragin et al. (1999). Our study confirms that conventional intracranial EEG macroelectrodes (sampling rate 1 kHz) can be used for HFO detection in both TLE and ETLE. However, as described in simultaneous recordings using macroelectrodes and microwires (Worrell et al., 2008), the patterns of the HFO detected by EEG is quantitatively different from those detected by microwires. The FR are spatially localized to a region of less than 1 $mm^3$ (Bragin et al., 2003), and thus spatial averaging of focal field potentials (larger surface area of macroelectrodes) leads to spatially undersampling HFO activity (fewer FR are disclosed by macroelectrodes than by microwires) (Worrell et al., 2008). These observations contrast with those of Jacobs et al. (2008), who published similar frequency findings of HFO with macroelectrodes as had been seen previously in microwires; the detection of HFO was even higher due to the spatial recording ability. Nevertheless, Jacobs did not simultaneously study microwires, and the electrodes used in the study had smaller contact areas than standard multicontact depth macroelectrodes and the subdural electrodes used by Worrell. To compare both methods (visual and automatic) we used previously recorded data with the advantage of knowledge of the histology results and outcomes. We had to compare data from wakefulness, as we did not have data from sleep in these patients, even though we know that HFO are more stable in sleep and the likelihood for artifact contamination is lower during sleep. Nevertheless, the differences of HFO rates (between the SOZ and other remote areas) were disclosed in wakefulness period as significant (Bagshaw et al., 2009).

Electrodes with HFO were visually detected in most of our subjects (19/20 for R and 16/20 for FR). Ripples and fast ripples occurred within and outside the SOZ. The sensitivity of both analyses (simple visual assessment and automated detection) was equivalent. The concordance between R and the identified SOZ was higher than between FR and the SOZ. This bias is probably related to the lower sensitivity of macroEEG for FR detection (Worrell et al., 2008). Other explanations might be the use of limited sampling rate or low signal to noise ratio in EEG, as with patient 16. It should also be mentioned that HFO in spikes might tend more towards the ripple range and thus explain the better result for ripples than fast ripples (Bénar et al., 2010).

Ripples denote the SOZ (using both visual assessment 9/10 and automated detection 9/10) better outside the mesiotemporal structures; the use of FR as the predictor of SOZ in this type of epilepsy might be confusing.

Crépon et al. (2010) implied that neocortical epileptic networks do not have to generate HFO if the hippocampus is not involved in this network. These findings contradict other recent studies (Jacobs et al., 2008, 2009; Brázdil et al., 2010) in which FR were detected in the pathologic neocortex (FCD), although FR were observed with a lower rate or were a less specific marker for SOZ than the mesiotemporal regions.

The false positive results (the results that were discordant with the actual SOZ) were found in R range, and were high in both methods, especially in TLE subjects. The explanation for this outcome is that ripples are very likely physiological for mesiotemporal structures, even though their confirmation in the extratemporal structures may contribute to detecting the SOZ (Brázdil et al., 2010).

Fast ripples are predominantly specific for the epileptic mesial temporal cortex as the result of a damaged physiological network (producing ripples), and thus this neuronal pathologic network (interconnected principle neurons within epileptogenic areas) enables the production of hypersynchronous events at frequencies above 200 Hz. This pattern may thus be specific for mesiotemporal SOZ (Bragin et al., 1999; Staba et al., 2004; Urrestarazu et al., 2007; Worrell et al., 2008; Crépon et al., 2010) and hippocampal atrophy/sclerosis (Staba et al., 2002; Crépon et al., 2010). In 10 subjects with TLE, FR were observed in the denoted SOZ in only 4 subjects visually and in 6 subjects by means of automated detection. Sufficient detection of FR (in addition to low signal to noise ratio and limited sampling rate) and false positivity might be explained by the subtle and discrete clusters of abnormally bursting neuronal cell assemblies (not homogeneously distributed over the whole epileptogenic tissue), which could generate FR not visible in standard SEEG (Bragin et al., 2003), as well as by the spatial propagation of these patterns to other areas (Crépon et al., 2010). HFO may be also generated by neuronal clusters outside the SOZ (Jacobs et al., 2008). Whether these FR (outside the SOZ) represent potentially epileptogenic areas is unclear (Jacobs et al., 2009). Although

in 10 subjects a contact with dominant FR was not detected, or was disclosed (by automated detection) in a region other than that of the identified SOZ, 3 subjects had outcome IV according to Engel's classification, and 2 subjects had level III. Only 9 patients (47.4%) in whom the presumed SOZ was removed had good outcomes (Engel I and II).The poor outcome in the subjects might be caused by responsible pathology localized in a different region, and a favorable outcome might be expected if this HFO generating tissue were removed (Jacobs et al., 2010; Wu et al., 2010; Akiyama et al., 2011; Modur et al., 2011). The extent of SOZ may not correspond with the extent of the epileptogenic zone. The epileptogenic zone may include the actual epileptogenic zone (generating seizures before surgery) as well as a potential epileptogenic zone which is an area of the cortex that may generate seizures after the presurgical SOZ has been resected (Rosenow and Lüders, 2004). It seems that for good postsurgical outcome, it is more important to detect the epileptogenic zone than the SOZ (Zijlmans et al., 2012), but further research is necessary. Problems may also arise if the electrode contact is not placed exactly in the SOZ and we identify the first EEG change during seizures from a contact actually distant from the actual SOZ.

Most HFO are found within sharp components (Urrestarazu et al., 2007; Jacobs et al., 2008; Crépon et al., 2010). Artifactual high frequency activities can be also caused by high-pass filtering these sharp components (spikes or sharp waves) of epileptiform discharges and therefore include high-frequency components that usually induce a broadband increase in the high frequency (Urrestarazu et al., 2007; Bénar et al., 2010) and therefore these inauthentic oscillations might cause bias in the data. These false HFO must be eliminated if an accurate count of R and FR is the main aim. The false HFO has the same time occurrence as a corresponding spike, and the power spectrum for the given time interval is monotonically decreases. We did not eliminate the false HFO with automatic or visual detection. With automated detection, we tested the common occurrence of spikes and HFO after analysis. The common occurrence was supposed if there was any overlapping of spikes and HFO. We detected 65% common occurrence over all subjects and analyzed channels with R and spikes, and 57% with FR and spikes. Nevertheless, whether or not these events were included, the results would not be changed (Urrestarazu et al., 2007; Jacobs et al., 2008). Subjects with spikes localized in one well-restricted region benefit from a higher probability of being seizure free than subjects with spikes generated in multiple pathologic areas (Bautista et al., 1999). This indicates that this abnormal pattern also represents an important pathology, and its importance in the neuronal network should not be omitted.

Several automated algorithms were introduced for automatically detecting and classifying HFO in human intracranial EEGs (Staba et al., 2002; Nelson et al., 2006; Gardner et al., 2007; Firpi et al., 2007; Blanco et al., 2010; Nikulin et al., 2011). In summary, different results can be obtained from varied parameter settings for automated HFO pattern detection, not merely with regard to the relative number (rate) of HFOs but also in the number of HFOs for particular contacts (and thus differences among regions). This algorithm as well as all algorithms to detect spontaneous HFOs typically has low specificity and manual review is needed to remove false positives. The optimal algorithm for HFO study is still being determined. Undoubtedly the elaboration of this algorithm is highly complex. We hypothesized that each region of epileptic brain tissue (primarily the mesiotemporal structures in comparison with neocortex) might produce specific HFO patterns. Different neocortical seizure-onset patterns and attributes recorded by intracranial EEG were presented with regard to the anatomic location or pathologic substrate (Lee et al., 2000). The different results of R and FR depending on the region of epilepsy (TLE compared to ETLE) may be seen in our study.

Automatic detection may be used for different reasons, such as to count R and FR, to classify patients, to detect seizures (Ayala et al., 2011; Cabrerizo et al., 2012), to predict seizures, and to assess the SOZ. A simple algorithm for automated HFO detection contributes comparably (similar sensitivity) to the visual identification of the SOZ. For the future, we think a more complex algorithm would be useful, where the training and more overlapped frequency bands will be used, as according to our experience (time frequency analysis of data with sampling frequency 5 kHz) the frequency of events is subject specific and events may exist in the frequency area over 500 Hz.

## 5. Conclusion

When using macroelectrodes in neocortical extratemporal epilepsies, the SOZ might be better determined (higher specificity) by the ripple range than by fast ripples. However these results might be influenced by the acquisition system used. Simple visual assessment of SEEG traces (filtered in frequency ranges 80–200 Hz and 200–450 Hz) and standard automated detection of HFO contribute comparably (similar sensitivity) to the identification of the SOZ in subjects with focal epilepsies. Nevertheless, automated detection has the considerable advantage of saving time. The major disadvantages of visual inspection are that it is a lot of work to assess all of the channels in all of the patients and it requires experienced reviewers. The widespread clinical use of HFO will only be possible if some kind of reliable automated or semiautomated method (Worrell et al., 2008; Crépon et al., 2010) for their identification is implemented. A semiautomated method allows for the removal of artifacts and the possible modification of the duration of the detected HFO, and it could be used for all types of recordings, nevertheless most clinicians probably would use the fully automated version. The evaluation of SEEG recordings does not require the control of a whole long-term invasive video EEG; it is possible to identify the SOZ with a high specificity by looking at only 5–10 min of interictal HFO activity (Urrestarazu et al., 2007; Jacobs et al., 2008; Andrade-Valença et al., 2012). Nevertheless, we should mention that more repeated measurements eliminate accidental interferences. We hypothesized that each region of epileptic brain tissue (primarily the mesiotemporal structures in comparison with neocortex) might produce specific HFO patterns. This might be also clarified by using several frequency bands, not only R and FR. It seems that for a good postsurgical outcome, it is more important to detect the epileptogenic zone than the SOZ by means of HFO (Zijlmans et al., 2012), but further research is necessary.

In summary, standard automated detection of HFO, in comparison with visual analysis of HFO, achieves analogous results and enables the evaluation of HFO characteristics (several frequency bands, changes in time, changes in relation to seizures) in whole data. This detection allows general purpose and objective evaluation without any bias from the neurophysiologist's experiences and practice.

## Acknowledgments

We thank Anne Johnson for grammatical assistance. The study was supported by the "CEITEC - Central European Institute of Technology" project (CZ.1.05/1.1.00/02.0068) from the European Regional Development Fund and by MŠMT ČR Research Program no. MSM0021622404. The technical part of the study was supported by the GACR project P103/11/0933 and the Application Laboratories of Advanced Microtechnologies and Nanotechnologies (CZ.1.05/2.1.00/01.0017), co-funded by the Operational

Programme "Research and Development for Innovations", the European Regional Development Fund, and the state budget.

We confirm that we have read the Journal's position on the issues involved in ethical publication and affirm that this report is consistent with those guidelines.

None of the authors has any conflict of interest to disclose.

## References


Andrade-Valença L, Mari F, Jacobs J, Zijlmans M, Olivier A, Gotman J, et al. Interictal high frequency oscillations (HFOs) in patients with focal epilepsy and normal MRI. Clin Neurophysiol 2012;123:100–5.

Akiyama T, McCoy B, Go CY, Ochi A, Elliott IM, Akiyama M, et al. Focal resection of fast ripples on extraoperative intracranial EEG improves seizure outcome in pediatric epilepsy. Epilepsia 2011;52:1802–11.

Axmacher N, Cohen MX, Fell J, Haupt S, Dümpelmann M, Elger CE, et al. Intracranial EEG correlates of expectancy and memory formation in the human hippocampus and nucleus accumbens. Neuron 2010;65:541–9.

Ayala M, Cabrerizo M, Jayakar P, Adjouadi M. Subdural EEG classification into seizure and nonseizure files using neural networks in the gamma frequency band. J Clin Neurophysiol 2011;28:20–9.

Bagshaw AP, Jacobs J, LeVan P, Dubeau D, Gotman J. Effect of sleep stage on interictal high-frequency oscillations recorded from depth macroelectrodes in patients with focal epilepsy. Epilepsia 2009;50:617–28.

Bautista RE, Cobbs MA, Spencer SS. Prediction of surgical outcome by interictal epileptiform abnormalities during intracranial EEG monitoring in patients with extrahippocampal seizures. Epilepsia 1999;40:880–90.

Bénar CG, Chauviére L, Bartolomei F, Wendling F. Pitfalls of high-pass filtering for detecting epileptic oscillations: a technical note on "false" ripples. Clin Neurophysiol 2010;121:301–10.

Blanco JA, Stead M, Krieger A, Viventi J, Marsh WR, Lee KH, et al. Unsupervised classification of high-frequency oscillations in human neocortical epilepsy and control patients. J Neurophysiol 2010;104:2900–12.

Bragin A, Engel Jr J, Wilson CL, Fried I, Mathern GW. Hippocampal and enthorhinal cortex high-frequency oscillations (100–500 Hz) in human epileptic brain and in kainic acid-treated rats with chronic seizures. Epilepsia 1999;40:127–37.

Bragin A, Wilson CL, Engel J. Spatial stability over time of brain areas generating fast ripples in the epileptic rat. Epilepsia 2003;44:1233–7.

Brázdil M, Halámek J, Jurák P, Daniel P, Kuba R, Chrastina J, et al. Interictal high-frequency oscillations indicate seizure onset zone in patients with focal cortical dysplasia. Epilepsy Res 2010;90:28–32.

Cabrerizo M, Ayala M, Goryawala M, Jayakar P, Adjouadi M. A new parametric feature descriptor for the classification of epileptic and control EEG records in pediatric population. Int J Neur Syst 2012;22:1250001–16.

Crépon B, Navarro V, Hasboun D, Clemenceau S, Martinerie J, Baulac M, et al. Mapping interictal oscillations greater than 200 Hz recorded with intracranial macroelectrodes in human epilepsy. Brain 2010;133:33–45.

Curio G, Mackert BM, Burghoff M, Neumann J, Nolte G, Scherg M, et al. Somatotopic source arrangement of 600 Hz oscillatory magnetic fields at the human primary somatosensory hand cortex. Neurosci Lett 1997;234:131–4.

Engel Jr J, Wilson C, Bragin A. Advances in understanding the process of epileptogenesis based on patient material: what can the patient tell us? Epilepsia 2003;44:60–71.

Engel Jr J, Bragin A, Staba R, Mody I. High-frequency oscillations: what is normal and what is not? Epilepsia 2009;50:598–604.

Firpi H, Smart O, Worrell G, Marsh E, Dlugos D, Litt B. High-frequency oscillations detected in epileptic networks using swarmed neural-network features. Ann Biomed Eng 2007;35:1573–84.

Gardner AB, Worrell GA, Marsh E, Dlugos D, Litt B. Human and automated detection of high-frequency oscillations in clinical intracranial EEG recordings. Clin Neurophysiol 2007;118:1134–43.

Jacobs J, LeVan P, Chander R, Hall J, Dubeau F, Gotman J. Interictal high-frequency oscillations (80–500 Hz) are an indicator of seizure onset areas independent of spikes in the human epileptic brain. Epilepsia 2008;49:1893–907.

Jacobs J, Levan P, Châtillon CE, Olivier A, Dubeau F, Gotman J. High frequency oscillations in intracranial EEGs mark epileptogenicity rather than lesion type. Brain 2009;132:1022–37.

Jacobs J, Zijlmans M, Zelmann R, Chatillon CE, Hall J, Olivier A, et al. High-frequency electroencephalographic oscillations correlate with outcome of epilepsy surgery. Ann Neurol 2010;67:209–20.

Jirsch JD, Urrestarazu E, LeVan P, Olivier A, Dubeau F, Gotman J. High-frequency oscillations during human focal seizures. Brain 2006;129:1593–608.

Lee SA, Spencer DD, Spencer SS. Intracranial EEG seizure-onset patterns in neocortical epilepsy. Epilepsia 2000;41:297–307.

Modur PN, Zhang S, Vitaz TW. Ictal high-frequency oscillations in neocortical epilepsy: implications for seizure localization and surgical resection. Epilepsia 2011;52:1792–801.

Nelson R, Myers SM, Simonotto JD, Furman MD, Spano M, Norman WM, et al. Detection of high frequency oscillations with Teager energy in an animal model of limbic epilepsy. Conf Proc IEEE Eng Med Biol Soc 2006;1:2578–80.

Nikulin VV, Nolte G, Curio G. A novel method for reliable and fast extraction of neuronal EEG/MEG oscillations on the basis of spatio-spectral decomposition. Neuroimage 2011;55:1528–35.

Rosenow F, Lüders HO. Overview. In: Rosenow F, Lüders HO, editors. Handbook of clinical neurophysiology, Presurgical assessment of the epilepsies with clinical neurophysiology and functional imaging, vol. 3. Amsterdam: Elsevier; 2004. p. 3–7.

Staba RJ, Wilson CL, Bragin A, Fried I, Engel Jr J. Quantitative analysis of high-frequency oscillations (80–500 Hz) recorded in human epileptic hippocampus and entorhinal cortex. J Neurophysiol 2002;88:1743–52.

Staba RJ, Wilson CL, Bragin A, Jhung D, Fried I, Engel Jr J. High-frequency oscillations recorded in human medial temporal lobe during sleep. Ann Neurol 2004;56:108–15.

Tito M, Cabrerizo M, Ayala M, Jayakar P, Adjouadi M. Seizure detection: an assessment of time- and frequency-based features in a unified two-dimensional decisional space using nonlinear decision functions. J Clin Neurophysiol 2009;26:381–91.

Urrestarazu E, Chander R, Dubeau F, Gotman J. Interictal high-frequency oscillations (100–500 Hz) in the intracerebral EEG of epileptic patients. Brain 2007;130:2354–66.

Usui N, Terada K, Baba K, Matsuda K, Nakamura F, Usui K, et al. Very high frequency oscillations (over 1000 Hz) in human epilepsy. Clin Neurophysiol 2010;121:1825–31.

Worrell GA, Parish L, Cranstoun SD, Jonas R, Baltuch G, Litt B. High-frequency oscillations and seizure generation in neocortical epilepsy. Brain 2004;127:1496–550.

Worrell GA, Gardner AB, Stead SM, Hu S, Goerss S, Cascino GJ, et al. High-frequency oscillations in human temporal lobe: simultaneous microwire and clinical macroelectrode recordings. Brain 2008;131:928–37.

Wu JY, Sankar R, Lerner JT, Matsumoto JH, Vinters HV, Mathern GW. Removing interictal fast ripples on electrocorticography linked with seizure freedom in children. Neurology 2010;75:1686–94.

Zelmann R, Zijlmans M, Jacobs J, Chatillon C, Gotman J. Improving the identification of high frequency oscillations. Clin Neurophysiol 2009;120:1457–64.

Zijlmans M, Jacobs J, Kahn YU, Zelmann R, Dubeau F, Gotman J. Ictal and interictal high frequency oscillations in patients with focal epilepsy. Clin Neurophysiol 2011;122:664–71.

Zijlmans M, Jiruska P, Zelmann R, Leijten FS, Jefferys JG, Gotman J. High-frequency oscillations as a new biomarker in epilepsy. Ann neurol 2012;71:169–78.

# CHAPTER 3

# Mechanisms of high-frequency oscillations genesis

Functional connectivity within the brain is commonly characterized by activity synchrony of neuronal subpopulations. These functional couplings are transient (with a duration in the order of hundreds of milliseconds), dynamic (the strength of association between two cortical regions has a time-varying nature), and frequency-specific (neuronal groups oscillate in specific bands according to a precise phase relationship) (Le Van Quyen & Bragin, 2007; Worrell et al., 2012). In epilepsy, synchrony is believed to play an essential role in forming epileptic networks and generating seizures.

Traditionally, only the postsynaptic currents (Buzsáki et al., 2012) are said to be the primary source of electrical activity in the brain since their relatively long duration (i.e., the long time constant) in conjunction with pyramidal neuron arrangement allows temporal and spatial summation of these potentials. These potentials can be registered with the help of extracellular electrodes, including electrodes located far away from the source, within the brain, or on the surface of the brain or scalp.

It is believed that research into the mechanisms of high-frequency oscillation genesis will also make it possible to understand the mechanisms responsible for the development of epileptic seizures and epilepsy, as well as the new knowledge of the physiological functions of the brain. Neocortical networks that perform critical physiological functions are organized across spatial scales from sub-millimeter cortical columns to centimeter-scale lobar structures. The brain's ability to generate oscillations at 80 Hz and higher is a fascinating phenomenon, reflecting collective oscillations of large neuronal assemblies – local field potentials oscillations (LFP). Mechanisms generating the extracellular currents responsible for the LFP are varied but primarily reflect synaptic activity (Buzsáki et al., 2003). Unfortunately, it is challenging to directly associate LFP characteristics (e.g., frequency, amplitude, entropy, waveform morphology, etc.) with mechanisms, physiology, or pathology (Worrell et al., 2012). HFOs are likely generated by multiple, possibly not exclusive, mechanisms occurring at the cellular and network level, with interneurons playing a complex role (Jiruska et al., 2017), which will be more precisely discussed further.

Neural brain networks show numerous patterns of oscillatory activity. HFOs refer to distinct types of brain activity occurring in a frequency band ranging from 80 Hz to 600 Hz (Jefferys et al. 2012; Zijlmans et al., 2012). To gain deeper insight into the function of these network oscillations in neuronal signal processing, the underlying cellular mechanisms need to be uncovered (Hájos & Paulsen, 2009). The underlying mechanisms of HFOs have been the subject of much research, both those associated with normal brain processes (Buzsáki, 2015) as well as with epileptic processes (Jefferys et al., 2012).

One of the HFO formation theory suggests that high-frequency activity is primarily generated by interneurons (Buzsáki & Chrobak, 1995; Fries et al., 2007; Buzsáki & Wang, 2012). Some types of interneurons (mainly basket cells) are equipped with mechanisms that predispose to the genesis of high-frequency activity (Buzsáki & Chrobak, 1995). Results from published research on the physiology of cortical interneurons suggested that through their interconnectivity, interneurons can maintain large-scale oscillations at various frequencies (4-12 Hz, 40-100 Hz, and 200 Hz) (Buzsáki & Chrobak, 1995). From this, neuronal not only gamma-band synchronization appears to be a fundamental mode of neuronal activity (Fries et al., 2007). Membrane properties and the presence of specific ion channels allow interneurons to generate high-frequency action potentials over a relatively long duration (Buzsáki et al., 1983). The axons of interneurons create numerous synaptic endings on membranes of pyramidal neurons (Klausberger & Somogyi, 2008), and therefore a single interneuron can control the activity of a large number of pyramidal neurons. Finally, this property is enhanced by interneurons' ability to have wide axonal projections with several targets, including other interneurons (Jiruška, 2013). This can lead to the creation of an extensive network, where individual neurons communicate with each other through both chemical synapses and non-synaptically through gap-junctions (Traub et al., 2003; Jiruška, 2013). Such interneuronal activity induces through GABAergic connections a sequence of rapid post-synaptic inhibitory potentials (IPSPs) that synchronized and summated, are extracellularly recorded as physiological HFOs. An example may be physiological hippocampal ripples (and underlying sharp wave-ripple /SPWR/ complexes) which appear to reflect summated synchronous IPSPs generated by subsets of interneurons regulating the discharges of principal cells (Buzsáki et al., 1983; Bragin et al., 1995; Ylinen et al., 2005; Brázdil et al., 2015). In addition to the classical pyramidal excitability control, interneurons play a crucial role in the genesis of brain oscillations – rhythmogenesis (Jiruška, 2013). These oscillations are driven by interneuronal activity and can facilitate temporal coding, fast processing, and flexible routing of neuronal activity, which are necessary, e.g., for cognition (Fries et al., 2007; Jiruska et al., 2017).

According to the theory of 'cell assembly', transient synchrony of anatomically distributed groups of neurons underlies the processing of both external sensory input and internal cognitive mechanisms (Harris et al., 2003). Network oscillations are considered instrumental in synchronizing the activity of anatomically distributed neuron populations (Buzsáki & Chrobak, 1995). The basic idea is that interneuronal networks impose an oscillatory synaptic input onto the principle cells. Such oscillations impose a periodic fluctuation of principal cells' membrane potential close to, but below, threshold (Buzsáki & Chrobak, 1995). The rhythmic high-frequency inhibitory potentials generated on pyramidal cells' membranes create a time window during which only specific pyramidal neurons can be active, and cell assemblies are synchronized (Harris et al., 2003; Singer & Gray, 1995). Active neurons that are involved in a particular cognitive process (processing relevant information) can overcome inhibition and generate action potentials. At a specific timescale, the cooperative activity is optimal for information transmission and storage in cortical circuits (Harris et al., 2003). This temporal window corresponds with the pyramidal neuronal membrane time constant, the cortical oscillation cycle, and the time window for synaptic plasticity (Harris et al., 2003).

The timing of action potential development in relation to the oscillation cycle phase depends on the intensity of activation of the individual neuron (Buzsáki & Chrobak, 1995). Conversely, neurons not involved in the information processing have a reduced probability of action potentials occurring during the oscillation cycle (Jiruška, 2013). Thus, oscillation has the ability to reduce the level of neuronal noise that could interfere with the processing of the information (Fries et al., 2007). Activation of the neuron during a specific phase of the oscillation cycle enables the so-called phase coding of information. It represents a very effective mechanism to combine information from individual stimuli into adequate units and thus create a complex image of the stimulus, e.g., stimulus awareness, shape, color, movement etc. (Singer & Gray, 1995; Jiruška, 2013). In such combined interneuronal-principal cell systems, interneuronal networks provide precision timing of the action potentials of principal cells, and the information is contained in the temporal sequence of their spike occurrences (Buzsáki & Chrobak, 1995). If these rapid synchronized inhibitory postsynaptic potentials appear on the membranes of a large population of pyramidal cells synchronously, they can be registered in the extracellular record as high-frequency oscillations (Buzsáki et al., 1983; Bragin et al., 1995; Ylinen et al., 2005; Hájos & Paulsen, 2009). It is believed that the above-described ways of the genesis of oscillations apply to the formation of physiological HFOs (Jiruška, 2013).

The second theory of high-frequency oscillations suggests that a single cycle of oscillation is an extracellular manifestation of the synchronization of the action potentials of principal cells, summated field excitatory postsynaptic potentials (EPSPs) (Bragin et al., 2000; Foffani et al., 2007; Ibarz et al., 2010; Jefferys et al., 2012). It is now considered that pathological HFOs, whether they are ripples or fast ripples, reflect mainly these principal cell action potentials (Foffani et al., 2007; Draguhn et al., 1998; Ibarz et al., 2010; Bragin et al., 2011; Demont-Guignard et al., 2012). Several structural, molecular, and functional changes have been found within epileptic neuronal networks. These changes have the potential to increase neuronal and tissue excitability and generate pathological HFOs (Jiruska & Bragin, 2011).

The first condition for the formation of these HFO events that can be registered extracellularly is synchronization in milliseconds of fast-firing within the population of interconnected neurons that leads to the formation of an episode of high-frequency population spikes (Jiruska et al., 2017). Synaptic connections between neurons, particularly recurrent excitatory synaptic transmission, are one of these mechanisms (Dzhala & Staley, 2004). These structural changes are conditioned by, e.g., sprouting of axon collaterals and formation of autapses (Jiruska & Bragin, 2011). Pathological high-frequency oscillations were found to be generated spontaneously only in those neuronal networks in which the recurrent excitatory collateral system among principal cells is significant, including the neocortex, the CA3 region of the hippocampus, and the basolateral amygdala (Hájos & Paulsen, 2009). In brain areas lacking local recurrent connections among excitatory cells, such as the dentate gyrus and the CA1 region of the hippocampus, higher oscillations appear to depend on extrinsic rhythmic inputs (Csicsvari et al., 2000; Hájos & Paulsen, 2009). Other mechanisms that can ensure rapid synchronization are of

non-synaptic origin (Jefferys, 1995; Jefferys et al., 2012). These mechanisms include gap junction coupling (Draguhn et al., 1998; Traub et al., 2001), ephaptic interactions - a synchronizing mechanism that depends on the specific geometric organization and tight cellular arrangement (Anastassious et al., 2001; Jiruska et al., 2017) or the influence of local electric fields (Grenier et al., 2003, Jefferys, 1995). All these mechanisms have been proven experimentally, and some of them are applied only in pathological conditions (Jiruška, 2013). It is evident from these mechanisms that the oscillation frequency resulting from the synchronization of high-frequency voltages of action potentials of pyramidal neurons will correspond to the frequency of these and will depend primarily on membrane properties and neuronal excitability (Ibarz et al., 2010). The generation of oscillations appears related to the dysbalance between tonic excitation, increased by the activation of NMDA or/and AMPA receptors (Draguhn et al., 1998; Yaari & Beck, 2002; Traub et al., 2005) and tonic inhibition (GABAA receptor-mediated inhibition) of interneurons (Köhling et al., 2000; Khazipov et al., 2003), which is the basic principle of seizure generation. Nevertheless, one recent study indicates that oscillations require only AMPA receptors, but not NMDA receptors, the latter of which has previously been shown (Naggar et al., 2020).

The second condition is principal neurons' ability to generate high-frequency bursts of action potentials (Jiruška, 2013). For example, principal neurons in the CA3 region of the hippocampus may generate salvage action potentials at a frequency of 200-300 Hz during eating, drinking, slow-wave sleep, and awake immobility (Chrobak, 1996; Traub et al., 2001; Ibarz et al., 2010), and some neocortical pyramidal neurons have similar properties (Kucewicz et al., 2014). The ability to generate high-frequency oscillations is one of the fundamental properties of epileptic neurons (Yaari & Beck, 2002). These neurons have undergone molecular and structural changes that have led to alteration of expression of some ion channels (e.g., sodium, potassium, calcium) (Bernard et al., 2004; Yaari & Beck, 2002), or their subunits, resulting in increased excitability of epileptic neurons and the ability to generate bursts of action potentials spontaneously (Jiruška, 2013). A typical intracellular manifestation of epileptic neurons is extensive membrane depolarization known as paroxysmal depolarization shift (Johnston & Brown, 1981), during which bursts of high-frequency potentials are generated (Jiruška, 2013).

HFO frequency can be determined purely from cellular behavior, i.e., from the principal cells' potential firing rate. These are called 'pure' HFOs (Ibarz et al., 2010). Notably, the mentioned theories do not explain the origin of high-frequency oscillations with frequencies around 500 Hz and higher (Bragin et al., 2002; Ibarz et al., 2010; Jiruska et al., 2010b). These are frequencies from the fast ripple (250-600Hz) band and above (i.e., very high-frequency oscillations) that occur very specifically in chronic endogenous epileptogenic tissue (Bragin et al., 2002b; Jiruska et al., 2010b; Jiruska & Bragin, 2011; Staba et al., 2002, Brázdil et al., 2017). With a few exceptions (Timofeev et al., 2002), the vast majority of neurons are unable to generate synchronized action potentials at such a high frequency, as mechanisms of action potential generation with such a high firing rate do not generally allow it (Jiruška, 2013). When these oscillations occur, network mechanisms must be applied, where the high oscillation is the result of interaction between individual neuronal subpopulations (Jiruška, 2013). It is assumed that

the mechanism of high-frequency oscillation with frequencies beyond the physiological limits is the result of the summation of the activity of independent neuronal subpopulations of synchronized neurons that have a phase delay (Jefferys et al., 2012; Jiruska et al., 2013). The suggestion is that multiple populations of neurons in epileptic focus possess decreased spike-timing reliability, which results in out-of-phase firing (Jiruska & Bragin, 2011). Individual neuronal subpopulations generate low-frequency oscillations, but there is a phase delay between each subpopulation activity (Foffani et al., 2007; Ibarz et al., 2010; Jiruska et al., 2010a), and so detected HFOs are much higher in the extracellular space. These oscillations are called 'emergent' HFOs (Ibarz et al., 2010; Jiruska et al., 2010a).

The currently accepted explanations for the several network mechanisms that are responsible for the out-of-phase firing are reduced spike time-variability, uncorrelated firing, delayed activation, disconnected neural populations, or complex network connectivity patterns with a high level of clustering due to the presence of hub neurons (Jiruska et al., 2017). One of the candidate mechanisms is also a neuronal loss (Foffani et al., 2007; Staba et al., 2007). It is believed that the death of several neurons may disrupt non-synaptic synchronization, which requires a small distance and close organization between neurons. Loss of neurons can disrupt this type of synchronization and disintegration of the population into two or more functionally independent subpopulations (Jiruška, 2013). The basis for this hypothesis is the observation that the incidence of high-frequency oscillation positively correlates with the severity of hippocampal sclerosis and negatively correlates with the number of cells in the hippocampus (Staba et al., 2007), probably by decreasing the synchronizing effect of ephaptic interactions (Foffani et al., 2007). A recent study, however, has shown that cell loss is not the major necessary factor for FR generation, but it may further contribute to their genesis (Jiruska et al., 2010b). Other mechanisms that can reduce the level of phase synchronization within a single neuronal population and increase the frequency of oscillations are synaptic noise, the level of which is amplified in epileptic tissue (Foffani et al., 2007) or disturbed topology of synaptic connections due to epileptic axonal rearrangement (Foffani et al., 2007; Jefferys et al., 2012; Jiruska & Bragin, 2011; Jiruška, 2013).

Clearly, some of the mechanisms involved in the generation of high-frequency oscillations require specific structural and functional changes that can be observed in tissue that has undergone epileptogenic rearrangement (Jiruska & Bragin, 2011). It is progressively recognized that HFOs are generated by multiple mechanisms at both cellular and network-level (Jiruska et al., 2017). Since HFOs are closely associated with epileptogenic tissue and ictogenesis, understanding their cellular and network mechanisms could provide useful information about epileptogenic networks' organization and how seizures emerge from these networks' abnormal activity (Jiruska et al., 2017). HFO pathogenesis has historically been studied mainly in patients with temporal lobe epilepsy and animal models that mimic this disease.

Further explanations of the possible fast ripple genesis are provided by computational models. Even within the microscopic scale of epileptic fast ripples in the hippocampus, thousands of cells are

involved, well beyond the resolution offered by conventional microelectrode arrays. Therefore, computational models have been necessary to guide research into HFO mechanisms (Jiruska et al., 2017). Previous modeling work had identified some potential mechanisms of fast ripples genesis: gap junction networks, ephaptic interactions, fast synaptic transmission, disrupted inhibitory coupling with asynchronous groups of firing cells (Foffani et al., 2007; Ibarz et al., 2010, Jefferys et al., 2012); activated, but weakly synchronized pyramidal cells (increase in NMDA conductance) (Demont-Guignard et al., 2012). Some studies have proposed mechanisms for the transition of physiological to epileptic HFOs through the loss of inhibition (reduction of GABAergic connections from interneurons) (Fink et al., 2015), or increased synaptic activity, or increased coupling from gap junctions and recurrent synapses (Stacey et al., 2009). The computational models also showed that at HFOs with frequencies below 250 Hz, both epileptic and physiological processes can produce HFOs with identical peak frequencies (Fink et al., 2015). The neuronal network can synchronize and produce HFOs. Nevertheless, fast ripple oscillations are a generic feature of highly active, desynchronized neurons or networks (Fink et al., 2015). Finally, large groups of hyper-excitable, hyper-synchronized pyramidal cells produce spikes, but if the connectivity of cells is disrupted, then cells would fire out of phase and produce fast ripples (Jiruska et al., 2017). Therefore, cell activity is not necessarily synchronized, but heterogeneous firing is typical for pathological HFOs (Jiruska et al., 2017).

Next to cross-location interactions between individual oscillations, analyzes of HFOs revealed that brain oscillations also interact across different spectral scales, resulting in various cross-frequency coupling dynamics. E.g., the phase of low-frequency rhythms (4-8 Hz) during cognitive tasks modulates the amplitude of higher frequency oscillations (80-150 Hz); called phase-amplitude modulation (Canolty & Knight, 2010). Two forms of cross-frequency phase interactions have been described, an amplitude-independent phase-locking of *n* cycles of one LFP to *m* cycles of an independent LFP (Palva et al., 2005) and 'nested oscillations' (Canolty et al., 2010). Based on published data, it has been suggested that global brain processes operate in a slow 'rhythmic mode' and use these differential excitability states as a mechanism of amplifying relevant activities at a small scale and suppressing irrelevant ones (Schroeder & Lakatos, 2009).

It is well documented that both ripples and fast ripples can be either physiological or pathological. HFOs, especially fast ripples, are a generic phenomenon of neural networks that have some complex relationship with epileptic processes. Although HFO potential biomarker value is very strong, it is clear that merely focusing on the peak frequency of HFOs may not be sufficient to determine whether they are pathological (Jiruska et al., 2017). Moreover, the brain's electrophysiological activity is not consistent across time and is affected by different states of vigilance (Staba et al., 2002). Since most of the knowledge about the genesis of HFOs comes from animal models of temporal epilepsy, whether similar pathophysiological principles are involved in HFOs of neocortical origin needs to be clarified (Jiruska et al., 2017).

# CHAPTER 4

# Ripples

When we refer to ripples, we mean the slowest oscillations in the HFO band, specifically between 80-250 Hz. HFOs, especially ripples, were firstly observed in invasive EEG recordings in normal animal models at the end of the 20th century (Buzsáki et al., 1992). Beyond the gamma frequency range, hippocampal ripple frequency oscillations (~250 Hz) are believed to play an essential role in memory function (Buzsáki et al., 1992). The presence of interictal HFOs of nonepileptic nature spontaneously emerging without external sensory stimuli during slow-wave sleep has been described in several human ECoG studies using macro- and micro-electrodes (Axmacher et al., 2008; Nagasawa et al., 2012; Le Van Quyen et al., 2016).

Physiological ripples are observed primarily in hippocampal-entorhinal networks of rodents, monkeys, and humans during quiet wakefulness, and slow-wave sleep (Buzsáki et al., 1992; Skaggs et al., 2007; Le Van Quyen et al., 2016), and have been linked to replay and consolidation of previously acquired information. Paraphrasing it, pyramidal cells display transient network oscillations in the ripple range (200 Hz) during behavioral immobility and slow-wave sleep (Buzsáki et al., 1992). Afterwards, Axmacher et al. (2008) reliably found that memory consolidation and generation of ripples occurred not only during sleep but also during waking states. They occur predominantly during negative half-waves of slow neocortical oscillations (Axmacher et al., 2008). These types of ripples appear to reflect summated synchronous inhibitory postsynaptic potentials (IPSPs) occurring during high-frequency bursts of inhibitory neurons regulating the discharges of principal cells. Simultaneously, multisite recordings revealed temporal and spatial coherence of neuronal activity during population oscillations, reflecting the state of network synchronization (Buzsáki et al., 1992).

More specifically, ripples commonly co-occur with large amplitude sharp waves ("sharp wave ripples" - SWR), which were first registered in the CA1 region of the hippocampus and parahippocampal areas and have similar properties to gamma oscillations (Buzsáki et al., 1992), one of the best understood locally-generated network patterns (Hájos & Paulsen, 2009). These sharp-wave ripples are fast oscillations with a frequency in the range of 140-220 Hz, superimposed on the sharp waves that are generated in the CA3 region of the hippocampus (synchronized firing of CA3 cells) and spread along the CA1-subicular-entorhinal axis (Chrobak & Buzsáki, 1996). Results from cross-correlation analysis confirmed that hippocampal events are closely locked to rhinal events and are consistent with findings on the transmission of ripples from the hippocampus into the rhinal cortex (Axmacher et al., 2008). These physiological oscillations result from phasic inhibitory input on the soma of pyramidal cells (Chrobak & Buzsáki, 1996) together with rhythmic excitatory potentials (Maier et al., 2010) and phase-

locked firing (Csicsvari et al., 2000). Perisomatic inhibitory cells provide prominent rhythmic inhibition to CA3 pyramidal cells and are themselves synchronized primarily by excitatory synaptic inputs derived from the local collaterals of CA3 pyramidal cells (Hájos & Paulsen, 2009). The recruitment of this recurrent excitatory-inhibitory feedback loop during hippocampal HFOs suggests that local oscillations control when and *how many* and *which* pyramidal cells will fire during each HFO cycle (Hájos & Paulsen, 2009). Inhibitory interneurons would then secure an orderly recruitment of pyramidal cells (Klausberger & Somogyi, 2008) together, perhaps with contributions to synchrony from gap junctions (Traub et al., 2003) and the ephaptic entrainment of neurons by large sharp-wave fields (Anastassiou et al., 2010).

Axmacher et al. (2008) were the first who recorded ripples in humans during a cognitive task and suggested that ripples are indeed related to behavioral performance. Co-activation of hippocampal and neocortical pathways during sharp-wave ripples may be crucial for memory consolidation and replay of previously acquired information (Buzsáki et al., 1992; Axmacher et al., 2008). In this context, the hippocampus serves as a model substrate for addressing fundamental questions about the population co-operativity of neuronal ensembles (Buzsáki & Chrobak, 1995).

Ripples has been studied in detail, and it has been shown to have been implicated in the process of declarative memory formation and reactivation of memory tracks (O'Neill et al., 2010). In two subsequent steps, the development of declarative memories was suggested to occur. While initial encoding, which occurs while receiving intense sensory input, involves the formation of transient representations via fast synaptic plasticity in the hippocampus (accompanied by prominent theta and gamma oscillations). The consolidation (accompanied by HFOs) refers to the transfer of information into the neocortex, where more stable networks are built (Buzsáki et al., 1992; Fries et al., 2007). Furthermore, this is also accompanied by findings that hippocampal ripples are significantly locked to the phase of hippocampal delta band activity (Axmacher et al., 2008). This might provide a mechanism for itself reported phase-locking to slow neocortical oscillations, which correspond to alternating states of enhanced and reduced cortical excitability (up- and down-states) due to membrane potential fluctuations (Axmacher et al., 2008). Subsequent work supported the concept that HFOs are associated with phasic increases of neural activity, namely during slow-wave oscillations, which is linked to hippocampal-neocortical information transfer during consolidation. It was suggested that such patterned activity in the sleeping brain (slow-wave sleep) could play a role in the offline processing of cortical networks and memory consolidation (Le Van Quyen et al., 2016). In detail, this offline processing mode is linked to hippocampal neurons fire in large asynchronous population bursts called sharp waves superimposed by high frequency 'ripple' oscillations (SWR events; Buzsáki et al., 1992; Hájos & Paulsen, 2009). Besides, Axmacher and colleagues (2008) observed consistently and frequently ripples also during the waking state. However, we must point out it was a resting state, not awake exploratory behavior.

There is a growing consensus that episodic and spatial memories both include the encoding of complex associations in hippocampal neuronal circuits through SWR events, which could coordinate

the reactivation of memory traces and direct their reinstatement in cortical circuits (O'Neill et al., 2010). The studies suggest that such SWR-driven reactivation of brain-wide memory traces could underlie memory consolidation (O'Neill et al., 2010). Loss of ability to generate these oscillations or disruption of their mechanisms results in a variety of cognitive deficits, such as perceptual grouping, attention-dependent stimulus selection, routing of signals across distributed cortical networks, sensory-motor integration, working memory, and perceptual awareness (Uhlhaas & Singer, 2006). Alterations of cerebral oscillations have been shown in several neurological and psychiatric diseases, such as cognitive and amnestic disorders in epilepsy, schizophrenia, autism, Alzheimer's and Parkinson's disease, and others. (Uhlhaas & Singer, 2006).

It has long been recognized that representations of information in the brain are embedded in the spatio-temporal co-operation of cell assemblies (Buzsáki & Chrobak, 1995). Mainly in association with sensory processing, it has been hypothesized that binding and segmentation in perception are dynamically encoded in the temporal relationship between a large number of co-activated neurons across structures (Gray, 1994). Such co-operation may be achieved by rhythmic or intermittent oscillations (Buzsáki & Chrobak, 1995). Concerning physiological oscillations, the emergence and function of inhibitory (i.e., GABAergic) networks are mentioned that produce network oscillations (Buzsáki & Chrobak, 1995).

However, the presumption of the exclusively physiological nature of ripples was impugned by evidence of HFOs in ripple ranges recorded in the dentate gyrus after epileptogenic insult in an animal model of kainate-induced status epilepticus (Bragin et al., 1999a; Bragin et al., 2004). Then, ripple activity similar to that previously described in the normal and epileptic rat was found in the hippocampus and entorhinal cortex of patients with epilepsy (Bragin et al., 1999b). Until now, multiple studies have now shown that HFO in the range of physiological gamma and ripple oscillations are also increased in the human epileptogenic hippocampus (Worrell et al., 2008; Crépon et al., 2010; Jacobs et al., 2010, Pail et al., 2017), and neocortex (Worrell et al., 2004; Jacobs et al., 2010; Blanco et al., 2011; Pail et al., 2017). These studies showing an increase in activity previously defined as physiological, i.e., ripple frequency oscillations, highlight the difficulty of attaching pathological specificity to high-frequency oscillation subclasses based on oscillation frequency within the epileptic brain (Engel et al., 2009; Blanco et al., 2011). Interestingly, some studies have observed an even higher incidence of R rates in the pathological hippocampus (Pail et al., 2017). Noteworthy, when using macro electrodes in neocortical extratemporal epilepsies, the SOZ might be better determined (higher specificity) by the ripple range than by fast ripples (Pail et al., 2013). However, these results might be influenced by the acquisition system used. Human intracranial recordings showed that immediately before or at the onset of anepileptic seizure, there is often an increase in the amplitude of the 40-120 Hz range (Fisher et al., 1992).

If we look at the best-studied area of the brain in terms of HFOs, based on several observations, LFP ripples of the human hippocampus may be detected in both non-epileptogenic and epileptogenic areas associated with both interictal and preictal events (Staba et al., 2002; Alvarado-

Rojas et al., 2015; Le Van Quyen et al., 2016). The occurrence of ripples is similar between epileptogenic and non-epileptogenic temporal lobe, increases during non-REM sleep and during REM sleep and wakefulness, ripple rates are lowest (Staba et al., 2004; Bagshaw et al., 2009). Specifically, in subiculum, ripples associated with (both interictal and preictal) discharges a proportion of events (up to 50 %) are confined to the 150-250 Hz band (Alvarado-Rojas et al., 2015), spectrally similar to ripples seen in vivo in non-epileptogenic regions of humans (Staba et al., 2002). Using combined intra- or juxta-cellular and extracellular recordings, it was revealed that these interictal and preictal ripple-like oscillations are associated with distinct cellular and synaptic processes (Alvarado-Rojas et al., 2015). Interictal ripples were associated with rhythmic γ-aminobutyric acidergic (confirmed by predominant IPSPs) and glutamatergic synaptic potentials with moderate neuronal firing. Such interictal ripples are reminiscent of physiological ripples, even if they reflect multiple processes, including IPSPs, EPSPs, and depolarizing GABA signaling (Alvarado-Rojas et al., 2015). In contrast, preictal ripples were associated with depolarizing synaptic inputs (linked to glutamatergic signals), frequently reaching the threshold for bursting in most pyramidal cells (Alvarado-Rojas et al., 2015). Thus, ripple-like oscillations in the human temporal lobe subicular circuits appear to be generated by different cellular and synaptic mechanisms, different forms of synchronizing mechanisms reflecting distinct dynamic changes in inhibition and excitation during interictal and preictal states. Thus, the ripple band could not help disambiguate the underlying cellular processes (Alvarado-Rojas et al., 2015).

# CHAPTER 5

# Fast ripples

Power spectral analysis showed distinct spectral frequency differences between ripples (R) and fast ripples (FR), although the peak spectral frequency associated with either of these oscillations could vary as much as 25% (Staba et al., 2004). Previous studies suggest that R and FR have separate sources because voltage depth profiles often show phase reversals for FR but not for R, even when they occur in association (Bragin et al., 2002b; Staba et al., 2004).

At first, in animal studies using the chronic kainate model of temporal lobe epilepsy, FR were observed only in epileptic rodents in areas adjacent to the site of spontaneous seizure onset and not in the non-pathological area (Bragin et al., 1999a,b). Therefore, these oscillations have been considered a highly specific indicator of epileptogenesis and, at the same time, which has a high predictive value of the future development of epilepsy, including its severity (Bragin et al., 1999a,b; Bragin et al., 2004). Even the sooner FR occur, the sooner the first epileptic seizure occurs, and the subsequent seizure frequency is higher (Bragin et al., 2004). The initial studies of recordings from the human hippocampus supported the hypothesis that HFOs above 250 Hz, named FR oscillations (Bragin et al., 1999a,b; Staba et al., 2004; Jirsch et al., 2006), were a unique pathological oscillation associated with the epileptic brain (epileptogenic zone or the seizure onset zone). A new biomarker for epileptogenic tissue has emerged, which promises to improve the understanding of epilepsy's pathophysiology of epilepsy and develop new clinical diagnostic methods (Zijlmans et al., 2012). The presence of FR reflects an epileptogenic reorganization of brain tissue, endogenous epileptogenicity, and the ability to generate spontaneous seizures (Jiruska & Bragin, 2011). Although FR (250-600 Hz) were first thought to be reliable markers of epileptic tissue, there is also increasing evidence of the possibility of the physiological origin of these oscillations (Kucewicz et al., 2014; Frauscher et al., 2018). Despite this, FR have proven particularly important and useful in epilepsy.

The pathophysiology of epileptic HFOs is complex and challenging, possibly requiring spontaneous asynchronously firing of independent neuronal populations. They differ from physiological HFOs in not being paced by rhythmic inhibitory activity and their possible origin from population spikes (Zijlmans et al., 2012). The cellular correlates of pathological FR were shown to be synchronous population firing of large groups of pyramidal cells and decreased inhibitory interneuron firing (Bragin et al. 2007, 2011; Matsumoto et al., 2013), while physiological FR likely reflecting multiunit cortical neuronal responses (Telenczuk et al., 2011). The analysis suggested that neuronal networks associated with FR generation are spatially smaller compared to networks underlying ripple generation (Bragin et al., 2002b). FR oscillations (250-600 Hz) are often localized to sub-millimeter volumes (<1 $mm^3$) in human

hippocampus (Bragin et al., 1999a,b, 2002a,b; Worrell et al., 2008; Staba et al., 2002). Recent observations of microdomain electrographic seizures (Stead et al., 2010) and periodic complexes (Schevon et al., 2009) supported the hypothesis that the pathological organization of epileptic brain extends to sub-millimeter scales (Worrell et al., 2012). Within a given brain area, there are several neuronal clusters that generate FR (Bragin et al., 2000a,b) and which have a high density of connections between principal cells (Jiruska & Bragin, 2011). R generation is thought to rely on the activation of both excitatory and inhibitory neurons (Ylinen et al., 1995). In contrast, the prevailing hypothesis on FR generation suggests that FR reflect synchronized population spikes within an interconnected network composed primarily of pyramidal cells (Bragin et al., 2000). The spatial extent of interictal oscillations is controlled by local inhibitory (GABA-A) mechanisms. Each individual cycle of a pathological HFO appears to represent the co-firing of small groups of principal cells, which are pathologically interconnected (Bragin et al., 2007; Foffani et al., 2007). Besides, the presented animal epileptic model suggests increased network excitability that produces high-frequency epileptiform activity due to alterations in cellular composition and synaptic connectivity associated with atrophic areas (Lehmann et al., 2000). Based on these data, a loss of inhibitory interneurons may impede HFO generation by removing an essential neuronal component that contributes to its generation. Consequently, the absence of interneuronal postsynaptic targets may promote synaptic reorganization among remaining excitatory cells forming an interconnected network presumed to support FR generation (Staba et al., 2004). For more detail, see chapter 3.

According to some studies, FR could also play a causal role in epileptogenesis (Bragin et al., 2004; Staba et al., 2002). As mentioned above, pathological FR represent the highly synchronous activity of neuronal populations. Propagation of action potentials to projection regions and their synchronous nature can significantly affect postsynaptic neurons' properties. It is hypothesized that continuous repeated synaptic input to postsynaptic neurons by synchronous excitation impulses may have a similar effect as kindling (in animal models) and potentiate epileptogenic neuronal conversion in given regions, thus becoming an active part of the epileptogenic network over time (Bragin et al. 2000; Jiruska & Bragin, 2011; Jiruška, 2013). One example may be secondary epileptogenesis in the contralateral hippocampus in the case of mesial temporal lobe epilepsy (Jiruska et al., 2010b).

FR have been observed predominantly in the epileptic region between seizures, at seizure onset, and during seizures (Zijlmans et al., 2012). HFOs in a wide frequency band (150-600 Hz) can be associated with both interictal and peri-ictal discharges (Staba et al., 2004; Alvarado-Rojas et al., 2015) or can occur independently of sharp waves (Staba et al., 2004). Despite this frequent co-occurrence, there is now sufficient evidence that FR and spikes represent different neurophysiological mechanisms (Frauscher et al., 2017). A separate but related question is whether only those FR that occur alone versus those occurring in association with epileptiform spikes are relevant (Worrell et al., 2012). Interestingly, it has been shown that the HFOs co-occurring with spikes are even more closely related to the SOZ than the HFOs without a spike (Wang et al., 2013). FR were also found using standard macro

electrodes during the ictal period (Jirsch et al., 2006). Also, ictal FR occur predominantly in the region of primary epileptogenesis (SOZ), and less are found in areas of secondary seizure spread (Jirsch et al., 2006). Based on the results of previously published papers, it seems that the SOZ can be determined with high specificity through the evaluation of 10 min of FR activity (Jacobs et al., 2008; Zelmann et al., 2008; Andrade-Valença et al., 2011). Remarkably, this biomarker can be found in brief invasive electroencephalography recordings and possibly even in extracranial magnetoencephalography (MEG) or EEG (Zijlmans et al., 2012). Besides, increased FR are reported to correlate with disease severity and activity (Zijlmans et al., 2009) and seizure frequency (Jacobs et al., 2009; Zijlmans et al., 2009) and possibly predict outcome after epilepsy surgery (Jacobs et al., 2010).

Sleep/wake state and anatomical location are factors that may strongly influence FR spectral frequency. Localization of FR concerning medial temporal lobe sites shows that the highest rates of FR are found within the subicular cortex as the subiculum is capable of supporting rhythmic interictal activity (Cohen et al., 2002; Staba et al., 2004). It is postulated that most subicular neurons can fire bursts of action potentials that may, if there is a coincident burst firing among a small neuronal group, initiate synchronous population discharge reflected as an FR oscillation (Staba et al., 2002). FR rates in areas ipsilateral to seizure onset are significantly higher than rates from areas contralateral to seizure onset (Staba et al., 2004). The generation of FR showed the highest rates of occurrence during NREM slow-wave sleep, similar to R (Staba et al., 2004; Jirsch et al., 2006; Urrestarazu et al., 2007; Worrell et al., 2008; Bagshaw et al., 2009). During REM sleep, FR rates remained elevated and were equivalent to rates observed during waking (Staba et al., 2004). The predominance of FR within the epileptogenic zone not only during NREM sleep but also during epileptiform-suppressing desynchronized episodes of waking and REM sleep supports the view that FR are the product of pathological neuronal hyper-synchronization associated with seizure-generating areas (Staba et al., 2004). Bagshaw et al. showed that HFOs have their maximal rate in the same sleep stages as the spikes, and HFO duration is relatively stable across the sleep-wake cycle (Bagshaw et al., 2009).

Next to temporal lobe epilepsy, FR have also been reported occurring in other epileptic disorders and models (Wu et al., 2010; Jacobs et al., 2012; Zijlmans et al., 2012; Jiruska et al., 2017; Pail et al., 2017). Thus, in epilepsy, transient fast oscillations in local field potentials called pathological high-frequency oscillations (pHFOs) have received intense interest as potential electrophysiological biomarkers to improve focal epileptic brain mapping, which led to the incorporation of measurements of pHFO properties into presurgical examinations (Frauscher et al., 2017; Jiruska et al., 2017). Whether pHFOs recorded in the epileptic brain are generated by unique pathological mechanisms or represent aberrations of normal physiological oscillations is not clear (Le Van Quyen et al., 2006). Traditionally, however, the pathogenesis of pHFOs was explored mainly in patients with temporal lobe epilepsy and in animal models mimicking this condition.

Whether pHFOs in the FR frequency range (>250-600 Hz) are uniquely pathological oscillations in humans remains an open question. Nevertheless, there is strong evidence that pHFOs are spatially

associated with the epileptic brain, and therefore, pHFOs have emerged as promising biomarkers of epileptogenic tissue, see reviews (Worrell & Gotman, 2011; Jacobs et al., 2012; Zijlmans et al., 2012). At the same time, however, it must be said that this is an indicator that is, to some extent, unreliable because the incidence of HFO changes significantly over time (Gliske et al., 2018).

While FR were considered a unique biomarker of epileptogenicity over time, there is increasing evidence that they may also have physiological genesis (Curio et al., 1994; Nagasawa et al., 2012; Matsumoto et al., 2013; Kucewicz et al., 2014; Pail et al., 2020). While physiological HFOs appear to reflect summated synchronous inhibitory postsynaptic potentials generated by subsets of interneurons regulating the discharges of principal cells (Buzsáki et al., 1992; Engel et al., 2009), epileptic HFOs represent field potentials of population spikes from clusters of abnormal synchronously bursting pyramidal cells, and decreased inhibitory interneuron firing (Engel et al., 2009; Bragin et al., 2011). So far, in some brain regions, the localizing value of pHFO is weakened by frequency overlap with physiological HFOs (Jiruska & Bragin, 2011).

# CHAPTER 6

# High-frequency oscillations and medically intractable epilepsy

The first broad application of pHFOs was in the context of epilepsy surgery. This is now accompanied by other applications such as assessing epilepsy severity or monitoring antiepileptic treatment response using non-invasive methods (Frauscher et al., 2017).

For patients with drug-resistant focal epilepsy, epilepsy surgery constitutes the approved and most promising treatment option in order to achieve seizure freedom (Thomschewski et al., 2019). The effectiveness of surgical procedures depends mainly on the location of the brain area responsible for seizure generation, defined as an epileptogenic zone. Accurate localization of epileptogenic tissue is critical for achieving optimal outcomes and minimizing the risk of side effects. However, identifying this brain region is challenging, as all available non-invasive diagnostic tools cannot directly delineate the epileptogenic zone. Consequently, the epileptogenic area is only a theoretical concept, and only based on the postoperative time, the achievement of seizure freedom will show the correctness of its localization. The results from multiple non-invasive modalities are considered in order to indirectly infer the location of the epileptogenic zone (EZ; Rosenow & Lüders, 2001). Its location is indirectly defined by the location of other zones: lesion, irritative zone (interictal discharges), functional deficit zone. When using invasive EEG, the current gold standard for identifying the epileptogenic zone is using the determination of seizure-onset zone (SOZ) by recording spontaneous seizures (Staba et al., 2002), but this approach is suboptimal. The fact that surgical outcomes are unfavorable in 40-50 % of well-selected patients (Najm et al., 2013) suggests that the SOZ is not an optimal approximation of the EZ and that new seizure-independent biomarkers resulting in better post-surgical outcomes are needed (Thomschewski et al., 2019).

Although the results regarding HFOs are limited to a unique epileptic population, many studies point to a prognostic value of HFOs (especially FR) in predicting the EZ (Jacobs et al., 2012; Zijlmans et al., 2012; Haegelen et al., 2013; van Klink et al., 2016; Frauscher et al., 2017). A recent clinical study showed an association between recurrent seizures following cortical resection and incomplete resection of sites showing interictal spontaneous pHFOs observed during slow-wave sleep (Jacobs et al., 2010; Nagasawa et al., 2012). Notably, residual HFOs in the postoperative electrocorticogram were shown to better predict epilepsy surgery outcomes than preoperative HFO rates (Frauscher et al., 2017).

Therefore, in the clinical setting, interictal pHFOs have been used as a biomarker for the location of seizure generating zones (Worrell et al., 2004), with a potential to improve surgical success in patients with drug-resistant epilepsy even without the need to record seizures (Thomschewski et al., 2019).

pHFOs are utilized by neurosurgeons to select which tissue to resect in surgical treatments of refractory epilepsy (Haegelen et al., 2013; Frauscher et al., 2017). Many epilepsy surgery centers are now equipped with facilities and analytical approaches that allow the recording of wide-band signals and provide relevant information about the spatiotemporal properties of pHFOs over long time scales to be extracted (Jiruska et al., 2017). This additional information may lead to a better delineation of the epileptogenic zone and thus improve the outcomes of epilepsy surgery (Frauscher et al., 2017).

In general, HFOs were shown to be more closely linked and more specific for the SOZ than interictal spikes (Jacobs et al., 2008), as spikes are often seen outside the SOZ as well. As it was shown by Jacobs et al. (2012), when applying a threshold with 95% specificity, fast ripples had the highest sensitivity (52 %) for identification of the SOZ, followed by ripples (38 %) and spikes alone (33 %). HFOs are unlikely to result from spikes as 64 % of HFOs; therefore, they started on average 10 ms before the spike's onset (van Klink et al., 2016). The most of HFOs (approximately 60 %) are visible as riding on the spike in the unfiltered signal, less (20 %) ale invisible in the unfiltered spikes, or 20 % occurred entirely independently of spikes in timing and localization (Urrestarazu et al., 2007). Despite the frequent co-occurrence of spikes and HFOs, there is now sufficient evidence that they represent different neurophysiological mechanisms (Frauscher et al., 2017). FR occur more focally than ripples and spikes, given that they probably arise from local pathological connections of out-of-phase firing neuronal clusters rather than from the larger-scale networks. FR are, therefore, considered more specific for epileptogenic tissue than ripples and spikes (Jacobs et al., 2010; Jefferys et al., 2012). HFOs seem to increase before the occurrence of seizures, immediately prior to or at seizure onset (Jirsch et al., 2006; Zijlmans et al., 2009), whereas spikes are more prominent postictally (Frauscher et al., 2017). In contrast to spikes, HFOs increase after medication reduction (Zijlmans et al., 2009). In a recent study of Jiruska et al. (2017), even specific HFO patterns associated with different seizure-onset patterns were revealed; ripples (>80 Hz) predominate during low-voltage fast activity seizures, whereas fast ripples (>250 Hz) predominate during periodic spiking seizures (Frauscher et al.,2017).

Similarly, in vitro models showed a progressive increase in total population neuronal activity before a seizure, which was manifested in extracellular records by an increase in HFA. This HFA increase corresponds to a progressive increase in synchronization between neural networks and spatial expansion of neuronal population activity. Interestingly, at the cellular level, there are complex but heterogeneous changes in the dynamics of individual neurons; their activity may increase, remain unchanged and in some cases even decrease (Jiruska et al., 2010a).

However, we should differentiate between the SOZ and the epileptogenic zone, the area of the brain necessary and sufficient for spontaneous seizures to occur (Rosenow & Lüders, 2001). Therefore, our efforts should be directed not to identifying the SOZ but to identifying the epileptogenic region. HFOs could be one such marker to improve the approximation of the epileptogenic zone with the ultimate aim of improving surgical outcome in people with epilepsy (Frauscher et al., 2017). It seems that incomplete removal of tissue with HFOs, especially FRs, is strongly linked to a poor surgical

outcome, whereas this relationship is not found for spikes (Jacobs et al., 2010; Wu et al., 2010). Importantly, it has been suggested, that pre-surgically assessed HFO rates might not be vital in predicting seizure outcome. A recent meta-analysis confirmed a higher resection ratio for HFOs in seizure-free versus non–seizure-free patients (Frauscher et al., 2017). Even better results can be achieved by using intraoperative electrocorticography (ECoG), which can measure epileptiform activity and HFOs directly from the cortex during epilepsy surgery, aiming to delineate the epileptogenic tissue. Residual FRs after resection, in post-ECoG, predict recurrent seizures, whereas spikes and ripples do not (van 't Klooster et al., 2017). Moreover, according to the recent study using postoperative ECoG, it is critical to disconnect networks generating HFOs (especially FR) rather than remove all areas that generate HFOs prior to surgery (van 't Klooster et al., 2017).

HFOs were revealed as a useful biomarker for epileptogenic areas in both hippocampal sclerosis and focal cortical dysplasia (Kerber et al., 2013), the most common causes of focal epilepsies in adults. It is believed that no specific HFO pattern could be identified for these different lesion types (Jacobs et al., 2009). Nevertheless, a recent Ferrari-Marinho´s study (2015) showed that the HFO rates might vary considerably with different pathologies and might hence reflect different types of neuronal derangements. Specifically, both mentioned mesial temporal lobe sclerosis and focal cortical dysplasia, plus nodular heterotopia, displayed higher HFO rates compared to tuberous sclerosis complex, polymicrogyria, or cortical atrophy (Ferrari-Marinho et al., 2015). HFO rates are higher in the hippocampal than in the neocortical lesions (Schönberger et al., 2020). In addition, higher rates of FRs are uniquely associated with atrophic sites ipsilateral to seizure onset, suggesting that primary seizure generating areas are specifically characterized by the presence of FR activity during interictal periods (Staba et al., 2004). Kerber et al. (2013) also emphasized the potential usefulness of HFOs as an additional method to better define and delineate the extent of the epileptogenic dysplastic tissue in FCD.

Regarding focal cortical dysplasia (FCD), the rates of HFOs are higher in patients with FCD type II compared to type I; usually, type II lesions are more epileptogenic with an earlier onset of seizures as well as a higher seizure frequency (Kerber et al., 2013). Therefore, rates of high-frequency oscillations mirror the disease activity of a lesion. Moreover, some studies have shown that the HFO rate correlates with disease severity; see the review of Frauscher et al. (2017).

FR may also be useful in the localization of epileptogenic area in nonlesional epilepsies, as has been shown, for example, in a model of mesial temporal lobe epilepsy (Jiruska et al., 2010b). This is an essential feature as it could improve preoperative diagnostics in terms of better delineation of the area of resection in these patients.

In individual studies, when investigating electrophysiological brain recordings, it is necessary to distinguish HF power (e.g., increased during spikes) and HFOs terms. Nevertheless, it was further shown that it might not be necessary for clinical application to separate real HFOs from “false oscillations” produced by the filter effect of sharp spikes (Burnos et al., 2016; Frauscher et al., 2017).

It is essential to highlight that the majority of previous studies evaluated results drawn from HFO analysis at a group level. Noteworthy, when considering individual patients, the rates of HFOs are often highly variable and less specific for epileptic brain localization (Blanco et al., 2011; Cimbalnik et al., 2016; Jacobs et al., 2018; Roehri et al., 2018). To this date, most investigations simply report increased HFOs when summed across all SOZ electrodes compared to all non-SOZ electrodes, which is not sufficient for guiding epilepsy surgery (Worrell & Gotman, 2011; Cimbalnik et al., 2016). Jacobs et al. (2018) reported on results from three tertiary epilepsy referral centers using individual analysis that HFO assessment (the surgical outcome was correlated and predicted by the ratio of interictal HFOs removal) was only associated with good surgical outcome in two-thirds of included patients. These results and their discrepancies further highlight the need for prospective trials (Thomschewski et al., 2019).

In conclusion, for patients with drug-resistant focal epilepsy, epilepsy surgery is the therapy of choice in order to achieve seizure freedom. Identifying the area responsible for seizure generation (EZ) is crucial for the successful ability of epilepsy surgery. Research of recent years revealed HFOs, especially FR, as a useful biomarker for epileptogenic areas in patients with intractable epilepsy, and removal of regions with highest FR rates (it seems that not necessarily all of them) is associated with an excellent postsurgical outcome (Frauscher et al., 2017). Even better results can be achieved by using intraoperative HFOs monitoring. Fast ripple analysis could provide helpful information for generating a hypothesis on seizure-generating networks, especially in cases with few or no recorded seizures (Schönberger et al., 2020).

Nevertheless, significant challenges still remain for the full clinical translation of HFOs (especially fast ripples) as epileptogenic brain biomarkers. There are still a few issues that need to be addressed. First of all, we have to deal with differentiating true HFO from the high-frequency power changes associated with increased neuronal firing and bandpass filtering sharp transients and distinguishing pathological HFOs from normal physiological HFOs (Cimbalnik et al., 2016). To guide surgical resection, biomarkers must be able to classify tissue under each individual electrode as pathological or normal. Moreover, the optimal biomarker would identify tissue at risk for generating seizures in the future (risk of epileptogenesis process) (Cimbalnik et al., 2016). However, as it turns out, HFOs do not always accomplish this condition. Prospective assessments of the use of HFOs for surgery planning using automatic HFO detection are needed in order to determine their clinical value, reproducibility, and reliability (Cimbalnik et al., 2016; Thomschewski et al., 2019).

**Published research**

# Hippocampal high-frequency oscillations in unilateral and bilateral mesial temporal lobe epilepsy

Pavel Řehulka

Jan Cimbálník

Martin Pail

Jan Chrastina

Markéta Hermanová

Milan Brázdil

**Clin Neurophysiol. 2019 Jul;130(7):1151-1159. doi: 10.1016/j.clinph.2019.03.026**

## Commentary on published paper

Research of recent years suggested that high-frequency oscillations (HFOs) are a promising biomarker of the epileptogenic zone, with the potential to improve surgical success in patients with drug-resistant epilepsy without the need to record seizures (Thomschewski et al., 2019). Interictal high-frequency oscillations (HFOs), ripples (80–250 Hz), and fast ripples (FR; 250-600 Hz) have been studied over the past two decades and have been detected in different brain areas under physiological and pathological conditions. In mesial temporal areas, ripples are associated mainly with the physiological functions, whereas the increase of FR have been repeatedly demonstrated in the seizure onset zone and is thought to be a biomarker of epileptogenicity (Jacobs et al., 2008, Staba et al., 2002, Worrell et al., 2008). Higher FR to ripple ratio was demonstrated in mesial temporal area ipsilateral to seizure onset than those contralateral (Staba et al., 2002; Staba et al., 2007). As shown in our previous study, FR might be used as a biomarker for SOZ not only in focal temporal but also extratemporal epilepsies (Pail et al., 2017), and HFOs may mark the cortex that needs to be removed to achieve seizure control (Zijlmans et al., 2012).

Nevertheless, focal epilepsy may not have only one epileptogenic area but may also be multifocal. One such example may be patients with associated/dual pathology or bitemporal epilepsy. The presurgical workup in dual pathology/ bitemporal epilepsy aims to evaluate the necessary scope of the surgical intervention. If we detect seizures in these patients, especially if only a few seizures are captured, from only one lesion or one side of temporal lobe epilepsy during invasive EEG monitoring, multifocal epilepsy may be misdiagnosed. The remaining uncertainty is considerable, and patients rarely become seizure-free after epilepsy surgery.

Patients with dual pathology have two potentially epileptogenic lesions: most often one in the hippocampus and one in the neocortex. It is often unclear which lesion is seizure-generating in these patients or if both lesions have such potential. Schönberger et al. (2020) reported a significant correlation between the patients' primary focus and the ratio $R_{\text{fast ripples}}$, i.e., the proportion of interictal fast ripples detected in this lesion. No such correlation was observed for interictal epileptic spikes (IES), ripples, and IES-ripples. In retrospect, using this approach, interictal fast ripples would have correctly "predicted" the primary focus in 69 % of their patients (Schönberger et al., 2020).

A similar problem as with dual pathology may be in patients with bitemporal epilepsy. Temporal lobe epilepsy is the most frequent cause of drug-resistant seizures. Bitemporal epilepsy is characterized by independent seizure origins (requires invasive EEG recordings) in both temporal lobes and should be considered as a dynamic, nonstationary condition (Hirsch et al., 1991). Consequently, some bitemporal epilepsy may be misdiagnosed, as it is not always possible to record seizures from both sides of the brain during SEEG monitoring. It remains unclear whether bitemporal epilepsy represents a specific type of a single extensive epileptogenic network or two independent networks.

The main aim of our retrospective study was to investigate the potential differences in terms of interictal high-frequency oscillations (HFOs) between both hippocampi in unilateral (U-MTLE) and bilateral mesial temporal lobe epilepsy (B-MTLE). This study was conducted as a group comparison of the interictal HFOs occurrence in hippocampi ipsilateral and contralateral to the side of the seizure onset zone in mesial temporal lobe epilepsy. Sixteen patients with MTLE underwent SEEG monitoring as a part of the epilepsy surgery evaluation. We used an automatic tool for HFO detection. The analyses entail comparisons of the rates and spatial distributions of ripples and fast ripples (FR) in hippocampi and amygdalae, with respect to the eventual finding of hippocampal sclerosis (HS).

In U-MTLE, higher ripple and fast ripple rates were found in the hippocampi ipsilateral to the seizure onset than in the contralateral hippocampi. Our results indicate that it is possible that neuronal loss in sclerotic hippocampi might cause additional increases in HFO rates and also in the ripple range, as it has been suggested in previous studies (Jacobs et al., 2009, Crépon et al., 2010; Worrell et al., 2008); however, other studies have not confirmed these findings (Staba et al., 2004). Perhaps another indicator is more important, namely FR / R ratio. Staba et al. (2004) showed that the ratio of FR / ripple occurrence in atrophic areas (including the hippocampus, entorhinal, and subicular cortex) ipsilateral to seizure onset was significantly higher than that of ipsilateral to seizure onset without atrophy, as well as contralateral sites. Non-epileptic hippocampi in U-MTLE were distinguished by a significantly lower ripple rate than in the remaining analyzed hippocampi. Nevertheless, it is doubtful whether the low interictal HFO rate might be used as a negative biomarker of the non-epileptic hippocampi, as some studies observed ripple occurrence similar between epileptogenic and non-epileptogenic temporal lobe (Staba et al., 2004; Bagshaw et al., 2009). There were no differences between the hippocampi in B-MTLE. The increased FR rate in mesial temporal structures was previously found to be associated with the characteristic features of HS, such as hippocampal neuronal loss (Staba et al., 2007) and reduced hippocampal volume (Jacobs et al., 2009; Staba et al., 2007). In the hippocampi with proven HS, higher FR rates were observed in the ventral than in the dorsal parts. Our finding of higher FR rates in the head than in the posterior parts of sclerotic hippocampi might be explained by the similar gradient of atrophy and neuronal loss within the sclerosis along the longitudinal hippocampal axis, which has been observed in both MRI and histopathological studies (Bernasconi et al., 2003; Thom et al., 2012).

To conclude our study, non-epileptic hippocampi in U-MTLE demonstrated significantly lower ripple rates than those epileptic hippocampi in U-MTLE and B-MTLE. Low interictal HFO occurrence might be considered as a marker of the non-epileptic hippocampi in MTLE. Based on HFO rates, it is possible to distinguish between unilateral and bilateral mesial temporal lobe epilepsy. This approach may improve the detection and diagnosis of bitemporal epilepsy without the need to detect the onset of seizures from both temporal lobes during SEEG monitoring.

Clinical Neurophysiology 130 (2019) 1151–1159

Contents lists available at ScienceDirect

Clinical Neurophysiology

journal homepage: www.elsevier.com/locate/clinph

# Hippocampal high frequency oscillations in unilateral and bilateral mesial temporal lobe epilepsy

Pavel Řehulka [a,*], Jan Cimbálník [b], Martin Pail [a], Jan Chrastina [c], Markéta Hermanová [d], Milan Brázdil [a,e]

[a] Brno Epilepsy Center, Department of Neurology, St. Anne's University Hospital and Faculty of Medicine, Masaryk University, Brno, Czech Republic
[b] International Clinical Research Center, St. Anne's University Hospital, Brno, Czech Republic
[c] Brno Epilepsy Center, Department of Neurosurgery, St. Anne's University Hospital and Faculty of Medicine, Masaryk University, Brno, Czech Republic
[d] Brno Epilepsy Center, First Department of Pathology, St. Anne's University Hospital and Faculty of Medicine, Masaryk University, Brno, Czech Republic
[e] Behavioral and Social Neuroscience Research Group, CEITEC – Central European Institute of Technology, Masaryk University, Brno, Czech Republic

ARTICLE INFO

*Article history:*
Accepted 13 March 2019
Available online 10 April 2019

*Keywords:*
High frequency oscillations
Hippocampus
Hippocampal sclerosis
Temporal lobe epilepsy
Bitemporal epilepsy

HIGHLIGHTS

- Hippocampal recordings in patients with mesial temporal lobe epilepsy were analyzed.
- Non-epileptic hippocampi demonstrated lower ripple rates than those epileptic.
- The highest fast ripple rate was seen in ventral parts of sclerotic hippocampi.

ABSTRACT

*Objective:* The main aim of this study was to investigate the potential differences in terms of interictal high frequency oscillations (HFOs) between both hippocampi in unilateral (U-MTLE) and bilateral mesial temporal lobe epilepsy (B-MTLE).
*Methods:* Sixteen patients with MTLE underwent bilateral hippocampal depth electrode implantation as part of epilepsy surgery evaluation. Interictal HFOs were detected automatically. The analyses entail comparisons of the rates and spatial distributions of ripples and fast ripples (FR) in hippocampi and amygdalae, with respect to the eventual finding of hippocampal sclerosis (HS).
*Results:* In U-MTLE, higher ripple and FR rates were found in the hippocampi ipsilateral to the seizure onset than in the contralateral hippocampi. Non-epileptic hippocampi in U-MTLE were distinguished by significantly lower ripple rate than in the remaining analyzed hippocampi. There were not differences between the hippocampi in B-MTLE. In the hippocampi with proven HS, higher FR rates were observed in the ventral than in the dorsal parts.
*Conclusions:* Non-epileptic hippocampi in U-MTLE demonstrated significantly lower ripple rates than those epileptic in U-MTLE and B-MTLE.
*Significance:* Low interictal HFO occurrence might be considered as a marker of the non-epileptic hippocampi in MTLE.


## 1. Introduction

Interictal high frequency oscillations (HFOs), ripples (80–250 Hz), and fast ripples (FRs; 250–600 Hz) have been studied over the past two decades and have been detected in different brain areas under physiological and pathological conditions. As the visual review of HFOs has several disadvantages (Gardner et al., 2007; Zelmann et al., 2009), interest has been dedicated to resolving problematic issues related to automated HFO detection (Birot et al., 2013; Navarrete et al., 2016; Waldman et al., 2018; Zelmann et al., 2012). Increase of FRs have been repeatedly demonstrated in the seizure onset zone and is thought to be a biomarker of epileptogenicity. In mesial temporal areas, ripples are associated mainly with the physiological functions of mesial temporal structures (Jacobs et al., 2008; Staba et al., 2002; Worrell et al., 2008). In the recordings from microelectrodes higher FR to ripple ratio were demonstrated in mesial temporal area ipsilateral to seizure onset than those contralateral (Staba et al., 2002, 2007). Moreover, the characteristic features of hippocampal sclerosis (hippocampal

* Corresponding author at: Department of Neurology, St. Anne's University Hospital and Faculty of Medicine, Pekařská 53, 656 91 Brno, Czech Republic. Fax: +420 543 182 624.
*E-mail address:* pavel.rehulka@fnusa.cz (P. Řehulka).

https://doi.org/10.1016/j.clinph.2019.03.026
1388-2457/

neuronal loss, reduced hippocampal volume) were found to be associated with greater FRs occurrence (Jacobs et al., 2009; Ogren et al., 2009; Staba et al., 2007).

Bitemporal epilepsy is characterized by independent seizure origins in both temporal lobes (Hirsch et al., 1991). The identification of bitemporal epilepsy requires invasive EEG recordings from both temporal lobes and should be considered as a dynamic, nonstationary condition due to possibility of the seizure clustering effect (Spencer et al., 2011) and long term seizure laterality switch (Smart et al., 2013). Consequently, it remains unclear whether bitemporal epilepsy represents a specific type of a single extensive epileptogenic network or two independent networks.

Several HFO studies have involved patients with bilateral mesial temporal seizure onset (Jacobs et al., 2008, 2009, 2010; Staba et al., 2002; Worrell et al., 2008), particularly when the investigated patients did not have a visible MRI lesion (Andrade-Valença et al., 2012). The involvement of patients with bitemporal epilepsy in such studies presumes the parity of both seizure onset zones and their equivalence with a seizure onset zone in unilateral temporal lobe epilepsy. This premise might carry a potential risk of selection bias. On the other hand, HFO analysis could reveal new insight into the pathophysiology of bitemporal epilepsy and provide useful information for the clinicians.

This retrospective study was conducted as a group comparison of the interictal HFOs occurrence in hippocampi ipsilateral and contralateral to the side of the seizure onset zone in mesial temporal lobe epilepsy. We hypothesize that in unilateral mesial temporal lobe epilepsy (U-MTLE) interictal HFO occurence is higher in epileptic than in non-epileptic hippocampi. In bilateral mesial temporal lobe epilepsy (B-MTLE) we aimed at both epileptic hippocampi (on the side with the higher and lower number of registered seizures) in order to establish potential differences between them. As the neuronal loss vary along the longitudinal axis of sclerotic hippocampi (Thom et al., 2012), the analyses were performed with respect to the underlying hippocampal pathology and recording site localization.

## 2. Methods

### 2.1. Patient selection

We reviewed all patients with intractable epilepsy who had undergone invasive EEG at a sampling rate of 5000 Hz at the Brno Epilepsy Center at St. Anne's University Hospital in Brno between January 2011 and March 2017. The study included the patients who fulfilled the following criteria: (1) seizure semiology compatible with mesial temporal lobe epilepsy (MTLE); (2) available recordings from depth electrodes implanted in both hippocampi; and (3) fitting in one of the two following groups:

1. Patients with U-MTLE who fulfilled criteria a and b:
   (a) All spontaneous seizures originated in the mesial structures of one temporal lobe;
   (b) At least one of the following three characteristics:
      (i) $\geq$ 5 recorded clinical seizures (implying acceptable confidence of only unilateral seizure onset zone (Blum, 1994)),
      (ii) 3 clinical and $\geq$3 subclinical (asymptomatic) seizures recorded (subclinical seizures are usually generated from the same temporal lobe as clinical seizures and predict favorable post-surgical outcomes (Sperling and O'Connor, 1990)),
      (iii) Engel IA classification for at least two years of follow-up care after anteromedial temporal resection.
2. Patients with B-MTLE – defined as those having recorded at least one independent spontaneous clinical seizure onset arising from both mesial temporal structures.

All patients underwent high-resolution MRI scans at 1.5 Tesla (Siemens Magnetom Symphony scanner) or 3 Tesla (GE Discovery 750 scanner). All patients signed an informed consent form. The study was approved by St Anne's University Hospital Research Ethics Committee and the Ethics Committee of Masaryk University.

### 2.2. Group and subgroup matching

In each patient with U-MTLE, the hippocampus on the side of all registered seizures was labelled as 'ipsilateral' (UNIP) and the other side as 'contralateral' (UNCO). Similarly, in each patient with B-MTLE, the hippocampus on the side with the higher number of registered seizures was labelled as 'ipsilateral' (BIP) and the other as 'contralateral' (BICO); in cases of parity of recorded seizures, the side of subsequent surgical intervention was labelled as 'ipsilateral'. In order to estimate the potential influence of underlying pathology on interictal HFOs occurrence, the following two groups of hippocampi with adjacent amygdalae were formed.

$HS^+$ group – hippocampus with evidence of hippocampal sclerosis (HS) based on MRI (clear hippocampal atrophy and an unequivocally increased signal from the hippocampus) and/or histopathological finding of HS as defined by the ILAE classification system (Blümcke et al., 2013).

$HS^-$ group – hippocampus with histopathological finding of 'no-HS/gliosis only' as defined by ILAE classification (Blümcke et al., 2013).

### 2.3. Recording methods

All patients underwent video-EEG monitoring with multicontact depth electrodes inserted orthogonally into different parts of the brain including both hippocampi. In all patients were used 5-, 10-, or 15-contact platinum semiflexible Microdeep intracerebral electrodes (Alcis, France) with an electrode diameter of 0.8 mm, a contact length of 2 mm, with 3.5 mm center-to-center spacing (1.5 mm between contacts) and a surface area of 5 $mm^2$ for each contact. The anatomical targeting of intracerebral electrodes was individualized in each patient according to available non-invasive data and hypotheses about the seizure onset zone location. Interictal EEG recordings were low-pass filtered at 1000 Hz at a sampling rate of 5000 Hz (a reference average montage was used). A recording session in a noiseless Faraday room was performed prior to initiating the reduction of antiepileptic drugs (usually during the second post-implant day between 8 a.m. and 12 noon), in a wakeful resting state. The session duration differed among patients depending on individual collaboration capacity and patient comfort. Thirty minutes of interictal EEG activity were selected, having no or minimal artifacts, recorded at least 2 hours after and before a seizure.

### 2.4. Recording sites

Only contacts verified as located in the hippocampus (Hip) or amygdala (Amy) were used for HFO analysis. Hippocampal contacts were further subdivided into those placed in the head of the hippocampus (aHip) and those in the body or tail of the hippocampus (pHip). The localization of all implanted electrodes and contacts was determined visually by two independent experienced researchers (P.R. and M.P.). Post-implant 1.5-Tesla MRI study (T2-weighted Turbo Inversion Recovery Magnitude sequence in axial, coronal, and sagittal planes) with depth electrodes in situ

was used. The location of each electrode and contact was ultimately determined using the MRI atlas by Tamraz and Comair (2000). The anatomical boundaries of the hippocampus were based on a reference atlas (Duvernoy et al., 2013).

### 2.5. Histopathological examination

Histopathological examinations were performed only for those patients who had undergone resective surgery. "All the paraffin-embedded tissue specimens, slides, and histopathology reports were retrieved from the files of the First Department of Pathology of St. Anne's University Hospital. All examined resected tissues were identically treated, fixed in a 10% neutral buffered formalin, grossly inspected, carefully oriented, measured, and cut so as to obtain representative 2–3 mm thick tissue slices perpendicular to the cortical surface. Smaller resection specimens were completely processed and paraffin embedded; in larger resection specimens, at least every second tissue slice was further processed. Five micrometer thick tissue sections were stained by hematoxylin and eosin (H&E), and evaluated under light microscope. NeuN immunohistochemistry (using mouse monoclonal anti-NeuN antibody, dilution 1:100, clone A-60, Millipore) was performed on preselected tissue sections if there was an inconclusive picture in H&E" (Kuba et al., 2013). The classification system for HS proposed by the ILAE (Blümcke et al., 2013) was applied.

### 2.6. Automated detection of HFOs

HFOs were detected by a custom-made Python detection algorithm (Kucewicz et al. 2014). The signal in the statistical window (10 s) was filtered in a series of 400 logarithmically spaced frequency bands ranging from 30–800 Hz. Power envelopes and their corresponding z-scores were computed for each band. Putative detections were obtained as events >3.5 of the z-score. Putative detections in adjacent frequency bands and overlaps in the temporal domain were joined and considered a single event. Event onsets and offset were determined as the first and last values above the threshold in all the frequency bands of the putative detections. The highest z-score values of the putative detections were used to obtain event frequencies. The detections were separated into ripples (80–250 Hz) and FRs (250–600 Hz). Events with frequencies below 80 Hz and above 600 Hz were disregarded as well as events shorter than 4 oscillations at the peak frequency. This led to the successful elimination of filter artifacts produced by sharp transients since the highest z-score values of such events are in low frequencies and their estimated frequency is below 80 Hz. The procedure is illustrated in Supplementary Fig. 1. Ripple and FR incidence was expressed as the rate of respective events per 10 minutes (No./10 min).

Detector validation was done in a similar fashion as in a study by Roehri et al. (2016). Simulated HFOs, HFOs on spike, and spikes were inserted into a signal recorded from non-pathological white matter. The parameters of each inserted HFO event were pseudo-randomized with varying frequency (80–600 Hz), duration (6–10 oscillations at the given frequency), and amplitude (0.05–0.25 of signal std). The HFOs were constructed as tapering sine waves. Similarly, the parameters of inserted spikes were varied for duration (0.05–0.2 s) and amplitude (2.5–12.5 of signal std). Events were inserted in 3 s time windows and algorithm precision-recall was calculated. The resulting performance was 0.94 precision and 0.72 recall.

### 2.7. Statistical analysis

Custom Python scripts were created for statistical analyses using the SciPy module. The data were tested for normal distribution using D'Agostino's normality test. Since most of the data sets failed this test, the Wilcoxon rank sum test was used to evaluate differences among them. Bonferroni's correction was applied where necessary.

To evaluate whether normal hippocampal tissue (UNCO) can be distinguished from pathological hippocampal tissue (UNIP, BIP, BICO), receiver operating characteristic (ROC) curves and their area under the curve (AUC) were calculated on per channel basis using HFO rates as the varying threshold. This analysis was performed on a per hippocampus basis and separately for aHip and pHip. The statistical significance of AUCs compared to chance (AUC = 0.5) was tested with Hanley-McNeil test.

## 3. Results

### 3.1. Description of study population and recording sites data set

Of the 62 consecutive patients recorded at a sampling rate of 5000 Hz, 16 patients met the inclusion criteria for the study: 9 patients with U-MTLE and 7 patients with B-MTLE. Individual characteristics of all patients are summarized in Table 1 and a comparison of clinical variables between both groups is provided in Table 2. Notably, in patients 7 and 14 temporopolar seizures that arose concurrently from the temporal pole and the hippocampus were observed. Interictal recordings were available from the both hippocampal sides in patients with U-MTLE (9 UNIP and 9 UNCO) or with B-MTLE (7 BIP and 7 BICO). The $HS^{+}$ group comprised 6 UNIP and 1 BIP, the $HS^{-}$ group had two pairs of UNIP and BIP. The localization of recording sites and contacts among these groups is indicated in Table 3.

### 3.2. Hippocampal HFOs in U-MTLE

First, to establish the potential difference between hippocampi ipsilateral and contralateral to seizure onset zone in U-MTLE, we compared homotopic recording sites in UNIP and UNCO. Higher rates were observed in UNIP than in UNCO, in both aHip (ripples: $126.17 \pm 102.93$ and $31.83 \pm 27.32$ [$p < 0.001$], FRs: $160.17 \pm 162.68$ and $32.13 \pm 24.67$ [$p = 0.003$], respectively) and pHip (ripples: $134.15 \pm 101.37$ and $18.25 \pm 21.60$ [$p \ll 0.001$], FRs: $71.30 \pm 69.44$ and $17.13 \pm 17.17$ [$p = 0.003$], respectively) recording sites. The results are illustrated in Fig. 1. In order to test whether difference between UNIP and UNCO might be attributed to the difference between epileptic and non-epileptic hippocampal tissue we proceeded with ROC analysis between the hippocampi contralateral (UNCO) and ipsilateral (UNIP, BIP, BICO) to seizure onset. Hanley-McNeil test reached statistical significance in the ripple range both in aHip (AUC = 0.734, $p = 0.014$) and pHip (AUC = 0.788, $p = 0.002$), indicating that a low hippocampal ripple rate might be sufficient to identify hippocampus without obvious involvement in seizure onset (Fig. 2). A similar but non-significant trend was found in the FR range within aHip (AUC = 0.668, $p = 0.057$).

### 3.3. Hippocampal HFOs in B-MTLE

Similarly were compared homotopic recording sites in B-MTLE. BIP and BICO did not differ significantly, in either aHip (ripples: $90.62 \pm 47.82$ and $80.41 \pm 78.29$, FRs: $54.29 \pm 34.52$ and $70.22 \pm 71.68$, respectively) or pHip (ripples: $60.61 \pm 38.79$ and $37.86 \pm 42.89$, FRs: $26.78 \pm 32.18$ and $22.04 \pm 24.32$, respectively) recording sites (Fig. 1).

**Table 1**
Individual characteristics of patients in the U-MTLE and B-MTLE groups.

| No./ Group | Sex/ Age | Duration (years)/PF | MRI finding/ scanner | PET hypo-metabolism | Explored brain lobes (No. of electrodes) | Side, No. and SOZ of seizures # | AMTR* | Histopathology** | VNS*** | Previous intervention/** |
|---|---|---|---|---|---|---|---|---|---|---|
| 1/U | F/56 | 28/- | R/HA/1.5T | R/mT | T (2), T′(3) | R: 5 mT [R] | R/IIIA (5) | NA | NP | NP |
| 2/U | F/33 | 31/ME | L/HS, PECLT/3T | L/mT | T(2), T′(6), F′(3) | L: 3 mT | L/IA (3) | HS type 1 | NP | NP |
| 3/U | F/27 | 18/ME | L/HS/3T | L/Tp | T′(8), T(2), P′(1), I′(1), F′(1) | L: 3 mT [L] | L/IIIA (3) | HS type 1, FCD IIIa | NP | NP |
| 4/U | M/51 | 49/FS | R/HA /3T | R/mT | T(5), F(3), T′(2) | R: 3 mT [R] | R/IA (3) | HS type 2 | NP | NP |
| 5/U | M/24 | 14/TBI | L/HS, MPTG/3T | L/mT, P | T(2), T′(7) | L: 3 mT [L] | L/IIA(2) | pHS | NP | NP |
| 6/U | F/45 | 19/- | L/HA/3T | normal | T(2), T′(8), I′(1), P′(1), F′(2) | L: 3 mT [L] | L/IIIA (2) | no-HS | NP | NP |
| 7/U | F/36 | 27/- | R,L/HIMAL/3T | normal | T(7), T′(3) | R: 2 Tp, 1 mT | R/IA (2) | no-HS | NP | NP |
| 8/U | F/26 | 20/- | R/HS/3T | R/mT | T(4), T′(2), F (4), I(1), P (1) | R: 6 mT | R/IA (1) | HS type 1 | NP | NP |
| 9/U | F/56 | 55/ME | R/HS/3T | R/mT | T(5), F(2),T′(4) | R: 7 mT | R/IVA (1) | HS type 2 | NP | VNS |
| 10/B | F/20 | 4/- | normal/1.5T | L/Tp | T (3), T′(2) § | R: 10 mT; L: 1 mT | NP | NA | IIIB (5) | LTPR†/normal |
| 11/B | F/34 | 30/- | R/HA/1.5T | R/mT | T′(3), T(3) | R: 3 mT; L: 1 mT [R > L] | R/IA (5) | pHS | NP | NP |
| 12/B | F/33 | 17/PI | normal/1.5T | R,L/mT | T′(4), T(4) | R: 4 mT; L: 1 mT | R/IIIA (5) | no-HS | NP | VNS |
| 13/B | M/38 | 11/- | normal/3T | L/Tp | T(3), I′(2), T′(6), P′(1), O′(1), F′(1) | R: 4 mT; L: 1 mT | NP | NA | IIB (4) | NP |
| 14/B | M/35 | 14/- | R,L/HA/3T | R > L mT | T(6), T′(2) | R: 4 Tp; L: 1 mT [L] | NP | NA | IIIB (2) | NP |
| 15/B | M/37 | 6/FS | normal/3T | L/mT, Tp | T′(8), F′(2), T(2) | L: 2 mT; R: 2 mT | L/IA (3) | no-HS | NP | NP |
| 16/B | F/58 | 46/- | L/HS/1.5T | NA | T (1), T′(2), F′(3) | R: 2 mT; L: 5 mT [L] | NP | pHS | NP | LAMTR††/pHS |

U – unilateral MTLE, B – bilateral MTLE; F – female; M – male; PF – precipitating factor; ME – meningoencephalitis; FS – febrile seizures; TBI – traumatic brain injury; PI – perinatal insult; MRI – magnetic resonance imaging; PET – positron emission tomography with $^{18}$F – fluorodeoxyglucose; R – right; L – left; HS – hippocampal sclerosis; HA – hippocampal atrophy; PECLT – postencephalic changes of left temporal lobe; MPTG – mild posttraumatic gliosis of left pericentral region; HIMAL – hippocampal malrotation; mT – mesial temporal region; Tp – temporal pole; NA – not available; T – right temporal; T′ – left temporal; F – right frontal; F′ – left frontal; P – right parietal; P′ – left parietal; I – right insular; I′ – left insular; O′ – left occipital; § – recordings from one oblique electrode inserted into the body and tail of the left hippocampus were not analysed; SOZ – seizure onset zone; # – only clinical spontaneous seizures are indicated, the lateralization of electrophysiological seizures is mentioned in square brackets, if applicable; AMTR – anteromedial temporal lobe resection; * – side of AMTR/outcome using Engel classification (follow-up in years); NP – not performed; ** – histopathological finding using ILAE 2013 classification for hippocampal sclerosis, ILAE 2011 classification for focal cortical dysplasia; FCD – focal cortical dysplasia; pHS – probable hippocampal sclerosis as defined by ILAE 2013 classification for hippocampal sclerosis; VNS – vagus nerve stimulation; *** – outcome using McHugh classification (follow-up in years); LTPR – left temporal pole resection, † – based on non-invasive findings and data acquired during previous invasive EEG using unilateral covering only; L – left AMTR; †† – only the anterior portion of the hippocampus with a length of 15 mm was removed.

**Table 2**
Comparison of clinical characteristics between U-MTLE and B-MTLE group (median is calculated; range is given in square brackets).

| | U-MTLE | B-MTLE | p-value |
|---|---|---|---|
| Number of patients | 9 | 7 | |
| Females | 7 | 4 | NS* |
| Age at evaluation (years) | 36 [26–56] | 35 [20–58] | NS** |
| Epilepsy duration (years) | 27 [18–55] | 14 [4–46] | p = 0.04** |
| Seizure frequency (per month) | 4 [1–20] | 6 [1–15] | NS** |

NS – non significant; * – Fisher's exact test; ** – Mann-Whitney test.

### 3.4. Differences along the longitudinal hippocampal axis in U-MTLE and B-MTLE

In order to elaborate the issue of the potential influence of recording site location, we compared HFO rates between ventral (aHip) and dorsal (pHip) hippocampal recording sites in U-MTLE and B-MTLE. Higher FR rates were found in aHip than in pHip in UNIP (160.17 ± 162.68 and 71.30 ± 69.44, respectively; $p = 0.038$) and BIP (54.29 ± 34.52 and 26.78 ± 32.18, respectively; $p = 0.027$); statistically significant differences were nearly reached in BICO (70.22 ± 71.68 and 22.04 ± 24.32, respectively; $p = 0.051$) and UNCO (32.13 ± 24.67 and 17.13 ± 17.17, respectively; $p = 0.057$). Conversely, in the ripple range no statistically significant differences were observed between aHip and pHip in any studied group (UNIP: 126.17 ± 102.93 and 134.15 ± 101.37; BIP: 90.62 ± 47.82 and 60.61 ± 38.79; UNCO: 31.83 ± 27.32 and 18.25 ± 21.60; BICO: 80.41 ± 78.29 and 37.86 ± 42.89, respectively).

### 3.5. Hippocampal HFOs in HS$^+$ and HS$^-$ subgroups

To estimate the potential influence of underlying hippocampal pathology, we compared homotopic recording sites in the HS$^+$ and HS$^-$ subgroups (Fig. 3). In aHip, higher ripple (141.72 ± 95.93, 70.46 ± 44.26; $p = 0.017$) and FR rates (173.59 ± 163.15, 54.54 ± 38.3; $p = 0.015$) were observed in the former subgroup than in the latter; in pHip, the higher rate was statistically significant only in the ripple range (151.45 ± 101.54, 49.43 ± 34.21; $p = 0.001$). In amygdalar recording sites, higher ripple rates were found in the HS$^+$ group (85.0 ± 52.13) than the HS$^-$ group (34.10 ± 20.78; $p = 0.006$); a similar trend in the FR band was statistically non-significant (61.18 ± 60.69 and 22.60 ± 15.57; $p = 0.06$).

### 3.6. Differences along the longitudinal hippocampal axis in HS$^+$ and HS$^-$ subgroups

Finally, potential differences in terms of HFO rates along the longitudinal axis of the amygdalo-hippocampal complex were examined. In the HS$^+$ subgroup, a higher ripple rate was found in pHip (151.45 ± 101.54) than in Amy (85.0 ± 52.13; $p = 0.03$); the difference between aHip and Amy nearly reached statistical significance (141.72 ± 95.93 and 85.0 ± 52.13, respectively; $p = 0.057$). In the FR band, the rate in aHip (173.59 ± 163.15) prevailed over those in both Amy (61.18 ± 60.69; $p = 0.013$) and pHip (71.25 ± 75.50; $p = 0.043$) (Fig. 4). In the HS$^-$ group, there were no significant differences among Amy, aHip, and pHip recording sites in the ripple range or in the FR range.

## 4. Discussion

### 4.1. Hippocampal HFOs and unilateral MTLE

Majority of the fundamental HFO literature is based upon the comparison of the seizure onset zone versus non-seizure zone HFO occurence, regardless the anatomical boundaries of the

**Table 3**
The location of analyzed contacts in different recording sites (the number of recording contacts in brackets) among the respective groups (UNIP, UNCO, BIP, BICO – as defined in Section 2.2).

| Patient no. | UNIP | UNCO | BIP | BICO |
|---|---|---|---|---|
| 1 | R: Amy (2), aHip (4) | L: Amy (3), aHip (3), pHip (4) | NA | NA |
| 2 | L*: Amy (3), aHip (3), pHip (3) | R: aHip (4), pHip (3) | NA | NA |
| 3 | L*: Amy (4), aHip (3), pHip (4) | R: aHip (3), pHip (3) | NA | NA |
| 4 | R*: Amy (2), aHip (3), pHip (2) | L: aHip (3), pHip (4) | NA | NA |
| 5 | L*: Amy (3), aHip (3), pHip (2) | R: aHip (2), pHip (2) | NA | NA |
| 6 | L**: Amy (3), aHip (3), pHip (3) | R: aHip (3), pHip (3) | NA | NA |
| 7 | R**: Amy (3), aHip (3), pHip (3) | L: Amy (3), aHip (2), pHip (3) | NA | NA |
| 8 | R*: Amy (3), aHip (3), pHip (3) | L: aHip (2), pHip (2) | NA | NA |
| 9 | R*: Amy (4), aHip (3), pHip (3) | L: Amy (4), aHip (2), pHip (1) | NA | NA |
| 10 | NA | NA | R: Amy (4), aHip (3), pHip (3) | L: aHip (4) |
| 11 | NA | NA | R*: Amy (3), aHip (4), pHip (3) | L: Amy (3), aHip (4), pHip (3) |
| 12 | NA | NA | R**: Amy (4), aHip (3), pHip (4) | L: Amy (2), aHip (4), pHip (3) |
| 13 | NA | NA | R: Amy (3), aHip (3), pHip (3) | L: Amy (4), aHip (7), pHip (2) |
| 14 | NA | NA | R: Amy (3), aHip (4), pHip (3) | L: aHip (2), pHip (3) |
| 15 | NA | NA | L**: aHip (4), pHip (4) | R: Amy (3), aHip (3) |
| 16 | NA | NA | L: pHip (3) | R: aHip (2) |
| **Amy contacts** | 27 | 10 | 17 | 12 |
| **aHip contacts** | 28 | 24 | 21 | 26 |
| **pHip contacts** | 23 | 25 | 23 | 11 |

R – right; L – left; Amy – amygdala; aHip – anterior hippocampus; pHip – posterior hippocampus; NA – not applicable; * – $HS^{+}$ subgroup as defined in Section 2.2; ** – $HS^{-}$ group subgroup as defined in Section 2.2. The sum of contacts for the respective groups in different recording sites is provided at the bottom of the table.

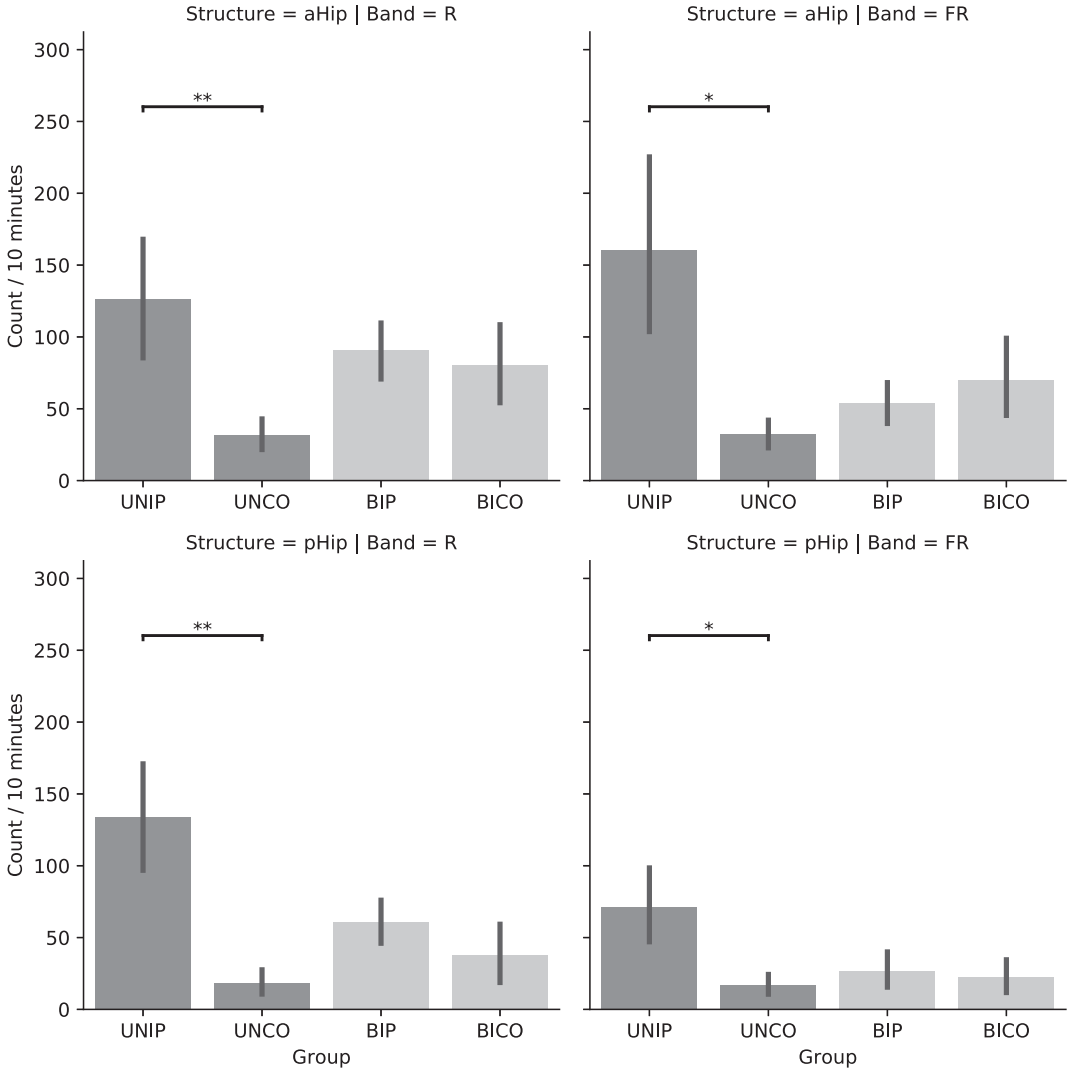


**Fig. 1.** Differences between ipsilateral and contralateral hippocampi in patients with unilateral (UNIP and UNCO, respectively) and bilateral (BIP and BICO, respectively) mesial temporal lobe epilepsy. The analysis was performed separately for ventral (aHip) and dorsal (pHip) hippocampal recording sites in ripple (R) and fast ripple (FR) bands. Significance levels are marked by asterisks (* < 0.05, ** < 0.001).

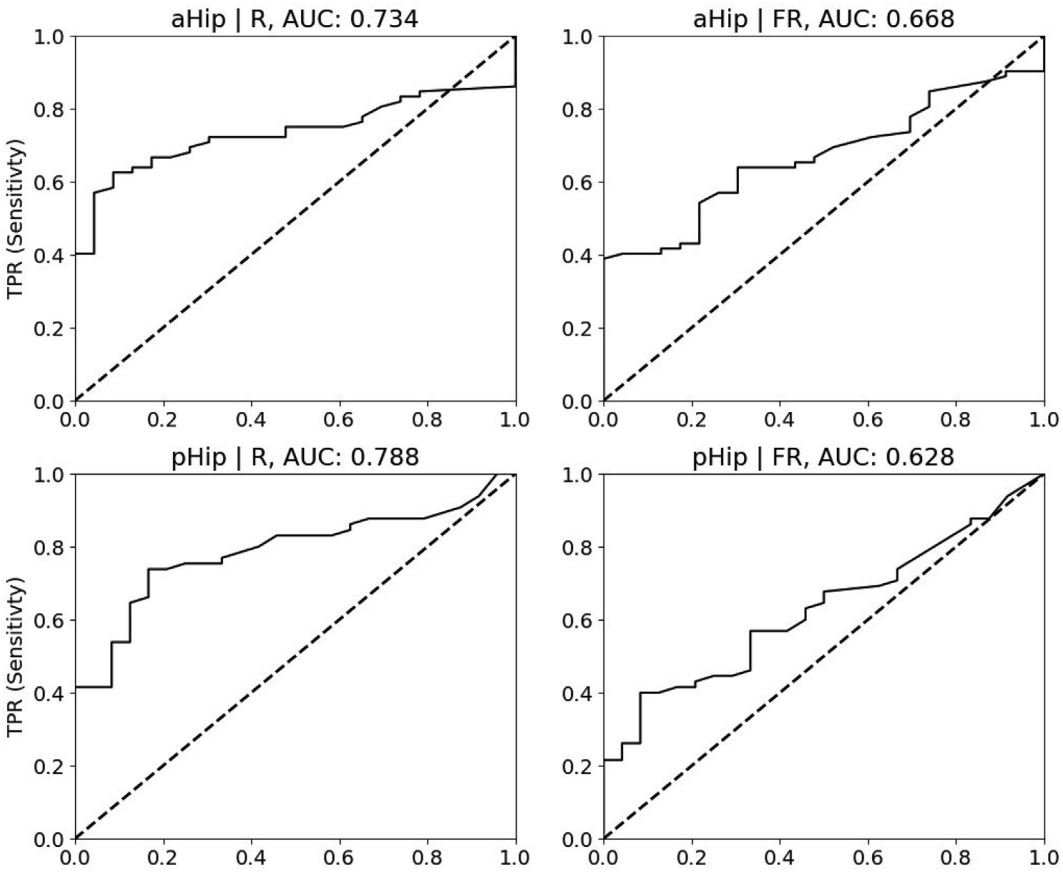


**Fig. 2.** The receiver operating characteristics (ROC) curves were created by plotting the true positive rates (TPR) against the false positive rates (FPR) in order to evaluate whether the hippocampi contralateral (UNCO) and ipsilateral to seizure onset (UNIP, BIP, BICO groups) can be distinguished. Each area under the curve (AUC) was compared to chance (AUC = 0.5 represented by the dashed line) and tested with Hanley-McNeil test. The statistical significance (p-value <0.05) was reached both for the anterior (aHip; AUC = 0.734) and posterior hippocampus (pHip; AUC = 0.788) in ripple (R), but not in fast ripple (FR) range.

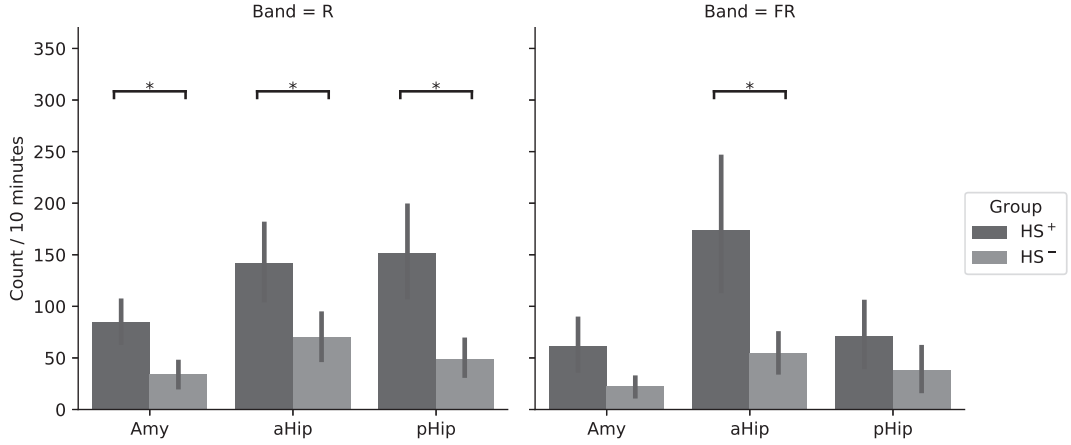


**Fig. 3.** Comparison of ripple (R) and fast ripple (FR) rates in homotopic recording sites (Amy – amygdala, aHip – anterior hippocampus, pHip – posterior hippocampus) with respect to the underlying pathology ($HS^+$ subgroup – hippocampal sclerosis, $HS^-$ subgroup – no– hippocampal sclerosis /gliosis only). The significance level <0.05 is indicated by asterisks (*). Please note the higher R rates in either Amy, aHip and pHip recording sites in $HS^+$ than in $HS^-$ subgroup. The similar trend in the FR range reached statistical significance only in the ventral parts of sclerotic hippocampi.

explored structures or mesial temporal and lateral neocortical localization. Indeed, ripple and FR rates that were found higher in the seizure onset zone than outside if clinical macroelectrodes were used (Jacobs et al., 2008; Jacobs et al., 2009; Andrade-Valença et al., 2012). In studies dedicated to the comparison between mesial temporal areas ipsilateral and contralateral seizure onset zones (recordings from microelectrodes) showed higher FR to ripple ratio in ipsilateral mesial area (Staba et al., 2002, 2007).

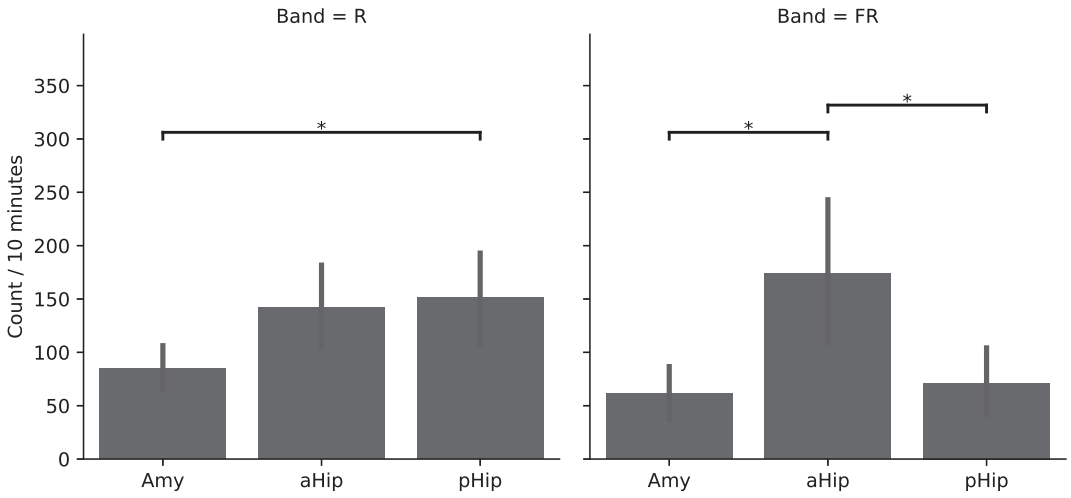


**Fig. 4.** Ripple (R) and fast ripple (FR) rates in recording sites along the longitudinal axis of the amygdalo-hippocampal complex in the HS$^{+}$ subgroup (Amy – amygdala, aHip – anterior hippocampus, pHip – posterior hippocampus). The significance level of <0.05 is marked by asterisks (*). Please note the most increased FR rate in the ventral part of sclerotic hippocampi and the lacking difference between ventral and dorsal part of sclerotic hippocampi in the R band. Differences in the HS$^{-}$ subgroup did not reach statistical significance (not illustrated).

In present study higher ripple and FR rates were found in the hippocampi ipsilateral to the seizure onset than in the contralateral hippocampi in U-MTLE. Moreover, non-epileptic hippocampi demonstrated significantly lower ripple rates than others. However, it remains questionable whether this finding might support the opinion that FR-generating areas are relatively stable (Bragin et al., 2003) as the recent study provided the detailed analysis indicating substantial spatiotemporal variability of HFOs (Gliske et al., 2018). It is doubtful whether the low interictal HFO rate might be used as a negative biomarker of the non-epileptic hippocampi. In any case, the challenging issue of HFO specificity should be resolved by prospective studies on a per subject basis.

### 4.2. Hippocampal HFOs and bilateral MTLE

In an experimental rat model of induced temporal lobe epilepsy, unilateral lesion in the hippocampus was sufficient for the later occurrence of independent bilateral seizures and interictal FRs within both hippocampi (Finnerty and Jefferys, 2002; Jefferys and Empson, 1990; Bragin et al., 2003; Jiruska et al., 2010). The literature presents limited evidence that the epileptogenic network in bilateral MTLE is more spatially extended, concerning the extrahippocampal mesial temporal structures, than that in unilateral MTLE (Aubert et al., 2016; Bragin et al., 2003; Jacobs et al., 2009). This might increase the number and variability of potential ictal generators among extrahippocampal structures; this has been demonstrated in unilateral MTLE (Spencer and Spencer, 1994; Van Paesschen et al., 2001; Wennberg et al., 2002). It might be interesting to clarify the role of the extrahippocampal structures within the epileptogenic network in bitemporal epilepsy.

Secondly, there is evidence for progressive cellular and network alterations in MTLE (Pitkänen and Sutula, 2002; Bartolomei et al., 2008). Some works have proposed a process of secondary epileptogenesis as a possible mechanism of bitemporal epilepsy development (Morrell, 1989; Wilder, 2001). Indeed, in an experimental rat model FRs within both hippocampi and bilateral spontaneous seizures developed during the first weeks after a unilateral intrahippocampal tetanus toxin injection (Finnerty and Jefferys, 2002; Jiruska et al., 2010). Nevertheless, this finding of a short-term process leading to bilateral disorder in rodents must be interpreted carefully when considering the different hippocampal commissural system arrangement in humans (Gloor et al., 1993). In the present study, patients with unilateral MTLE demonstrated significantly longer epilepsy duration than patients with bilateral MTLE, although previously no difference was observed between both groups (Hirsch et al., 1991). Unfortunately, in the present study, the small sample size did not allow the correlation between the HFO rates and epilepsy duration. We wonder if a prospective design could be applied in human studies.

### 4.3. Interictal HFOs in MTLE, underlying hippocampal pathology and recording site localization

The increased FR rate in mesial temporal structures was previously found to be associated with the characteristic features of HS, such as hippocampal neuronal loss (Staba et al., 2007) and reduced hippocampal volume (Jacobs et al., 2009; Ogren et al., 2009; Staba et al., 2007). Our results indicate that it is possible that neuronal loss in sclerotic hippocampi might cause additional increases in HFO rates also in the ripple range, as has been suggested in previous studies (Jacobs et al., 2009; Worrell et al., 2008). Our finding of higher FR rates in the head than in the posterior parts of sclerotic hippocampi might be explained by the similar gradient of atrophy and neuronal loss within the sclerosis along the longitudinal hippocampal axis, which has been observed in both MRI and histopathological studies (Babb et al., 1984; Bernasconi et al., 2003; Thom et al., 2012). Another question is whether the HFO rate in amygdalar recording sites might be affected by amygdalar sclerosis, which is often associated with HS (Yilmazer-Hanke et al., 2000). It seems necessary to confirm and estimate the potential influence of these variables on the occurrence of HFOs.

### 4.4. Study limitations

Our results might be influenced by the high inter-individual variability of interictal HFOs and the small sample size. As bitemporal epilepsy might be a cause of surgery failure, in two patients the recordings were acquired during the re-evaluation procedure after a previous intervention in the temporal lobe (both hippocampi of patient 10 were completely intact; only registrations from contacts located in the spared left pHip were available in patient 16). As we understand the potential influence of previous interventions on hippocampal epileptogenicity, the influence is thought to be linked to the nature of mesial temporal sclerosis

per se, rather than its maturation in a surgical scar (Hennessy et al., 2000).

Visual inspection of the hippocampus with 3-Tesla MRI is not considered sensitive enough to detect all cases of HS (Blümcke et al., 2013). It is not possible to definitively exclude the possibility of HS in any hippocampi not examined histopathologically. Another limitation of this work was caused by the lack of criteria and the variable terminology used in bitemporal epilepsy description. Our B-MTLE patients were definitely characterized by independent seizure onsets; in patients with U-MTLE, it was not possible to exclude certain levels of involvement of both temporal lobes (as might be suggested by, e.g., frequent findings of bilateral interictal discharges (Ergene et al., 2000)). We minimized the risk of contamination in U-MTLE patients using multiple inclusion criteria. We used the terms 'ipsilateral'/'contralateral' to label each side of the hippocampi in order to avoid similar terms (such as 'primary', 'leading'/'secondary', 'mirror') that might suggest a certain pathophysiological concept.

Ultimately, the question remains whether bitemporal epilepsy represents a specific type of a single extensive epileptogenic network, as supported by a favorable outcome after unilateral surgery (Aghakhani et al., 2014), or two independent networks, as is indirectly expressed in its definition. We encourage further research with the purpose of bringing together the two perspectives.

## Conflict of interest

None of the authors has any conflict of interest to disclose.

## Acknowledgments

This work was supported by funds from the Faculty of Medicine, Masaryk University, provided to the junior researcher (Martin Pail).

We confirm that we have read the journal's position on the issues involved in ethical publication and affirm that this report is consistent with those guidelines.

We thank Anne Johnson for grammatical assistance.

## Appendix A. Supplementary material

Supplementary data to this article can be found online at https://doi.org/10.1016/j.clinph.2019.03.026.

## References

Aghakhani Y, Liu X, Jette N, Wiebe S. Epilepsy surgery in patients with bilateral temporal lobe seizures: a systematic review. Epilepsia 2014;55:1892–901.
Andrade-Valença L, Mari F, Jacobs J, Zijlmans M, Olivier A, Gotman J, et al. Interictal high frequency oscillations (HFOs) in patients with focal epilepsy and normal MRI. Clin Neurophysiol 2012;123:100–5.
Aubert S, Bonini F, Curot J, Valton L, Szurhaj W, Derambure P, et al. The role of subhippocampal versus hippocampal regions in bitemporal lobe epilepsies. Clin Neurophysiol 2016;127:2992–9.
Babb TL, Lieb JP, Brown WJ, Pretorius J, Crandall PH. Distribution of pyramidal cell density and hyperexcitability in the epileptic human hippocampal formation. Epilepsia 1984;25:721–8.
Bartolomei F, Chauvel P, Wendling F. Epileptogenicity of brain structures in human temporal lobe epilepsy: a quantified study from intracerebral EEG. Brain 2008;131:1818–30.
Bernasconi N, Bernasconi A, Caramanos Z, Antel SB, Andermann F, Arnold DL. Mesial temporal damage in temporal lobe epilepsy: a volumetric MRI study of the hippocampus, amygdala and parahippocampal region. Brain 2003;126:462–9.
Birot G, Kachenoura A, Albera L, Bénar C, Wendling F. Automatic detection of fast ripples. J Neurosci Methods 2013;213:236–49.
Blum D. Prevalence of bilateral partial seizure foci and implications for electroencephalographic telemetry monitoring and epilepsy surgery. Electroencephalogr Clin Neurophysiol 1994;91:329–36.
Blümcke I, Thom M, Aronica E, Armstrong DD, Bartolomei F, Bernasconi A, et al. International consensus classification of hippocampal sclerosis in temporal lobe epilepsy: a Task Force report from the ILAE Commission on Diagnostic Methods. Epilepsia 2013;54:1315–29.
Bragin A, Wilson CL, Engel J. Spatial stability over time of brain areas generating fast ripples in the epileptic rat. Epilepsia 2003;44:1233–7.
Duvernoy HM, Cattin F, Risold PY. The Human Hippocampus: Functional Anatomy, Vascularization and Serial Sections with MRI. Berlin Heidelberg: Springer-Verlag; 2013.
Ergene E, Shih JJ, Blum DE, So NK. Frequency of bitemporal independent interictal epileptiform discharges in temporal lobe epilepsy. Epilepsia 2000;41:213–8.
Finnerty GT, Jefferys JGR. Investigation of the neuronal aggregate generating seizures in the rat tetanus toxin model of epilepsy. J Neurophysiol 2002;88:2919–27.
Gardner AB, Worrell GA, Marsh E, Dlugos D, Litt B. Human and automated detection of high-frequency oscillations in clinical intracranial EEG recordings. Clin Neurophysiol 2007;118:1134–43.
Gliske SV, Irwin ZT, Chestek C, Hegeman GL, Brinkmann B, Sagher O, Garton HJL, Worrell GA, Stacey WC. Variability in the location of high frequency oscillations during prolonged intracranial EEG recordings. Nat Commun 2018;9:2155.
Gloor P, Salanova V, Olivier A, Quesney LF. The human dorsal hippocampal commisure. An anatomically identifiable and functional pathway. Brain 1993;116:1249–73.
Hennessy MJ, Elwes RD, Binnie CD, Polkey CE. Failed surgery for epilepsy. A study of persistence and recurrence of seizures following temporal resection. Brain 2000;123:2445–66.
Hirsch LJ, Spencer SS, Williamson PD, Spencer DD, Mattson RH. Comparison of bitemporal and unitemporal epilepsy defined by depth electroencephalography. Ann Neurol 1991;30:340–6.
Jacobs J, LeVan P, Chander R, Hall J, Dubeau F, Gotman J. Interictal high-frequency oscillations (80–500 Hz) are an indicator of seizure onset areas independent of spikes in the human epileptic brain. Epilepsia 2008;49:1893–907.
Jacobs J, Levan P, Châtillon CE, Olivier A, Dubeau F, Gotman J. High frequency oscillations in intracranial EEGs mark epileptogenicity rather than lesion type. Brain 2009;132:1022–37.
Jacobs J, Zijlmans M, Zelmann R, Chatillon CE, Hall J, Olivier A, et al. High-frequency electroencephalographic oscillations correlate with outcome of epilepsy surgery. Ann Neurol 2010;67:209–20.
Jefferys JGR, Empson RM. Development of chronic secondary epileptic foci following intrahippocampal injection of tetanus toxin in the rat. Exp Physiol 1990;75:733–6.
Jiruska P, Finnerty GT, Powell AD, Lofti N, Cmejla R, Jefferys JG. Epileptic high-frequency network activity in a model of non-lesional temporal lobe epilepsy. Brain. 2010;133:1380–90.
Kuba R, Musilová K, Vojvodič N, Tyrlíková I, Rektor I, Brázdil M. Rhythmic ictal nonclonic hand (RINCH) motions in temporal lobe epilepsy: invasive EEG findings, incidence, and lateralizing value. Epilepsy Res 2013;106:386–95.
Kucewicz MT, Cimbalnik J, Matsumoto JY, Brinkmann BH, Bower MR, Vasoli V, et al. High frequency oscillations are associated with cognitive processing in human recognition memory. Brain 2014;137:2231–44.
Morrell F. Varieties of human secondary epileptogenesis. J Clin Neurophysiol 1989;6:227–75.
Navarrete M, Pyrzowski J, Corlier J, Valderrama M, Le Van Quyen M. Automated detection of high-frequency oscillations in electrophysiological signals: methodological advances. J Physiol Paris 2016;110:316–26.
Ogren JA, Wilson CL, Bragin A, Lin JJ, Salamon N, Dutton RA, et al. Three-dimensional surface maps link local atrophy and fast ripples in human epileptic hippocampus. Ann Neurol 2009;66:783–91.
Pitkänen A, Sutula TP. Is epilepsy a progressive disorder? Prospects for new therapeutic approaches in temporal-lobe epilepsy. Lancet Neurol 2002;1:173–81.
Roehri N, Lina JM, Mosher JC, Bartolomei F, Bénar CG. Time-frequency strategies for increasing high frequency oscillation detectability in intracerebral EEG. IEEE Trans Biomed Eng 2016;63:2595–606.
Smart O, Rolston JD, Epstein CM, Gross RE. Hippocampal seizure-onset laterality can change over long timescales: a same-patient observation over 500 days. Epilepsy Behav Case Rep 2013;1:56–61.
Spencer D, Gwinn R, Salinsky M, O'Malley JP. Laterality and temporal distribution of seizures in patients with bitemporal independent seizures during a trial of responsive neurostimulation. Epilepsy Res 2011;93:221–5.
Spencer SS, Spencer DD. Entorhinal-hippocampal interactions in medial temporal lobe epilepsy. Epilepsia 1994;35:721–7.
Sperling MR, O'Connor MJ. Auras and subclinical seizures: characteristics and prognostic significance. Ann Neurol 1990;28:320–8.
Staba RJ, Wilson CL, Bragin A, Fried I, Engel Jr J. Quantitative analysis of high-frequency oscillations (80–500 Hz) recorded in human epileptic hippocampus and entorhinal cortex. J Neurophysiol 2002;88:1743–52.
Staba RJ, Frighetto L, Behnke EJ, Mathern GW, Fields T, Bragin A, et al. Increased fast ripple to ripple ratios correlate with reduced hippocampal volumes and neuron loss in temporal lobe epilepsy patients. Epilepsia 2007;48:2130–8.
Tamraz JC, Comair YG. Atlas of regional anatomy of the brain using MRI: with functional correlations. Berlin Heidelberg: Springer-Verlag; 2000.
Thom M, Liagkouras I, Martinian L, Liu J, Catarino CB, Sisodiya SM. Variability of sclerosis along the longitudinal hippocampal axis in epilepsy: a post mortem study. Epilepsy Res 2012;102:45–59.
Van Paesschen W, King MD, Duncan JS, Connelly A. The amygdala and temporal lobe simple partial seizures: a prospective and quantitative MRI study. Epilepsia 2001;42:857–62.

Waldman ZJ, Shimamoto S, Song I, Orosz I, Bragin A, Fried I, et al. A method for the topographical identification and quantification of high frequency oscillations in intracranial electroencephalography recordings. Clin Neurophysiol 2018;129:308–18.
Wennberg R, Arruda F, Quesney LF, Olivier A. Preeminence of extrahippocampal structures in the generation of mesial temporal seizures: evidence from human depth electrode recordings. Epilepsia 2002;43:716–26.
Wilder BJ. The mirror focus and secondary epileptogenesis. Int Rev Neurobiol 2001;45:435–46.
Worrell GA, Gardner AB, Stead SM, Hu S, Goerss S, Cascino GJ, et al. High-frequency oscillations in human temporal lobe: simultaneous microwire and clinical macroelectrode recordings. Brain 2008;131:928–37.
Yilmazer-Hanke DM, Wolf HK, Schramm J, Elger CE, Wiestler OD, Blümcke I. Subregional pathology of the amygdala complex and entorhinal region in surgical specimens from patients with pharmacoresistant temporal lobe epilepsy. J Neuropathol Exp Neurol 2000;59:907–20.
Zelmann R, Zijlmans M, Jacobs J, Châtillon CE, Gotman J. Improving the identification of high frequency oscillations. Clin Neurophysiol 2009;120:1457–64.
Zelmann R, Mari F, Jacobs J, Zijlmans M, Dubeau F, Gotman J. A comparison between detectors of high frequency oscillations. Clin Neurophysiol 2012;123:106–16.

**Published research**

# Multi-feature localization of epileptic foci from interictal, intracranial EEG

Jan Cimbálník

Petr Klimeš

Vladimír Sladký

Petr Nejedlý

Pavel Jurák

Martin Pail

Robert Roman

Pavel Daniel

Hari Guragain

Benjamin Brinkmann

Milan Brázdil

Gregory A. Worrell

**Clin Neurophysiol. 2019 Oct;130(10):1945-1953.**

## Commentary on published paper

When considering all patients with focal drug-resistant epilepsy, as high as 40-50% of patients suffer seizure recurrence after surgery. To achieve seizure freedom without side effects, precise localization of the focal brain region generating a patient's seizures, known as the epileptogenic zone, is required before its resection. As mentioned, research of recent years suggested that high-frequency oscillations (HFOs) are a promising biomarker of the epileptogenic zone without the need to record seizures (Thomschewski et al., 2019). However, these methods considered promising for pathological tissue localization have been shown successfully in ⅔ of the patients (Jacobs et al., 2018). What other features in interictal invasive EEG could, together with HFOs, improve the accuracy of the delineation of the epileptogenic area? In the presented retrospective study, we investigated an automated, fast, objective mapping process that used only interictal data.

We proposed a novel approach based on multiple invasive EEG (iEEG) features (the combination of univariate and bivariate iEEG features), which were used to train a support vector machine (SVM) model for classification of invasive EEG electrodes as normal or pathologic using 30 min of inter-ictal recording. It was the first study to our knowledge to combine conventional iEEG features and iEEG connectivity measures. This model was used to identify electrodes with the highest probability of being in the epileptogenic region. We used the validation of the SVM models based on post-surgical outcome. We analyzed the data from patients with intractable focal epilepsy in Brno Epilepsy Center (43) or Mayo Clinic (34) in the epilepsy surgery program recorded between years 2011 and 2016. In all patients, non-invasive studies could not adequately localize the seizure onset zone. We compared the results of postoperative outcomes, resected contacts with the delineation of the epileptogenic zone provided by SVM model. Unfortunately, the information about the resected area was available only in 30 patients (16 in Brno dataset, 14 in Mayo dataset) mostly due to low quality of imaging data (slices > 2 mm) or due to the implantation of a vagus nerve stimulator.

In our data, bivariate measures, especially the relative entropy, substantially contributed to the detector's performance. The HFO rate and relative entropy (higher values) were the most relevant for the epileptogenic zone distinction from all calculated features. The tissue under the iEEG electrodes, classified as epileptogenic, was removed in 17/18 excellent outcome patients and was not entirely resected in 8/10 poor outcome patients. The overall best result was achieved in a subset of 9 excellent outcome patients with the area under the receiver operating curve = 0.95. Validating the SVM models using post-surgical outcomes proved that resection of channels classified as pathologic led to excellent outcomes while failure to resect these channels resulted in poor outcomes.

Despite the promise of seizure-independent biomarkers, no single marker has been consistently shown to be effective and useful for all patients (Jacobs et al., 2018). SVM models combining multiple iEEG features show better performance than algorithms using a single iEEG marker (in most studies

used HFO rates). The current findings in iEEG connectivity studies suggest that changes of connectivity in epileptogenic tissue may be a clinically useful signature of ictogenesis and can substantially contribute to conventional methods for automatic localization of seizure generating tissue. We corroborated a statistically higher rate of spectrally rich events (HFOs) compared to a healthy brain (Frauscher et al., 2017). Importantly, our approach and underlying software's architecture is modular, allowing to add other potentially useful features (advanced processing pipelines, potential biomarkers of epileptogenicity,..) without the need to modify the whole data and model training pipelines.

Multiple invasive EEG and connectivity features in presurgical evaluation could improve epileptogenic tissue localization and is superior to using a single feature like the most used HFO rates alone. This approach may improve surgical outcomes and minimize the risk of side effects.

Clinical Neurophysiology 130 (2019) 1945–1953

Contents lists available at ScienceDirect

Clinical Neurophysiology

journal homepage: www.elsevier.com/locate/clinph

# Multi-feature localization of epileptic foci from interictal, intracranial EEG

Jan Cimbalnik [a,b,*,1], Petr Klimes [a,b,c,1], Vladimir Sladky [a,b], Petr Nejedly [a,b,c], Pavel Jurak [c], Martin Pail [d], Robert Roman [e], Pavel Daniel [d], Hari Guragain [b], Benjamin Brinkmann [b,f], Milan Brazdil [d,e], Greg Worrell [b,f]

[a] International Clinical Research Center, St. Anne's University Hospital, Brno, Czech Republic
[b] Mayo Systems Electrophysiology Laboratory, Department of Neurology, Mayo Clinic, 200 First St SW, Rochester, MN 55905, USA
[c] Institute of Scientific Instruments, The Czech Academy of Sciences, Brno, Czech Republic
[d] Brno Epilepsy Center, Department of Neurology, St. Anne's University Hospital and Faculty of Medicine, Masaryk University, Brno, Czech Republic
[e] Behavioral and Social Neuroscience Research Group, CEITEC – Central European Institute of Technology, Masaryk University, Brno, Czech Republic
[f] Department of Physiology and Biomedical Engineering, Mayo Clinic, 200 First St SW, Rochester, MN 55905, USA

ARTICLE INFO

*Article history:*
Accepted 19 July 2019
Available online 5 August 2019

*Keywords:*
Drug resistant epilepsy
Epileptogenic zone localization
Multi-feature approach
High frequency oscillations
Connectivity
Machine learning

HIGHLIGHTS

- Multi-feature approach in localization of epileptogenic tissue is superior to using single feature.
- Multi-feature approach can improve epileptogenic brain localization.
- The presented algorithm performed well on datasets from different institutions.

ABSTRACT

*Objective:* When considering all patients with focal drug-resistant epilepsy, as high as 40–50% of patients suffer seizure recurrence after surgery. To achieve seizure freedom without side effects, accurate localization of the epileptogenic tissue is crucial before its resection. We investigate an automated, fast, objective mapping process that uses only interictal data.
*Methods:* We propose a novel approach based on multiple iEEG features, which are used to train a support vector machine (SVM) model for classification of iEEG electrodes as normal or pathologic using 30 min of inter-ictal recording.
*Results:* The tissue under the iEEG electrodes, classified as epileptogenic, was removed in 17/18 excellent outcome patients and was not entirely resected in 8/10 poor outcome patients. The overall best result was achieved in a subset of 9 excellent outcome patients with the area under the receiver operating curve = 0.95.
*Conclusion:* SVM models combining multiple iEEG features show better performance than algorithms using a single iEEG marker. Multiple iEEG and connectivity features in presurgical evaluation could improve epileptogenic tissue localization, which may improve surgical outcome and minimize risk of side effects.
*Significance:* In this study, promising results were achieved in localization of epileptogenic regions by SVM models that combine multiple features from 30 min of inter-ictal iEEG recordings.


## 1. Introduction

Epilepsy is one of the most prevalent neurological diseases (Leonardi and Ustun, 2002). While roughly two-thirds of patients with epilepsy are successfully managed with anti-seizure drugs (ASDs), the remaining patients continue to have seizures and may be candidates for surgical treatment options (Wiebe et al., 2001).

* Corresponding author at: Department of Biomedical Engineering, International Clinical Research Center (FNUSA-ICRC), St. Anne's University Hospital in Brno, Pekařská 53, Brno 656 91, Czech Republic.
*E-mail address:* jan.cimbalnik@fnusa.cz (J. Cimbalnik).
[1] Co-first authors for this study.

https://doi.org/10.1016/j.clinph.2019.07.024
1388-2457/

Precise localization of the focal region generating a patient's seizures is required for surgical resection, the most effective (Téllez-Zenteno et al., 2010) and commonly performed treatment (Kelly and Chung, 2011), and to guide implantation of electrodes for therapeutic brain stimulation (Fisher and Velasco, 2014; Bergey et al., 2015). Accurate localization of epileptogenic tissue is critical for achieving optimal outcomes and minimizing risk of side effects.

Currently, the clinical gold-standard for localization of epileptogenic tissue is obtained by recording spontaneous seizures with intracranial EEG (iEEG). This requires days to weeks of recording and can be associated with patient discomfort and risk, (Van Gompel et al., 2008). The iEEG is used in combination with other modalities to ensure concordance of the multi-modal information but when considering all types of focal epilepsy the seizure-free outcome is achieved in only approximately 50% of patients (Téllez-Zenteno et al., 2010).

The visual analysis of the massive iEEG datasets is time consuming and subject to observer biases. Naturally, this has led to many attempts for automated localization of epileptogenic tissue from inter-ictal iEEG recordings, which would significantly speed up the pre-surgical evaluation process. Many of these seizure-independent methods use high-frequency EEG power or rates of high-frequency oscillations (HFO) (Bragin et al., 2002; Jacobs et al., 2008; Worrell et al., 2008; Cimbalnik et al., 2016). These methods show promise for pathological tissue localization, and have been shown successful in ⅔ of the patients (Cimbálník et al., 2018; Jacobs et al., 2018). The reason for the failures might be caused by false positive detections (Bénar et al., 2010) or by the fact that physiological HFOs (Kucewicz et al., 2014; Brázdil et al., 2015) are challenging to distinguish from pathological HFOs (Matsumoto et al., 2013; Cimbalnik et al., 2018).

Recently, functional connectivity was described as a new biomarker of the epileptogenic zone, i.e. the tissue that must be resected or disconnected for seizure freedom (Lüders and Comair, 2001). During the inter-ictal period, different connectivity patterns have been reported in a normal epileptic brain compared to the seizure onset zone (SOZ) (Bettus et al., 2008; Dauwels et al., 2009; Warren et al., 2010), which is also functionally isolated from surrounding healthy tissue (Warren et al., 2010; Klimes et al., 2016). Altered connectivity pattern in the epileptic brain has also been used to predict surgery outcome (Antony et al., 2013).

Despite the promise of seizure-independent biomarkers, no single marker has been consistently shown to be effective for all patients (Cimbalnik et al., 2018; Jacobs et al., 2018). Electrophysiological activity of the brain is not consistent across time (Pearce et al., 2013; Gliske et al., 2018) and is affected by different states of vigilance (Gross and Gotman, 1999; Staba et al., 2002; Kremen et al., 2017). Therefore, utilizing the HFO rate, or connectivity as a stand-alone biomarker is unlikely to be successful in all cases (Khadjevand et al., 2017; Cimbalnik et al., 2018; Jacobs et al., 2018). Combination of multiple features might provide a more robust estimation (Gnatkovsky et al., 2014; Varatharajah et al., 2018).

Here we explore the utility of combining different information represented by multiple iEEG biomarkers. A previous study by Varatharajah et al. (2018) used a combination of univariate features (HFO rate and phase-amplitude coupling) for SOZ localization (Varatharajah et al., 2018). We investigated a combination of univariate and bivariate iEEG features given they are likely to carry different information. These features are used to train the Support Vector Machine (SVM) model which is used to identify electrodes with the highest probability of being in the epileptogenic region.

## 2. Methods

To promote transparency and ensure reproducibility of our results, the SVM code and feature data are available online (https://github.com/ICRC-BME/machine_learn_module).

### 2.1. Patients

All patients underwent intracranial depth and subdural electrode implantation as part of their evaluation for epilepsy surgery when non-invasive studies could not adequately localize the seizure onset zone. All patients recorded in the Brno Epilepsy Center or Mayo Clinic between years 2011 and 2016 were selected for this study. Patients without implanted white matter, electrode coordinates, SOZ information or with poor recording quality were omitted from the cohort. The final cohort of patients, who participated in the study, consisted of 43 patients from Brno Epilepsy Center and 34 from Mayo Clinic (Supplementary Table 1).

Since we used three different targets for classification (1. SOZ contacts, 2. Resected contacts, 3. SOZ overlapped with resected contacts), the final cohort was further divided into three subgroups. For SOZ target all patients were included. For resected contacts target only patients with information about surgical outcome and resected area were included resulting in a subgroup of 30 patients (9 good and 7 bad outcome patients in Brno Epilepsy Center, 9 good and 5 bad outcome patients in Mayo Clinic). For SOZ overlapped with resected contacts target the subgroup consisted of 28 patients (9 good and 5 bad outcome patients in Brno Epilepsy Center, 9 good and 5 bad outcome patients in Mayo Clinic). The information about the resected area was available only in 30 patients (16 in Brno dataset, 14 in Mayo dataset) mostly due to poor quality of imaging data (slices > 2 mm) or implantation of vagus nerve stimulator. The numbers of patients in each group are available in Table 1.

The study was approved by the Brno Epilepsy Center - St. Anne's University Hospital Research Ethics Committee and the Mayo Clinic Institutional Review Board. All patients provided informed consent.

### 2.2. Intracranial EEG recordings

#### 2.2.1. Brno Epilepsy Center, St. Anne's University Hospital

43 patients implanted with standard intracranial depth electrodes (5, 10 and 15 contact semi-flexible multi-contact platinum electrodes DIXI (DIXI MEDICAL; CHAUDEFONTAINE, FRANCE) or ALCIS(ALCIS, Besançon, France), contact surface area 5.02 $mm^2$ and inter-contact distance 1.5 mm). All iEEG was acquired with a common reference, an average signal from all iEEG channels. The iEEG was recorded with a sampling frequency of 25 kHz. The data was down-sampled to 5 kHz for further processing. 30 min of relaxed awake activity was selected for the analysis. Anatomical

**Table 1**
The receiver operating curve classification results for different datasets and different definition of epileptogenic tissue.

| Target | SOZ | Resected | | SOZ + Resected | |
|---|---|---|---|---|---|
| Outcome | All | Good | Bad | Good | Bad |
| Mayo | 0.770 (N = 34) | 0.729 (N = 9) | 0.558 (N = 5) | 0.803 (N = 9) | 0.623 (N = 5) |
| Brno | 0.770 (N = 43) | 0.842 (N = 9) | 0.776 (N = 7) | 0.952 (N = 9) | 0.827 (N = 5) |
| Joined | 0.745 (N = 77) | 0.747 (N = 18) | 0.560 (N = 12) | 0.838 (N = 18) | 0.592 (N = 10) |

localization of electrodes was achieved using post-implant MRI co-registered to the patient's pre-implant MRI.

*2.2.2. Electrophysiology Laboratory, Mayo Clinic*

34 patients, all implanted with intracranial depth electrodes (AD-Tech Medical Inc, Racine, WI, 4 and 8 contact clinical depth electrodes with Platinum/Iridium clinical macro-electrode contacts, contact surface area 9.4 $mm^2$ and inter-contact distance 10 mm) and subdural grids and strips (4.0 mm diameter Platinum/Iridium discs (2.3 mm diameter exposed) with 10 mm inter-contact distance). All intracranial EEG was acquired with a stainless steel suture as a common reference placed in the vertex region of the scalp midline between the international 10–20 Cz and Fz electrode positions. The iEEG was recorded with a sampling frequency of 32 kHz and down-sampled to 5 kHz, with a 1 kHz Bartlett-Hanning window low-pass filter. 30 min from 1 AM to 1:30 AM of the patient's first night at ICU was selected for analysis. The location of electrodes was determined from post-implant CT data co-registered to the patient's pre-implant MRI using normalized mutual information (SPM8). Electrode coordinates were then automatically labeled by SPM Anatomy toolbox, with an estimated accuracy of 5 mm (Tzourio-Mazoyer et al., 2002).

*2.3. EEG signal pre-processing*

A visual inspection and automated detection based on convolutional neural networks was used to detect noise, technical artifacts, muscle and movement artifacts (Nejedly et al., 2018). Bad data segments or whole EEG channels were omitted from further analysis. To remove scalp reference and suppress far-field potentials caused predominantly by volume conduction a reference signal was calculated and subtracted from each iEEG signal. The reference signal was calculated as an average signal from iEEG electrodes placed in the white matter.

*2.4. Identification of seizure onset zone*

The seizure onset electrodes and time of seizures were determined from the clinical report and verified independently by identifying the electrodes with the earliest iEEG seizure discharge. Seizure onset times and location were determined by visual identification of a clear electrographic seizure discharge, followed by a look back in the iEEG recordings for the earliest electroencephalographic change contiguously associated with the seizure.

*2.5. Identification of resected tissue*

Post-resection MRI was used to identify areas of the brain that were surgically removed. The electrodes localized within the resected areas were marked.

*2.6. Surgical outcomes*

Surgical outcomes were classified according to the International League Against Epilepsy (ILAE) classification system at Mayo Clinic and Engel Surgical Outcome Scales at Brno. ILAE Class-1 and Engel class IA were considered good outcome.

*2.7. Calculated features*

The EEG features were computed in three distinct groups: (1) HFO features – computed from detections of oscillatory events in the iEEG signal, (2) univariate features – computed on iEEG signal from individual iEEG channel on a depth electrode, (3) bivariate features – computed between two iEEG signals from two adjacent iEEG channels on a depth electrode. In grid contacts the adjacent channels were determined along the longitudinal axis of the grid. HFOs and oscillatory events below HFO frequency bands (<80 Hz) were detected in 10 sec, non-overlapping statistical windows. Mean rate per channel was then calculated for the whole length of recording. Univariate and bivariate EEG features were calculated in 1 sec non-overlapping windows. The mean feature value of all 1 sec windows was calculated for each channel or channel pair. To obtain one value per contact for bivariate features only the higher of the two mean feature values was selected. All features were calculated in 9 different frequency bands (1–4 Hz, 4–8 Hz, 8–12 Hz, 12–20 Hz, 20–45 Hz, 55–80 Hz, 80–250 Hz, 250–600 Hz, 600–1000 Hz), except frequency- and phase-amplitude coupling, which were calculated for fixed pair of frequencies only. The data were filtered using 2nd order IIR bandpass Butterworth filters. All features were normalized by z-score normalization before SVM model training and testing.

*2.7.1. HFO rate*

Various HFO detectors have been described in the literature, and direct comparison of detectors remains challenging (Roehri et al., 2017). In this study, two different HFO detectors were used: (1) The line-length detector (Gardner et al., 2007) which is sensitive to any increase in band power but its specificity is low, especially with regard to false ripples created by sharply contoured transients. This detector was run in all frequency bands. The detection thresholds were set to 3 standard deviations of the line-length metric above the mean and the duration threshold was set to a minimum of 5 oscillations. (2) The CS detector has been proven to successfully eliminate false ripples produced by band pass filtering of sharp transients (Cimbálník et al., 2018). The threshold for the detection was set to 0.1 and the duration threshold set to a minimum of 5 oscillations. This detector was run in parallel with the LL detector. Since the CS detector provides detections with determined frequency, the HFO rate in individual frequency bands was determined ad-hoc by the sum of detections that fell within the frequency cut-offs of each frequency band.

The resulting HFO rates of the LL and CS detectors were treated as separate features.

*2.7.2. Power in band (univariate feature)*

Increased Local Field Potential (LFP) amplitude is primarily caused by synchronized activity of local neuronal synapses and provides information about electrophysiological activity of measured region (Katzner et al., 2009). Relative power in band (PB) for each iEEG channel was calculated as $PB = \langle X_t^2 \rangle / \langle X_{t\_raw}^2 \rangle$, where $\langle\rangle$ stands for mean, $X_t$ for the signal in selected frequency band and $X_{t\_raw}^2$ for the non-filtered signal.

*2.7.3. Frequency amplitude coupling (univariate feature)*

Frequency amplitude coupling reflects how the signal amplitude is modulated by a particular frequency band. Unlike other features, this method used fixed pair of frequency bands: lower (1–30 Hz) for time signal and higher (65–180 Hz) for signal envelope (Varatharajah et al., 2018). Frequency amplitude coupling (FAC) was calculated as $FAC = [cov(|x_H|, x_t)/std(|x_H|) \cdot std(x_t)]$, where $x_t$ is the time signal filtered in lower frequency band, $x_H$ is the Hilbert transformation of the time signal *filtered in higher frequency band*, *cov* stands for the covariance and *std* for the standard deviation. The value of FAC varies in interval $\langle -1,1 \rangle$. $FAC = 1$ indicates perfect dependence between frequency and amplitude, $FAC = -1$ indicates opposite dependence, and $FAC = 0$ indicates no dependence.

*2.7.4. Phase amplitude coupling (univariate feature)*

Phase amplitude coupling reflects how the signal amplitude is modulated by its instantaneous phase of particular frequency band. Similarly to FAC, this method used fixed pair of frequency

bands: lower (1–30 Hz) for instantaneous phase and higher (65–180 Hz) for signal envelope (Varatharajah et al., 2018). Instantaneous phase was calculated as $\Phi_t = arctan(x_H/x_t)$, where $x_H$ is the Hilbert transformation of the time signal $x_t$, which was previously filtered in lower frequency band. Phase amplitude coupling (PAC) was then calculated as $PAC = [cov(|X_H|,\Phi_t)/std(|X_H|)\cdot std(\Phi_t)]$, where $X_H$ is the Hilbert transformation of the time signal, which was previously filtered in higher frequency band, *cov* stands for the covariance and *std* for the standard deviation. The value of PAC varies in interval <−1,1>. $PAC = 1$ indicates perfect dependence between phase and amplitude, $PAC = -1$ indicates opposite dependence, and $PAC = 0$ indicates no dependence.

*2.7.5. Power spectral entropy (univariate feature)*

In general, information entropy is defined as the average amount of information in observed data. In signal processing, entropy reflects a randomness and spectral richness in continuous time-series. Power spectral entropy (PSE) was calculated as $PSE = -sum[ps\cdot log_2(ps)]$, where *ps* is a fraction of particular examples in the dataset, in this case normalized spectral power density obtained by Fourier transformation.

*2.7.6. Relative entropy (bivariate feature)*

To evaluate the randomness and spectral richness between two time-series, the Kullback-Leibler divergence, i.e. relative entropy (REN), was calculated. REN is a measure of how entropy of one signal diverges from a second, expected one. The value of REN varies in interval <0,+Inf>. $REN = 0$ indicates the equality of statistical distributions of two signals, while $REN > 0$ indicates that the two signals are carrying different information.

*REN* was calculated between adjacent iEEG channels X,Y as $REN = sum[pX\cdot log(pX/pY)]$, where *pX* is a probability distribution of investigated signal and *pY* is a probability distribution of expected signal. Because of asymmetrical properties of REN, REN (X, Y) is not equal to REN(Y, X). *REN* was calculated in two steps for both directions (both distributions from channel pair were used as expected distributions). The maximum value of *REN* was then considered as the final result, regardless of direction.

*2.7.7. Correlation (bivariate feature)*

The linear correlation (LC) varies in interval <−1,1> and reflects shape similarities between two signals. $LC = 1$ indicates perfect conformity between two signals, $LC = -1$ indicates opposite signals and $LC = 0$ indicates two different signals. LC was calculated by Pearson's correlation coefficient as: $LC_{X,Y} = [cov(X_t,Y_t)/std(X_t)\cdot std(Y_t)]$, where $X_t,Y_t$ are the two evaluated signals, *cov* is the covariance and *std* is the standard deviation.

*2.7.8. Correlation with time-lag (bivariate feature)*

The linear correlation between all adjacent iEEG channels was calculated in 1 second non-overlapping intervals with a time-lag. Maximum time-lag was equal to $f_{max}/2$ of selected frequency band. Lagged linear correlation (LLC) for each time-lag *k* was calculated by Pearson's correlation coefficient as: $LLC_{X(k),Y(k)} = [cov(X_{t(k)},Y_{t(k)})/std(X_{t(k)})\cdot std(Y_{t(k)})]$, where $X_t,Y_t$ are the two evaluated signals, *cov* is the covariance and *std* is the standard deviation. The maximum value of correlation was stored with its time-lag value. Time-lag of maximum LLC value was evaluated as a separate feature.

*2.7.9. Phase lag index (bivariate feature)*

Phase lag index (PLI) represents evaluation of statistical interdependencies between time series, which is supposed to be less influenced by the common sources (Stam et al., 2007). PLI calculation is based on the phase synchronization between two signals with constant, nonzero phase lag, which is most likely not caused by volume conduction from a single strong source. Phase lag index was calculated as $PLI = |<sign[\Delta\Phi(t_k)]>|$, where *sign* represents signum function, <> stands for mean and $\Delta\Phi$ is a phase difference between two iEEG signals. For calculation of instantaneous phase see the phase-amplitude coupling paragraph. PLI was calculated in 1 second non-overlapping intervals with time-lag. Maximum time-lag was equal to $f_{max}/2$ of selected frequency band. The maximum value of PLI was stored with its time-lag value. Time-lag of maximum PLI value was evaluated as a separate feature.

*2.7.10. Phase synchrony (bivariate feature)*

Instantaneous phase of each signal was calculated the same way as in phase-amplitude coupling section. Phase synchrony (PS) was then calculated as $PS = \sqrt{[(<\cos(\Phi X_t)>)^2 + (<\sin(\Phi Y_t)>)^2]}$, where $\Phi X_t$ is instantaneous phase of signal *X*, $\Phi Y_t$ is instantaneous phase of signal *Y*, <> stands for mean and $\sqrt{}$ for square root.

*2.7.11. Phase consistency (bivariate feature)*

Calculation of phase consistency between two signals, regardless of any phase shift between signals. First, phase synchrony (PS, defined above) was calculated for multiple steps of time delay between two signals. Phase consistency (PC) was then calculated as $PC = <PS>\cdot(1-std(PS)/0.5)$, where std is the standard deviation and <> stands for mean.

*2.8. Feature selection*

Feature selection was carried out to determine the relevant features for classification (in both datasets separately and together for joined dataset). The features were separated into three groups: HFO features, univariate features and bivariate features (connectivity) to take into account different information they represent. Each group of features was evaluated separately by ANOVA. F-score values were used to determine the features that carry the most information for pathological tissue localization. The relevant features in each group were selected by determining outliers of F-score values using modified z-score with threshold set to 3 (Iglewicz and Hoaglin, 1993). Only features selected in respective dataset were used in SVM model for all patients in that dataset.

*2.9. Support vector machine classifier*

Selected features were used to train and test an SVM model for classification of tissue under individual electrodes as normal or pathologic. Weights were applied to correct for the imbalanced dataset resulting from more non-pathological channels than the pathological ones. The weights were calculated as inversely proportional to class frequencies. Leave-one-patient-out cross validation was used to train and test the SVM. In each iteration, the data of one patient was held out for testing while the SVM was trained on the remaining data. To obtain the best possible performance, both linear and radial basis function (RBF) kernels were tested and a parameter sweep was carried out to determine the optimal value of the penalty parameter C and gamma parameters. The best performing parameters were used for final classification (Table 2). To evaluate the performance of the SVM models, the probability estimate of correct target classification was used to create receiver operating curves (ROC) and area under the curves (AUC) for each leave-one-out iteration.

*2.10. Model evaluation*

To evaluate the feasibility of SVM for different usage scenarios the feature selection and subsequent SVM model training were done for three definitions of pathological tissue: **(1) Seizure onset zone**, as a standard definition of pathological tissue commonly defined in clinical practice. **(2) Resected tissue,** in patients with

**Table 2**
The best performing parameters for Support Vector Machine for different datasets and different definition of epileptogenic tissue.

| Dataset | SOZ | Resected | SOZ + Resected |
|---|---|---|---|
| Mayo | rbf, C = 0.1, gamma = 0.001 | rbf, C = 10, gamma = 0.001 | rbf, C = 10, gamma = 0.001 |
| Brno | rbf, C = 10, gamma = 0.001 | rbf, C = 0.1, gamma = 0.01 | linear, C = 0.001 |
| Joined | rbf, C = 0.01, gamma = 0.001 | rbf, C = 1, gamma = 0.001 | rbf, C = 0.1, gamma = 0.001 |

excellent post-surgical outcome (ILAE 1 & Engel 1). **(3) Resected tissue overlapped with SOZ** in patients with excellent post-surgical outcome. This overlap was used to compensate for non-pathological tissue removed as part of the surgical margin. For example, in patients that have a standard anterior temporal lobectomy approximately 3–4 cm of lateral temporal neocortex is resected (Wiebe et al., 2001), even if apparent pathology is confined to the mesial temporal structures. The trained SVM model was also used to classify pathological channels in patients with poor surgical outcome to assess if tissue under contacts classified as pathologic was not resected during the surgery. The evaluation was done on the whole dataset as well as separately on the datasets from two institutions. Testing for seizure onset zone, resected tissue, and resected tissue overlapped with SOZ in Mayo Clinic, Brno center and both datasets together resulted in 9 runs of the algorithm. Statistical significance of the average AUCs was tested with a Hanley-McNeil test by comparing them to chance (AUC = 0.5).

To evaluate the clinical relevance of the SVM model for individual patients, model training and classification were performed on resected tissue overlapped with SOZ in excellent outcome patients in a leave-one-out fashion. The classification of contacts in poor outcome patients was done by a model trained on all excellent outcome patients. To eliminate contacts misclassified due to residual noise the contacts classified as pathologic were clustered based on their spatial distribution in MNI space with the nearest neighbor clustering algorithm were radius was set to 2*shortest distance between contacts, i.e. 2 cm in patient space. Only the cluster with the highest mean probability of being pathologic was chosen (Fig. 1). We defined true positive (TP) finding when all channels classified as pathological were within the resected area and patient had excellent outcome. False positive finding (FP) was defined when all channels classified as pathological were resected but the patient had poor surgical outcome. True negative (TN) finding was defined when at least one channel classified as pathological was outside the resected area and the patient had poor outcome. False negative (FN) finding was defined when at least one channel classified as pathological was outside the resected area and the patient had an excellent outcome. Negative predictive value (NPV) defined as TN/(TN + FN) and positive predictive value (PPV) defined as TP/(TP + FP) were calculated.

## 3. Results

### 3.1. Feature selection

The best performing features for all targets and both institutions are summarized in Table 3. Relative entropy was the most selected feature especially above the alpha (8–12 Hz) frequency range. Relative entropy in the low gamma (20–45 Hz) and ripple (80–250 Hz) bands were selected in all runs of the algorithm. Oscillatory events detected by the line-length algorithm were the second most selected feature from alpha (8–12 Hz) band to ripple band (80–250 Hz). Fast ripple HFO detected by CS algorithm (Cimbálník et al., 2018) was selected in 6 runs of the algorithm. Fig. 2 shows distributions of two best performing features in Brno center dataset.

Notably, oscillatory event features were more often selected in runs using the Brno center dataset, whereas in runs with Mayo Clinic dataset the connectivity features were selected.

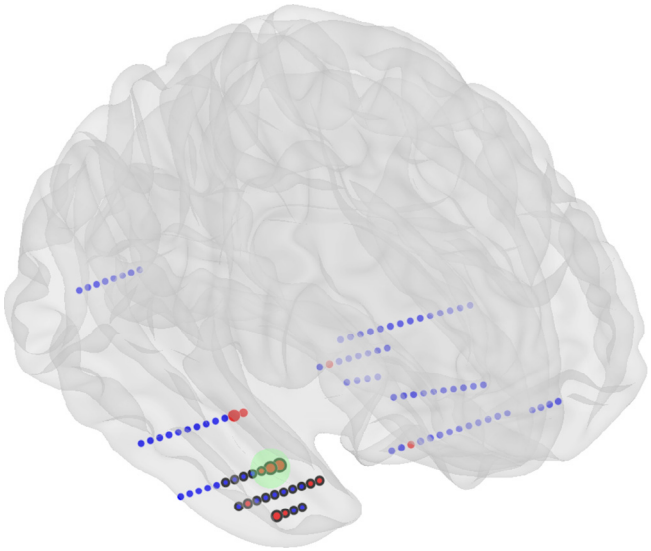

**Fig. 1.** Schematic illustration depth electrodes implanted in a brain. Localization of pathological tissue example. Red disks represent the channels identified by the SVM as pathological. The cluster (green circle) with the highest mean probability is selected as the final localization. Channels with black border were localized in the resected tissue.

### 3.2. Pathologic tissue localization

The performance of the algorithm was evaluated for three different classifications of pathologic tissue (SOZ contacts; resected contacts; and SOZ overlapped with resected contacts) in both dataset separately as well as combined dataset from both centers. All runs of the algorithm showed AUCs significantly better than chance ($p < 0.001$). The lowest AUCs were obtained for classification of SOZ targets 0.770, 0.770, 0.745 for Brno center and Mayo Clinic and combined datasets. Classification of channels over the resected tissue in excellent outcome patients showed better performance than classification of SOZ channels for the Brno center dataset (0.842) and combined datasets (0.747) but worse performance for Mayo dataset (0.729). Classification of channels in poor outcome patients showed decreased performance in all datasets. Classification of SOZ contacts within resected area in excellent outcome patients had the best performance compared to the other targets (0.952, 0.803, 0.838). The classification performance was reduced in poor outcome patients (Fig. 3). The ROC classification results are summarized in Table 1. In the subset of 28 patients where the contacts in SOZ overlapped with the resected contacts, the tissue under the iEEG electrodes, classified as epileptogenic, was removed in 17/18 excellent outcome patients and was not entirely resected in 8/10 poor outcome patients.

Evaluation of the SVM models for individual cases showed NPV = 1.0 and PPV = 0.9 for Brno center dataset, NPV = 0.8 and PPV = 0.89 for Mayo dataset and NPV = 0.7 and PPV 0.83 for the whole dataset which included patients from both institutions, summarized in Table 4.

**Table 3**
The best performing features.

| Bands (Hz) | 1-4 | | | 4-8 | | | 8-12 | | | 12-20 | | | 20-45 | | | 55-80 | | | 80-250 | | | 250-600 | | | 600- | | |
|---|---|---|---|---|---|---|---|---|---|---|---|---|---|---|---|---|---|---|---|---|---|---|---|---|---|---|---|
| | B | M | J | B | M | J | B | M | J | B | M | J | B | M | J | B | M | J | B | M | J | B | M | J | B | M | J |
| **HFO** | | | | | | | | | | | | | | | | | | | | | | | | | | | |
| Line Length | | | | | ○ ◉ | | ○ ◉ | ◉ | ○ ◉ | ○ ● ◉ | ◉ | ● ◉ | ● ◉ | ◉ | ● ◉ | | ◉ | ◉ | ○ ◉ | | ○ ◉ | | | | | ● | |
| CS detector | | | | | | | | | | | | | | | | | ○ | | | | | ○ ● ◉ | ○ ◉ | ○ ◉ | | | |
| **Univariate** | | | | | | | | | | | | | | | | | | | | | | | | | | | |
| Power in band | | | ● | | | ● | | ◉ | ● | | ○ ◉ | ● | | ○ ◉ | | | ○ | | | | | | | | | | |
| Freq - amp coupling | | | | | | | | | | | | | | | | | | | | | | | | | | | |
| Phase - ampcoupling | | | | | | | | ○ | | | | | | | | | | | | | | | | | | | |
| Power spectral entropy | | | | | | | | | | | | | | | | | | | | | | | | | | | |
| **Bivariate** | | | | | | | | | | | | | | | | | | | | | | | | | | | |
| Correlation | | ○ | | | ○ | | | | | | | | | | | | | | | ● ◉ | | | ● | | | | |
| Correlation with lag | | | | | | | | | | | | | | ● | | | | | | ● ◉ | | | ● | | | | |
| Correlation delay | | | | | ◉ | | | ◉ | | | | | | | | | | | | | | | | | | | |
| Phase synchrony | | | | | | | | | | | | | | | | | | | | ● ◉ | | | ● | | | | |
| Phase consistency | | | | | | | | | | | | | | | | | | | | ● | | | ● | | | | |
| Phase lag index | | | | | | | | | | | | | | | | | | | | ◉ | ● | | | | | | |
| Phase pal index delay | ○ | ● | ● | | | ● | | | | | | | | | | | | | | | | | ○ ◉ | ● | | | |
| Relative entropy | | | | | ○ | ● | | ○ ◉ | ● ◉ | ● | ○ ● ◉ | ○ ● ◉ | ○ ● ◉ | ○ ● ◉ | ○ ● ◉ | ● | ○ ● | ● ◉ | ● ◉ | ○ ● ◉ | ○ ● ◉ | ○ ● ◉ | ○ ● ◉ | ○ ◉ | ○ ● ◉ | | | |

Seizure onset zone=○, Resected=●, Resected+SOZ=◉
B = Brno
M = Mayo
J = Joined

## 4. Discussion

This study reports a multi-feature, machine learning approach for classification of electrodes placed in epileptogenic tissue. It is the first study to our knowledge to combine conventional iEEG features and iEEG connectivity measures. Current inter-ictal methods have largely been focused on a single biomarker of epileptogenic zone, e.g. HFO rate (Worrell et al., 2012). To date, this has been insufficient for clinical practice (Jacobs et al., 2018).

The recent study by Varatharajah et al. (2018) shows that the combination of multiple biomarkers can out-perform algorithms based on a single biomarker. However, this study did not assess connectivity measures. In our data, bivariate measures, especially the relative entropy, substantially contributed to the detector's performance.

From all calculated features the HFO rate and relative entropy were the most relevant for the epileptogenic zone distinction. The limitations of HFOs as a unique biomarker of epileptogenic brain are now widely appreciated and include distinguishing physiological (Buzsaki et al., 1992) and pathological (Matsumoto et al., 2013) HFOs and false positive detections (Bénar et al., 2010; Roehri et al., 2017). The CS detector efficiently eliminates false detections by phase correlation of bandpass filtered signal with a low pass filtered signal, which leads to clear distinction of true oscillations (Cimbálník et al., 2018). But even with optimal HFO detectors the ability to localize epileptogenic brain using HFOs alone is challenging. The current findings in iEEG connectivity studies suggest that changes of connectivity in epileptogenic tissue may be a clinically useful signature of ictogenesis and can substantially contribute to conventional methods for automatic localization of seizure generating tissue. Entropy has the ability to characterize signal randomness and spectral richness. Epileptogenic regions are known for a statistically higher rate of spectrally rich events, e.g., HFOs or epileptiform discharges, compared to healthy brain (Frauscher et al., 2017; Khoo et al., 2018). Therefore, the calculation of relative values of entropy between pathological and non-pathological areas makes this measure compelling in achieving the best possible score. In the Brno center and Mayo Clinic datasets, different features were selected as the most relevant (Table 3). This implies that there may be a dependence on the electrodes, reference signals, and acquisition system used. Studies with different datasets are needed to elucidate the impact of these variables on pathologic tis-

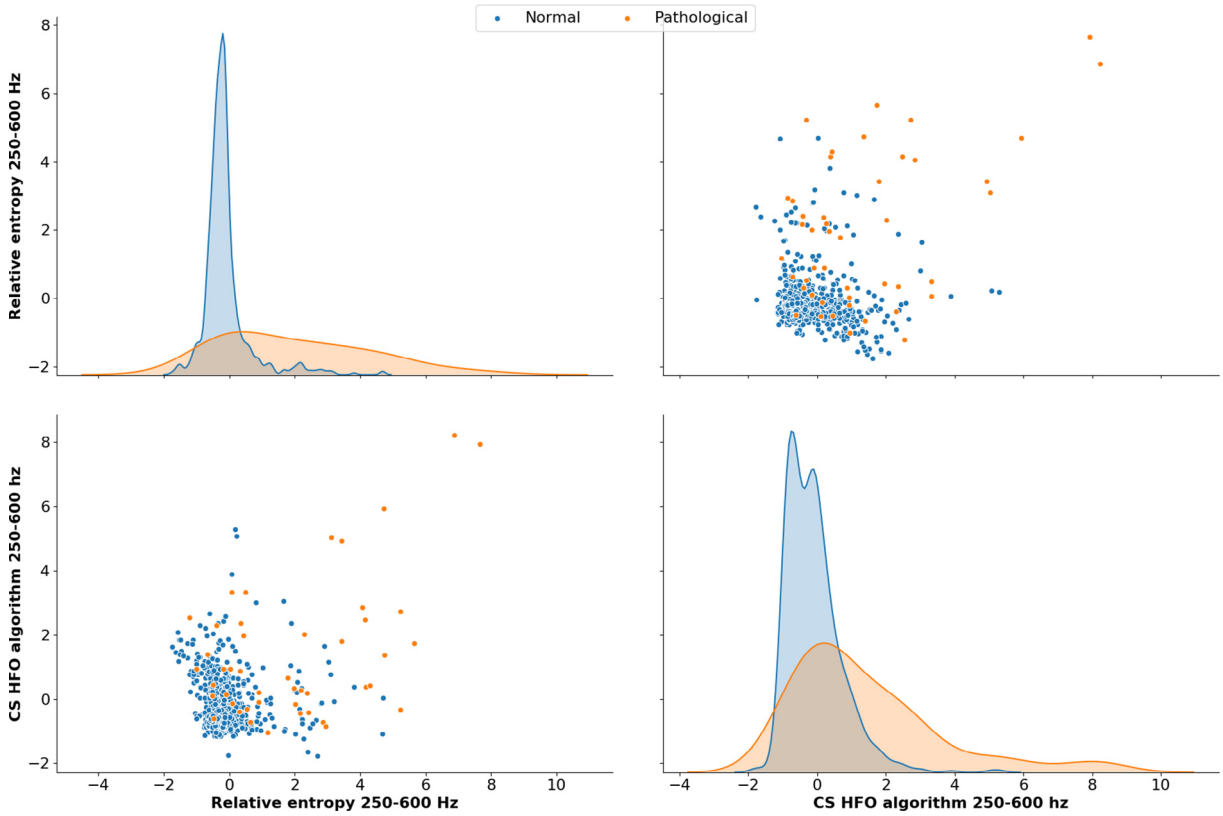


**Fig. 2.** Two best performing features in Brno dataset with SOZ ⋂ resected area target. Relative entropy in FR frequency band and FR HFO show the highest association with the pathology. Distributions of both features demonstrate a long tail.

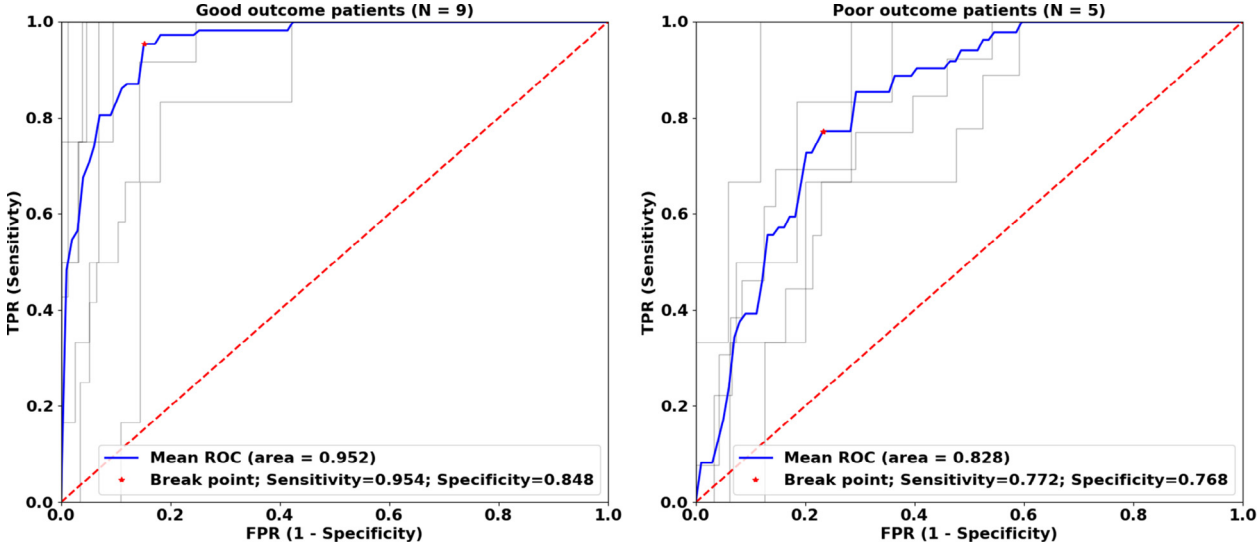


**Fig. 3.** ROC curves for Brno dataset with SOZ ⋂ resected area target. Grey lines represent classification of electrodes in individual patients during cross-validation iterations. Blue lines represent mean ROC curves. ROC analysis in poor outcome patients shows decreased performance indicating that some channels classified by the SVM model as pathologic were not resected.

**Table 4**
Evaluation of the Support Vector Machine models for individual cases.

| Dataset | TP | FP | TN | FN | PPV | NPV | Sensitivity | Specificity |
|---|---|---|---|---|---|---|---|---|
| Mayo | 8 | 1 | 4 | 1 | 0.89 | 0.80 | 0.89 | 0.80 |
| Brno | 9 | 1 | 4 | 0 | 0.90 | 1.00 | 1.00 | 0.80 |
| Joined | 15 | 3 | 7 | 3 | 0.83 | 0.70 | 0.83 | 0.70 |

sue localization. Further, it is well recognized that variability of vigilance levels can have impact on electrophysiological features for localization of epileptogenic tissue (Baud et al., 2018; Gliske et al., 2018). Rates of HFO and epileptiform discharges were shown to be the highest in non-rapid eye movement (NREM) sleep (Staba et al., 2004) which could further enhance the precision of the SVM model. Patients from Brno center were recorded during the day, whereas patients from Mayo Clinic were recorded at night. Therefore it is likely that differences between datasets and subsequent feature selection might also be caused by different states of vigilance. All of these variables had likely some influence on the presented results. Future studies with larger datasets should explore their impact on pathological tissue localization in more detail.

Pathological tissue classification by SVM models which combine HFO features with univariate and bivariate features show superior performance to algorithms utilizing these features or groups of features separately (Cimbalnik et al., 2018; Varatharajah et al., 2018). Classification of tissue under individual electrodes, which is the clinically relevant classification, was the most successful for the definition of SOZ contacts overlapped with resected area in excellent outcome patients. Using the trained SVM models on patients with poor surgical outcome resulted in worse AUC suggesting that channels identified by the algorithm as pathologic were not resected during surgery. Indeed, validating the SVM models using post-surgical outcome proved that resection of channels classified as pathologic led to excellent outcome while failure to resect these channels resulted in poor outcome. The presented algorithm showed similar performance on datasets from two institutions in different day times and clinical settings. Combining the datasets from both institutions resulted in worse performance both in ROC analysis and individual patient analysis which is likely due to difference in selected features.

The architecture of our approach and underlying software is modular, allowing to add other potentially useful features without the need to modify the whole data and model training pipelines. The modularity of the algorithm allows for easy utilization of other advanced processing pipelines (Fedele et al., 2017) or potential biomarkers of epileptogenicity such as very high-frequency oscillations (Brázdil et al., 2017), spike onset zone (Khoo et al., 2018), or low frequency activity (Vanhatalo et al., 2005). Further improvements in pathological tissue classification might be achieved by normalization of calculated features by the values found in normal human brain (Frauscher et al., 2018; Guragain et al., 2018). Recent studies have also reported that epileptogenic activity is changing over time, different states of vigilance and in different brain structures (Baud et al., 2018; Gliske et al., 2018; Guragain et al., 2018). Advanced iEEG signal processing methods might also be dependent on the length of the analyzed segment (Fraschini et al., 2016). In this study, either resting-state or sleep recordings were analyzed, with a minimum length of 30 min without distinction of the states of vigilance or anatomical structure. Testing of the algorithm in specific sleep stages, resting-state conditions, different length of recording and specific anatomical structures can further improve its classification performance.

## 5. Limitations

Three definitions of pathological tissue used in this study are not optimal surrogate for pathological tissue definition. The definition of SOZ suffers from subjective visual determination by medical staff and the resection of such tissue does not guarantee seizure freedom (Téllez-Zenteno et al., 2010). Resected areas in excellent outcome patients often includes normal brain tissue in addition to electrophysiologically abnormal tissue. To overcome the problems of the former two definitions, we considered iEEG channels on a depth electrode pathological, if they were resected, and previously marked as SOZ. However, this definition is not guaranteed to encompass the whole pathological area of the epileptic brain. All of the definitions used suffer from substantial spatial undersampling of the brain tissue due to the limitations of clinical iEEG recordings (Stead et al., 2010; Worrell et al., 2012).

The presented method cannot be applied to multifocal patients due to spatial clustering, which was used to obtain the cluster of contacts with the highest probability of being pathologic. Nonetheless, this can likely be overcome in the clinical setting by visualization of all contact clusters and their probability (Fig. 1) which could potentially be an invaluable tool for surgery planning. In addition, the referential signal was computed as average signal from contacts located in white matter which makes this method inapplicable to cases where white matter was not implanted.

Utilization of connectivity measures in a bivariate manner, i.e. calculation of relations between two adjacent contacts on one depth electrode, can introduce potential bias in final results. This is a well known limitation of bivariate measures in EEG signal processing, which is caused by ignoring possible relation with a third source.

The fact that no features were selected in the highest frequency band might reflect low signal-to-noise ratio in these frequencies. Conversely, absence of useful features in the lowest frequency bands could be caused by the short data segments used in this study. Further study of long-term recordings might reveal useful information in these bands.

Lastly, the use of this algorithm was limited to retrospective analysis of patients who had previously undergone surgery. Although the ‘leave-one-out’ approach can be interpreted as pseudo-prospective study, a true prospective study is required to clearly establish its effectiveness.

## 6. Conclusion

In this retrospective study in a modest number of patients, promising results were achieved in localization of epileptogenic regions by SVM models that combine multiple features from 30 min of inter-ictal iEEG recordings. Pilot testing of the proposed algorithm in two different datasets suggests it is suitable for further testing in prospective studies, and ultimately, its possible implementation in clinical practise. Our results also suggests better performance of multi-feature methods in epileptogenic tissue localization than methods, which are using single iEEG feature, e.g. HFO.

## Acknowledgements

The authors would like to thank Drs. Gregory Cascino, Jeffry Britton, Elson So, Cheolsu Shin, Terry Lagerlund, Fredric Meyer, Richard Marsh, Elaine Wirrell, Lily Wong-Kisel, and Kate Nickels for clinical care of patients and assistance with translational research. We appreciate the technical support provided by Cindy Nelson and Karla Crockett. We acknowledge the core facility MAFIL of CEITEC supported by the MEYS CR (LM2015062 Czech-BioImaging). This research was supported by the National Institutes of Health R01-NS063039(GW), R01-NS078136, Mayo Clinic Discovery Translation Grant, projects no. LQ1605 and LO1212 from the National Program of Sustainability II (MEYS CR), and Ministry of Education, Youth and Sports of the Czech Republic project no. LTAUSA18056.

## Appendix A. Supplementary material

Supplementary data to this article can be found online at https://doi.org/10.1016/j.clinph.2019.07.024.

## References


Antony AR, Alexopoulos AV, González-Martínez JA, Mosher JC, Jehi L, Burgess RC, et al. Functional connectivity estimated from intracranial EEG predicts surgical outcome in intractable temporal lobe epilepsy. PLoS ONE 2013;8(10). e77916.

Baud MO, Kleen JK, Mirro EA, Andrechak JC, King-Stephens D, Chang EF, et al. Multi-day rhythms modulate seizure risk in epilepsy. Nat Commun 2018;9(1). Available from: https://doi.org/10.1038/s41467-017-02577-y.

Bénar CG, Chauvière L, Bartolomei F, Wendling F. Pitfalls of high-pass filtering for detecting epileptic oscillations: a technical note on "false" ripples. Clin Neurophysiol 2010;121(3):301–10.

Bergey GK, Morrell MJ, Mizrahi EM, Goldman A, King-Stephens D, Nair D, et al. Long-term treatment with responsive brain stimulation in adults with refractory partial seizures. Neurology 2015;84(8):810–7.

Bettus G, Wendling F, Guye M, Valton L, Régis J, Chauvel P, et al. Enhanced EEG functional connectivity in mesial temporal lobe epilepsy. Epilepsy Res 2008;81(1):58–68.

Bragin A, Mody I, Wilson CL, Engel Jr J. Local generation of fast ripples in epileptic brain. J Neurosci 2002;22(5):2012–21.

Brázdil M, Cimbálník J, Roman R, Shaw DJ, Stead MM, Daniel P, et al. Impact of cognitive stimulation on ripples within human epileptic and non-epileptic hippocampus. BMC Neurosci 2015;16:47.

Brázdil M, Pail M, Halámek J, Plešinger F, Cimbálník J, Roman R, et al. Very high-frequency oscillations: Novel biomarkers of the epileptogenic zone. Ann Neurol 2017;82(2):299–310.

Buzsaki G, Horvath Z, Urioste R, Hetke J, Wise K. High-frequency network oscillation in the hippocampus. Science 1992;256(5059):1025–7.

Cimbalnik J, Brinkmann B, Kremen V, Jurak P, Berry B, Van Gompel J, et al. Physiological and pathological high frequency oscillations in focal epilepsy. Ann Clin Transl Neurol 2018. Available from: https://doi.org/10.1002/acn3.618.

Cimbálník J, Hewitt A, Worrell G, Stead M. The CS algorithm: A novel method for high frequency oscillation detection in EEG. J Neurosci Methods 2018;293:6–16.

Cimbalnik J, Kucewicz MT, Worrell G. Interictal high-frequency oscillations in focal human epilepsy. Curr Opin Neurol 2016;29(2):175–81.

Dauwels J, Eskandar E, Cash S. Localization of seizure onset area from intracranial non-seizure EEG by exploiting locally enhanced synchrony. Conf Proc IEEE Eng Med Biol Soc 2009;2009:2180–3.

Fedele T, Burnos S, Boran E, Krayenbühl N, Hilfiker P, Grunwald T, et al. Resection of high frequency oscillations predicts seizure outcome in the individual patient. Sci Rep 2017;7(1):13836.

Fisher RS, Velasco AL. Electrical brain stimulation for epilepsy. Nat Rev Neurol 2014;10(5):261–70.

Fraschini M, Demuru M, Crobe A, Marrosu F, Stam CJ, Hillebrand A. The effect of epoch length on estimated EEG functional connectivity and brain network organisation. J Neural Eng 2016;13(3). 036015.

Frauscher B, Bartolomei F, Kobayashi K, Cimbalnik J, van 't Klooster MA, Rampp S, et al. High-frequency oscillations: The state of clinical research. Epilepsia 2017;58(8):1316–29.

Frauscher B, von Ellenrieder N, Zelmann R, Doležalová I, Minotti L, Olivier A, et al. Atlas of the normal intracranial electroencephalogram: neurophysiological awake activity in different cortical areas. Brain 2018;141(4):1130–44.

Gardner AB, Worrell GA, Marsh E, Dlugos D, Litt B. Human and automated detection of high-frequency oscillations in clinical intracranial EEG recordings. Clin Neurophysiol 2007;118(5):1134–43.

Gliske SV, Irwin ZT, Chestek C, Hegeman GL, Brinkmann B, Sagher O, et al. Variability in the location of high frequency oscillations during prolonged intracranial EEG recordings. Nat Commun 2018;9(1):2155.

Gnatkovsky V, de Curtis M, Pastori C, Cardinale F, Lo Russo G, Mai R, et al. Biomarkers of epileptogenic zone defined by quantified stereo-EEG analysis. Epilepsia 2014;55(2):296–305.

Gross DW, Gotman J. Correlation of high-frequency oscillations with the sleep-wake cycle and cognitive activity in humans. Neuroscience 1999;94(4):1005–18.

Guragain H, Cimbalnik J, Stead M, Groppe DM, Berry BM, Kremen V, et al. Spatial variation in high-frequency oscillation rates and amplitudes in intracranial EEG. Neurology 2018;90(8):e639–46.

Iglewicz B, Hoaglin DC. How to detect and handle outliers. Asq Press; 1993.

Jacobs J, LeVan P, Chander R, Hall J, Dubeau F, Gotman J. Interictal high-frequency oscillations (80–500 Hz) are an indicator of seizure onset areas independent of spikes in the human epileptic brain. Epilepsia 2008;49(11):1893–907.

Jacobs J, Wu JY, Perucca P, Zelmann R, Mader M, Dubeau F, et al. Removing high-frequency oscillations: A prospective multicenter study on seizure outcome. Neurology 2018. Available from: https://doi.org/10.1212/WNL.0000000000006158.

Katzner S, Nauhaus I, Benucci A, Bonin V, Ringach DL, Carandini M. Local origin of field potentials in visual cortex. Neuron 2009;61(1):35–41.

Kelly KM, Chung SS. Surgical treatment for refractory epilepsy: review of patient evaluation and surgical options. Epilepsy Res Treat 2011;2011. 303624.

Khadjevand F, Cimbalnik J, Worrell GA. Progress and remaining challenges in the application of high frequency oscillations as biomarkers of epileptic brain. Curr Opin Biomed Eng 2017;4:87–96.

Khoo HM, von Ellenrieder N, Zazubovits N, He D, Dubeau F, Gotman J. The spike onset zone: The region where epileptic spikes start and from where they propagate. Neurology 2018;91(7):e666–74.

Klimes P, Duque JJ, Brinkmann B, Van Gompel J, Stead M, St Louis EK, et al. The functional organization of human epileptic hippocampus. J Neurophysiol 2016;115(6):3140–5.

Kremen V, Duque JJ, Brinkmann BH, Berry BM, Kucewicz MT, Khadjevand F, et al. Behavioral state classification in epileptic brain using intracranial electrophysiology. J Neural Eng 2017;14(2). 026001.

Kucewicz MT, Cimbalnik J, Matsumoto JY, Brinkmann BH, Bower MR, Vasoli V, et al. High frequency oscillations are associated with cognitive processing in human recognition memory. Brain 2014;137:2231–44.

Leonardi M, Ustun TB. The global burden of epilepsy. Epilepsia 2002;43(Suppl 6):21–5.

Lüders H, Comair YG. Epilepsy surgery. Lippincott Williams & Wilkins; 2001.

Matsumoto A, Brinkmann BH, Matthew Stead S, Matsumoto J, Kucewicz MT, Marsh WR, et al. Pathological and physiological high-frequency oscillations in focal human epilepsy. J Neurophysiol 2013;110(8):1958–64.

Nejedly P, Cimbalnik J, Klimes P, Plesinger F, Halamek J, Kremen V, et al. Intracerebral EEG artifact identification using convolutional neural networks. Neuroinformatics 2018. Available from: https://doi.org/10.1007/s12021-018-9397-6.

Pearce A, Wulsin D, Blanco JA, Krieger A, Litt B, Stacey WC. Temporal changes of neocortical high-frequency oscillations in epilepsy. J Neurophysiol 2013;110(5):1167–79.

Roehri N, Pizzo F, Bartolomei F, Wendling F, Bénar C-G. What are the assets and weaknesses of HFO detectors? A benchmark framework based on realistic simulations. PLoS ONE 2017;12(4). e0174702.

Staba RJ, Wilson CL, Bragin A, Fried I, Engel Jr J. Sleep states differentiate single neuron activity recorded from human epileptic hippocampus, entorhinal cortex, and subiculum. J Neurosci 2002;22(13):5694–704.

Staba RJ, Wilson CL, Bragin A, Jhung D, Fried I, Engel Jr J. High-frequency oscillations recorded in human medial temporal lobe during sleep. Ann Neurol 2004;56(1):108–15.

Stam CJ, Nolte G, Daffertshofer A. Phase lag index: assessment of functional connectivity from multi channel EEG and MEG with diminished bias from common sources. Hum Brain Mapp 2007;28(11):1178–93.

Stead M, Bower M, Brinkmann BH, Lee K, Marsh WR, Meyer FB, et al. Microseizures and the spatiotemporal scales of human partial epilepsy. Brain 2010;133(9):2789–97.

Téllez-Zenteno JF, Ronquillo LH, Moien-Afshari F, Wiebe S. Surgical outcomes in lesional and non-lesional epilepsy: A systematic review and meta-analysis. Epilepsy Res 2010;89(2–3):310–8.

Tzourio-Mazoyer N, Landeau B, Papathanassiou D, Crivello F, Etard O, Delcroix N, et al. Automated anatomical labeling of activations in SPM using a macroscopic anatomical parcellation of the MNI MRI single-subject brain. Neuroimage 2002;15(1):273–89.

Van Gompel JJ, Worrell GA, Bell ML, Patrick TA, Cascino GD, Raffel C, et al. Intracranial electroencephalography with subdural grid electrodes: techniques, complications, and outcomes. Neurosurgery 2008;63(3):498–506.

Vanhatalo S, Voipio J, Kaila K. Full-band EEG (FbEEG): an emerging standard in electroencephalography. Clin Neurophysiol 2005;116(1):1–8.

Varatharajah Y, Berry B, Cimbalnik J, Kremen V, Van Gompel J, Stead M, et al. Integrating artificial intelligence with real-time intracranial EEG monitoring to automate interictal identification of seizure onset zones in focal epilepsy. J Neural Eng 2018;15(4). 046035.

Warren CP, Hu S, Stead M, Brinkmann BH, Bower MR, Worrell GA. Synchrony in normal and focal epileptic brain: the seizure onset zone is functionally disconnected. J Neurophysiol 2010;104(6):3530–9.

Wiebe S, Blume WT, Girvin JP, Eliasziw M. Effectiveness and efficiency of surgery for temporal lobe epilepsy study group. A randomized, controlled trial of surgery for temporal-lobe epilepsy. N Engl J Med 2001;345(5):311–8.

Worrell GA, Gardner AB, Stead SM, Hu S, Goerss S, Cascino GJ, et al. High-frequency oscillations in human temporal lobe: simultaneous microwire and clinical macroelectrode recordings. Brain 2008;131:928–37.

Worrell GA, Jerbi K, Kobayashi K, Lina JM, Zelmann R, Van Quyen ML. Recording and analysis techniques for high-frequency oscillations. Prog Neurobiol 2012;98(3):265–78.

# CHAPTER 7

# Characteristics of high-frequency oscillations

Understanding the mechanisms of pathological high-frequency oscillations (HFOs) should lead to a better understanding of epileptogenic tissue's functional organization and the abnormal dynamics of epileptic neuronal networks (Jiruska et al., 2017). Invasive EEG, the recording of electrical activity using electrodes placed directly on or within the brain, is used when non-invasive modalities like non-invasive scalp EEG, MRI, and functional imaging are unable to unambiguously identify epileptogenic brain area (Blanco et al., 2011). Despite the recording of seizures with invasive EEG (iEEG), considered the 'gold standard' for localizing focal epileptogenic brain and the seizure onset zone (SOZ), epilepsy surgery is often unsuccessful (Urrestarazu et al., 2007; Najm et al., 2013; Cimbalnik et al., 2017). It seems that for an excellent postsurgical outcome, it is more important to detect the epileptogenic zone than the SOZ by means of HFOs (Zijlmans et al., 2012). In this context, there has been a growing interest in the analysis of interictal high-frequency oscillations (HFOs), primarily with the goal of understanding their value for identifying the epileptogenic zone and their correlation with epileptogenicity. However, the reliability of HFOs as a biomarker of epileptogenicity and of the epileptogenic zone remains still uncertain (Haegelen et al., 2013; Wang et al., 2013). It was presented, that combining multiple HFO features shows better performance than algorithms using a single HFO marker, mentioned HFO rates (Cimbalnik et al., 2019). Moreover, physiological, non-epileptic HFOs and their existence pose a challenge, as disentangling them from clinically relevant pathological HFOs still is an unsolved issue with considerable influence on HFO research (Thomschewski et al., 2019). The HFO frequency range, in general, is not sufficient to differentiate "epileptogenic" and "non-epileptogenic" HFOs. Despite the promise of seizure-independent other biomarkers, no single HFO marker has been consistently shown to be effective for all patients (Jacobs et al., 2018).

Epileptic high-frequency oscillations include not only pathological activities with frequencies above 80Hz recorded in epileptic brain in vitro, in animals, and in human patients (Zijlmans et al., 2012; Frauscher et al., 2017; Jiruska et al., 2017). Several researchers studied the incidence, spatial distribution, and signal characteristics of high-frequency oscillations within and also outside the epileptic network (Jiruska & Bragin, 2011; Jefferys et al., 2012; Matsumoto et al., 2013; Alkawadri et al., 2014; Pail et al., 2017). High-frequency oscillations represent a very heterogeneous group of (patho)physiological phenomena, which includes a number of different oscillations that can be classified by many criteria, most often frequency. It is proven that HFOs from nonepileptic sites had lower peak frequency than HFOs from epileptic sites (Alkawadri et al., 2015; Frauscher et al., 2018). Furthermore, oscillations can be classified according to the mechanisms of origin, pathogenicity, location, morphology, duration, amplitude, entropy, and other characteristics.

The main aim of describing individual HFO events is to find clearly pathological ones because their epileptogenicity may differ. HFOs could reflect increased cortical excitability, perhaps more than epileptogenicity. Despite the potential to delineate the epileptogenic zone, ripples and even fast ripples have also been reported in normal cortical areas (Axmacher et al., 2008; Nagasawa et al., 2012; Matsumoto et al., 2013; Melani et al. 2013; Kucewicz et al., 2014). The study of Alkawadri et al., (2014) illustrated the frequent, consistent, and symmetric occurrence of nonepileptic ripples over vast areas of the neocortex. The following sublobes were consistently involved: lateral frontal, lateral parietal (specifically perirolandic), all occipital subregions, basal temporal, and orbitofrontal (Alkawadri et al., 2014). Regions with the nonepileptic FR were suggested in the occipital lobes and extraoccipitally, in the lateral perirolandic region (Alkawadri et al., 2014). The HFO frequency range, in general, is not sufficient to differentiate “physiological” and “pathological” HFOs. One challenge in the interpretation of HFO rates is that different brain regions generate highly variable rates of physiological HFOs (von Ellenrieder et al., 2016). This is given above all by the relatively rare placement of electrodes in healthy brain tissue, by the difficulty in identifying healthy brain regions, and by the lack of standardization for electrode placement, compared to scalp EEG, resulting in problems in accumulating data from multiple individuals with heterogeneous implantation schemes (Frauscher et al., 2018). Therefore, some authors have suggested clustering HFOs based on characteristics and features such as frequency, rates, spectral properties, duration, amplitude, and so on (Matsumoto et al., 2013; Alkawadri et al., 2014; Malinowska et al., 2015; Pail et al., 2017). Nevertheless, none of the cutoffs of the signal parameters is both highly sensitive and specific for reliable distinction.

There are two basic approaches to measuring, assessing, and categorization of individual HFOs. One of them is monitoring and measuring the characteristics of spontaneous HFOs in particular areas and their further comparison. The second one is monitoring the effect of particular modulation on individual HFOs, whether spontaneous or induced. This modulation can be physiological, such as sleep phases, or artificial - a specific cognitive or motor task or sensory stimulation. Subsequently, due to the different reactivity of individual HFOs, HFOs are categorized, e.g., as either pathological or physiological.

**Published research**

# Frequency-independent characteristics of high-frequency oscillations in epileptic and non-epileptic regions

Martin Pail

Pavel Řehulka

Jan Cimbálník

Irena Doležalová

Jan Chrastina

Milan Brázdil

**Clin Neurophysiol. 2017 Jan;128(1):106-114. doi: 10.1016/j.clinph.2016.10.011.**

## Commentary on published paper

The purpose of the published study was to determine whether there are frequency-independent high-frequency oscillation parameters that may differ in epileptic (epileptogenic zone) and non-epileptic regions. We hypothesized that epileptic brain tissue might produce specific pathological HFO patterns, as was shown using power spectral density in our previous study (Brázdil et al., 2010).

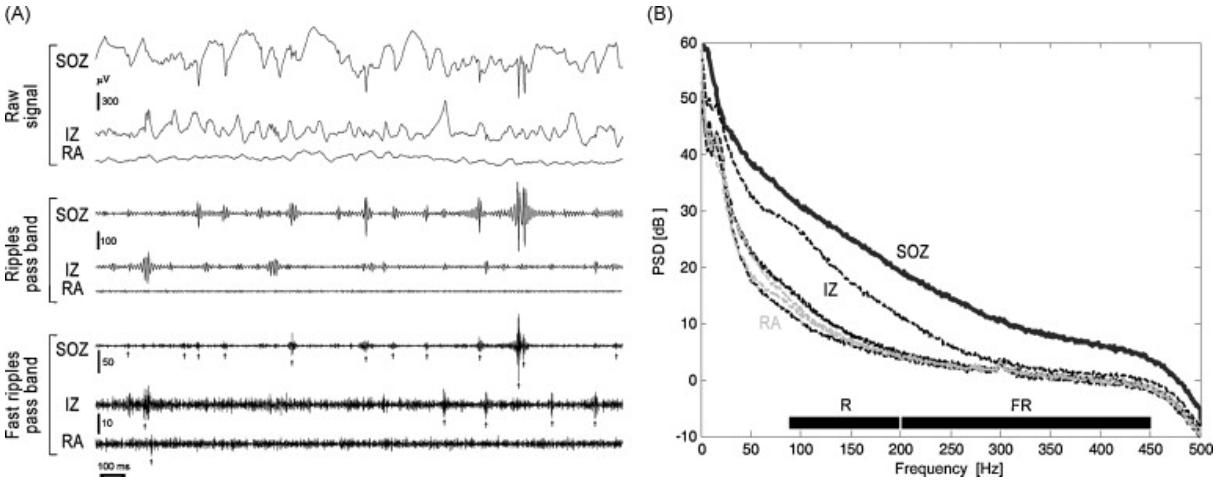


*Figure 8: Examples of ripples and fast ripples (A) and power spectral density (B) for the investigated frequencies in the same patient with focal cortical dysplasia. Left panel: signals from SOZ, IZ, and RA. 2 s time window, from top: raw signal, ripples and fast ripples pass band. In the case of fast ripples, there is the different vertical scale for SOZ and IZ/RA. Arrows mark the position of detected FR – automated detection of HFOs (Gardner et al., 2007). Right panel: black (SOZ), dashed black (IZ – irritative zone), dashed gray (RA – remote area). (Brázdil et al., 2010)*

We studied 31 consecutive patients with medically intractable focal (temporal and extratemporal) epilepsies who were examined by either intracerebral or subdural electrodes. Automated detection was used to detect HFOs during resting states. The characteristics (rate, amplitude, and duration) of HFOs were statistically compared within three groups: the seizure onset zone (SOZ), the irritative zone (IZ), and areas outside the IZ and SOZ (nonSOZ/nonIZ), determined by iEEG results.

In all patients, fast ripples (FR) and ripples (R) were significantly more frequent and shorter in the SOZ than in the nonSOZ/nonIZ region. In the group of patients with favorable surgical outcomes, the relative amplitude of FR was higher in the SOZ than in the IZ and nonIZ/nonSOZ regions; in patients with poor outcomes, the results were reversed. Ripple's relative amplitude was significantly higher in the SOZ (in contrast, what was seen by Alkawadri et al., 2014), with no difference between patients with poor and favorable surgical outcomes. The highest rate of FR was in the seizure onset zone.

According to previously published data, which was further corroborated by our study, the FR and R rate were significantly higher in the SOZ than in nonSOZ/nonIZ regions (Urrestarazu et al., 2007, Jacobs et al., 2008, Jacobs et al., 2009; Andrade-Valença et al., 2012). As in a study by Jacobs et al. (2008), the distinction between pathological and normal areas was worse for R than for FR. There is cumulative evidence that more extensive networks influence R generation; smaller pathological networks (a region of less than 1 $mm^3$) are involved in FR generation (Bragin et al., 2002a; Brázdil et al., 2017). Concerning the duration of HFOs, as in the study by Wang et al. (2013), our data suggested longer durations of both R and FR outside SOZ. Regarding the R, this finding might also be explained by Nagasawa's (2012) and Alkawadri (2014) works, who revealed that the duration of spontaneous R HFOs of a presumably physiological nature were significantly longer than that of epileptogenic HFOs. In other studies, however, the duration of pathological (in the SOZ) and non-pathological (nonSOZ region) FR was not diverse (Nagasawa et al., 2012, Alkawadri et al., 2014), or the longer duration of both R (Brázdil et al., 2015) and FR was revealed within the SOZ (Jacobs et al., 2008, Matsumoto et al., 2013, Pail et al., 2020). The discrepancies among studies in the duration of R and FR in various regions might be explained by different proportions of included focal epilepsies (hippocampus vs. neocortex). There have been noteworthy results regarding relative HFO amplitude in epileptic and non-epileptic regions in particular subgroups of patients. Interestingly, in the group of patients with favorable outcomes, the relative HFO amplitude (especially FR) was higher in the SOZ than in other regions; in other patients with “poor outcomes”, the results of FR analysis were reversed. Based on these results, R and FR relative amplitude might contribute to neurosurgical resection planning, showing possible worse prognosis in patients with higher amplitudes, especially of FR outside the SOZ. This indicates it is possible that the true SOZ was not adequately detected or a more dispersed or multifocal epileptogenic zone/SOZ is present, a pattern that is too diffuse to permit a successful resective strategy.

Nevertheless, the limitation of this study was that seizures originating from areas not covered by electrodes but propagating to the actual electrode positions might lead to misinterpretation (Zijlmans et al., 2012). There is, however, no exact cut-off value for all mentioned characteristics (both duration and amplitude), which can separate the SOZ, the IZ, and other regions. Detection of HFOs in specific sleep stages, resting-state conditions, different length of recording, and specific anatomical structures can further improve the classification performance of HFOs. Further improvements in pathological tissue classification might be achieved by normalization of calculated features by the values found in the average human brain (Frauscher et al., 2018).

To conclude our study concerning the characteristics of HFOs, various HFO parameters, especially of FR, differ in epileptic and non-epileptic regions. We suggested that the amplitude and duration may be as important as the frequency band and rate of HFO in marking the seizure onset region or the epileptogenic area and may provide additional information on epileptogenicity. In summary, FR are more frequent, shorter, and have higher relative amplitudes in the SOZ area than in other regions. The study suggested a possible worse prognosis in patients with higher amplitudes of FR outside the

SOZ. This feature may imply a greater extent of the epileptogenic region. Although duration, amplitude, and peak frequency are the most effective distinguishing features, there was extensive overlap between the groups.

Clinical Neurophysiology 128 (2017) 106–114

Contents lists available at ScienceDirect

Clinical Neurophysiology

journal homepage: www.elsevier.com/locate/clinph

# Frequency-independent characteristics of high-frequency oscillations in epileptic and non-epileptic regions

Martin Pail [a,*], Pavel Řehulka [a], Jan Cimbálník [b], Irena Doležalová [a], Jan Chrastina [c], Milan Brázdil [a,d]

[a] Brno Epilepsy Center, Department of Neurology, St. Anne's University Hospital and Faculty of Medicine, Masaryk University, Brno, Czech Republic
[b] International Clinical Research Center, St. Anne's University Hospital, Brno, Czech Republic
[c] Brno Epilepsy Center, Department of Neurosurgery, St. Anne's University Hospital and Faculty of Medicine, Masaryk University, Brno, Czech Republic
[d] Behavioral and Social Neuroscience Research Group, CEITEC – Central European Institute of Technology, Masaryk University, Brno, Czech Republic

ARTICLE INFO

*Article history:*
Accepted 15 October 2016
Available online 29 October 2016

*Keywords:*
High frequency oscillations
Ripples
Fast ripples
Temporal lobe epilepsy
Extratemporal lobe epilepsy
Seizure onset zone
Epileptogenic zone
Irritative zone

HIGHLIGHTS

- The highest rate of fast ripples is in the seizure onset zone (SOZ).
- A worse prognosis (no seizure freedom after surgery) is associated with higher amplitudes of fast ripples outside the SOZ.
- In the SOZ, high frequency oscillations are more frequent, shorter, and have higher amplitudes.

ABSTRACT

*Objective:* The purpose of the presented study is to determine whether there are frequency-independent high-frequency oscillation (HFO) parameters which may differ in epileptic and non-epileptic regions.
*Methods:* We studied 31 consecutive patients with medically intractable focal (temporal and extratemporal) epilepsies who were examined by either intracerebral or subdural electrodes. Automated detection was used to detect HFO. The characteristics (rate, amplitude, and duration) of HFO were statistically compared within three groups: the seizure onset zone (SOZ), the irritative zone (IZ), and areas outside the IZ and SOZ (nonSOZ/nonIZ).
*Results:* In all patients, fast ripples (FR) and ripples (R) were significantly more frequent and shorter in the SOZ than in the nonSOZ/nonIZ region. In the group of patients with favorable surgical outcomes, the relative amplitude of FR was higher in the SOZ than in the IZ and nonIZ/nonSOZ regions; in patients with poor outcomes, the results were reversed. The relative amplitude of R was significantly higher in the SOZ, with no difference between patients with poor and favorable surgical outcomes.
*Conclusions:* FR are more frequent, shorter, and have higher relative amplitudes in the SOZ area than in other regions. The study suggests a worse prognosis in patients with higher amplitudes of FR outside the SOZ.
*Significance:* Various HFO parameters, especially of FR, differ in epileptic and non-epileptic regions. The amplitude and duration may be as important as the frequency band and rate of HFO in marking the seizure onset region or the epileptogenic area and may provide additional information on epileptogenicity.


## 1. Introduction

Over the past few years, there has been growing interest in the analysis of interictal high frequency oscillations (HFO), primarily with the goal of understanding their value for identifying the epileptogenic zone and their correlation with epileptogenicity. HFO promise to be more specific than interictal spikes for epileptogenic brain tissue and even more specific than the seizure-onset area (Jacobs et al., 2008).

HFO are short-lasting field potentials, which arise as a result of the synchronization of neuronal populations. HFO have been identified and defined in terms of frequency: ripples (80–250 Hz), fast ripples (250–600 Hz) (reviewed in Bragin et al., 2010; Engel et al.,

* Corresponding author at: Department of Neurology, St. Anne's University Hospital and Faculty of Medicine, Pekařská 53, 656 91 Brno, Czech Republic. Fax: +420 543 182 624.
*E-mail address:* martin.pail@fnusa.cz (M. Pail).

http://dx.doi.org/10.1016/j.clinph.2016.10.011
1388-2457/

2009), and very high frequency oscillations (1000–2500 Hz) (Usui et al., 2015). HFO have been widely studied in animals and humans, in mesial temporal and neocortical structures, under physiological and pathological conditions, using microelectrodes or commercial macroelectrodes, and during interictal and ictal periods (Bragin et al., 1999a,b; Staba et al., 2002; Worrell et al., 2004, 2008; Urrestarazu et al., 2007; Jacobs et al., 2008, 2009; Bagshaw et al., 2009; Brázdil et al., 2010; Crépon et al., 2010). However, the reliability of HFO as a biomarker of epileptogenicity and the seizure-onset zone remains uncertain (Haegelen et al., 2013; Jobst, 2013; Wang et al., 2013).

Ripples, observed as a physiological finding in the hippocampus and parahippocampal structures, are thought to be functionally involved in memory consolidation (Buzsáki et al., 1992; Axmacher et al., 2010; Lachaux et al., 2012). The spontaneous occurrence of ripples in humans is also believed to be physiological in the primary visual cortex (Nagasawa et al., 2012; Wang et al., 2013) and in the primary motor cortex (Wang et al., 2013). The presumption of the exclusively physiological nature of ripples was, however, impugned by evidence of HFO in ripple ranges recorded in the dentate gyrus after epileptogenic insult in an animal model of kainate-induced status epilepticus (Bragin et al., 1999b, 2004).

Conversely, fast ripples were repeatedly reported as a biomarker of epileptogenesis and epileptogenicity, both in animal models and in human epilepsy (Bragin et al., 1999a,b; Staba et al., 2002). It is important that HFO in the fast ripple range (at about 600 Hz) can also be considered physiological, as they were previously evoked during stimulation of the somatosensory cortex (Curio et al., 1997). Thus the HFO frequency range, in general, is not sufficient to differentiate physiological and pathological HFO (Bragin, 2007). On the other hand, there is evidence of favorable epilepsy surgery outcome after the removal of tissue generating interictal HFO, especially fast ripples (Jacobs et al., 2010; Wu et al., 2010; Akiyama et al., 2011).

Several authors have tried to distinguish between pathological and physiological HFO on the basis of a specific regional distribution in respective mesial temporal structures (Jiruska and Bragin, 2011); some have investigated the difference between task-induced and spontaneous HFO (Nagasawa et al., 2012; Matsumoto et al., 2013; Brázdil et al., 2015); others have studied the association of HFO with epileptiform discharges (Crépon et al., 2010; Urrestarazu et al., 2007; Wang et al., 2013). Interictal HFO (both ripples and fast ripples) rates were proven significantly higher within the seizure onset zone (SOZ) than outside it (Jacobs et al., 2009).

The purpose of the present study is to identify whether there are any other frequency-independent HFO parameters that potentially differ in areas within the SOZ, within the irritative zone (IZ), and in areas outside the IZ/SOZ.

## 2. Methods

### 2.1. Subjects

Our sample comprised 31 patients (19 females; 12 males) ranging in age from 13 to 56 years (mean age 33.4 years, SD = 10.5), all with medically intractable focal epilepsies (Table 1). All the subjects fulfilled the diagnostic criteria for either medically intractable temporal lobe epilepsy (TLE) – 22 subjects or extratemporal lobe epilepsy (ETLE) – 9 subjects. The diagnosis was made according the ILAE criteria (Commission on Classification and Terminology of ILAE, 1989). The main demographic and clinical characteristics of the included subjects are shown in Table 1.

#### 2.1.1. Presurgical evaluation

All 31 patients underwent a comprehensive presurgical evaluation, including a detailed history and neurological examination, magnetic resonance imaging (MRI), neuropsychological testing, and scalp and invasive video-EEG monitoring (Table 1). Most of the subjects had not previously undergone intracranial surgery. One subject underwent resection of venous malformation within the left P-O region before SEEG and re-operation; in one subject a resection of the pole of the left temporal lobe had been performed, and in one subject a limited left AMTR was performed before SEEG monitoring. Prior to invasive EEG, two subjects had a vagus nerve stimulation system implanted, with unfavorable seizure frequency outcome. The duration of clinical monitoring and the location and number of implanted electrodes were determined in accordance with clinical considerations.

#### 2.1.2. Surgery and outcome measure

Most of the patients (28) underwent surgical intervention (implantation of VNS was performed in 7 patients and brain resection in 21 patients; details are shown in Table 1). The follow-up interval after epilepsy surgery was at least 12 months. After surgical resection, 8 patients were rated as Engel IA, one patient was Engel IIA, and 11 patients were Engel III or IV; the Engel rating is unknown for one patient (due the loss to follow-up care).

This study was approved by the St. Anne's University Hospital Research Ethics Committee and the Ethics Committee of Masaryk University. All patients signed an informed consent form.

### 2.2. SEEG

Depth electrodes (mostly SEEG; grids and strips were used in two patients) were implanted to localize the seizure origin prior to surgical treatment. The sites of electrode placements were individualized according to seizure semiology, clinical history, noninvasive EEG investigations, and neuroimaging results. Standard intracerebral 5-, 10-, and 15-contact Micro Deep semi-flexible multicontact platinum electrodes (ALCIS) were used with a diameter of 0.8 mm, a contact length of 2 mm, an inter-contact distance of 1.5 mm, and a contact surface area of 5 $mm^2$. Their position within the brain was afterwards verified by MRI with electrodes in situ (see Table 1). In two patients, platinum subdural strip and grid electrodes (Radionics) were used. Thirty minutes of artifact-free continuous interictal SEEG data (recorded during wakefulness) was analyzed for each subject. This period is sufficient based on the results of previously published papers (Jacobs et al., 2008; Zelmann et al., 2009; Andrade-Valença et al., 2012). The EEGs were acquired at 25 kHz sampling frequency and subsequently low-pass filtered and downsampled to 5 kHz. High harmonics produced by the system (artificial harmonics) are accounted for during EEG acquisition. A reference average montage was used for the analysis.

#### 2.2.1. Labeling of analyzed contacts

The contacts in each subject were divided into three groups for further HFO analysis. The distribution was done visually (by co-authors M.P. and I.D.) by a standard analysis of ictal and interictal SEEG recordings. The first group was labelled SOZ contacts: the channels that revealed the first ictal activity. The second group was labelled IZ contacts: the channels where interictal epileptiform discharges were detected, but no seizure onset was detected. The remaining non-spiking contacts were labelled nonSOZ/nonIZ. Only contacts localized in gray matter were included in the study.

#### 2.2.2. Automated detection of HFO in resting awake SEEG

The algorithm for HFO detection is explained in more detail in the Supplementum. HFO were detected by a custom Matlab detection algorithm. The raw signal (Supplementary Fig. S1) was divided

**Table 1**
Demographic and clinical data of the patients.

| Subject gender | Age at seizure onset | Age at invasive EEG | Seizure frequency/monthly | Febrile seizures/precipitating events | MRI (signs of) | Brain lobes explored and number of implanted electrodes | Region SOZ (epileptogenic zone) | Intervention/histopathology | Postsurgical outcomes (Engel) (years) |
|---|---|---|---|---|---|---|---|---|---|
| 1 (F) | 16 | 20 | CPS/4plus | 0 | Normal | T (3), T′(2) | H bilaterally | VNS | – |
| 2 (F) | 19 | 57 | CPS/2plus, sGTCS/6 | 0 | Postischemic lesions within left T-O and H | F′(1), T′(5) | Left H | AMTR/gliosis, hemosiderin within T pole | IA (3.5) |
| 3 (F) | 4 | 34 | CPS/50 | 0 | Hypotrophic right H | T′(3), T(3) | Right H | AMTR/hippocampal sclerosis grade III | IA (3.5) |
| 4 (F) | 6 | 19 | CPS/4 | Perinatal hypoxia | Gliosis and cortical abnormalities left PO | O′(2), T′(2), P′(1), O(2), F(2) | Left TPO region | Cortectomy/negat | IV (3) |
| 5 (F) | 2 | 34 | SPS,CPS/4 | Perinatal asphyxia | Polymicrogyria left F, postoperative changes of left PO | F′ (8), P′(2), T′(1) | Left P lobe, pericentral area | VNS | – |
| 6 (F) | 16 | 33 | CPS/5 | Perinatal hypoxia | Bilat. HS | T′(4), T(4) | H bilaterally (mainly right side) | Right AMTR/negat | III (2.5) |
| 7 (M) | 0.5 | 21 | CPS/30, MS/300 | 0 | Abnormality of left H | F′(9), P′(1), T′(1), F(2) | Left SMA (myoclonic seizures), left F pole (CPS) | Resection of left F pole/negat | IV (2.5) |
| 8 (F) | 9.5 | 13 | CPS/30 | Perinatal asphyxia | Malrotation of left H | P′(5), T′(5), F′(1), O(1), P(1) | Undetected | – | – |
| 9 (M) | 9 | 27 | CPS/30 plus | Perinatal asphyxia | Bilat. abnormal gyrification and gliotic changes of PO | O (2), T (3), P(3), O′(3), T′(1), P′(3) | O lobe bilaterally (mainly right side) | Partial resection of right O lobe/ ulegyria, FCD IIIA | IIIA (2) |
| 10 (F) | 9 | 30 | CPS/3 | Perinatal asphyxia | Normal | T (3), T′(8), O′(2) | Left lateral T lobe, GTS | Incomplete resection of left GTS/ negat | IVA (2) |
| 11 (F) | 17 | 26 | CPS/12 | Meningoencephalitis | Normal | T (1), T′(8) | Lateral mesial T lobe | Left AMTR/FCD IB | IA (2) |
| 12 (F) | 28 | 56 | CPS/8 | 0 | Right hippocampal sclerosis | T (2), T′(3) | Right H | Right AMTR/negat | IIIA (2) |
| 13 (M) | 1 | 40 | CPS/2 plus | 0 | Hypotrophic left H | T′(6), P′(2), O′(2) | Left H | Left AMTR/negat | IA (2) |
| 14 (F) | 11 | 27 | sGTCS/3 | 0 | Normal | F(4), F′(8) | Left GFS, GFM, GFMed | Partial cortectomy of left F lobe | IIIA (2) |
| 15 (M) | 19 | 26 | CPS/4 | 0 | FCD left T and hyperintensity of H | T′(7), F′(1), T (1) | Left anterotemporal, right mesial temporal | VNS | – |
| 16 (F) | 10 | 34 | SPS, CPS/10 plus | Perinatal asphyxia | Normal | F′(5), P′(2), F(6), P(2) | Right dorsolateral parasagittal premotoric area | Partial cortectomy of right F lobe, partial callosotomy/FCD 1C | Not available |
| 17 (M) | 27 | 38 | CPS/25 plus | 0 | Normal | T(3), I′(2), T′(6), P′(1), O′(1), F′(1) | Mesial T region bilaterally | VNS | – |
| 18 (F) | 6 | 48 | CPS/60 plus | Febrile seizures | Postoperative gliosis right P | P(6), T(3), O(1) | Right TP cortex, right hippocampus | VNS | – |
| 19 (M) | 33 | 41 | CPS/30 | 0 | Focal hyperintensity right basal T | T(4), T′(3) | Right H | Right AMTR/FCD IIIb gangliogliom | IA(1.5) |
| 20 (M) | 11 | 25 | CPS/12 plus | 0 | Normal | TPO grids | Right lateral T lobe | Cortical resection of right T a TO region/negat | IIA(2) |
| 21 (F) | 17 | 40 | CPS/20 | 0 | Normal | F′(1),O′(2),T′(7),T(2) | Undetected | – | – |
| 22 (F) | 17 | 40 | CPS/20 | 0 | Normal | FTPO′ grids | Left laterobasal posterior T lobe | Cortectomy of left laterobasal posterior T lobe/negat | IIIA (1.5) |
| 23 (M) | 8 | 29 | CPS/20 plus | 0 | Normal | T′(7), F′(2), T(2) | Bitemporal | Left AMTR/negat | IVA (1) |
| 24 (F) | 2 | 33 | CPS/6 plus | Meningoencephalitis | Postencephalitic changes left T | T(2), T′(6), F′(3) | Left H | Left AMTR/hippocampal sclerosis, postmeningoencephalitic changes | IA (1) |
| 25 (M) | 12 | 40 | CPS/40 plus | Trauma | Posttraumatic changes of left T and GFI | F′(6), T′(5) | Left T pole, lateral T, lateral prefrontal area | Resection of temporal pole, lesionectomy F left/posttraumatic changes | IIIA (1) |
| 26 (F) | 2 | 33 | sGTCS/10 | 0 | Postoperative changes right PO | T(3), P(2), O(2) | Right GTS, LPI | – | – |
| 27 (F) | 2 | 22 | CPS/4 | 0 | Postoperative changes right PO | P(2), F(2), T(3) | Undetected (right posterior quadrant) | VNS | – |

**Table 1** (*continued*)

| Subject gender | Age at seizure onset | Age at invasive EEG | Seizure frequency/monthly | Febrile seizures/precipitating events | MRI (signs of) | Brain lobes explored and number of implanted electrodes | Region SOZ (epileptogenic zone) | Intervention/histopathology | Postsurgical outcomes (Engel) (years) |
|---|---|---|---|---|---|---|---|---|---|
| 28 (M) | 21 | 35 | CPS/5 | Commotio cerebri | Bilat. hypotrophic hippocampi | T(6), T′(2) | H bilaterally (mainly right side) | VNS | – |
| 29 (M) | 31 | 37 | CPS/4 | Prolonged febrile seizures | Normal | T′(8), F′(2), T(2) | H bilaterally (mainly left side) | Left AMTR/negat | IA (1) |
| 30 (F) | 9 | 27 | CPS/5 | Meningoencephalitis | Left HS | T′(8), T(2), P′(1), I′(1), F′(1) | Left H | Left AMTR/FCDIIIA | IIIA (1) |
| 31 (M) | 2 | 51 | CPS/3 plus | Febrile seizures | Right H atrophy, slight changes of density | T(5), F(3), T′(2) | Right H | Right AMTR/negat | IA (1) |

CPS – complex partial seizure; MS – myoclonic seizures; plus – sporadic ictal generalization; SOZ – seizure onset zone; SMA – supplementary motor area; LPI – lobulus parietalis inferior; GTS – gyrus temporalis superior; GFS – gyrus frontalis superior; GFM – gyrus frontalis medius; GFMed – gyrus frontalis medius; H – hippocampus; HS – hippocampal sclerosis; DNET – dysembryoplastic neuroepithelial tumor; FCD – focal cortical dysplasia; AMTR – anteromedial temporal resection; E – extratemporal; T – temporal; R – right; L – left; FCD – focal cortical dysplasia; F – frontal; P – parietal; T – temporal; O – occipital, I – insular; ′ - left.

into sliding statistical windows (10 s) and filtered in a series of overlapping, logarithmically spaced frequency bands. Each band was processed as follows:

The power envelope was computed using the Hilbert transform and normalized by Eq. (1) to stress the signal peaks (Supplementary Fig. S2).

$$x_{normed} = \frac{x - P_{2/3}}{P_{1/3} - P_{2/3}} \quad (1)$$

To overcome the effects of Gibb's phenomenon, a "frequency stability" metric was computed. The band passed filtered signal (narrow band) was transformed to a cosine representation of its phase. The same transformation was applied to a band passed filtered signal with the same high cut-off frequency but a four times lower low cut-off frequency (broad band) (Supplementary Fig. S3a, b). A sliding window with the width of four cycles of the narrow band low cut-off frequency was applied to the narrow band signal and the root mean square (RMS) was calculated, thus generating the "signal". Similarly, the RMS was calculated on the signal created by subtracting the narrow band signal from the broad band signal, generating "noise". The frequency stability was calculated as a "signal-to-noise" ratio. The produced signal was normalized Eq. (1).

The dot product of the amplitude and frequency stability metric was calculated. Negative values were set to 0. Putative HFO detections were obtained by thresholding the normalized Eq. (1) dot product of the power envelopes and frequency stability with 0.1 (Supplementary Fig. S4).

To increase algorithm specificity, amplitude, and frequency stability, the dot product and duration minimum/maximum thresholds were applied on putative HFO detections. The metric threshold values were obtained from cumulative distribution functions fitted to the HFO metric distributions previously marked by expert reviewers. The parameters of the fitted gamma functions were specific for each band. The parameters (Supplementary Table S1) and examples of true positive detection and false positive detection (Supplementary Fig. S5) are included in the Supplementum.

### 2.3. Statistical analysis

The rates of HFO per contacts within the three groups (SOZ, IZ, and nonSOZ/nonIZ) were statistically compared (SOZ × IZ; SOZ × nonSOZ/nonIZ; IZ × nonSOZ/nonIZ). This statistical analysis was performed using an independent two sample *t*-test separately for ripple range and fast ripple range. We performed statistical analyses on the whole dataset and separately for patients with favorable postoperative outcomes (Engel I or II – 9 patients) and the other patients with "poor outcomes" (postsurgical outcomes of Engel III or IV and patients with presumed poor outcomes due to more than one detected SOZ according to SEEG). Furthermore, we performed a statistical analysis comparing the duration and relative amplitude of HFO (separately for R and FR ranges) for contacts in the areas, as defined above. This analysis was performed in all patients and subsequently in patients with favorable or poor surgical outcomes. For this analysis, we again used an independent two sample *t*-test. Bonferroni's correction for multiple comparisons was applied where needed.

## 3. Results

The statistical analysis and complete results of HFO detection (rates, duration, and amplitudes) are shown in Table 2 and Supplementary Table S2, respectively.

### 3.1. Rates

As expected, the HFO rate per contact in all patients was statistically higher in the SOZ than in the nonSOZ/nonIZ regions (Fig. 1) in the fast ripple frequency range ($p = 0.018$) and ripple range ($p = 0.038$).

Specifically, HFO in the ripple range were identified. The mean number of HFO per contact (per 30 min) was 109.13 within the SOZ (SD = 79.19), 96.03 in the IZ (SD = 82.24) and 68.65 for nonSOZ/nonIZ regions (SD = 49.24). The differences between groups of contacts were significant only between SOZ and nonSOZ/nonIZ regions. In the fast ripple range, the mean HFO count per contact (per 30 min) were 50.02 in the SOZ (SD = 50.75), 31.56 in the IZ (SD = 34.89) and 23.23 in nonSOZ/nonIZ (SD = 21.84). The only significant result was in the comparison of SOZ and nonSOZ/nonIZ regions; see above.

No statistically significant results were seen in comparison of regions separately in groups of patients with favorable or poor outcomes.

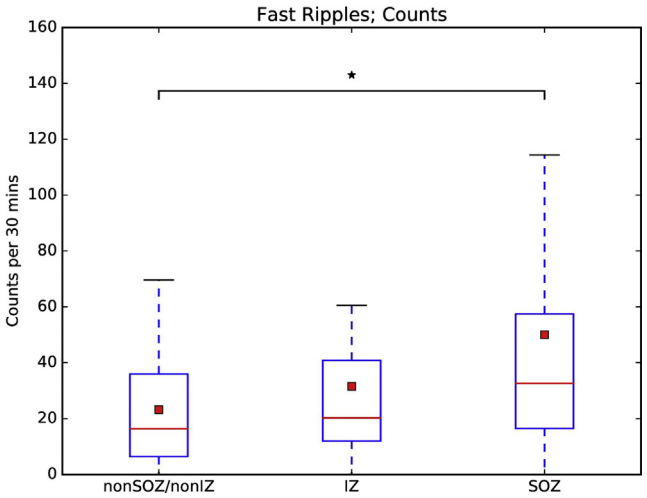


**Fig. 1.** Counts of fast ripples per 30 min in particular areas (SOZ, IZ, and nonSOZ/nonIZ) in all patients.

### 3.2. Duration

#### 3.2.1. Ripples

The mean duration of detected HFO was 54.40 ms in the SOZ (SD = 25.58), 56.31 ms in the IZ (SD = 27.52) and 56.12 ms in nonSOZ/nonIZ regions (SD = 29.16). Statistical analysis showed significantly shorter durations of HFO in the SOZ than in either the IZ or nonSOZ/nonIZ regions ($p < 0.001$); the difference between the IZ and nonSOZ/nonIZ regions was not significant ($p = 0.361$).

#### 3.2.2. Fast ripples

Similarly, automated detection in the fast ripple range detected the mean durations of HFO of 27.43 ms in the SOZ (SD = 16.04), 29.13 ms in the IZ (SD = 18.30) and 30.41 ms, in nonSOZ/nonIZ regions (SD = 20.94); the shortest durations of FR were in the

**Table 2**
The results of statistical analysis (two sample *t*-test, *p* values) comparing the rates, duration, and relative amplitudes of HFO (all over separately for ripples [first column] and fast ripples range [second column]) per contacts in the redefined areas (SOZ, IZ, nonSOZ/nonIZ); also in this analysis particularly in all patients and in patients with favorable or poor outcomes.

Rates

| | nonSOZ/nonIZ | | | | | | IZ | | | | | |
|---|---|---|---|---|---|---|---|---|---|---|---|---|
| | All | | Favorable outcome | | Poor outcome | | All | | Favorable outcome | | Poor outcome | |
| SOZ | 0.038 | 0.018 | 0.417 | 0.143 | 0.102 | 0.076 | 1.078 | 0.228 | 0.102 | 0.092 | 0.974 | 0.407 |
| IZ | 0.245 | 0.543 | 1.243 | 1.136 | 0.464 | 0.491 | x | x | x | x | x | x |
| nonSOZ/nonIZ | x | x | x | x | x | x | | | | | | |

Duration

| | nonSOZ/nonIZ | | | | | | IZ | | | | | |
|---|---|---|---|---|---|---|---|---|---|---|---|---|
| | All | | Favorable outcome | | Poor outcome | | All | | Favorable outcome | | Poor outcome | |
| SOZ | <<0.001 | <<0.001 | <<0.001 | <<0.001 | 0.877 | <<0.001 | <<0.001 | <<0.001 | <<0.001 | <0.001 | <<0.001 | <<0.001 |
| IZ | 0.361 | <<0.001 | <<0.001 | 0.460 | <<0.001 | 0.027 | x | x | x | x | x | x |
| nonSOZ/nonIZ | x | x | x | x | x | x | | | | | | |

Amplitude

| | nonSOZ/nonIZ | | | | | | IZ | | | | | |
|---|---|---|---|---|---|---|---|---|---|---|---|---|
| | All | | Favorable outcome | | Poor outcome | | All | | Favorable outcome | | Poor outcome | |
| SOZ | <<0.001 | 0.430 | <<0.001 | <<0.001 | <<0.001 | <<0.001 | <<0.001 | 0.309 | <<0.001 | 0.014 | 0.030 | <<0.001 |
| IZ | <<0.001 | 0.013 | <<0.001 | <<0.001 | <<0.001 | 1.136 | x | x | x | x | x | x |
| nonSOZ/nonIZ | x | x | x | x | x | x | | | | | | |

SOZ, HFO durations were longer in nonSOZ/nonIZ regions than in the IZ ($p < 0.001$) and in nonSOZ/nonIZ regions than in the SOZ ($p < 0.001$). The difference between the IZ and SOZ was also significant ($p < 0.001$).

In the group of patients with favorable outcomes, shorter R and FR durations were seen in the SOZ ($p < 0.001$) than in nonSOZ/nonIZ and IZ regions (see Fig. 2).

In the group of patients with poor outcomes, the longest duration of R was in the IZ ($p < 0.001$); the difference between nonSOZ/nonIZ × SOZ was not significant ($p = 0.877$). In both subgroups of patients, the shortest FR duration was seen in the SOZ ($p < 0.001$).

### 3.3. Amplitudes

#### 3.3.1. Ripples

Automated detection in the ripple range detected the relative amplitudes of HFO in the SOZ of 77.47 (SD = 164.35), in the IZ of 66.14 (SD = 231.74) and in nonSOZ/nonIZ regions of 56.30 (SD = 151.74). Statistical analysis showed significantly higher amplitudes of HFO in the SOZ than in either the IZ or nonSOZ/nonIZ regions ($p < 0.001$); the difference between the IZ and nonSOZ/nonIZ regions was also significant ($p < 0.001$).

#### 3.3.2. Fast ripples

Automated detection in the fast ripple range detected relative amplitudes of HFO in the SOZ of 76.04 (SD = 164.95), in the IZ of 80.93 (SD = 458.49) and in nonSOZ/nonIZ regions of 73.79 (SD = 241.17). The differences between SOZ and IZ or nonSOZ/nonIZ were not significant.

Nevertheless, in the group of patients with favorable outcomes, the relative amplitude of HFO (both R and FR) was higher in the SOZ than in the IZ and nonIZ/nonSOZ region ($p < 0.001$) (see Figs. 3 and 4). In the group of patients with poor outcomes, the highest amplitude of R was seen in the SOZ ($p < 0.001$) (versus nonSOZ/IZ); $p = 0.030$ (IZ) and the lowest in nonIZ/nonSOZ region ($p < 0.001$). The relative amplitude of FR was lower in the SOZ than in either the IZ or nonSOZ/nonIZ regions ($p < 0.001$) (see Fig. 5).

## 4. Discussion

Interictal HFO analyses in patients with epilepsy have been reported useful for SOZ identification (Urrestarazu et al., 2007;

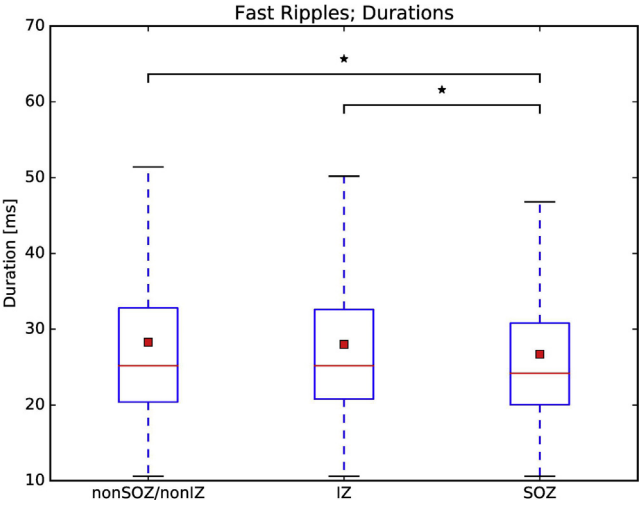


**Fig. 2.** Durations (ms) of fast ripples in particular areas (SOZ, IZ, and nonSOZ/nonIZ) in patients with favorable outcomes.

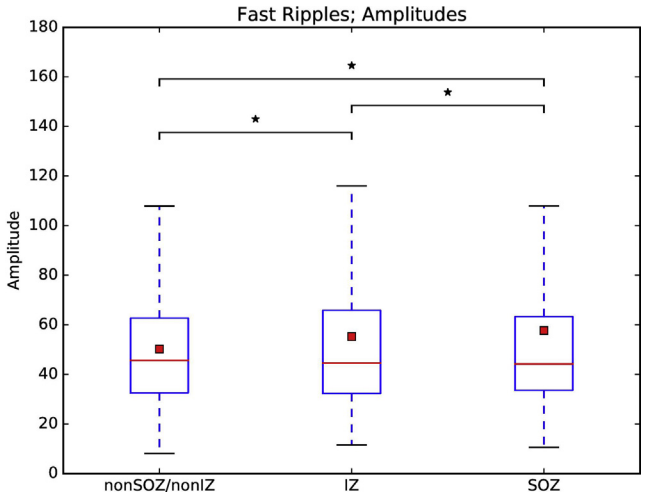


**Fig. 3.** Relative amplitudes of fast ripples in particular areas (SOZ, IZ, and nonSOZ/nonIZ) in patients with favorable outcomes.

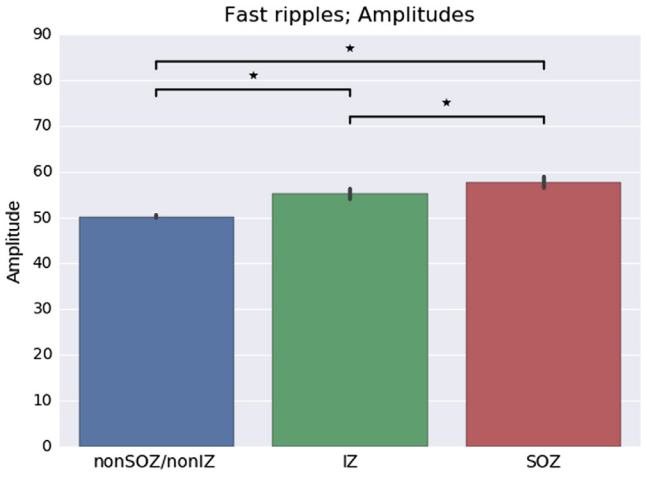


**Fig. 4.** Relative amplitudes of fast ripples in particular areas (SOZ, IZ, and nonSOZ/nonIZ) in patients with favorable outcomes. Bar graphs represent the population mean. Ticks represent a 95% confidence interval of the mean calculation.

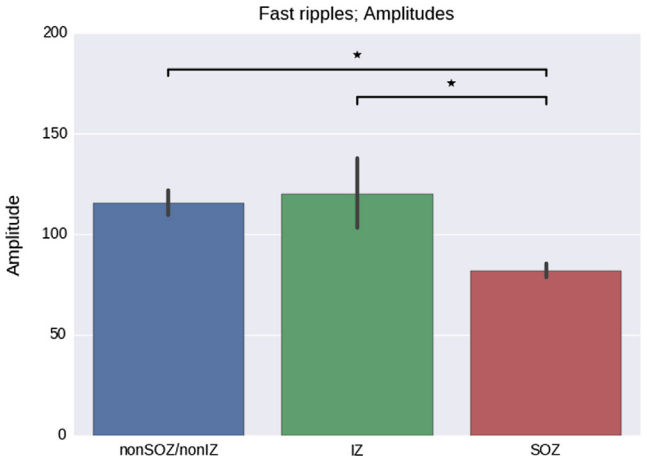


**Fig. 5.** Relative amplitudes of fast ripples in particular areas (SOZ, IZ, and nonSOZ/nonIZ) in patients with poor outcomes. Bar graphs represent the population mean. Ticks represent a 95% confidence interval of the mean calculation.

Jacobs et al., 2008, 2009). In the present study, patients with both temporal and extratemporal epilepsy were examined to ascertain facts about HFO characteristics in areas within and outside the SOZ and the IZ. For these purposes, we used the concept of an epileptogenic zone (Lüders and Awad, 1992; Rosenow and Lüders, 2001), and used the term "irritative zone" as it has been used elsewhere (Blanco et al., 2011) to investigate HFO characteristics in more detail, to observe the area between the SOZ and non-SOZ, and to eliminate potential overlap of interictal active ("spiking") channels within SOZ and non-SOZ. Only patients who underwent surgical resections and had good postsurgical outcomes reflect the correct determination of the seizure onset zone. For that reason, we divided patients into two subgroups: favorable outcome and others ("poor outcome").

In our study, HFO were detected in all (SOZ, IZ, and nonSOZ/nonIZ) areas, with a higher absolute HFO rate for events in the R range than in the FR range. These findings are not surprising; the occurrence of high frequency activity unassociated with the SOZ is well documented in the hippocampi (Staba et al., 2002; Axmacher et al., 2010) and in the primary motor, somatosensory, and visual cortices (Curio, 2000; Nagasawa et al., 2012; Matsumoto et al., 2013; Wang et al., 2013). The results indicate that the detection algorithm, in addition to detecting pathological HFO, may also detect HFO that might be physiological, might be a fragment or propagation of pathological HFO arising from elsewhere (Crépon et al., 2010), or might be false positive detections. Higher HFO rates in the R range than in the FR range may be explained by an association between HFO and interictal spiking (Urrestarazu et al., 2007; Jacobs et al., 2008; Wang et al., 2013). There is evidence that larger networks are involved in R than in FR generation in SOZ areas (Chrobak and Buzsáki, 1996; Bragin et al., 2002) and that FR generators are spatially localized to a region of less than 1 $mm^3$ (Bragin et al., 2002). Furthermore there is evidence of HFO under detection, especially in higher frequency bands when using macroelectrodes (as in our cases), i.e. in the FR range, which results in a lower mean frequency of detected HFO (Worrell et al., 2008).

According to previously published data, which is further corroborated by our study, the FR and R rate are significantly higher in the SOZ than in nonSOZ/nonIZ regions (Urrestarazu et al., 2007; Jacobs et al., 2008, 2009; Andrade-Valença et al., 2012). Interestingly, in patients with favorable outcomes, a prominent (though not significant) difference between rates of FR and R in the SOZ and the IZ can be observed, which might represent a more focal generator (epileptogenic tissue) of these pathological HFO; this difference was less seen in other patients. As in a study by Jacobs et al. (2008), the distinction between pathological and normal areas was worse for R than for FR. Nevertheless, the explanation for the high rates of R and FR in nonSOZ/nonIZ regions is unclear. It cannot be definitely demonstrated whether all of these marked events were actually pathological, physiological, or the propagation of pathological HFO arising from elsewhere, as was mentioned above. Spontaneous HFO of a physiological nature are difficult to distinguish from epileptogenic ones, particularly during wakefulness (Jacobs et al., 2008; Curio, 2000) since the frequency and amplitude measures alone cannot be used for this purpose (Engel et al., 2009; Nagasawa et al., 2012; Matsumoto et al., 2013). Finally, the overlap (in both amplitude and duration) between the pathological and physiological ripples is extensive (Alkawadri et al., 2014).

The main reason for focusing on the IZ is evidence of HFO linking with interictal epileptiform discharges in both mesiotemporal and neocortical epilepsy (Urrestarazu et al., 2007; Jacobs et al., 2008; Wang et al., 2013). The vast majority of interictal HFO (up to 73% of R and 92% of FR) is associated with interictal spikes or sharp waves (Urrestarazu et al., 2007; Jacobs et al., 2008). A comparison of HFO associated with interictal epileptiform discharges and unassociated HFO revealed no differences in terms of the duration (Urrestarazu et al., 2007), or the associated HFO had longer durations than the unassociated HFO with spikes (Jacobs et al., 2008). Wang and colleagues (2013) showed HFO detected in the SOZ area were of shorter duration than those not correlated to the SOZ area. As in the study by Wang et al. (2013), our data suggest longer durations of both R and FR in the IZ or nonSOZ/nonIZ than in the SOZ. These findings might be also a consequence of analyzing awake recordings with less expressed interictal discharges, and so more HFO detected this phenomenon and with shorter duration. This finding might be also explained by the work of Nagasawa (2012), who revealed that the duration of spontaneous HFO in the ripple range (namely from the occipital cortex) of a physiological nature were significantly longer than that of epileptogenic ripple HFO. Similar results were presented by Alkawadri et al. (2014). These observations are still consistent with the hypothesis that longer durations of HFO may represent longer excitatory neural processing (Niessing et al., 2005; Nishida et al., 2008; Koch et al., 2009; Manning et al., 2009; Nagasawa et al., 2012). In other studies, however, the duration of pathological (in the SOZ) and physiological (nonSOZ region) FR was not diverse (Nagasawa et al., 2012; Alkawadri et al., 2014), or the longer duration of both R (Brázdil et al., 2015) and FR was revealed within the SOZ (Jacobs et al., 2008; Matsumoto et al., 2013). The discrepancies among studies in the duration of R and FR in various regions might be explained by different proportions of included focal epilepsies (hippocampus vs. neocortex).

There have been noteworthy results regarding relative HFO amplitude in epileptic and non-epileptic regions in particular subgroups of patients. Interestingly, in the group of patients with favorable outcomes, the relative HFO amplitude (especially FR) was higher in the SOZ than in other regions; in other patients with "poor outcomes", the results of FR analysis were reversed. These results for both R and FR might contribute to neurosurgical resection planning, showing possible worse prognosis in patients with higher amplitudes especially of FR outside the SOZ. This indicates that it is possible that the true SOZ was not adequately detected. Another reason may be a more dispersed or multifocal epileptogenic zone/SOZ, a pattern which is too diffuse to permit a successful resective strategy, and so usually results in VNS implantation. Yet another reason for poor outcome may be that the result of the epileptogenic zone may include the actual epileptogenic zone (generating seizures before surgery) as well as a potential epileptogenic zone which is an area of the cortex that may generate seizures after the presurgical SOZ has been resected (Rosenow and Lüders, 2001). Seizures originating from areas not covered by electrodes but propagating to the actual electrode positions might lead to misinterpretation (Zijlmans et al., 2012).

HFO are more stable and more expressed, and the likelihood for artifact contamination is lower, during sleep. However, a review of recently presented data indicates that the effect of sleep on HFO expression differs among regions (Dümpelmann et al., 2015) and so this phenomenon might influence the observation. Some patients also experience postoperative nausea and general discomfort so they rarely reach deep stages of sleep. The differences in HFO rates between the SOZ and other remote areas were disclosed in wakefulness periods as significant (Bagshaw et al., 2009). Based on this data we decided to analyze awake recordings.

Our findings emphasize the importance of the careful interpretation of HFO, especially in cases with extensive spatial sampling or when there is an overlap between the epileptic and physiologic areas (Alkawadri et al., 2014). Based on our data, it is useful to include both ripples and fast ripples in the evaluation of the potential epileptogenic region (Zijlmans et al., 2012). Currently, there are no established criteria for distinguishing physiological from pathological HFO and SOZ areas (Engel et al., 2009; Jacobs et al.,

2016). Nevertheless, it seems that FR generated in the SOZ are more frequent, shorter, and have higher relative amplitudes than in other regions. There is, however, no clear cut-off value for these characteristics which can separate the SOZ, the IZ, and other regions.

## 5. Conclusion

HFO parameters (rate, amplitude, and duration) differ in epileptic and non-epileptic regions. We suggest that amplitude and duration may be as important as frequency band and rate of HFO in marking the seizure onset region or epileptogenic area and may provide additional information on epileptogenicity. To conclude, FR are more frequent, shorter, and have higher relative amplitudes in the SOZ area than in other regions. The study suggests a possible worse prognosis in patients with higher amplitudes of FR outside the SOZ.

## Acknowledgments

The study was supported by the "CEITEC – Central European Institute of Technology" project (CZ.1.05/1.1.00/02.0068) from the European Regional Development Fund and by MŠMT ČR Research Program no. MSM0021622404. The technical part of the study was supported by the GACR project P103/11/0933 and the Application Laboratories of Advanced Microtechnologies and Nanotechnologies (CZ.1.05/2.1.00/01.0017), co-funded by the Operational Programme "Research and Development for Innovations", the European Regional Development Fund, and the state budget.

Supported by European Regional Development Fund - Project FNUSA-ICRC (No. CZ.1.05/1.1.00/02.0123) and Ministry of Education, Youth and Sports of the Czech Republic project no. LH15047 (KONTAKT II).

*Conflict of interest:* None of the authors has any conflict of interest to disclose.

## Appendix A. Supplementary data

Supplementary data associated with this article can be found, in the online version, at http://dx.doi.org/10.1016/j.clinph.2016.10.011.

## References

Akiyama T, McCoy B, Go CY, Ochi A, Elliott IM, Akiyama M, et al. Focal resection of fast ripples on extraoperative intracranial EEG improves seizure outcome in pediatric epilepsy. Epilepsia 2011;52:1802–11.

Alkawadri R, Gaspard N, Goncharova II, Spencer DD, Gerrard JL, Zaveri H, et al. The spatial and signal characteristics of physiologic high frequency oscillations. Epilepsia 2014;55:1986–95.

Andrade-Valença L, Mari F, Jacobs J, Zijlmans M, Olivier A, Gotman J, et al. Interictal high frequency oscillations (HFOs) in patients with focal epilepsy and normal MRI. Clin Neurophysiol 2012;123:100–5.

Axmacher N, Cohen MX, Fell J, Haupt S, Dümpelmann M, Elger CE, et al. Intracranial EEG correlates of expectancy and memory formation in the human hippocampus and nucleus accumbens. Neuron 2010;65:541–9.

Bagshaw AP, Jacobs J, LeVan P, Dubeau F, Gotman J. Effect of sleep stage on interictal high-frequency oscillations recorded from depth macroelectrodes in patients with focal epilepsy. Epilepsia 2009;50:617–28.

Blanco JA, Stead M, Krieger A, Stacey W, Maus D, Marsh E, et al. Data mining neocortical high-frequency oscillations in epilepsy and controls. Brain 2011;134:2948–59.

Bragin A, Wilson CL, Engel Jr J. Voltage depth profiles of high-frequency oscillations after kainic acid-induced status epilepticus. Epilepsia 2007;48(Suppl 5):35–40. Erratum in: Epilepsia 2007; 48:2379.

Bragin A, Engel Jr J, Wilson CL, Fried I, Buzsáki G. High-frequency oscillations in human brain. Hippocampus 1999;9:137–42.

Bragin A, Engel Jr J, Wilson CL, Fried I, Mathern GW. Hippocampal and entorhinal cortex high-frequency oscillations (100–500 Hz) in human epileptic brain and in kainic acid-treated rats with chronic seizures. Epilepsia 1999;40:127–37.

Bragin A, Mody I, Wilson CL, Engel Jr J. Local generation of fast ripples in epileptic brain. J Neurosci 2002;22:2012–21.

Bragin A, Wilson CL, Almajano J, Mody I, Engel Jr J. High-frequency oscillations after status epilepticus: epileptogenesis and seizure genesis. Epilepsia 2004;45:1017–23.

Bragin A, Engel Jr J, Staba RJ. High-frequency oscillations in epileptic brain. Curr Opin Neurol 2010;23:151–6.

Brázdil M, Halámek J, Jurák P, Daniel P, Kuba R, Chrastina J, et al. Interictal high-frequency oscillations indicate seizure onset zone in patients with focal cortical dysplasia. Epilepsy Res 2010;90:28–32.

Brázdil M, Cimbálník J, Roman R, Shaw DJ, Stead MM, Daniel P, et al. Impact of cognitive stimulation on ripples within human epileptic and non-epileptic hippocampus. BMC Neurosci 2015;16:47.

Buzsáki G, Horváth Z, Urioste R, Hetke J, Wise K. High frequency network oscillation in the hippocampus. Science 1992;256(5059):1025–7.

Chrobak JJ, Buzsáki G. High-frequency oscillations in the output networks of the hippocampal–entorhinal axis of the freely behaving rat. J Neurosci 1996;16:3056–66.

Crépon B, Navarro V, Hasboun D, Clemenceau S, Martinerie J, Baulac M, et al. Mapping interictal oscillations greater than 200 Hz recorded with intracranial macroelectrodes in human epilepsy. Brain 2010;133:33–45.

Curio G. Linking 600 Hz "spikelike" EEG/MEG wavelets ("ς-bursts") to cellular substrates: concepts and caveats. J Clin Neurophysiol 2000;17:377–96.

Curio G, Mackert BM, Burghoff M, Neumann J, Nolte G, Scherg M, et al. Somatotopic source arrangement of 600 Hz oscillatory magnetic fields at the human primary somatosensory hand cortex. Neurosci Lett 1997;234:131–4.

Dümpelmann M, Jacobs J, Schulze-Bonhage A. Temporal and spatial characteristics of high frequency oscillations as a new biomarker in epilepsy. Epilepsia 2015;56:197–206.

Engel Jr J, Bragin A, Staba R, Mody I. High-frequency oscillations: what is normal and what is not? Epilepsia 2009;50:598–604.

Haegelen C, Perucca P, Châtillon C-E, Andrade-Valença L, Zelmann R, Jacobs J, et al. High-frequency oscillations, extent of surgical resection, and surgical outcome in drug-resistant focal epilepsy. Epilepsia 2013;54:848–57.

Jacobs J, LeVan P, Chander R, Hall J, Dubeau F, Gotman J. Interictal high-frequency oscillations (80–500 Hz) are an indicator of seizure onset areas independent of spikes in the human epileptic brain. Epilepsia 2008;49:1893–907.

Jacobs J, LeVan P, Châtillon C-E, Olivier A, Dubeau F, Gotman J. High frequency oscillations in intracranial EEGs mark epileptogenicity rather than lesion type. Brain 2009;132:1022–37.

Jacobs J, Zijlmans M, Zelmann R, Châtillon C-E, Hall J, Olivier A, et al. High-frequency electroencephalographic oscillations correlate with outcome of epilepsy surgery. Ann Neurol 2010;67:209–20.

Jacobs J, Vogt C, LeVan P, Zelmann R, Gotman J, Kobayashi K. The identification of distinct high-frequency oscillations during spikes delineates the seizure onset zone better than high-frequency spectral power changes. Clin Neurophysiol 2016;127(1):129–42.

Jiruska P, Bragin A. High-frequency activity in experimental and clinical epileptic foci. Epilepsy Res 2011;97:300–7.

Jobst BC. Are HFOs still UFOs? The known and unknown about high frequency oscillations in epilepsy surgery. Epilepsy Curr. 2013;13:273–5.

Koch SP, Werner P, Steinbrink J, Fries P, Obrig H. Stimulus-induced and state-dependent sustained gamma activity is tightly coupled to the hemodynamic response in humans. J Neurosci 2009;29:13962–70.

Lachaux JP, Axmacher N, Mormann F, Halgren E, Crone NE. High-frequency neural activity and human cognition: past, present and possible future of intracranial EEG research. Prog Neurobiol 2012;98:279–301.

Lüders HO, Awad I. Conceptual considerations. In: Lüders HO, editor. Epilepsy surgery. New York: Raven Press; 1992. p. 51–62.

Manning JR, Jacobs J, Fried I, Kahana MJ. Broadband shifts in local field potential power spectra are correlated with single-neuron spiking in humans. J Neurosci 2009;29:13613–20.

Matsumoto A, Brinkmann BH, Stead SM, Matsumoto J, Kucewicz MT, Marsh WR, et al. Pathological and physiological high-frequency oscillations in focal human epilepsy. J Neurophysiol 2013;110:1958–64.

Nagasawa T, Juhász C, Rothermel R, Hoechstetter K, Sood S, Asano E. Spontaneous and visually driven high-frequency oscillations in the occipital cortex: intracranial recording in epileptic patients. Hum Brain Mapp 2012;33:569–83.

Niessing J, Ebisch B, Schmidt KE, Niessing M, Singer W, Galuske RA. Hemodynamic signals correlate tightly with synchronized gamma oscillations. Science 2005;309(5736):948–51.

Nishida M, Juhász C, Sood S, Chugani HT, Asano E. Cortical glucose metabolism positively correlates with gamma-oscillations in nonlesional focal epilepsy. Neuroimage 2008;42:1275–84.

Rosenow F, Lüders H. Presurgical evaluation of epilepsy. Brain 2001;124:1683–700.

Staba RJ, Wilson CL, Bragin A, Fried I, Engel Jr J. Quantitative analysis of high-frequency oscillations (80–500 Hz) recorded in human epileptic hippocampus and entorhinal cortex. J Neurophysiol 2002;88:1743–52.

Urrestarazu E, Chander R, Dubeau F, Gotman J. Interictal high-frequency oscillations (100–500 Hz) in the intracerebral EEG of epileptic patients. Brain 2007;130:2354–66.

Usui N, Terada K, Baba K, Matsuda K, Usui K, Tottori T, et al. Significance of very-high-frequency oscillations (over 1000 Hz) in epilepsy. Ann Neurol 2015;78:295–302.

Wang S, Wang IZ, Bulacio JC, Mosher JC, Gonzalez-Martinez J, Alexopoulos AV, et al. Ripple classification helps to localize the seizure-onset zone in neocortical epilepsy. Epilepsia 2013;54:370–6.

Worrell GA, Parish L, Cranstoun SD, Jonas R, Baltuch G, Litt B. High-frequency oscillations and seizure generation in neocortical epilepsy. Brain 2004;127:1496–550.

Worrell GA, Gardner AB, Stead SM, Hu S, Goerss S, Cascino GJ, et al. High-frequency oscillations in human temporal lobe: simultaneous microwire and clinical macroelectrode recordings. Brain 2008;131:928–37.

Wu JY, Sankar R, Lerner JT, Matsumoto JH, Vinters HV, Mathern GW. Removing interictal fast ripples on electrocorticography linked with seizure freedom in children. Neurology 2010;75:1686–94.

Zelmann R, Zijlmans M, Jacobs J, Châtillon C-E, Gotman J. Improving the identification of high frequency oscillations. Clin Neurophysiol 2009;120:1457–64.

Zijlmans M, Jiruska P, Zelmann R, Leijten FS, Jefferys JG, Gotman J. High-frequency oscillations as a new biomarker in epilepsy. Ann Neurol 2012;71:169–78.

# CHAPTER 8

# Physiological vs. pathological high-frequency oscillations

Transient high-frequency oscillations (HFOs; 80-600Hz) in local field potentials generated by especially human hippocampal but also extrahippocampal areas have been related in nature to both physiological and pathological processes. In this situation, only detailed knowledge of the regional physiological activity may provide relevant information, which pathological HFOs (pHFOs) provide localizing information of epileptogenic brain tissue (Jiruska & Bragin, 2011). However, this situation poses a significant problem: how can be physiological and pathological HFOs distinguished? From a clinical point of view, when assessing the validity of HFOs as a marker for epilepsy, distinguishing normal physiological HFO (nHFO) (Buzsáki et al., 1992; Buzsáki & Silva, 2012; Kucewicz et al., 2014) from pathological, epileptiform HFOs (pHFO) (Le Van Quyen et al., 2006; Engel et al., 2009; Matsumoto et al., 2013; Wang et al., 2013) remains a fundamental challenge in clinical epileptology (Alvarado-Rojas et al., 2015; Jefferys et al., 2012; Menendez de la Prida et al., 2015). Moreover, distinguishing pathological from physiologic HFOs might increase the specificity of that marker. Separating normal and pathological HFOs in clinical studies, similar to the animal studies, would require electrodes with high spatial resolution, unit recordings, and precise recorded sites anatomical localization (Buzsáki et al., 2015). These electrodes could identify differences in EEG and unit firing that help to separate normal and pHFOs (Weiss et al., 2020). However, most clinical centers (like our center) use classical clinical invasive EEG macro-electrodes to examine drug-resistant epileptic patients during SEEG exploration.

It is now considered that physiological R are thought to reflect summated inhibitory postsynaptic potentials, while pathological HFOs, whether they be R or FR, reflect mainly principal cell action potentials of synchronously bursting neurons (Foffani et al., 2007; Draguhn et al., 1998; Bragin et al., 2011; Demont-Guignard et al., 2012; Ibarz et al., 2010). Some authors believe that pathological R are only slower FR (Jiruska et al., 2017; Frauscher et al., 2017).

Although currently, it is unclear how to definitively differentiate pathological HFOs from physiological HFOs in clinical invasive EEG recordings, until now, various analytical approaches have been sought to solve this problem. The methods used most commonly are based on, for example, a specific regional distribution in mesial temporal structures (Jiruska & Bragin, 2011); e.g., R frequency HFOs are recorded in dentate gyrus of epileptic rats, but not in control rodents. Higher rates of FR occurrence were observed within the subicular cortex compared with both hippocampus and entorhinal cortex, in contrast, no difference in the rates of R occurrence were found between these structures (Staba et al., 2004). Sleep/wake state and anatomical location are factors that may strongly influence R and FR spectral frequency (Staba et al., 2004). Thus, the anatomic location of implanted electrodes may identify what is pathological (Engel et al., 2009; Wang et al., 2013; Alkawadri et al., 2014). Some studies

investigated the association of HFOs with epileptiform discharges (Urrestarazu et al., 2007; Crépon et al., 2010; Wang et al., 2013), slow waves (Nagasawa et al., 2012; von Ellenrieder et al., 2016) or spindles (Bruder et al., 2017). Some authors have suggested separating them by clustering HFOs based on characteristics and features such as frequency, rates, spectral properties, duration, amplitude, and so on (Matsumoto et al., 2013; Alkawadri et al., 2014; Malinowska et al., 2015; Pail et al., 2017). Another approach is to simply classify HFOs as pHFO - produced spontaneously and associated with epileptiform sharp waves and identify nHFOs as being physiologic by associating them with specific physiologic processes (e.g., cognitive, sensory, motor,…) that can be observed in particular conditions or can be even evoked (event-related HFOs) by tasks or stimuli (Matsumoto et al., 2013; Kucewicz et al., 2014; Brázdil et al., 2015; Pail et al., 2020; Cimbalnik et al., 2020). Using this approach, a study of event-related evoked nHFO in the human motor cortex had higher mean frequencies, lower amplitudes, and shorter duration than pHFO associated with epileptiform sharp waves (Matsumoto et al., 2013). Evoked physiologic HFOs detected within the determined SOZ also differed from evoked HFOs recorded from electrodes placed within other sites and appeared to be more similar to epileptic HFOs (Matsumoto et al., 2013). Comparable results have been obtained for HFOs that can be evoked by visual stimulation (Nagasawa et al., 2012). Other reports have addressed this problem proposing several methods for dissociating different origins based on the width of the spectral frequency content of individual events, the number of distinct cycles observed, and the presence of actual oscillations in the unfiltered raw signal (Waldert et al., 2013; Kucewicz et al., 2017).

The most difficult is to classify in particular R that may have similarly both physiological (sharp-wave R complex) and pathological genesis (Buzsáki et al., 1992; Ylinen et al., 1995; Bragin et al., 2002b; Buzsáki & Silva, 2012). Of course, it would be possible to differentiate nHFOs and pHFOs by frequency, but multiple studies in humans report a wide range of overlapping pHFO and nHFO frequencies (Worrell et al., 2004; Worrell et al., 2008; Blanco et al., 2011). Moreover, ripples' rates vary substantially across different brain areas, as shown by von Ellenrieder et al. (2016). For instance, semicontinous/ continuous HFA exceeding 80Hz in the background EEG has been suggested to reflect physiologic activity distinctive for certain healthy brain regions, such as the occipital lobe or the hippocampus (Melani et al., 2013). Next to rates of HFOs, the duration of presumably physiological R seems to be significantly longer than that of epileptogenic R (Nagasawa et al., 2012; Alkawadri et al., 2014; Pail et al., 2017; Weiss et al., 2020); these observations are still consistent with the hypothesis that the longer duration of HFOs may represent the longer excitatory neural processing (Ray et al., 2008). However, in other studies, ripples' longer duration was revealed within the SOZ (Brázdil et al., 2015; Pail et al., 2020).

As far as the FR are concerned, in this case, it is easier to determine and categorize the origin because they are mainly a pathological genesis. Nevertheless, even here, it is not definite, as we will show below. The spontaneous FR of presumably physiological nature are difficult to distinguish from epileptogenic HFOs arising from elsewhere, based on their spectral frequency (Nagasawa et al.,2012; Pail et al., 2017, Weiss et al., 2020), amplitude (Nagasawa et al., 2012) but also duration (Nagasawa et

al., 2012, Alkawadri et al., 2014). Conversely, in some studies, longer duration and higher amplitude of FR was revealed within the SOZ (Jacobs et al., 2008; Matsumoto et al., 2013; Pail et al., 2020). The amplitude of LFP, however, is highly variable and sensitively depends on the distance between recording electrodes and the local HFO generators (Cimbalnik et al., 2016). Concerning the HFO entropy, Liu et al. (2018) presented the typical HFOs with the highest degree of waveform similarity (we can use the term "low entropy") were localized within the seizure onset zone only. In contrast, the sites generating HFOs embedded in random waveforms ("high entropy") were found in the functional regions independent from the epileptogenic locations (Liu et al., 2018).

Based on other observations, Wang et al. (2013) showed that neocortical R and FR coupled with spikes, are specific markers of the SOZ, whereas R not going along with spikes are not. Accordingly, other studies found that areas with FR occurring on spikes that were not resected during surgery were linked to a poor surgical outcome (Weiss et al., 2018; Thomschewski et al., 2019).

In humans, physiological HFOs are reported most frequently in the hippocampus, paracentral areas, and occipital cortex (Nagasawa et al., 2012; Matsumoto et al., 2013). Based on published observations, the eloquent cortex spontaneously generates physiological HFOs, which may stand out on ECoG traces as prominently as pathological HFOs arising from elsewhere (Nagasawa et al., 2012). Presumable physiological HFOs are often coupled with phases of delta oscillations (swiftly decayed from 1 to 3 Hz) during slow-wave sleep, which plays a crucial role in the effective consolidation of visual perceptual learning (Nagasawa et al., 2012; von Ellenrieder et al., 2016) This was not observed in case of pathologic HFOs, which had the strength of phase coupling from 1 to 3 Hz similar. Differences in delta-phase coupling between epileptogenic and spontaneous occipital HFOs could be explained by differences in responsiveness to larger network rhythms generated by healthy brain structures (Nagasawa et al., 2012). Based on the results of published studies can be assumed sleep-specific characteristics such as coupling to slow waves, and the suppressive effect of REM sleep, particularly during phasic REM sleep (desynchronization is even more increased) on HFO rates, less expressed in SOZ, which might help to delineate better the epileptogenic zone (Frauscher et al., 2017). Presumable physiologic HFOs appear predominantly during phasic REM sleep and seem to increase in rate overnight during REM sleep. Interestingly, pathologic R and FR decrease with increased sleep duration (von Ellenrieder et al., 2016). Spindle-linked physiological memory-related R seem to be shorter and appear to have lower amplitudes in contrast to supposedly epileptic R (Bruder et al., 2017).

In one recent study, the researchers observed that pathological FR occurred preferentially during the trough-peak or On-Off state transition of the slow wave in the hippocampal SOZ. In the hippocampal SOZ, ripples on slow waves (RoSW) also have a higher probability of coupling during the On-Off state, nevertheless in the hippocampal non-epileptogenic zone, RoSW are more likely to couple during the Off-On state transition (Fig.9; Weiss et al., 2020).

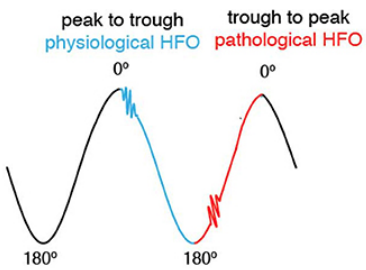


Figure 9: Illustration of the main hypothesis. Pathological ripples and fast ripples preferentially occur during the trough-peak transition of the slow wave.

The ability of HFOs as a biomarker for the epileptogenic zone might be improved by correcting HFO rates according to their topographic localization. Recently Frauscher et al. (2018) presented the multicenter atlas to provide region-specific quantitative normative values for physiological ripple (80-250Hz), fast ripple (>250Hz) rates and HFA in common stereotactic space. According to the collected data, physiological R are ubiquitous in normal regions, with particularly high rates in the eloquent cortex (the occipital and sensorimotor cortices, and in the mesiotemporal region, followed by basal temporal region, transverse temporal gyrus and planum temporale, and medial parietal lobe) and rare outside these regions. In contrast, physiological FR are very rare, even in eloquent cortical areas (medial occipital lobe, pre- and postcentral gyri, transverse temporal gyri and planum temporale, and lateral occipital lobe), making FR a good candidate for defining the epileptogenic zone, when present (Frauscher et al., 2018). This atlas is an open resource available for augmentation and consultation on the web (http://mni-open-ieegatlas.research.mcgill.ca). However, this atlas is mainly based on limited datasets and short pieces of recordings, not describing the overall electrophysiology of the human brain.

The issue of separating physiological from pathological HFOs is important, but not easy to address, and so far, based on the presented results, there are no specific characteristics of HFOs that would distinguish pathological and physiological HFOs in both Rand FR range. All studies have found a considerable overlap in their characteristics, and none has managed to separate these two entities correctly. Individual studies show no significant difference in individual characteristics; what is more, some studies contradict each other in the results (Nagasawa et al., 2012; Matsumoto et al., 2013; Wang et al., 2013; Alkawadri et al., 2014; Malinowska et al., 2015; von Ellenrieder et al., 2016; Pail et al., 2017, 2020). Whether the combination of different features and properties, including region-adjusted HFO rates might better delineate the epileptogenic zone remains to be investigated. And so, there are currently no established criteria of HFO features for distinguishing physiological HFOs from pathological ones.

**Published research**

# High-frequency oscillations in epileptic and non-epileptic human hippocampus during a cognitive task

Martin Pail

Jan Cimbálník

Robert Roman

Pavel Daniel

Jan Chrastina

Daniel J. Shaw

Milan Brázdil

**Sci Rep. 2020 Oct 23;10(1):18147. doi: 10.1038/s41598-020-74306-3.**

## Commentary on published paper

Hippocampal high-frequency electrographic activity (HFOs) represents one of the significant discoveries not only in epilepsy research but also in cognitive science over the past few decades. Several research groups have already addressed the issue of physiological and pathological HFOs. A fundamental challenge, however, has been the fact that physiological HFOs associated with normal brain function overlap in frequency with pathological HFOs. They assessed task-induced presumably physiological HFOs using visual tasks, visual-motor tasks, and visual memory tasks (Nagasawa et al., 2012, Matsumoto et al., 2013) or investigated the morphological characteristics of HFOs in epileptic and nonepileptic regions (Alkawadri et al., 2014; Malinowska et al., 2015; Pail et al., 2017). Despite the different approaches, a clear differentiation of presumably physiological HFOs and pathological epileptic HFOs was not possible, as both types largely overlap with respect to spectral frequency, duration, and amplitude (Nagasawa et al., 2012; Matsumoto et al., 2013; Alkawadri et al., 2014; Frauscher et al., 2017).

Our research looked at HFOs separately in the pathological and non-pathological hippocampus in the resting state, and especially during the simple cognitive task. We asked two fundamental questions. The first question was whether there was a difference in HFOs and their characteristics between the pathological and non-epileptic hippocampus. The second question was whether the HFOs found would change during the course of the cognitive task.

In a previous recent study, we used a simple cognitive task to investigate whether the effect of cognitive task on hippocampal ripples can be used as a new approach for distinguishing normal HFOs in the non-epileptic hippocampus (NEH) from pathological HFOs in the epileptic hippocampus (EH; Brázdil et al., 2015). In this study was shown different and, in some cases, opposing behavior of ripples within EH and NEH (Fig. 10; Brázdil et al., 2015).

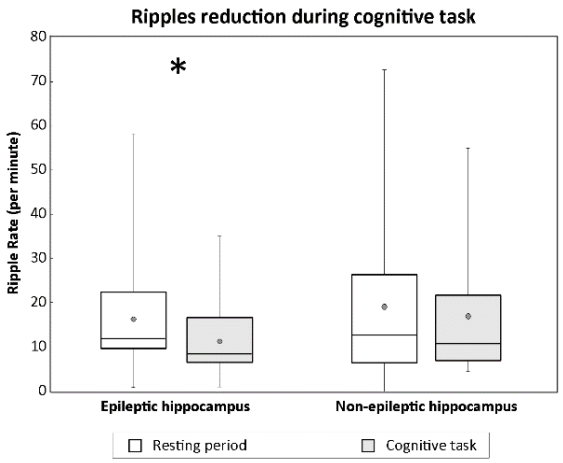


*Figure 10: Ripple rates during resting-state and cognitive-task periods within epileptic and non-epileptic hippocampi across all investigated subjects. A black asterisk means a significant difference in the epileptic hippocampus ($p < 0.05$). (Brázdil et al., 2015)*

R were significantly more reduced during a cognitive task than in quiet wakefulness in EH; in NEH, however, the difference remained statistically marginal.

Moreover, we observed a significant suppression of ripples in the first second after stimulus onset in NEH (Fig.11; Brázdil et al., 2015).

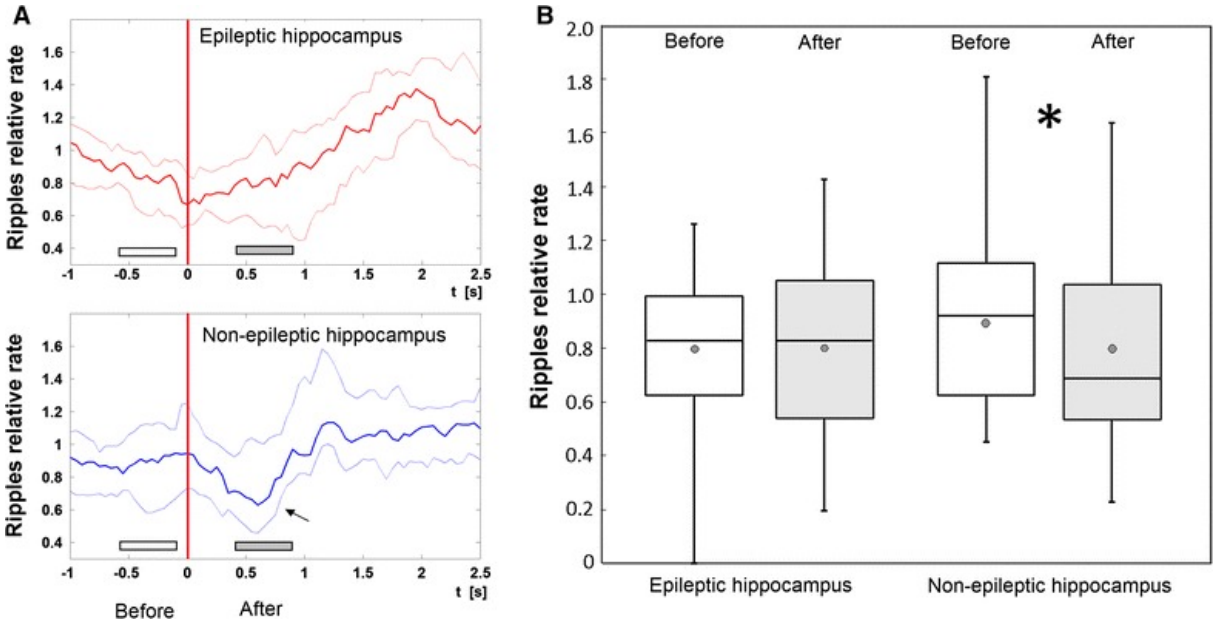


*Fig.11 Immediate short-lasting impact of cognitive stimuli on ripple rate across subjects. A) Transient suppression of relative ripple rate within epileptic (upper a) and non-epileptic (bottom a) hippocampus. Red vertical line defines visual stimulation onset (trigger). Full lines represent median, dotted lines 25 and 75 percentile across all subjects and all recording contacts. The figure clearly demonstrates task-induced HFOs reduction in the non-epileptic hippocampus in time period approximately 0.3–1 s after the stimulation (arrow). White and gray horizontal bars indicate an area that corresponds to the box plots in the right B. B) Box plots computed in baseline period before stimuli (−0.6 to −0.1 s) and after cognitive stimulation (0.4–0.9 s). A black asterisk means a significant difference in the non-epileptic hippocampus ($p < 0.02$).*

Importantly, however, in this study were not examined fast ripples due to a low sampling frequency. The study results we followed up with a new study in which we tested the hypothesis, that not only ripples but also fast ripples are modulated during wakefulness by cognitive tasks. We aimed to find different characteristics of HFOs in the hippocampus using a cognitive task. We hypothesized a distinct impact of a cognitive task on ripples and fast ripples (and their characteristics) within EH and NEH.

To test this hypothesis, we analyzed hippocampal SEEG of 15 patients during quiet wakefulness and during a simple visual cognitive oddball task. We investigated the impact of a cognitive task on HFOs with the aim of improving differentiation between epileptic and non-epileptic hippocampi in humans. HFOs in ripple and fast ripple frequency ranges were evaluated in both conditions, and their rate,

spectral entropy, relative amplitude, and duration were compared in epileptic and non-epileptic hippocampi.

The similarity of HFOs properties recorded at rest in epileptic and non-epileptic hippocampi suggests that they cannot be used alone to distinguish between hippocampi. However, both R and FR were observed with higher rates, higher relative amplitudes, and longer durations at rest as well as during a cognitive task in epileptic compared with non-epileptic hippocampi. Moreover, during a cognitive task, significant reductions of HFOs rates were found in epileptic hippocampi. These reductions were not observed in non-epileptic hippocampi. Our results indicate that although both hippocampi generate HFOs with similar features that probably reflect non-pathological phenomena, it is possible to differentiate between epileptic and non-epileptic hippocampi using a simple oddball task.

Hippocampal neurons are involved in many physiological cognitive processes. These functions are reflected, e.g., in cognitive event-related potentials (ERPs) that were repeatedly and consistently detected within the hippocampi using depth EEG recordings. How these functions are reflected in HFOs is nevertheless unclear. We revealed a significant decrease in HFO rates within epileptic hippocampal tissue but not in non-epileptic hippocampal tissue during discriminative task processing. Our results observed within the epileptic hippocampi show that the specific discriminative task modified its activity. It is very well known that even within epileptic hippocampi, some portion of physiological cognitive functions is often preserved. Besides clinical and neuropsychological indices, several studies with intracerebral event-related potentials have detected cognitive P3 phenomena in both normal and epileptic hippocampi (Meador et al., 1987; Puce et al., 1989; Brázdil et al., 1999). In epileptic hippocampi, these ERPs are often changed but not completely missing. Thus, the observed HFO changes within affected structures may suggest an increased involvement of the preserved normal hippocampal neurons that are active in some physiological cognitive processing and reduced involvement of the synchronously bursting neurons within the epileptic network that are generating pathological HFOs (Brázdil et al., 2015; Cimbalnik et al., 2020). Not observing a significant change in HFO rates within non-epileptic hippocampi makes it possible for us to hypothesize that healthy hippocampal neurons activated in our specific cognitive task are not involved in physiological HFO genesis. It is widely accepted that described physiological hippocampal HFOs reflect replay and consolidation of previously acquired information and are much more active during sleep (Axmacher et al., 2008).

Based on our results using a visual oddball task, it is possible to differentiate between epileptic and non-epileptic hippocampi, even though both hippocampi have HFOs with similar features that probably reflect non-pathological phenomena. And so, fast ripples recorded in the hippocampus should not be considered as only a pathological. Our results confirm the distinct impact of a particular discriminative task processing on ripples and fast ripples within epileptic and non-epileptic hippocampi, particularly the suppression of pathological HFOs in the epileptic hippocampus.

scientific reports

Check for updates

OPEN

# High frequency oscillations in epileptic and non-epileptic human hippocampus during a cognitive task

Martin Pail[1]✉, Jan Cimbálník[2], Robert Roman[1,3], Pavel Daniel[1,3], Daniel J. Shaw[3,4], Jan Chrastina[5] & Milan Brázdil[1,3]

**Hippocampal high-frequency electrographic activity (HFOs) represents one of the major discoveries not only in epilepsy research but also in cognitive science over the past few decades. A fundamental challenge, however, has been the fact that physiological HFOs associated with normal brain function overlap in frequency with pathological HFOs. We investigated the impact of a cognitive task on HFOs with the aim of improving differentiation between epileptic and non-epileptic hippocampi in humans. Hippocampal activity was recorded with depth electrodes in 15 patients with focal epilepsy during a resting period and subsequently during a cognitive task. HFOs in ripple and fast ripple frequency ranges were evaluated in both conditions, and their rate, spectral entropy, relative amplitude and duration were compared in epileptic and non-epileptic hippocampi. The similarity of HFOs properties recorded at rest in epileptic and non-epileptic hippocampi suggests that they cannot be used alone to distinguish between hippocampi. However, both ripples and fast ripples were observed with higher rates, higher relative amplitudes and longer durations at rest as well as during a cognitive task in epileptic compared with non-epileptic hippocampi. Moreover, during a cognitive task, significant reductions of HFOs rates were found in epileptic hippocampi. These reductions were not observed in non-epileptic hippocampi. Our results indicate that although both hippocampi generate HFOs with similar features that probably reflect non-pathological phenomena, it is possible to differentiate between epileptic and non-epileptic hippocampi using a simple odd-ball task.**

The discovery of high-frequency electrographic activity represents one of the essential milestones not only in epilepsy research, but also in cognitive science over the past few decades. These transient high and very high-frequency oscillations (HFOs/VHFOs) in invasive EEG (stereoelectroencephalography; SEEG) have been recorded repeatedly in several allocortical and neocortical structures. These short-lasting field potentials, both ictal and interictal phenomena, can be divided further into "ripples" (80–250 Hz), "fast ripples" (250–600 Hz), "very fast ripples" (VFR; 600–1000 Hz), and "ultra-fast ripples" (UFR; 1–2 kHz), all of which have been studied widely in humans under physiological and pathological conditions[1–12].

HFOs are believed to stem from the short-term synchronization of neuronal populations and their activity, and it appears that they are connected to normal as well as pathological brain functions[6,13]. While physiological HFOs seem to represent summated synchronous inhibitory postsynaptic potentials (IPSP) generated by interneuronal cell subpopulations regulating the principal cell activity and their discharges[14]. Epileptic HFOs might reflect the field potentials which are formed by the activity from clusters of abnormal synchronously bursting pyramidal cells, generating population spikes, and decreased inhibitory interneuron firing[6,15]. The detected HFO frequency can be determined purely from the behavior and activity of one cell subpopulation ("pure" HFOs). However, the observed HFOs (especially beyond the physiologic limits of neuronal firing; > 300 Hz), may also represent the net frequency of neuronal populations, more specifically due to the activity of different cell subpopulations of

[1]First Department of Neurology, Brno Epilepsy Center (Full member of the ERN EpiCARE), St. Anne's University Hospital and Medical Faculty of Masaryk University, Pekařská 53, Brno 65691, Czech Republic. [2]International Clinical Research Center, St. Anne's University Hospital, Brno, Czech Republic. [3]CEITEC – Central European Institute of Technology, Masaryk University, Brno, Czech Republic. [4]School of Life and Health Sciences, Aston University, Birmingham, UK. [5]Department of Neurosurgery, Brno Epilepsy Center, St. Anne's University Hospital and Medical Faculty of Masaryk University, Brno, Czech Republic. ✉email: martin.pail@fnusa.cz

synchronized neurons between which is a phase delay in activity. Each cell assembly then usually oscillate with a lower frequency than observed ("emergent" HFOs)[16,17].

There is evidence that ripple generation is influenced by larger networks; smaller networks are involved in fast ripples and even less in VFR and UFR generation, which can be observed focally[9]. Interest in HFOs is related primarily to the localization of the epileptogenic zone, since they are considered as being more focal and specific than classical epileptic spikes[18] that are only partially concordant with the epileptogenic zone[19]. As HFO rates are higher in focal seizure-generating tissue, they have attracted attention as a possible clinical biomarker[3].

Unfortunately, pathological and physiological HFOs cannot be distinguished by rate of their occurrence, as some regions are identified as generators of physiological HFOs[12]. Moreover, another significant problem, has been the fact that pathological HFOs overlap in frequency with physiological HFOs associated with normal brain function[8,20–22]. How these two types of electrographic phenomena can be separated remains unclear[6], as frequency and/or amplitude analysis alone seem to be insufficient for their delineation[23–25]. Therefore, the translation of HFOs into clinical practice is hindered by the inability to differentiate between pathological and normal HFOs in SEEG recordings. And so, more than twenty years after their discovery, there still exist questions about HFOs as biomarkers of epileptogenic brains and epileptogenic zones, and about their utility in clinical practice[12,26,27].

Until now, various analytical approaches have been sought to distinguish pathological and physiological HFOs. The methods used most commonly are based on, for example, a specific regional distribution in mesial temporal structures[28]; the association of HFOs with epileptiform discharges[4,26,29], slow waves[30] o spindles[31], or the difference between HFOs produced spontaneously and those induced by a cognitive task[8,23,24]. In the recent study of Sakuraba et al., epileptogenic region was determined based on less suppressive effect of REM sleep on HFOs in contrast to non-epileptogenic/physiological region[32]. Some authors have suggested separating HFOs by clustering them based on features such as frequency, duration, and amplitude[24,25,33]. Other reports have addressed this problem proposing several methods for dissociating different origins based on the width of the spectral frequency content of individual events, number of distinct cycles observed, and the presence of actual oscillations in the unfiltered raw signal[34,35]. Finally, when investigating electrophysiological brain recordings, the term HFO should be used to describe true high-frequency local field potential oscillations in the invasive EEG, that is oscillations visible in the raw recording and not the high-frequency Fourier components from a bandpass filter[36]. The ability to distinguish between pathological and physiological HFOs is crucial for understanding normal cognitive functions and no less important for the translation of HFOs into clinical practice.

In a recent study, we tested the hypothesis whether the presumed effect of cognitive task on hippocampal ripples can be used as a new approach for distinguishing pathological HFOs in the epileptic hippocampus (EH) from physiological HFOs in the non-epileptic hippocampus (NEH)[8]. To differentiate them, a simple oddball task was used. This study revealed different and, in some cases, opposing behavior of ripples within EH and NEH: Ripples were significantly more reduced during a cognitive task than in a resting period in EH, but in NEH this difference remained statistically marginal[8]. Moreover, we observed a significant suppression of ripple rate in the first second after stimulus onset only in NEH[8]. Importantly, however, we did not examine fast ripples due to a low sampling frequency.

In the present study, we tested the hypothesis that not only ripples, but also fast ripples are modulated by cognitive tasks. We aimed to find a distinct impact of a cognitive task on HFOs (the rate and other HFO characteristics) within EH and NEH. To test the hypothesis, we analyzed hippocampal SEEG of 15 patients during resting period and during a simple cognitive oddball task.

## Methods

**Subjects.** In our study we included 15 patients (7 females) ranging in age from 24 to 56 (mean: 38.3 ± 9.3) years. All patients suffered from medically intractable focal temporal epilepsies. For demographic and clinical characteristics of the included subjects, see Table 1. In most patients, chronic anticonvulsant medication was reduced slightly for the purposes of video-SEEG monitoring. The study procedures were approved by Masaryk University and St. Anne's University Hospital Ethics Committees. All subjects gave their written informed consent prior to the study investigation. All methods were performed in accordance with the relevant guidelines and regulations.

**EEG recordings.** Patients underwent the implantation of depth electrodes as part of their evaluation for pharmacoresistant focal epilepsy in order to localize seizure origin prior to surgical treatment. The location of the implanted electrodes was determined by clinical requirements. Each patient received 3–14 intracerebral electrodes containing either 5, 8, 10 or 15 individual contacts, in the temporal lobe and facultatively in other brain lobes using the Talairach stereotaxic system[37]. Standard platinum depth electrodes (ALCIS) were used (diameter = 0.8 mm; inter-contact distance = 1.5 mm, contact surface area = 5 $mm^2$; contact length = 2 mm). After implantation, each patient underwent MRI scanning to localize electrode placement. We used a 192-channel research EEG acquisition system (M&I; Brainscope, Czech Republic) for recording 30 min of an awake resting interictal period as well as the cognitive task. The sampling rate was 25 kHz and dynamic range of ± 25 mV with 10 nV (24 bits). The EEGs were low-pass filtered and downsampled to 5 kHz for further processing. All recordings were referenced to the average of intracranial signals. EEG data from a total of 111 electrode contacts positioned in either epileptic hippocampi (76) or non-epileptic hippocampi (35) were investigated (Table 1). No other structures were analyzed for the presence of spikes and HFOs. In identifying epileptic (EH) and non-epileptic hippocampi (NEH), we followed a process similar to that reported elsewhere[8,24]—specifically, based on the results of a standard visual analysis of interictal and ictal SEEG recordings: EH were identified by the presence of a seizure onset zone (confirmed by recording multiple seizures): the site in which contacts showed the first EEG ictal activity, with characteristic desynchronization and low voltage fast activity pattern. As presented

| Subject | Gender | Age at SEEG | FS | Age at Seizure onset | MRI before SEEG | Side of epilepsy | SOZ | Intervention/ histopathology | Postoperative outcome Engel (follow-up, year) | Number of analyzed contacts in EH | Number of analyzed contacts in NEH | Number of analyzed events in EH (spikes/R/FR) | Number of analyzed events in NEH (spikes/R/FR) |
|---|---|---|---|---|---|---|---|---|---|---|---|---|---|
| 1 | F | 26 | – | 17 | Normal | Left | Left hippocampus | Left AMTR/ FCD IB | IA (5) | 6 (left) | 3 (right) | 1950/517/835 | 205/69/302 |
| 2 | F | 56 | – | 28 | Right hippocampal atrophy | Right | Right hippocampus | Right AMTR/not available | IIIA (5) | 6 (right) | – | 1623/1991/1380 | – |
| 3 | M | 40 | – | 1 | Left hippocampal atrophy | Left | Left hippocampus | Left AMTR/negat | IA (5) | 8 (left) | – | 4501/2212/1454 | – |
| 4 | M | 38 | – | 27 | Normal | Bilaterally | Hippocampus bilaterally (mainly right side) | VNS | – | 3 (right) | – | 812/420/404 | – |
| 5 | M | 41 | – | 33 | Focal hyperintensity within right basal temporal lobe | Right | Right hippocampus, lesion | Right AMTR/FCD IIIb ganglioglioma | IA (5) | 7 (right) | 3 (left) | 1735/672/623 | 499/209/286 |
| 6 | F | 33 | – | 2 | Postencephalitic changes of left T lobe, left hippocampal atrophy | Left | Left hippocampus, lesion | Left AMTR/hippocampal sclerosis, postencephalitic changes | IA (5) | 6 (left) | 5 (right) | 1241/1029/97 | 155/50/297 |
| 7 | M | 35 | – | 21 | Bilateral hippocampal atrophy, RX > LT | Bilaterally | Hippocampus bilaterally (mainly right side) | VNS | – | 7 (right) | – | 2314/978/560 | – |
| 8 | M | 37 | FS | 31 | Normal | Bilaterally | Hippocampus bilaterally (mainly left side) | Left AMTR/negat | IA (4) | 8 (left) | – | 1149/1247/1002 | – |
| 9 | F | 27 | – | 9 | Left hippocampal atrophy | Left | Left hippocampus | Left AMTR/FCD IIIA | IIIA (4) | 7 (left) | – | 2767/1878/1767 | – |
| 10 | M | 51 | FS | 2 | Right hippocampal atrophy | Right | Right hippocampus | Right AMTR/hippocampal sclerosis | IA (4) | 5 (right) | 7 (left) | 636/568/895 | 222/171/435 |
| 11 | M | 24 | – | 10 | Left hippocampal atrophy, mild posttraumatic gliosis of left pericentral region | Left | Left hippocampus | Left AMTR/hippocampal sclerosis | IIA (4) | 5 (left) | – | 815/507/228 | – |
| 12 | F | 33 | – | 29 | Asymetry of colateral sulci in temporal lobe | Left | Temporal pole and lateral temporal cortex | Resection of temporal pole and anterior part of lateral temporal cortex/negat | IIIA (4) | – | 5 (left) | – | 308/69/125 |
| 13 | F | 45 | – | 26 | Left hippocampal atrophy | Left | Left T pole | Left AMTR / negat | IIIA (4) | – | 6 (right) | – | 155/53/328 |
| 14 | F | 36 | – | 16 | Nodular heterotopia along dorsal part of lateral ventricle and lateral cortex TO left | Left | Left lateral cortex TO junction | Lateral cortical resection TO left/ FCD IIA | IIA (4) | – | 4 (left) | – | 326/181/137 |
| 15 | M | 53 | – | 33 | Left hippocampal atrophy | Left | Left hippocampus | Left AMTR | IA (1) | 8 (left) | – | 3560/1641/1064 | – |

**Table 1.** Demographic and clinical data. M = male, F = female; SEEG = stereoelectroencephalography; T = temporal; O = occipital; FS = febrile seizures; SOZ = seizure onset zone; AMTR = anteromedial temporal resection; FCD = focal cortical dysplasia; EH = epileptic hippocampus; NEH = non-epileptic hippocampus; VNS = vagus nerve stimulation, R = ripples, FR = fast ripples.

in the Table 1, epileptic hippocampus was selected in 12 patients. A unilateral hippocampal epileptic region was found in 9 patients (6 patients with Engel IA (seizure free), 1 patient with Engel IIA (histologically confirmed hippocampal sclerosis), 2 patients with Engel IIIA (in one case histologically confirmed hippocampal sclerosis)). Bilateral epileptic hippocampal regions were determined in three, in which we analyzed the data only within a more pathologically active hippocampus. Putative NEH were defined by the absence of (a) a seizure onset zone and (b) frequent interictal spikes (IEDs; > 50 per 10 min). The putative non-epileptic hippocampi with spiking above the threshold were visually reviewed whether the IEDs were propagated from other brain structures. The putative non-epileptic hippocampi that generated IEDs were excluded from the analysis. NEH were identified in either the left or right hippocampus in extramesiotemporal epilepsy, but contralateral to the epileptogenic hippocampus in unilateral mesiotemporal epilepsy. In this way, each hippocampus could be classified either as epileptic or non-epileptic. We always analyzed all the electrode contacts within a particular hippocampus. In each subject, all the obtained data were reviewed to identify artifactual and pathological traces by expert neurologists (M.B. and M.P.).

Awake resting state was recorded with the subject's eyes closed with the minimization of possible external stimuli.

**Behavioral tasks.** Subjects were seated comfortably in a moderately lighted room. A monitor screen was placed approximately 100 cm in front of their eyes. During the task, they were asked to focus their gaze on a small fixation point in the center of the monitor screen. We performed a standard visual oddball task: three types of stimuli (target, frequent, and distractor) were presented in the center of the screen (black background) for 500 ms in random order at a ratio of 1:4.6:1. The interstimulus interval varied randomly between 4 and 6 s. Specifically, the experimental stimuli comprised clearly visible yellow capital letters "X" (target), "O" (frequent), and various other capital letters (distractor). The number of targets was 50. The task was divided into four blocks, each block consisting of 12 or 13 target stimuli. Each subject was instructed to count the target stimuli subvocally and to report the calculated number after each block.

**Data analysis.** Using a modified pipeline for automated HFO detection[21], we analyzed potential ripple and fast ripple rates in EH and NEH. We also carried out an automated detection of interictal spikes in the dataset used in this study[38]. Further, we compared the influence of the cognitive task on HFO and spikes occurrence in EH and NEH. Analyses of the HFO and spike occurrences and HFO features (relative amplitude, duration, and spectral entropy) were performed separately in the first 10-min window of the visual oddball task (i.e. throughout the whole epoch, not just in the short segments after specific stimuli) and during the resting state.

The detector of HFOs utilizes a sequence of power envelopes in consecutive logarithmically spaced frequency bands within a 10 s statistical window. The z-score of each separate power envelope is computed and a matrix of the z-scored power envelopes is created. The segment of each power envelope above the threshold (> 3) and with the number of oscillations larger than 1 is marked as a band detection. Band detections overlapping in the temporal domain are joined into one event (Fig. 1).

The relative amplitude is calculated as the highest z-score value of the event and the frequency is determined as the frequency band in which this value occurred. The duration is derived from the first and last value above the threshold across frequency bands. Spectral entropy was computed as the entropy of normalized power spectral density of detected events. Only detections longer than 5 oscillations at the determined frequency were processed.

To investigate how many HFOs occurred simultaneously with spikes and could be influenced by the changes in spike rates, we analyzed the number of HFOs that are superimposed on detected spikes. We analyzed the counts of spike-HFOs as well as standalone HFOs.

**Statistical analysis.** The statistical analysis was performed using in-house Python scripts. The individual data sets were first tested for distribution normality with D'Agostino's normality test. Subsequently, since most of the data sets were not normally distributed, the Wilcoxon rank-sum test was used to investigate differences between studied data sets (the average for individual channels were compared statistically). Bonferroni correction for multiple comparisons was applied where necessary. We also performed an analysis of differences between task-induced and resting HFO rates in each hippocampus (for each contact) using the Wilcoxon paired signed-rank test.

**Ethics approval and consent to participate.** We confirm that we have read the Journal's position on the issues involved in ethical publication and affirm that this report is consistent with those guidelines. All subjects gave their written informed consent prior to the investigation.

## Results

Interictal spikes, ripples, and fast ripples were detected in the hippocampi of all subjects included in the study. The mean percentage of HFOs that occurred simultaneously with spikes was 41% (in detail see Table 2); that is, most HFOs were observed independently of spikes. The degree of success in completing the cognitive task across all patients was at least 96%; this translates to a maximum of 2 errors out of 50 targets.

During the resting period, a comparison of HFO features revealed that both epileptic and non-epileptic hippocampi exhibited HFOs with similar properties. In the EH compared with NEH, however, we observed both ripples and fast ripples significantly more frequently and with higher relative amplitude and longer duration (Table 3). Furthermore, there was no significant difference in HFO spectral entropy. An illustration of these comparisons for ripples and fast ripples are presented in Figs. 2, 3 and 4.

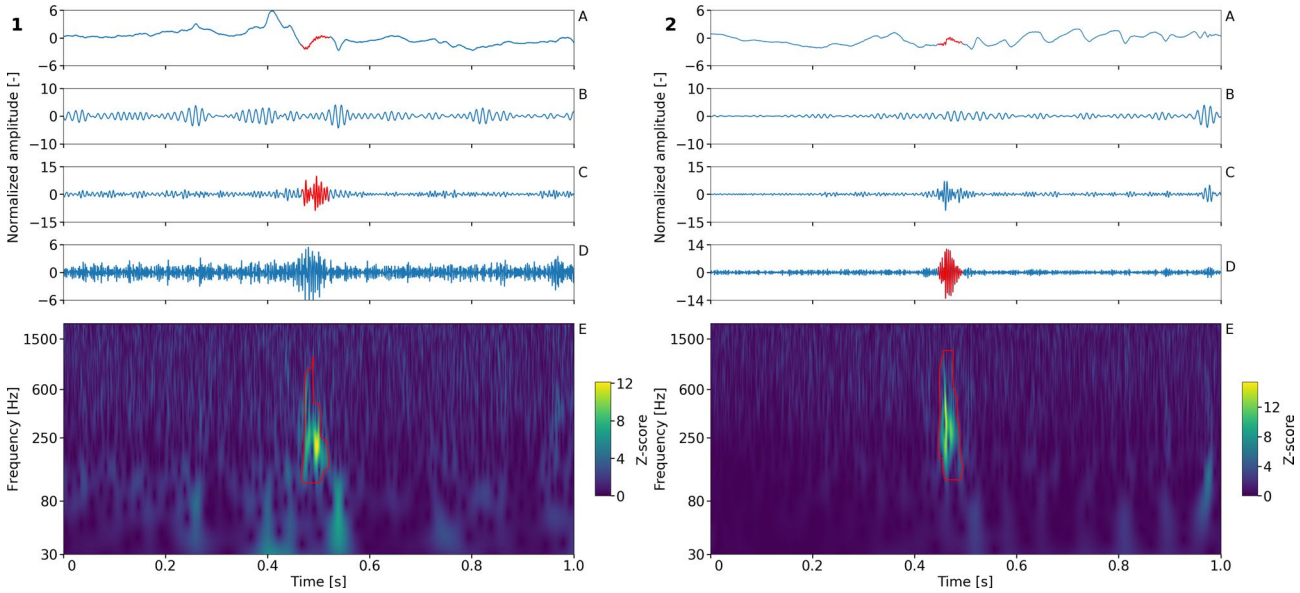


**Figure 1.** HFO detection. Raw data (A) and band-pass filtered data in the high gamma band frequency (65–80 Hz; (B), ripple band (80–250 Hz; (C) and fast ripple band (250–600 Hz; (D,E) Z-scored power envelopes in a series of log spaced band-pass filtered bands. The time scale of all subplots (A–E) is identical. The detection is represented by red lines in (A,C,E). The brightest spot of the detected event in (E) corresponds to the maximum peak relative amplitude. The frequency of the event is determined by the frequency band in which this peak occurred. The duration of the event is calculated as the difference between earliest onset and latest offset across frequency bands.

| | Epileptic hippocampus | | | Non-epileptic hippocampus | | |
|---|---|---|---|---|---|---|
| Subject | Spikes | Spike-HFOs | Standalone HFOs | Spikes | Spike-HFOs | Standalone HFOs |
| 1 | 1950 | 586 | 766 | 205 | 0 | 371 |
| 2 | 1623 | 840 | 2531 | – | – | – |
| 3 | 4501 | 2841 | 838 | – | – | – |
| 4 | 812 | 477 | 347 | – | – | – |
| 5 | 1735 | 1012 | 299 | 499 | 254 | 241 |
| 6 | 1241 | 138 | 988 | 155 | 0 | 347 |
| 7 | 2314 | 832 | 706 | – | – | – |
| 8 | 1149 | 391 | 1858 | – | – | – |
| 9 | 2767 | 1450 | 2204 | – | – | – |
| 10 | 636 | 295 | 1168 | 222 | 30 | 576 |
| 11 | 815 | 277 | 458 | – | – | – |
| 12 | – | – | – | 308 | 6 | 188 |
| 13 | – | – | – | 155 | 5 | 376 |
| 14 | – | – | – | 326 | 168 | 150 |
| 15 | 3560 | 1195 | 1106 | – | – | – |

**Table 2.** Rates of spikes, spike-HFOs and standalone HFOs per 10 min for individuals within resting-state recording.

The mean HFO rate in the resting period across all contacts was 219.9 ± 151.6 and 40.1 ± 44.3 per 10 min within EH and NEH, respectively. In cognitive-task periods, the mean HFOs rate within EH and NEH changed to 95.5 ± 82.9 and 43.3 ± 19.0 per 10 min, respectively. The change of HFO rate during the cognitive task was significant in EH ($p < 0.001$) but not in NEH. Similar results were revealed by statistical analysis of the differences between the task-induced and the resting period HFO rates using Wilcoxon signed-rank test: A significant reduction of HFO was observed only in contacts within EH ($p < 0.001$).

HFO rates were significantly different in EH compared to NEH during resting state as well as during the cognitive task ($p < 0.001$ and $p = 0.002$, respectively). Looking at HFOs separately in the ripple and fast ripple frequency ranges, we obtain similar results. Ripple and fast ripple rates were significantly reduced during the

| | Rate (N/10 min) | | | Log relative amplitude | | | Duration (ms) | | | Spectral entropy | | |
|---|---|---|---|---|---|---|---|---|---|---|---|---|
| | Rest | Oddball | *p* value | Rest | Oddball | *p* value | Rest | Oddball | *p* value | Rest | Oddball | *p* value |
| **Ripples** | | | | | | | | | | | | |
| NEH | 16.06 (±16.57) | 9.0 (±6.74) | Nonsig | 1.92 (±0.30) | 1.95 (±0.22) | Nonsig | 45.73 (±10.83) | 38.39 (±13.58) | Nonsig | 4.32 (±0.51) | 4.71 (±0.25) | 0.001 |
| EH | 125.50 (±75.91) | 54.96 (±52.29) | <0.001 | 2.32 (±0.21) | 2.25 (±0.27) | Nonsig | 52.71 (±10.97) | 53.06 (±14.12) | Nonsig | 4.46 (±0.29) | 4.61 (±0.35) | <0.05 |
| *p* value | <0.001 | <0.001 | | <0.001 | <0.001 | | <0.05 | <0.001 | | Nonsig | Nonsig | |
| **Fast ripples** | | | | | | | | | | | | |
| NEH | 28.52 (±22.09) | 34.54 (±18.82) | Nonsig | 1.89 (±0.23) | 1.88 (±0.12) | Nonsig | 19.14 (±10.90) | 16.40 (±5.31) | Nonsig | 4.82 (±0.39) | 4.89 (±0.22) | Nonsig |
| EH | 94.38 (±93.88) | 41.26 (±39.47) | <0.001 | 2.16 (±0.27) | 2.02 (±0.25) | <0.005 | 27.51 (±11.55) | 21.75 (±8.66) | <0.005 | 4.65 (±0.34) | 4.87 (±0.34) | <0.001 |
| *p* value | <0.005 | Nonsig | | <0.001 | <0.01 | | <0.01 | <0.01 | | Nonsig | Nonsig | |

**Table 3.** HFO characteristics per contact in the ripple and fast ripple ranges during rest and the oddball task.

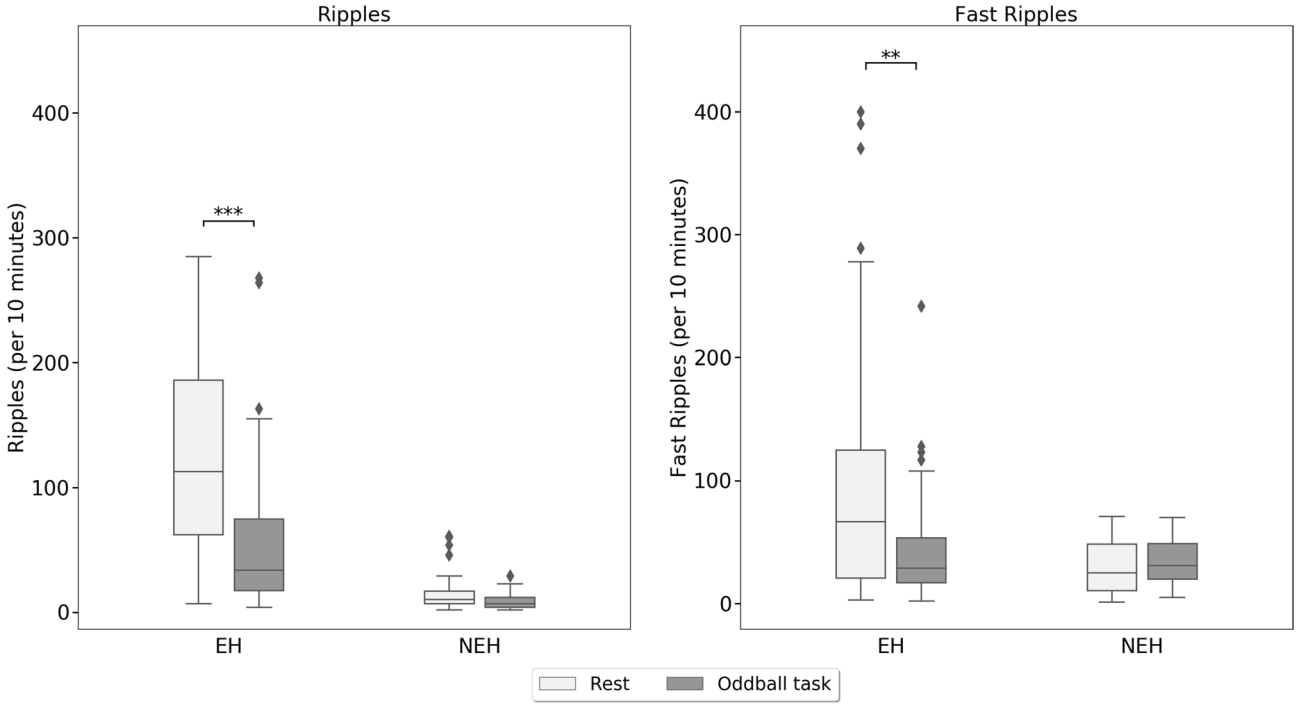


**Figure 2.** Fast ripple and ripple rates during resting and cognitive-task periods within the epileptic and non-epileptic hippocampi across all investigated subjects. Black asterisks indicate significant differences in epileptic hippocampi ($p < 0.001$). Black diamonds indicate outliers.

cognitive task in EH only, however ($p < 0.001$); the rate of HFOs was not significantly influenced by the cognitive task in NEH (Fig. 2).

During the cognitive task, HFOs (both ripples and fast ripples) were detected with the same features as during the resting period in epileptic and non-epileptic hippocampi. However, ripples exhibited higher spectral entropy in both EH and NEH during the cognitive task compared with the resting period. The relative amplitude and duration of R did not change in neither NEH nor EH.

During performance of the cognitive task, more HFOs in the fast ripple frequency range with lower relative amplitude, shorter duration, and higher spectral entropy were detected in EH than during the resting period. In NEH, all characteristics of fast ripples did not differ significantly between rest and the cognitive task. The comparisons of the specific HFO characteristics in the ripple and fast ripple ranges are summarized in Table 3.

Spikes exhibited a similar significant decrease in their rate during the cognitive task in the epileptic hippocampus, but this was observed also in non-epileptic hippocampus. Counts of spike-HFOs as well as standalone HFOs also showed significant reductions during the cognitive task in the epileptic hippocampi (Table 4).

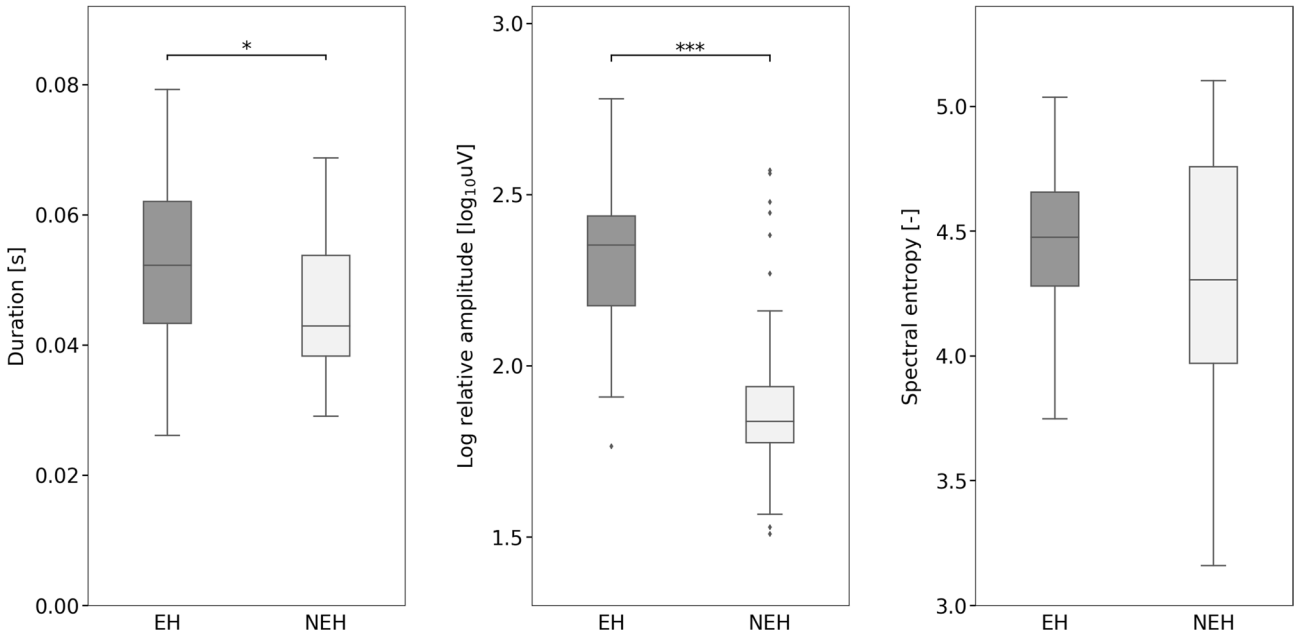


**Figure 3.** Ripple duration, relative amplitudes and spectral entropy during the resting period within the epileptic and non-epileptic hippocampi across all subjects. Black asterisks indicate significant differences ($p < 0.001$). Black diamonds indicate outliers.

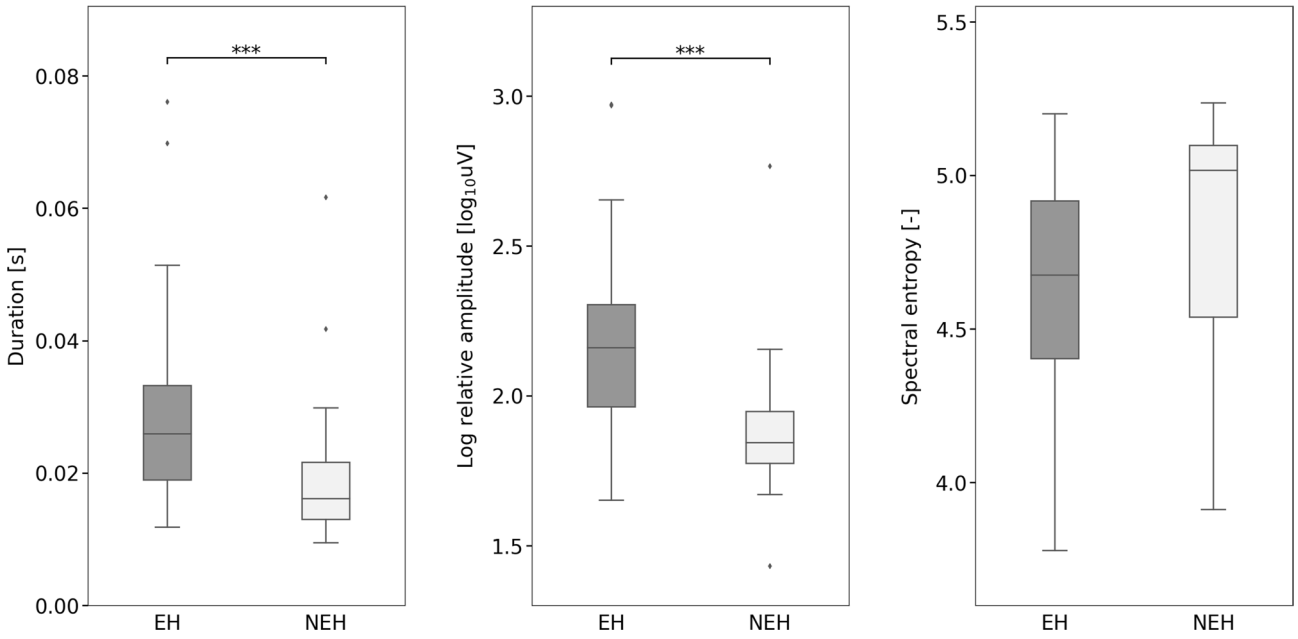


**Figure 4.** Fast ripple duration, relative amplitudes and spectral entropy during resting periods within the epileptic and non-epileptic hippocampi across all investigated subjects. Black asterisks indicate significant differences ($p < 0.001$). Black diamonds indicate outliers.

## Discussion

Widespread cortical and subcortical neuronal networks are thought to be coordinated into synchronous oscillations spanning ripples or fast ripples frequency ranges during cognitive phenomena but also pathologic epileptic processes[20]. In this study, we investigated HFOs only in the hippocampus, which plays a pivotal role in both cognitive (especially learning and memory) and epileptogenic processes and which is the most studied brain structure in relation to HFOs. Unsurprisingly, we observed that the ripples and fast ripples were detected at relatively low rates in NEH but at much higher rates in the EH (seizure onset zone), which confirms previously published data concerning the pathogenicity of this phenomena[4,18,39,40]. Importantly, our results not only confirm

| | Spikes | | | Spike-HFOs | | | Standalone HFOs | | |
|---|---|---|---|---|---|---|---|---|---|
| | Rate (N/10 min) | | | Rate (N/10 min) | | | Rate (N/10 min) | | |
| | Rest | Oddball | *p* value | Rest | Oddball | *p* value | Rest | Oddball | *p* value |
| NEH | 27.15 (± 18.86) | 14.13 (± 13.57) | < 0.01 | 0.72 (± 0.97) | 0.88 (± 1.76) | Nonsig | 33.88 (± 29.69) | 38.88 (± 19.34) | Nonsig |
| EH | 187.9 (± 120.34) | 114.00 (± 83.59) | < 0.001 | 98.68 (± 77.77) | 41.25 (± 47.30) | < 0.001 | 122.51 (± 122.65) | 56.88 (± 68.94) | < 0.001 |
| *p* value | < 0.001 | < 0.001 | | < 0.001 | < 0.001 | | < 0.001 | Nonsig | |

**Table 4.** Spikes, spike-HFOs and standalone HFOs rates per contact during rest and the oddball task.

our previous findings of significantly different behavior of ripples within the EH and NEH, suggesting diverse mechanisms of their generation[8], but also extend these previous findings by revealing similar results in the fast ripples frequency range.

Our results suggests that a distinction between epileptic and non-epileptic hippocampus cannot be based solely on HFO rates or characteristics at rest; there is no clear limit of HFO rates per 10 min of recording, nor any HFO characteristics that could be used to classify the hippocampal tissue surrounding individual contacts as epileptic or non-epileptic. Only during the very specific discriminative task did we observe a differential decrease in the rate of HFOs in EH. Our results observed within epileptic hippocampi show that its activity is modified by the cognitive task and confirm that a specific discriminative task suppresses pathological HFOs in the epileptic hippocampus, which we discuss below.

Hippocampal and parahippocampal physiological ripples have been proposed to be functionally involved in memory consolidation, strengthening and reorganizing memory traces during both rest and slow wave sleep and providing a link between information transfer and memory formation[20,41–44]. However, this concept of ripples as a physiological phenomenon in the hippocampus during memory-related memory processes has been questioned several times[8,12]. Our previous study showed a significant decrease of ripple rate in epileptic hippocampus during event processing. This may suggest increased involvement of normal hippocampal neurons in physiological cognitive processing and reduced involvement in the epileptic network impelled by synchronously bursting neurons[8]. The prevalence of pathologic ripples is seen usually during non-REM sleep, likely resulting from the sleep-dependent enhancement of network synchronization[5,45–47]. This suggests that a proportion of ripples present in EH are connected to underlying pathological network activity[8]. Our observation that a cognitive task only partly affects general ripple rate within NEH (a large overlap was observed between both EH and NEH) may be explained by the expected physiological role of normal hippocampal neurons during both rest (memory consolidation/awake neuronal replay) and task (complex event discrimination processing) periods[8].

Conversely, hippocampal fast ripples, VFR, and UFR have been repeatedly reported and considered as biomarkers of epileptogenesis and epileptogenicity, related to pathological processes and occurring in close proximity to the epileptic focus[1,9,10]. VFR and UFR seem to be more localized to the epileptogenic zone than fast ripples; surgical removal of the tissue generating these interictal HFOs leads to favorable surgery outcome[9]. Although fast ripples are considered pathological, they were also detected in a non-epileptic hippocampus[48]. Based on our results, both epileptic and non-epileptic hippocampi have a population of fast ripples with similar properties (i.e. with low fast ripple counts, low relative amplitude, short duration, and non-significant higher spectral entropy), but in the epileptic hippocampus, higher rates of HFOs with extra values of properties tend to occur more often. In other words, the variance is much larger for all the HFO features measured in EH than in NEH.

In line with published data, by evaluating fast ripple occurrence in resting and active periods, we observed the rates of fast ripples spreading to much higher values in EH, and a decreasing number of fast ripples in EH during the discriminative task processing. A similar mechanism like ripple range could be supposed, i.e. the increased involvement of preserved normal hippocampal neurons that are active in some physiological cognitive processing and the reduced involvement of synchronously bursting neurons within the epileptic network generating pathological HFOs[8]. Since the degree of success in completing the cognitive task in all patients was at least 96%, it can be assumed that the changes observed in task performance are really related to the mental processing during the cognitive task. The observed HFO changes in the epileptic hippocampus during the cognitive paradigm could partially reflect the result of activity in many neuronal networks and cognitive processes, including e.g. attention, conscious processing of an event, working memory, stimulus evaluation and response preparation[49,50]. Therefore, the HFO changes observed in the epileptic hippocampus during the oddball task cannot be assigned to a specific function but rather generally related to mental processing.

According to published studies, most brain cortical areas react (with task-induced modulation of high frequency activity) to at least one of the cognitive tasks performed by the patient[51], except for brain epileptogenic regions that are heavily contaminated by epileptiform activity[51]. Similarly, in a recent animal study, the authors revealed that pathological HFO rate is independent of brain state, though they did not test cognitive load[52]. Based on these results, we would expect that the occurrence of interictal spikes and HFOs is unlikely to be altered during state changes or by stimulation in the epileptic hippocampal region, compared to areas not responsible for seizure generation. Nevertheless, we observed changes just in EH. This would suggest that the epileptic hippocampus was actually participating in processing the stimulus. It is very well known that even within the epileptic hippocampi, some portion of physiological cognitive functions is often preserved. Ewell´s group confirmed that both pathological and non-pathological HFOs can co-occur in the same memory circuits and moreover, up to 28% CA1 principal cells participate in generating both events[52]. However, as can be seen, the majority of hippocampal

neurons are modulated by only one event type or the other[52]. Besides clinical and neuropsychological indices, several studies with intracerebral event-related potentials detected cognitive P3 phenomena in both normal and epileptic hippocampi[53–55]. In epileptic hippocampi, these ERPs are often changed but not completely missing.

As mentioned already, in our study fast ripples were also observed in NEH distant from the epileptogenic zone. The fast ripples detected in NEH cannot be clearly defined as pathological or physiological or as a manifestation of the propagation of pathological HFO generated elsewhere. But this propagation effect will not play a significant role, as SEEG measures the local field potentials generated within a centimeter radius and the field formed by neurons over a centimeter from a recording site contribute only a marginal part of the signal[56].

Moreover, which is essential, the cognitive task obviously did not change the rate of HFOs in NEH. This of course raises the question of whether fast ripples are the result of the non-epileptic activity of neurons in the NEH, since the fast ripple number did not change between resting state and cognitive task. If there were only pathological fast ripples within NEH, we assume that their number would decrease during a cognitive task, similarly to what we found in EH. Not observing a significant change in HFO rate within non-epileptic hippocampi, we hypothesize that healthy hippocampal neurons activated in our specific cognitive task are not involved in physiological HFO genesis. It is widely accepted that physiological HFOs are reflecting memory consolidation and are much more active during sleep[20,41–44]; this is the opposite of our task, which demands a very high attentional load.

Actually, the phenomenon of physiological fast ripples (up to 600 Hz) induced in the hippocampus during a cognitive task was also described in a recent study by Kucewicz et al.[21]. The number of induced HFO was decreasing with increasing frequencies. Most of these induced oscillations lasted between 10 and 25 ms, similarly to the gamma cycle synchronization time frame (correlating with memory formation, loading and maintenance) and the time window for synaptic interactions of neuronal ensembles[21]. This finding supports a physiological origin of fast ripples also in the hippocampus, not only within the primary motor cortex, somatosensory cortex, and visual cortices as was previously published[23,24,26,57]. All things considered, Kucewicz et al.[21] hypothesized that these induced both ripples and fast ripples likely reflect the coordinated activity of a number of stimulus-specific neurons responding to stimuli. Finally, these phenomena play an important role for fast network synchronization in human cognition.

Concerning the HFO entropy, we found that fast ripples had higher entropy during oddball task than in the rest in the EH. Our results are congruent with those published recently by Liu et al.[58]. Consistently, in all patients, the typical HFOs with the highest degree of waveform similarity (in our case, we can use the term "low entropy") were seen within epileptogenic tissue only, whereas HFOs embedded in random waveforms (high entropy) were generated by sites in the functional regions independent from the epileptogenic locations[58]. The repetitive waveform pattern was evident in fast ripple range also in our data. This result confirms the possibility of physiological fast ripples in NEH and reduced pathological FR in EH, since these oscillations had higher entropy than those seen during rest in EH and therefore probably have a different origin.

Additionally, we have shown that the "physiological" HFOs have significantly different properties from "pathological" HFOs, primarily shorter duration and lower amplitude[21,24]. In line with this, during the cognitive task in EH the fast ripples were detected with lower mean relative amplitude and shorten duration. In summary, during the cognitive task, more fast ripples were observed in EH with similar characteristics as in the NEH.

The fundamental question remains of whether the resting state and task-related ripples and fast ripples (normal and pathological) exhibit similar or different mechanisms of generation or possess any functional significance. As was shown, HFOs can simply represent a marker of highly activated and synchronized neurons, regardless of the structure or mechanism underlying them. These high frequency signals appear to aggregate local (spiking) activity of neuronal populations or network oscillations[59]. However, the spectral content of local field potential oscillations, which reflects high spectral components arising from sharply contoured transients, is not considered true/standalone HFOs in the invasive EEG[36,60]. Neurons firing broader spikes contaminate the local field potential to a greater extent because their waveforms have stronger components in lower frequencies than short spikes. Moreover, neurons that fire coupled to a certain rhythm and spike synchrony can increase the extent of spike contamination[34]. Signals occurring over larger spatial extents are expected to have greater effect on high frequencies and contribute to a broader range of frequencies[34]. In our study we analyzed true HFOs in the majority of cases as the mean percentage of HFOs that occurred simultaneously with spikes was only 35% (46% in EH and 6% in NEH). We also analyzed the counts of spike-HFOs as well as standalone HFOs. Both analyses showed significant reduction during the cognitive task in the epileptic hippocampus.

Physiological HFOs result from phasic inhibitory input on the soma of pyramidal cells, while epileptic HFOs, usually superimposed on interictal epileptiform sharp waves, appear to reflect the field potentials which are formed by the activity from clusters of abnormal synchronously bursting pyramidal cells, generating population spikes, and decreased inhibitory interneuron firing[6,15]. Based on the functioning of synaptic transmission, the contribution of this mechanism to HFO genesis is limited to approximately 80–150 Hz[61]. The true high frequency local field potential oscillations above ~ 250 Hz are above the physiological firing rate of pyramidal neurons and cannot be generated by synaptic currents[61]. It is assumed, these local field potential oscillations are an arising rhythm generated by the in and out of phase action potential firing of populations of neuronal cell assemblies or clusters[9,61]. Originally suggested pathologically interconnected neurons emitting hypersynchronous bursts, as the source of fast ripple oscillations[15] and a population of these clusters might underlie generation of activity above ~ 500 Hz[9].

The fact that our study consists of analyses of chronic epileptic patients is an obvious limitation. The brain tissue from which the signal is acquired is not organized in the same way as normal tissue; this may lead to a bad and misleading model of physiological human neural processing and functional organization[56]. The possibility of the disease-related processes interfering with the reported physiological oscillations cannot be completely ruled out

and must be taken into account, although usually many epileptic patients perform behaviorally as well as normal subjects[56]. Certain caution must be taken when interpreting "normal" results onto normal hippocampal behavior.

It is important to highlight that the majority of previous studies evaluated results drawn from HFO analysis at a group level, and when considering individual patients the rates of HFOs are often highly variable and less specific for epileptic brain localization[12,36]. HFOs could reflect increased cortical excitability, perhaps more than epileptogenicity. Our results support a possible physiological origin of fast ripples as well. Thus, in individual patients, the count of fast ripples may include fast ripples of physiological origin and therefore fast ripples may not be a sensitive and unique biomarker of epileptogenicity[12]. This finding, however, does not alter the fact that pathological fast ripples clearly prevail in epileptic hippocampi.

## Conclusion

Based on our results using a visual oddball task, it is possible to differentiate between epileptic and non-epileptic hippocampi, even though both hippocampi have HFOs with similar features that probably reflect non-pathological phenomena. And so, fast ripples recorded in the hippocampus should not be considered as only a pathological. Our results confirm the distinct impact of a very specific discriminative task processing on ripples and fast ripples within epileptic and non-epileptic hippocampi, particularly the suppression of pathological HFOs in epileptic hippocampus.

Received: 27 December 2019; Accepted: 23 September 2020
Published online: 23 October 2020

## References

1. Bragin, A., Engel, J. Jr., Wilson, C. L., Fried, I. & Buzsáki, G. High-frequency oscillations in human brain. *Hippocampus* **9**, 137–142 (1999).
2. Worrell, G. A. *et al.* High-frequency oscillations and seizure generation in neocortical epilepsy. *Brain* **127**, 1496–1550 (2004).
3. Worrell, G. & Gotman, J. High-frequency oscillations and other electrophysiological biomarkers of epilepsy: clinical studies. *Biomark. Med.* **5**, 557–566 (2011).
4. Urrestarazu, E., Chander, R., Dubeau, F. & Gotman, J. Interictal high-frequency oscillations (100–500 Hz) in the intracerebral EEG of epileptic patients. *Brain* **130**, 2354–2366 (2007).
5. Bagshaw, A. P., Jacobs, J., LeVan, P., Dubeau, F. & Gotman, J. Effect of sleep stage on interictal high-frequency oscillations recorded from depth macroelectrodes in patients with focal epilepsy. *Epilepsia* **50**, 617–628 (2009).
6. Engel, J. Jr., Bragin, A., Staba, R. & Mody, I. High-frequency oscillations: What is normal and what is not?. *Epilepsia* **50**, 598–604 (2009).
7. Brázdil, M. *et al.* Interictal high-frequency oscillations indicate seizure onset zone in patients with focal cortical dysplasia. *Epilepsy Res.* **90**, 28–32 (2010).
8. Brázdil, M. *et al.* Impact of cognitive stimulation on ripples within human epileptic and non-epileptic hippocampus. *BMC Neurosci.* **16**, 47 (2015).
9. Brázdil, M. *et al.* Very high-frequency oscillations: Novel biomarkers of the epileptogenic zone. *Ann. Neurol.* **82**, 299–310 (2017).
10. Jacobs, J. *et al.* High-frequency oscillations (HFOs) in clinical epilepsy. *Prog. Neurobiol.* **98**, 302–315 (2012).
11. Usui, N. *et al.* Significance of very-high-frequency oscillations (over 1,000 Hz) in epilepsy. *Ann. Neurol.* **78**, 295–302 (2015).
12. Roehri, N. *et al.* High-frequency oscillations are not better biomarkers of epileptogenic tissues than spikes. *Ann. Neurol.* **83**, 84–97 (2018).
13. Engel, J. Jr. & da Silva, F. L. High-frequency oscillations—Where we are and where we need to go. *Prog. Neurobiol.* **98**, 316–318 (2012).
14. Buzsáki, G., Horváth, Z., Urioste, R., Hetke, J. & Wise, K. High-frequency network oscillation in the hippocampus. *Science* **256**, 1025–1027 (1992).
15. Bragin, A., Benassi, S. K., Kheiri, F. & Engel, J. Jr. Further evidence that pathologic high-frequency oscillations are bursts of population spikes derived from recordings of identified cells in dentate gyrus. *Epilepsia* **52**, 45–52 (2011).
16. Jiruska, P. *et al.* Synchronization and desynchronization in epilepsy: Controversies and hypotheses. *J. Physiol.* **591**, 787–797 (2013).
17. Jiruska, P. *et al.* Update on the mechanisms and roles of high-frequency oscillations in seizures and epileptic disorders. *Epilepsia* **58**, 1330–1339 (2017).
18. Jacobs, J. *et al.* Interictal high-frequency oscillations (80–500 Hz) are an indicator of seizure onset areas independent of spikes in the human epileptic brain. *Epilepsia* **49**, 1893–1907 (2008).
19. Bartolomei, F. *et al.* What is the concor-dance between the seizure onset zone and the irritative zone? A SEEG quantified study. *Clin. Neurophysiol.* **127**, 1157–1162 (2016).
20. Buzsáki, G. & Silva, F. L. High frequency oscillations in the intact brain. *Prog. Neurobiol.* **98**, 241–249 (2012).
21. Kucewicz, M. T. *et al.* High frequency oscillations are associated with cognitive processing in human recognition memory. *Brain* **137**, 2231–2244 (2014).
22. Alkawadri, R. *et al.* The spatial and signal characteristics of physiologic high frequency oscillations. *Epilepsia* **55**, 1986–1995 (2014).
23. Nagasawa, T. *et al.* Spontaneous and visually driven high-frequency oscillations in the occipital cortex: Intracranial recording in epileptic patients. *Hum. Brain Mapp.* **33**, 569–583 (2012).
24. Matsumoto, A. *et al.* Pathological and physiological high-frequency oscillations in focal human epilepsy. *J. Neurophysiol.* **110**, 1958–1964 (2013).
25. Pail, M. *et al.* Frequency-independent characteristics of high-frequency oscillations in epileptic and non-epileptic regions. *Clin. Neurophysiol.* **128**, 106–114 (2017).
26. Wang, S. *et al.* Ripple classification helps to localize the seizure-onset zone in neocortical epilepsy. *Epilepsia* **54**, 370–376 (2013).
27. Zijlmans, M. *et al.* How to record high-frequency oscillations in epilepsy: A practical guideline. *Epilepsia* **58**, 1305–1315 (2017).
28. Jiruska, P. & Bragin, A. High-frequency activity in experimental and clinical epileptic foci. *Epilepsy Res.* **97**, 300–307 (2011).
29. Crépon, B. *et al.* Mapping interictal oscillations greater than 200 Hz recorded with intracranial macroelectrodes in human epilepsy. *Brain* **133**, 33–45 (2010).
30. von Ellenrieder, N., Frauscher, B., Dubeau, F. & Gotman, J. Interaction with slow waves during sleep improves discrimination of physiologic and pathologic high-frequency oscillations (80–500 Hz). *Epilepsia* **57**, 869–878 (2016).
31. Bruder, J. C. *et al.* Physiological ripples associated with sleep spindles differ in waveform morphology from epileptic ripples. *Int. J. Neural. Syst.* **27**, 1750011 (2017).
32. Sakuraba, R. *et al.* High frequency oscillations are less frequent but more specific to epileptogenicity during rapid eye movement sleep. *Clin. Neurophysiol.* **127**, 179–186 (2016).

33. Malinowska, U., Bergey, G. K., Harezlak, J. & Jouny, C. C. Identification of seizure onset zone and preictal state based on characteristics of high frequency oscillations. *Clin. Neurophysiol.* **126**, 1505–1513 (2015).
34. Waldert, S., Lemon, R. N. & Kraskov, A. Influence of spiking activity on cortical local filed potentials. *J. Physiol.* **591**, 5291–5303 (2013).
35. Kucewicz, M. T. *et al.* Dissecting gamma frequency activity during human memory processing. *Brain* **140**, 1337–1350 (2017).
36. Cimbalnik, J., Kucewicz, M. T. & Worrell, G. Interictal high-frequency oscillations in focal human epilepsy. *Curr. Opin. Neurol.* **29**, 175–181 (2016).
37. Talairach, J. *Atlas d´anatomie stéréotaxique du telencéphale: etudes anatomo-radiologiques* (Masson, Paris, 1967).
38. Barkmeier, D. T. *et al.* High inter-reviewer variability of spike detection on intracranial EEG addressed by an automated multi-channel algorithm. *Clin. Neurophysiol.* **123**, 1088–1095 (2012).
39. Jacobs, J. *et al.* High frequency oscillations in intracranial EEGs mark epileptogenicity rather than lesion type. *Brain* **132**, 1022–1037 (2009).
40. Andrade-Valença, L. *et al.* Interictal high frequency oscillations (HFOs) in patients with focal epilepsy and normal MRI. *Clin. Neurophysiol.* **123**, 100–105 (2012).
41. Axmacher, N., Elger, C. E. & Fell, J. Ripples in the medial temporal lobe are relevant for human memory consolidation. *Brain* **131**, 1806–1817 (2008).
42. Carr, M. F., Jadhav, S. P. & Frank, L. M. Hippocampal replay in the awake state: A potential substrate for memory consolidation and retrieval. *Nat. Neurosci.* **14**, 147–153 (2011).
43. Girardeau, G., Benchenane, K., Wiener, S. I., Buzsáki, G. & Zugaro, M. B. Selective suppression of hippocampal ripples impairs spatial memory. *Nat. Neurosci.* **12**, 1222–1223 (2009).
44. Lachaux, J. P., Axmacher, N., Mormann, F., Halgren, E. & Crone, N. E. High-frequency neural activity and human cognition: Past, present and possible future of intracranial EEG research. *Prog. Neurobiol.* **98**, 279–301 (2012).
45. Steriade, M., Contreras, D. & Amzica, F. Synchronized sleep oscillations and their paroxysmal developments. *Trends Neurosci.* **17**, 199–208 (1994).
46. Dinner, D. S. Effect of sleep on epilepsy. *J. Clin. Neurophysiol.* **19**, 504–513 (2002).
47. de Guzman, P. H., Nazer, F. & Dickson, C. T. Short-duration epileptic discharges show a distinct phase preference during ongoing hippocampal slow oscillations. *J. Neurophysiol.* **104**, 2194–2202 (2010).
48. Staba, R. J., Wilson, C. L., Bragin, A., Fried, I. & Engel, J. Jr. Quantitative analysis of high-frequency oscillations (80–500 Hz) recorded in human epileptic hippocampus and entorhinal cortex. *J. Neurophysiol.* **88**, 1743–1752 (2002).
49. Polich, J. Updating p300: An integrative theory of P3a and P3b. *Clin. Neurophysiol.* **118**, 2128–2148 (2007).
50. Pail, M. *et al.* Connectivity of superior temporal sulcus during target detection. *J. Psychophysiol.* **30**, 29–37 (2016).
51. Lachaux, J. P. Dynamic spectral imaging: Online and offline functional brain mapping using high-frequency activity [50–150 Hz] in SEEG. In *Invasive Studies of the Human Epileptic Brain* (eds Lhatoo, S. D. *et al.*) 453–464 (Oxford University Press, Oxford, 2019).
52. Ewell, L. A., Fischer, K. B., Leibold, C., Leutgeb, S. & Leutgeb, J. K. The impact of pathological high-frequency oscillations on hippocampal network activity in rats with chronic epilepsy. *eLife* **8**, e42148 (2019).
53. Meador, K. J. *et al.* Limbic evoked potentials predict site of epileptic focus. *Neurology* **37**, 494–497 (1987).
54. Puce, A., Kalnins, R. M., Berkovic, S. F., Donnan, G. A. & Bladin, P. F. Limbic P3 potentials, seizure localization, and surgical pathology in temporal lobe epilepsy. *Ann. Neurol.* **26**, 377–385 (1989).
55. Brázdil, M. *et al.* Hippocampal visual P3 potential in lateralization of primary epileptogenic focus and in assessment of hippocampal memory function in temporal lobe epilepsy. *Epilepsia* **40**(Suppl 2), 261 (1999).
56. Lachaux, J. P., Rudrauf, D. & Kahane, P. Intracranial EEG and human brain mapping. *J. Physiol. Paris* **97**, 613–628 (2003).
57. Curio, G. Linking 600-Hz "spikelike" EEG/MEG wavelets ("ς-bursts") to cellular substrates: Concepts and caveats. *J. Clin. Neurophysiol.* **17**, 377–396 (2000).
58. Liu, S. *et al.* Stereotyped high-frequency oscillations discriminate seizure onset zones and critical functional cortex in focal epilepsy. *Brain* **141**, 713–730 (2018).
59. Rich, E. L. & Wallis, J. D. Spatiotemporal dynamics of information encoding revealed in orbitofrontal high-gamma. *Nat. Commun.* **8**, 1139 (2017).
60. Bénar, C. G., Chauvière, L., Bartolomei, F. & Wendling, F. Pitfalls of high-pass filtering for detecting epileptic oscillations: A technical note on "false" ripples. *Clin. Neurophysiol.* **121**, 301–310 (2010).
61. Menendez de la Prida, L., Staba, R. J. & Dian, J. A. Conundrums of high-frequency oscillations (80–800 Hz) in the epileptic brain. *J. Clin. Neurophysiol.* **32**, 207–219 (2015).


## Acknowledgements

The results of this research were acquired within the CEITEC 2020 (LQ1601) project, with financial support from the Ministry of Education, Youth and Sports of the Czech Republic (MEYS CR) within special support paid from the National Programme for Sustainability II funds. Supported by MEYS CR project (Nos. LH15047, KONTAKT II). Supported by funds from the Faculty of Medicine MU to junior researcher (Martin Pail).

## Author contributions

M.P., J.C., R.R., and M.B. contributed to the conceptualization of the study. M.P., R.R., P.D., J.Ch. were responsible for project administration. M.P., R.R., J.C., J.Ch., P.D. were responsible for data curation. M.P., R.R., D.J.S. and M.B. wrote the main manuscript text. All authors reviewed and approved the final manuscript.

## Competing interests

The authors declare no competing interests.

## Additional information

**Correspondence** and requests for materials should be addressed to M.P.

**Reprints and permissions information** is available at www.nature.com/reprints.

**Publisher's note** Springer Nature remains neutral with regard to jurisdictional claims in published maps and institutional affiliations.

**Published research**

# Cognitive processing impacts high frequency intracranial EEG activity of human hippocampus in patients with pharmacoresistant focal epilepsy

Jan Cimbálník

Martin Pail

Petr Klimeš

Vojtěch Trávníček

Robert Roman

Adam Vajčner

Milan Brázdil

**Front. Neurol. 2020 Oct 27; 11: 578571. doi: 10.3389/fneur.2020.578571**

## Commentary on published paper

The electrophysiological EEG features such as high-frequency oscillations, spikes, and functional connectivity are often used to delineate epileptogenic tissue and study the normal function of the brain. The epileptogenic activity is also known to be suppressed by cognitive processing (Pail et al., 2020). However, differences between epileptic and healthy brain-behavior during rest and task were not studied in detail.

Our latest published study investigated iEEG features during resting state and task performance to elucidate the impact of cognitive processing on underlying brain electrophysiology under the hypothesis that HFO, interictal epileptiform discharges, and functional connectivity are modulated differently by cognitive processes in epileptic (EH) and non-epileptic (NEH) hippocampus. We investigated iEEG in 22 epileptic and 23 non-epileptic hippocampi in patients with intractable focal epilepsy during a resting state period and during the performance of various cognitive tasks (Visual oddball task, Go/NoGo task, Ultimatum Game task, and Mismatch negativity). We evaluated the behavior of features derived from high-frequency oscillations, interictal epileptiform discharges, functional connectivity and their changes concerning cognitive processing. Subsequently, we analyzed whether cognitive processing can contribute to epileptic and non-epileptic hippocampus classification using a machine learning approach. We studied multiple invasive EEG and connectivity features, as was published, to improve epileptogenic tissue localization and is superior to using a single feature (Cimbalnik et al., 2019).

The results show that cognitive processing suppresses epileptogenic activity (reduction of FR rates) in the epileptic hippocampus, similarly to our previous study (Pail et al., 2020), while it causes a shift toward higher frequencies in NEH. It was further confirmed that FR in EH have a higher rate and amplitude and longer duration. We also observed the increase in local FR linear correlation during cognitive tasks, which likely reflects high neuronal synchronization (Kucewicz et al., 2014). A decrease in relative entropy (reflecting pathological processes) in EH during cognitive tasks further supports the hypothesis that cognitive processing suppresses pathological activity in the brain (Cimbalnik et al., 2019). Statistical analysis using the machine learning approach reveals significantly different electrophysiological reactions of epileptic and non-epileptic hippocampus during cognitive processing, which can be measured by high-frequency oscillations, interictal epileptiform discharges, and functional connectivity. The calculated features showed high classification potential for the epileptic hippocampus.

In conclusion, the differences between epileptic and non-epileptic hippocampus during cognitive processing bring new insight into delineation between pathological and physiological processes. Analysis using the machine learning approach of computed iEEG features in rest and in task conditions can improve the functional mapping during pre-surgical evaluation. This approach provides additional guidance for distinguishing between epileptic and non-epileptic structure, which is absolutely crucial for achieving the best possible outcome with as little side effects as possible.

frontiers in Neurology

ORIGINAL RESEARCH
published: 27 October 2020
doi: 10.3389/fneur.2020.578571

# Cognitive Processing Impacts High Frequency Intracranial EEG Activity of Human Hippocampus in Patients With Pharmacoresistant Focal Epilepsy

*Jan Cimbalnik[1*†], Martin Pail[2], Petr Klimes[1,3], Vojtech Travnicek[1,3], Robert Roman[2,4], Adam Vajcner[2,5] and Milan Brazdil[2,4]*

*[1] International Clinical Research Center, St. Anne's University Hospital, Brno, Czechia, [2] Department of Neurology, Faculty of Medicine, Brno Epilepsy Center, St. Anne's University Hospital, Masaryk University, Brno, Czechia, [3] Institute of Scientific Instruments, The Czech Academy of Sciences, Brno, Czechia, [4] Behavioral and Social Neuroscience Research Group, CEITEC - Central European Institute of Technology, Masaryk University, Brno, Czechia, [5] Department of Sports Medicine and Rehabilitation, Faculty of Medicine, St. Anne's University Hospital, Masaryk University, Brno, Czechia*

OPEN ACCESS

**Edited by:**
*Maeike Zijlmans, University Medical Center Utrecht, Netherlands*

**Reviewed by:**
*Luiz E. Mello, Federal University of São Paulo, Brazil*
*Dinesh Upadhya, Manipal Academy of Higher Education, India*

***Correspondence:**
*Jan Cimbalnik*
*jan.cimbalnik@fnusa.cz*

**†ORCID:**
*Jan Cimbalnik*
*orcid.org/0000-0001-6670-6717*

**Specialty section:**
*This article was submitted to Epilepsy, a section of the journal Frontiers in Neurology*

**Received:** *10 July 2020*
**Accepted:** *18 September 2020*
**Published:** *27 October 2020*

**Citation:**
*Cimbalnik J, Pail M, Klimes P, Travnicek V, Roman R, Vajcner A and Brazdil M (2020) Cognitive Processing Impacts High Frequency Intracranial EEG Activity of Human Hippocampus in Patients With Pharmacoresistant Focal Epilepsy. Front. Neurol. 11:578571. doi: 10.3389/fneur.2020.578571*

The electrophysiological EEG features such as high frequency oscillations, spikes and functional connectivity are often used for delineation of epileptogenic tissue and study of the normal function of the brain. The epileptogenic activity is also known to be suppressed by cognitive processing. However, differences between epileptic and healthy brain behavior during rest and task were not studied in detail. In this study we investigate the impact of cognitive processing on epileptogenic and non-epileptogenic hippocampus and the intracranial EEG features representing the underlying electrophysiological processes. We investigated intracranial EEG in 24 epileptic and 24 non-epileptic hippocampi in patients with intractable focal epilepsy during a resting state period and during performance of various cognitive tasks. We evaluated the behavior of features derived from high frequency oscillations, interictal epileptiform discharges and functional connectivity and their changes in relation to cognitive processing. Subsequently, we performed an analysis whether cognitive processing can contribute to classification of epileptic and non-epileptic hippocampus using a machine learning approach. The results show that cognitive processing suppresses epileptogenic activity in epileptic hippocampus while it causes a shift toward higher frequencies in non-epileptic hippocampus. Statistical analysis reveals significantly different electrophysiological reactions of epileptic and non-epileptic hippocampus during cognitive processing, which can be measured by high frequency oscillations, interictal epileptiform discharges and functional connectivity. The calculated features showed high classification potential for epileptic hippocampus (AUC = 0.93). In conclusion, the differences between epileptic and non-epileptic hippocampus during cognitive processing bring new insight in delineation between pathological and physiological processes. Analysis of computed iEEG features in rest and task condition can improve the functional mapping during

pre-surgical evaluation and provide additional guidance for distinguishing between epileptic and non-epileptic structure which is absolutely crucial for achieving the best possible outcome with as little side effects as possible.

**Keywords: pharmacoresistant epilepsy, high frequency oscillation (HFO), interictal epileptiform discharge, functional connectivity, hippocampus, cognitive processing**

## INTRODUCTION

Epilepsy is one of the mostcommon chronic neurological diseases (1) and approximately one third of epileptic patients suffer from a medically intractable form. Those patients are candidates for intracranial EEG (iEEG) monitoring and subsequent surgical treatment of their condition.

The hippocampus is a brain structure that is often involved in temporal lobe epilepsy (TLE). In particular, hippocampal sclerosis is often found in TLE, even though it is not clear whether it is the primary cause of epilepsy, its alteration or consequence (2). Nonetheless, its surgical removal often leads to improvement of the epileptic condition and substantial reduction of seizures (3). The correct determination of epileptic hippocampus and whether the particular hippocampus or its part should be removed can improve the outcome of epileptic surgeries and reduce the unnecessary removal of possible healthy tissue.

In the end of the last millennium, high frequency oscillations (HFO) emerged as a marker of normal function of the brain and epileptic activity (4, 5). Since then, numerous studies have been conducted to evaluate their potential for localization of epileptogenic tissue from iEEG signals (6–11). The distinction of pathological HFO and normal HFO based on their features has been investigated but the results never showed that their separation is possible (12, 13).

The hippocampus is the brain structure where the first HFO were described (4). Physiological HFO in the hippocampus are often studied as markers of cognitive processes and as part of memory formation (14). On the other hand, epileptic hippocampus is often abundant with pathologic HFO (15). It is, therefore, likely that both types of HFO occur simultaneously in epileptic hippocampus and physiological HFO are likely to interfere with the interpretation of the pathological HFO occurrence.

Another iEEG phenomenon connected to epileptogenic tissue and the hippocampus are interictal epileptic discharges (IEDs). They have been proven to be insufficiently specific for the pathological tissue (16), they propagate across multiple brain structures or are generated in zones not generating seizures (green spikes) (17) and can even occur in non epileptic hippocampus (6).

Apart from distinct electrophysiological events such as IEDs and HFO, high frequency functional brain connectivity in ripple and fast ripple frequency range has been used both for studying normal function of the brain and epileptogenic areas (18, 19).

**Abbreviations:** iEEG, intracranial EEG; TLE, temporal lobe epilepsy; HFO, high frequency oscillation; IED, interictal epileptiform discharge; EH, epileptic hippocampus; NEH, non- epileptic hippocampus; SEEG, stereo EEG.

The mentioned high frequency iEEG features represent different underlying electrophysiology. In recent years, the use of machine learning algorithms that combine the diverse information carried by the iEEG features have been shown to outperform the single feature approaches in localization tasks (20–23).

In this study we investigated iEEG features during resting state and task performance to elucidate the impact of cognitive processing on underlying brain electrophysiology under the hypothesis that HFO, IEDs and functional connectivity are modulated differently by cognitive processes in epileptic (EH) and non-epileptic (NEH) hippocampus. The secondary goal of this study was to provide evidence whether these modulations can contribute to better classification of epileptic and non-epileptic hippocampus.

## MATERIALS AND METHODS

### Subjects

The study was carried out on the data of 36 patients (17 females) with age ranging from 22 to 58 (mean: 37.4 ± 11.3) suffering from medically intractable focal epilepsies. All patients provided a written consent to participate in the study approved by the Ethics Committee of St. Anne's University Hospital in Brno and Masaryk University. Patient information is summarized in **Table 1**. In most patients, chronic anticonvulsant medication was reduced slightly for the purposes of video-EEG monitoring. All methods were performed in accordance with the relevant guidelines and regulations.

### Recordings

All patients participating in this study underwent stereotactic depth electrode implantation as part of their presurgical evaluation for treatment of pharmacoresistant focal epilepsy. The localization of the electrodes was determined solely by clinical needs. Used electrodes were either DIXI or ALCIS (diameter = 0.8 mm; inter-contact distance = 1.5 mm, contact surface area = 5 $mm^2$; contact length = 2 mm). All used electrodes were MRI compatible. The acquired iEEG was low-pass filtered and downsampled from 25 kHz to 5,000 Hz for subsequent storage and analysis. The used recording reference was the average of all intracranial signals. We analyzed hippocampal stereo EEG (SEEG) during an awake resting interictal period and various simple cognitive tasks.

### Behavioral Tasks

#### Oddball Task

The oddball task was performed similarly to the previous study by Polich (24). Subjects were seated in a moderately lit room with a

**TABLE 1 |** Study subjects overview with regard to individual hippocampi.

| Analyzed hippocampus | Epilepsy side | Epilepsy type | Engel outcome | MRI | Histopathology |
|---|---|---|---|---|---|
| Epileptic $N = 22$ | Left $N = 8$<br>Right $N = 9$<br>Bilateral $N = 5$ | Temporal $N = 22$ | Engel IA $N = 12$<br>Engel II-III $N = 6$<br>NA $N = 4$ | Normal $N = 6$<br>Abnormal $N = 16$ | FCD $N = 3$<br>HS $N = 8$<br>Negative $N = 5$<br>NA $N = 6$ |
| Non-epileptic $N = 23$ | Left $N = 12$<br>Right $N = 11$ | Temporal $N = 16$<br>Extratemporal $N = 7$ | Engel IA $N = 10$<br>Engel II-III $N = 12$<br>NA $N = 1$ | Normal $N = 5$<br>Abnormal $N = 18$ | AVM $N = 1$<br>FCD $N = 9$<br>HS $N = 5$<br>Heterotophy $N = 1$<br>Negatvie $N = 4$<br>NA $N = 3$ |

*FCD, focal cortical dysplasia; AVM, arteriovenous malformation; HS, hippocampal sclerosis; NA, not available.*
*Some subjects had both epileptic and non-epileptic hippocampi.*

monitor screen positioned approximately 100 cm in front of their eyes. During the task, they were requested to focus their eyes on the small fixation point in the center of the screen. A standard visual oddball task was performed: three types of stimuli (target, frequent, and distractor) at a ratio of 1:4.6:1, were presented in the center of the screen in random order. The number of targets was 50. Clearly visible yellow capital letters X (target), O (frequent), and various other capital letters (distractor) on a black background were used as experimental stimuli that were presented for 500 ms. The task was divided into four blocks, each block consisted of 12 or 13 target stimuli. The interstimulus interval randomly varied between 4 and 6 s. Each subject was instructed to count the target stimuli in their mind and to report the calculated number after each block.

## Go/NoGo Task

The Go/NoGo task was replicated from work of Albares et al. (25). Experimental stimuli, i.e., white capital letters A and B, were displayed in the center of the black screen for 0.2 s, followed by a black screen for 2 s. Each letter was preceded by a red or green fixation cross presented with a random duration of 2–6 s. The red fixation cross was followed by the letter A (Go stimulus) or B (NoGo stimulus) with an equal probability. The green fixation cross was always followed by the letter A (Go stimulus). The red cross was twice as common as the green one. In total, 72 NoGo stimuli and 144 Go stimuli were presented, divided into four blocks of the experiment. Participants were instructed to press a button as quickly as possible on Go stimuli and to suppress this action when a NoGo stimulus appeared. Before the experiment, participants completed a short practice.

## Ultimatum Game Task

The Ultimatum Game task was previously used in an fMRI study by Shaw et al. (26). It presents a simple paradigm to investigate dyadic interaction. The patient was randomly assigned to the role of a Proposer or a Responder. The opposite role was assigned to a nurse willing to participate in the game. Roles were fixed for all rounds.

Each round of the ultimatum game started with the Proposer being given 4 s to choose one of two divisions of a sum of money (of 100 CZK, i.e.,∼€4) that differed in the degree of inequity, between themselves and the Responder. After this fixed period, the Proposer's offer was highlighted for 4 s, during which the Responder could either accept or reject the proposal. If they accepted it, then the money was divided accordingly, but if they rejected it, then neither player received any payoff. After this 4-s period, the Responder's decision was then presented for a final 4 s.

The exact same procedure was followed on control rounds, but the choice set comprised two alternative divisions of different colors between the players; rather than dividing a sum of money, Proposers were required to choose the color they preferred for themselves and the color that should go to the Responder, and the Responder then accepted or rejected that offer. Both players were instructed that control rounds had no monetary consequence. Each round ended with a jittered inter-trial interval, with a fixation cross presented pseudo-randomly for 2–4 s. All stimuli were presented to both players simultaneously—Responders saw the initial choice set from which Proposers selected their offer, and Proposers saw the Responder's accept/reject decision. Players were instructed at the start that they would receive the outcome of six rounds selected at random. At no point was any information given to participants on the number of rounds remaining in the task. The whole experiment consisted of two functional runs performed successively in a single session. The two runs together comprised 120 rounds of the experimental condition and 60 rounds of a control condition.

## Mismatch Negativity

Mismatch negativity (MMN) protocol was based on studies of (27–29).

We recorded a passive task of attention called MMN protocol to find out the presence of MMN/MMN-like response in aiming structures. Each patient lay on the bed in a semi-sitting position with eyes opened. Patient's task was to concentrate voluntary selective attention on watching a self-selected movie and ignore the tones of auditory stimulation, no further information was received. Simultaneously, auditory stimulation was presented binaurally through loudspeakers (∼2 m far from ears) in parameters of roving paradigm (frequent and infrequent stimuli).

Frequent and infrequent stimuli (standard and deviant tones of 50/100 ms duration) were randomly presented with the presentation probability of 0.8/0.2. Interstimulus intervals' (ITS)

duration was 2,000 ms. All tones were 54 dB (SD ± 4, adjusted subjectively for patient's comfort) SPL, frequency 1,000 Hz, and with jump increase and gradual decrease of the tones' course. The experiment protocol lasted 17 min. This part of investigation was focused on the preattentive detection mechanism on the unconscious level for auditory stimuli which is illustrated by Mismatch negativity.

## Determination of Anatomical Location

To localize the MRI compatible electrode contacts in patients' brains the preoperative MRI was coregistered with postoperative MRI/CT using a custom made Matlab (The MathWorks, Inc.) based on Statistical Parametric Mapping module. After the software coregistration the brain volume was transformed to MNI space and the MNI coordinates of individual contacts were determined. The coregistered volume was used to estimate he anatomical location of each contact by two clinical neurologists using Co-Planar Stereotaxic Atlas of the Human Brain (Talairach-Tournoux system). Only the contacts clearly located in the hippocampus were included in the analysis of iEEG.

## Selection of Hippocampi

The hippocampi in individual patients were classified as epileptic or non-epileptic specifically, according to the results of a standard visual analysis of interictal and ictal SEEG recordings. If contacts implanted in the hippocampus were included in seizure onset zone (SOZ) the hippocampus was classified as epileptic. Conversely, if all contacts implanted in the hippocampus were outside of SOZ and did not exhibit excessive spiking (<50 per 10 min) they were classified as putative non-epileptic hippocampi. The putative non-epileptic hippocampi with spiking above the threshold were visually reviewed whether the IEDs were propagated from other brain structures. The putative non-epileptic hippocampi that generated IEDs were excluded from the analysis.

## Data Processing and Feature Extraction

The iEEG data were processed by automated algorithms that were already used in other published studies. The Python codes of these algorithms are part of the ElectroPhYsiology Computation Module (EPYCOM) and can be found online at https://gitlab.com/icrc-bme/epycom.

### HFO Detection

The automated detection of HFO was performed by an algorithm used in our previous studies (30, 31). A statistical window of 10 s was used to compute z-scored amplitude envelopes using Hilbert transforms in a series of logarithmically spaced frequency bands (300 bands between 60 and 800 Hz). The detection of putative HFO was done by thresholding the amplitude envelopes by three standard deviations above the mean in each frequency band. The detections overlapping in temporal domain in adjacent frequency bands were joined into one HFO detection obtaining temporal and spectral span of the putative HFO. Final detections were obtained by selecting HFO that have time span >4 cycles at their peak frequency and HFO with minimal frequency at 60 Hz were discarded to remove false positive detections of spikes. HFO amplitude, peak frequency and duration were extracted along with the HFO detections. The detector thresholds were chosen to achieve high sensitivity in order to detect physiological HFO which were shown to have smaller amplitude than pathological HFO (12).

Detected HFO were split into broadband ripple (R; 80–250 Hz) and fast ripple (FR; 250–600 Hz) HFO based on their dominant frequency. Subsequently, HFO rate, mean relative amplitude, duration and dominant frequency per 10 min was calculated for each channel and R/FR and used as features.

### IED Detection

IED detection was done using the spike detector developed by Barkmeier et al. (32). The detector utilizes filtration in two frequency bands. 20–50 Hz band to detect putative spikes and 1–35 Hz band to determine scaling factor which is used to scale the data in all iEEG channels and to determine amplitude and slope thresholds for final spike detections.

The spike rate and mean spike amplitude per 10 min was calculated for each channel.

### Functional Connectivity Calculation

Recorded signals were filtered in ripple (80–250 Hz) and fast ripple (250–600 Hz) frequency bands and non-overlapping 1-s sliding windows were used to calculate linear correlation and relative entropy to estimate functional connectivity between iEEG signals recorded by adjacent contacts on an electrode implanted in the hippocampus. For iEEG signals X and Y, the linear correlation was calculated as $corr(X,Y) = cov(X,Y)/std(X)\cdot std(Y)$, where cov stands for covariance and std for standard deviation. The relative entropy was calculated as $REN(X,Y) = sum[pX\cdot log(pX/pY)]$, where pX is a probability distribution of investigated signal and pY is a probability distribution of expected signal.

The connectivity metrics were calculated for R and FR frequency bands and mean value per channel was used in subsequent processing as an iEEG feature.

## Statistical Analysis and Machine Learning

All statistical analyzes and machine learning tasks in this study were performed using custom-made Python scripts, open-source statistical libraries (scipy, statsmodels) and machine learning libraries (scikit-learn).

### Statistical Analysis

Paired *t*-tests were carried out to evaluate the changes in iEEG features between resting state and during task performance when the patients were under cognitive load for EH and NEH. The statistical difference between EH and NEH during rest and cognitive processing was tested with Mann-Whitney test.

To assess the potential of individual signal features for discrimination of epileptic and non-epileptic hippocampi the receiver operating curve (ROC) and its area under the curve (AUC) was calculated for values during resting state, task performance and for difference of values between resting state

**TABLE 2 |** Mean values and standard deviations of iEEG features per channel in EH and NEH channels during rest and cognitive task performance.

| Hippocampus type | EH | NEH | EH | NEH |
|---|---|---|---|---|
| **Task** | **Rest** | | **Cognitive task** | |
| R/10 min | 120.1 ± 141.92 | 44.94 ± 37.07 | 64.84 ± 79.77 | 21.13 ± 14.71 |
| FR/10 min | 214.16 ± 327.25 | 44.28 ± 50.18 | 137.15 ± 176.33 | 35.39 ± 24.36 |
| R amplitude [–] | 6.87 ± 1.26 | 5.35 ± 0.93 | 6.28 ± 1.06 | 4.95 ± 0.81 |
| FR amplitude [–] | 6.62 ± 1.26 | 5.15 ± 0.86 | 6.12 ± 0.93 | 5.05 ± 0.54 |
| R frequency [Hz] | 176.75 ± 13.83 | 153.99 ± 17.42 | 175.69 ± 11.37 | 156.96 ± 18.25 |
| FR frequency [Hz] | 399.6 ± 28.81 | 400.05 ± 30.43 | 412.24 ± 29.2 | 412.36 ± 22.14 |
| R duration [ms] | 34.56 ± 4.13 | 38.09 ± 4.2 | 34.41 ± 3.61 | 35.78 ± 4.19 |
| FR duration [ms] | 18.19 ± 2.68 | 15.11 ± 3.35 | 17.11 ± 2.69 | 14.07 ± 1.86 |
| IED/10 min | 158.84 ± 154.96 | 44.81 ± 54.86 | 105.03 ± 127.74 | 16.27 ± 31.74 |
| IED amplitude [μV] | 378.61 ± 152.44 | 339.8 ± 172.27 | 370.88 ± 139.48 | 320.24 ± 214.9 |
| R linear correlation [–] | 0.43 ± 0.21 | 0.43 ± 0.26 | 0.44 ± 0.21 | 0.44 ± 0.27 |
| FR linear correlation [–] | 0.49 ± 0.22 | 0.44 ± 0.2 | 0.51 ± 0.24 | 0.48 ± 0.17 |
| R relative entropy [–] | 0.29 ± 0.26 | 0.1 ± 0.05 | 0.19 ± 0.15 | 0.08 ± 0.04 |
| FR relative entropy [–] | 0.15 ± 0.15 | 0.06 ± 0.03 | 0.1 ± 0.08 | 0.05 ± 0.02 |

*The statistical evaluation of differences between the values in this table are shown in **Figure 1**.*

and task performance. Hanley-McNeil test was used to determine the ROCs significantly different from chance (AUC = 0.5).

The statistical tests were carried out per channel for each task individually as well as for all the tasks grouped together. In case one subject performed multiple tasks, the mean value of iEEG features across all performed tasks was calculated for statistical testing. To verify that the statistics are not influenced by a subgroup of channels with outlying iEEG features we performed the same analysis per hippocampus where the median of iEEG features from all hippocampal channels was used.

The chosen significance level for all statistical tests was $\alpha = 0.05$.

### Machine Learning

The iEEG features with ROC significantly different from chance (AUC = 0.5) either for resting state, task performance or difference between the two states were used to create an SVM model for classification of EH and NEH channels. Only the grouped task ROC values were used for this analysis. To decorrelate the features we used principal component analysis (PCA) during training and testing of the model.

The SVM model was trained and tested in a similar fashion as in our previous work (22) where we performed leave-one-patient-out cross validation for localization of contacts in epileptogenic tissue. Here we use leave-one-hippocampus-out cross validation. The SVM model was trained on all data apart from one hippocampus which was used for classification by the trained model. To optimize the SVM performance, linear and radial basis function kernels were tested and their hyperparameters were tuned by an iterative grid search approach. The performance of the model was evaluated by mean ROC and corresponding AUC calculated from ROCs of each leave-one-hippocampus-out iteration. The evaluated hippocampus was classified as pathologic if the mean probability for classification of the channels as pathologic exceeded 50%. To assess whether iEEG features during rest, cognitive task or the difference between the two states carry different information the SVM model was created separately for each group and for all groups joined.

## RESULTS

### Statistical Analysis

The total number of analyzed channels was 254 (140 EH, 114 NEH) in 45 analyzed hippocampi (22 EH, 23 NEH). The numerical results for all iEEG features are summarized in **Table 2** while the results of individual statistical tests are visualized in **Figure 1**.

### HFO

The influence of cognitive processing on HFO was evaluated by comparing the difference in HFO features during resting state and cognitive task performance (**Figure 1A**). The rate of R was significantly reduced both in EH and NEH as a result of cognitive processing while FR rate was reduced only in EH and remained practically unchanged in NEH. The HFO amplitude was significantly reduced by cognitive processing in EH for both explored HFO groups but in NEH this trend was observed only in the R range. The evaluation of cognitive task influence on HFO duration revealed that the duration was significantly shorter in R band only in NEH and in FR in both NEH and EH. The frequency of HFO in EH and NEH was significantly higher during cognitive stimulation in FR while in R band the significant change occurred only in NEH.

To inspect how HFO features are different between EH and NEH the analysis during resting state and cognitive tasks was performed (**Figure 1B**).

During resting state, the rate and amplitude of HFO was significantly lower in NEH than in EH in both frequency bands.

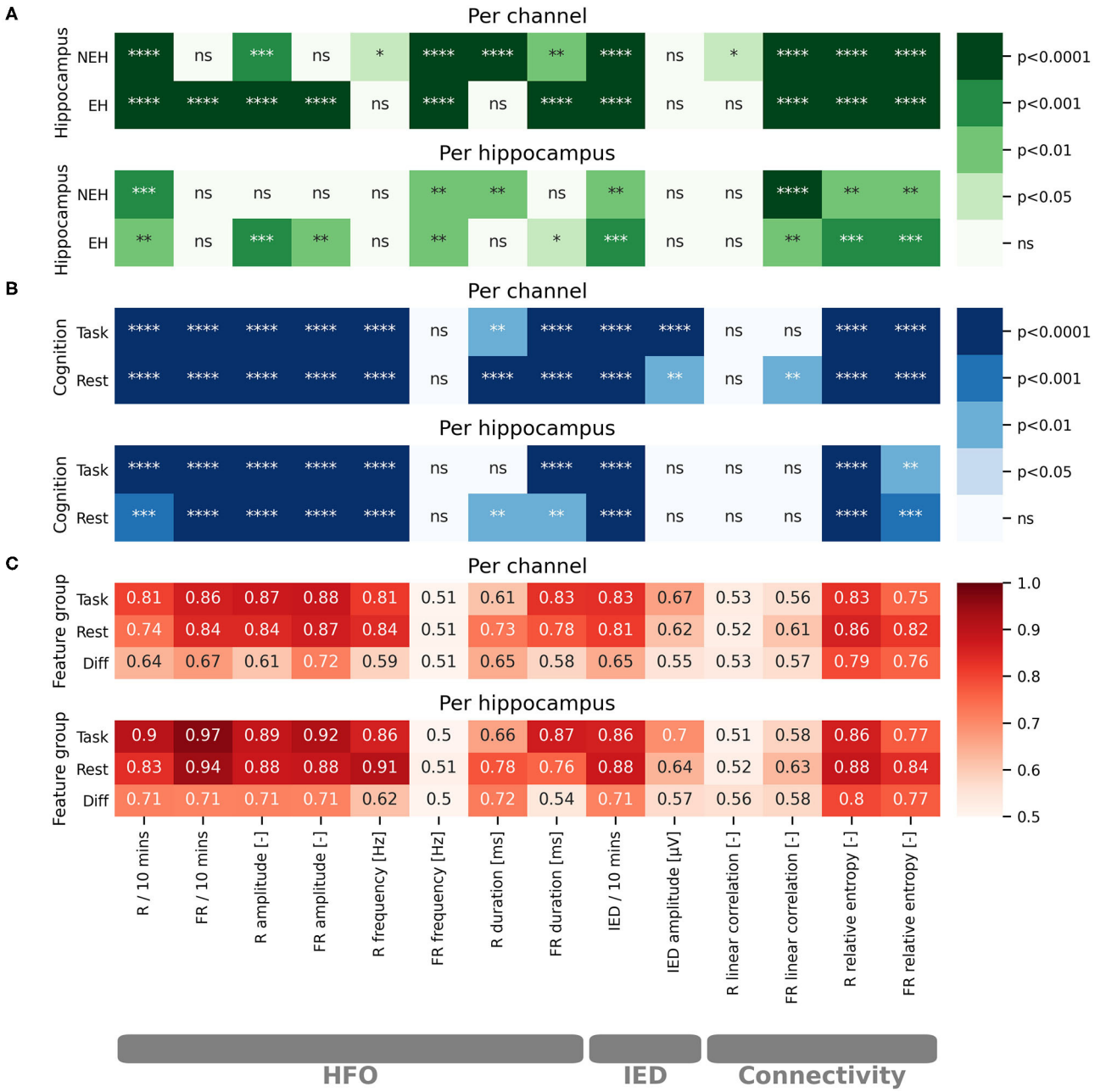


**FIGURE 1 |** Statistical evaluation of the impact of cognitive processing on iEEG features and evaluation of iEEG feature potential for classification of EH and NEH. The results are visualized for per channel and per hippocampus evaluations. The stars represent the level of significance as marked on the colorbars. Non significant results are marked by "ns." **(A)** Color-coded paired *t*-test significance level of iEEG features in EH and NEH as a result of cognitive stimulation. **(B)** Color-coded significance between EH and NEH during resting state period and cognitive task. **(C)** Color-coded values of ROC-AUC for classification of EH. ****($p < 0.0001$), ***($p < 0.001$), **($p < 0.01$), *($p < 0.05$), ns ($p < 1$).

The duration of HFO in EH compared to NEH was significantly longer in the R band but significantly shorter in the FR band. Significantly lower HFO frequencies in NEH were observed for R band but the difference in FR band was insignificant. During task performance, the HFO rate and amplitude changed similarly to resting state where they were significantly lower in NEH both for R and FR. The duration of R was significantly increased in NEH and, conversely, decreased in FR. HFO frequency during cognitive task was significantly different only in R band, where the NEH exhibited lower HFO frequencies.

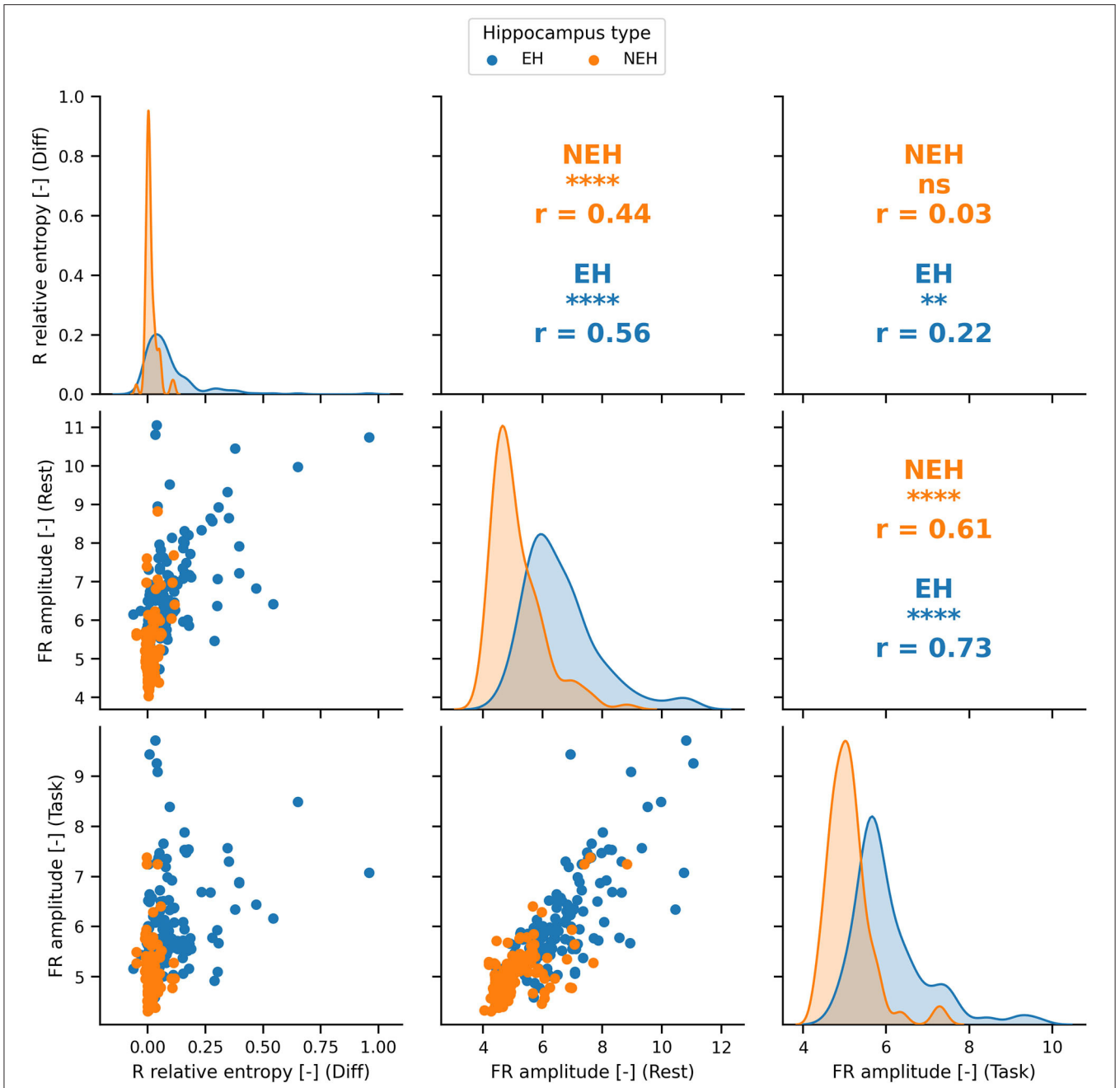


**FIGURE 2 |** The distributions and Pearson correlation coefficient (*r*) of the best performing features in rest, cognition and the difference between the two states. The best performing features are significantly correlated (significance denoted by stars) in most cases apart from FR amplitude during task and R relative entropy difference in NEH. PCA was therefore used to obtain uncorrelated principal components. ****($p < 0.0001$), ***($p < 0.001$), **($p << 0.01$), *($p < 0.05$), ns($p < 1$).

The analysis of HFO features utility for classification of EH and NEH was assessed by ROC-AUC during rest, during cognitive task and by the change between the two states (**Figure 1C**). More than half of the explored HFO features were significantly better than chance (14 out of 24). The HFO rate and amplitude along with R frequency and FR duration showed the highest classification potential both during resting state and task performance.

## IED

The changes in IED occurrence and amplitude as a result of cognitive task performance was evaluated in a similar fashion as HFO. IED rate was significantly reduced during task in EH and NEH. Conversely, the amplitude of spikes was not influenced neither in EH nor in NEH.

The rate of IED, and IED amplitude were significantly higher in EH during resting state and task performance.

While IED amplitude did not exhibit an ROC significantly better than chance, IED rate reached similar values of AUC as HFO rate and amplitude and was significant for resting state and task performance.

### Functional Connectivity

The changes in functional connectivity resulting from cognitive stimulation were estimated by linear correlation and relative entropy in the R and FR band. Linear correlation significantly increased during cognitive task in NEH in the R band. In the FR band the significant increase was observed in EH and NEH. The effect on relative entropy was reversed as it was significantly decreased in both bands and hippocampus types.

During resting state, linear correlation was significantly increased in EH compared to NEH only in the FR band while relative entropy was increased in both frequency bands. During cognitive task, relative entropy remained significantly increased in EH but linear correlation did non exhibit any significant difference between EH and NEH.

Hippocampus classification ROC-AUC of linear correlation was slightly higher in FR range but the ROCs were not significantly different from chance. On the other hand, relative entropy showed similar performance as HFO rate and amplitude with highly significant ROCs.

Per hippocampus analysis yielded similar results to per channel bases (**Figure 1**) with some tests showing nonsignificant results where per channel results were significant. This is a natural effect of performing statistical tests on fewer samples.

## Machine Learning

The features with ROC significantly different than chance during rest, task or the difference between the two states were chosen for the SVM model creation (**Figure 1C**). The top performing features and their correlation is presented in **Figure 2**.

The best performing SVM model hyperparameters were determined by an iterative grid search approach (**Table 3**). This approach was performed for iEEG features during rest, during task performance, the difference between the two states and for all feature groups joined.

ROC-AUC for classification of EH and NEH channels was calculated for each feature group. The lowest AUC was revealed for rest-task feature differences, followed by features during resting state and task performance. Combination of all features resulted in the highest AUC.

**TABLE 3 |** Best performing SVM hyperparameters for individual groups of features and for their aggregate.

| Group | Kernel | C | Gamma | AUC |
|---|---|---|---|---|
| Only rest | Linear | 0.001 | – | 0.90 |
| Only task | Linear | 0.001 | – | 0.92 |
| Only diff | rbf | 0.1 | 10 | 0.79 |
| All | rbf | 0.1 | 0.01 | 0.93 |

# DISCUSSION

Functional brain connectivity is commonly characterized by activity synchronization of neuronal subpopulations. Widespread neuronal networks including studied hippocampus are thought to be coordinated into synchronous oscillations, HFO during cognitive phenomena but also pathologic epileptic processes. In the presented study we investigated how the iEEG features are influenced by cognitive processing in EH and NEH. We subsequently used the results of this analysis to create an SVM model for classification of channels as EH and NEH.

The higher HFO rate and amplitude in EH during rest and task suggest the possible absence of pathological HFO in NEH and corroborates the results of previous studies (6, 12, 13, 33, 34). Higher resting state R frequency in EH compared to NEH is likely the result of imperfect labeling of FR as R due to the strict frequency boundary of 250 Hz and thus reflects the presence of pathological FR in EH. Some authors have put forward a hypothesis that pathological ripples are only slower fast ripples (11). In NEH, the longer R duration during rest and task performance is not surprising (35, 36). Nevertheless, these results contradict other previously published results (6, 12). This discrepancy might be caused by the fact that the work of Matsumoto et al. was mainly focused on motor cortex which might produce physiological HFO exhibiting disparate features from those in the hippocampus due to histologically different underlying tissue. Conversely to R, FR were longer in EH both during resting state and cognitive task performance reflecting the presence of pathological oscillations (12).

Cognitive processing induced reduction of HFO rates in EH and NEH across all explored frequency bands apart from FR in NEH. The observation that cognitive processing causes R rate decrease and no change in FR in NEH could be the result of decrease in number of R and increase of FR rates observed by Kucewicz et al. (30) in multiple structures including the hippocampus. As other studies previously suggested (37, 38), we hypothesize that the decrease of HFO rate and amplitude in EH as a result of cognitive processing is caused by suppression of epileptic activity in this structure. HFO changes within affected structures may suggest an increased involvement of the preserved normal hippocampal neurons that are active in some physiological cognitive processing and a reduced involvement of the synchronously bursting neurons within the epileptic network that are generating pathological HFO (38). The same explanation can be applied to similar results of possible pathologic ripple reduction in EH. In contrast to EH, the suppression of R rates and amplitude in NEH might be caused by shift of general HFO frequency toward FR band and, therefore, reduction of HFO amplitude and rate. This shift is further supported by the increased R and FR frequency along with shorter R and FR duration in NEH. It is likely that some residual physiological function remains in EH and the effect of reduction of epileptic activity is mingled with the shift observed in NEH.

IED rate was influenced in a similar way as R, being significantly higher in EH during rest as well as during cognitive task and decreased during cognitive task in both types of hippocampus which might reflect the suppression in epileptic activity not only in the hippocampus but also in non hippocampal structures from which the IEDs propagated to NEH. As was shown, specific tasks can suppress focal discharges over the brain regions that mediate the cognitive activity in question (37). IED amplitude was higher in EH than in NEH for both states which is an expected result.

Increased FR linear correlation in resting state EH could be ascribed to functional isolation of epileptic tissue as previously reported (18, 39). The increase in local FR linear correlation during cognitive task likely reflects high neuronal synchronization which is manifested through increased rate of FR HFO (30). Conversely to linear correlation, relative entropy was shown in our previous studies to reflect pathological processes (22, 23). This effect is further confirmed by the results in this study. Decrease in relative entropy during cognitive task further supports the hypothesis that cognitive processing suppresses pathological activity in the brain.

The AUC for classification of NEH and EH using resting state features in an SVM showed good performance. The task performance shower slightly higher AUC suggesting that the changes occurring during cognitive stimulation might carry unique information for localization of hippocampal epileptogenic tissue. The highest AUC was achieved when the SVM model was created with a combination of rest, task and difference features.

We show statistically different electrophysiological reactions of epileptic and non-epileptic hippocampus, which can be measured by HFO, IED and functional connectivity. We propose a hypothesis that cognitive processing reduces pathological electrophysiological activity in EH. Whether this effect is tied directly to stimuli presented to the patient and whether it is present in other brain structures remains to be explored. Analysis of the computed iEEG features in rest and task condition can improve functional mapping during pre-surgical evaluation and provide additional guidance for distinguishing between epileptic and non-epileptic structure which is absolutely crucial for achieving the best possible outcome with as little side effects as possible.

## LIMITATIONS OF THE STUDY

The NEH classification is problematic because even though such hippocampus is outside of the epileptogenic zone it is still likely influenced by epileptic networks and might exhibit traces of pathological behavior. The influence of different anti-epileptic drugs on the results could not be analyzed due to many variations in medication of individual patients.

## DATA AVAILABILITY STATEMENT

The datasets generated for this study are available on request to the corresponding author.

## ETHICS STATEMENT

The studies involving human participants were reviewed and approved by Ethics Committee of St. Anne's University Hospital in Brno. The patients/participants provided their written informed consent to participate in this study.

## AUTHOR CONTRIBUTIONS

JC carried out the statistical analyses and result visualizations. JC, MP, PK, VT, and MB participated on collection of metadata, writing of the manuscript and interpretation of the results. RR and AV provided data and metadata for cognitive task and assisted in interpretation of the cognitive task results. All authors contributed to the article and approved the submitted version.

## FUNDING

This work was supported by Ministry of Education, Youth and Sports of the Czechia Republic project no. LTAUSA18056 (programme INTER-EXCELLENCE). This study was also supported by the project no. LQ1605 from the National Program of Sustainability II (MEYS CR).

## REFERENCES

1. Leonardi M, Ustun TB. The global burden of epilepsy. *Epilepsia.* (2002) 43 (Suppl. 6):21–5. doi: 10.1046/j.1528-1157.43.s.6.11.x
2. Jefferys JGR. Hippocampal sclerosis and temporal lobe epilepsy: cause or consequence? *Brain.* (1999) 122:1007–8. doi: 10.1093/brain/122.6.1007
3. Wiebe S, Blume WT, Girvin JP, Eliasziw M. A randomized, controlled trial of surgery for temporal-lobe epilepsy. *N Engl J Med.* (2001) 345:311–8. doi: 10.1056/NEJM200108023450501
4. Buzsaki G, Horvath Z, Urioste R, Hetke J, Wise K. High-frequency network oscillation in the hippocampus. *Science.* (1992) 256:1025–7. doi: 10.1126/science.1589772
5. Bragin A, Engel J Jr, Wilson CL, Fried I, Mathern GW. Hippocampal and entorhinal cortex high-frequency oscillations (100–500 Hz) in human epileptic brain and in kainic acid–treated rats with chronic seizures. *Epilepsia.* (1999) 40:127–37. doi: 10.1111/j.1528-1157.1999.tb02065.x
6. Jacobs J, LeVan P, Chander R, Hall J, Dubeau F, Gotman J. Interictal high-frequency oscillations (80-500 Hz) are an indicator of seizure onset areas independent of spikes in the human epileptic brain. *Epilepsia.* (2008) 49:1893–907. doi: 10.1111/j.1528-1167.2008.01656.x
7. Worrell G, Gotman J. High-frequency oscillations and other electrophysiological biomarkers of epilepsy: clinical studies. *Biomark Med.* (2011) 5:557–66. doi: 10.2217/bmm.11.74
8. Zijlmans M, Jacobs J, Kahn YU, Zelmann R, Dubeau F, Gotman J. Ictal and interictal high frequency oscillations in patients with focal epilepsy. *Clin Neurophysiol.* (2011) 122:664–71. doi: 10.1016/j.clinph.2010.09.021
9. Engel J Jr, da Silva FL. High-frequency oscillations - where we are and where we need to go. *Prog Neurobiol.* (2012) 98:316–8. doi: 10.1016/j.pneurobio.2012.02.001
10. Fedele T, Burnos S, Boran E, Krayenbühl N, Hilfiker P, Grunwald T, et al. Resection of high frequency oscillations predicts seizure outcome in the individual patient. *Sci Rep.* (2017) 7:13836. doi: 10.1038/s41598-017-13064-1

11. Frauscher B, Bartolomei F, Kobayashi K, Cimbalnik J, van't Klooster MA, Rampp S, et al. High-frequency oscillations: the state of clinical research. *Epilepsia*. (2017) 58:1316–29. doi: 10.1111/epi.13829
12. Matsumoto A, Brinkmann BH, Matthew Stead S, Matsumoto J, Kucewicz MT, Marsh WR, et al. Pathological and physiological high-frequency oscillations in focal human epilepsy. *J Neurophysiol.* (2013) 110:1958–64. doi: 10.1152/jn.00341.2013
13. Cimbalnik J, Brinkmann B, Kremen V, Jurak P, Berry B, Van Gompel J, et al. Physiological and pathological high frequency oscillations in focal epilepsy. *Ann Clin Transl Neurol.* (2018) 5:1062–76. doi: 10.1002/acn3.618
14. Buzsáki G, da Silva FL. High frequency oscillations in the intact brain. *Prog Neurobiol.* (2012) 98:241–9. doi: 10.1016/j.pneurobio.2012.02.004
15. Bragin A, Engel J, Staba RJ. High-frequency oscillations in epileptic brain. *Curr Opin Neurol.* (2010) 23:151–6. doi: 10.1097/WCO.0b013e3283373ac8
16. Jacobs J, Zijlmans M, Zelmann R, Chatillon C-É, Hall J, Olivier A, et al. High-frequency electroencephalographic oscillations correlate with outcome of epilepsy surgery. *Ann Neurol.* (2010) 67:209–20. doi: 10.1002/ana.21847
17. Serafini R. Similarities and differences between the interictal epileptiform discharges of green-spikes and red-spikes zones of human neocortex. *Clin Neurophysiol.* (2019) 130:396–405. doi: 10.1016/j.clinph.2018.12.011
18. Klimes P, Duque JJ, Brinkmann B, Van Gompel J, Stead M, St Louis EK, et al. The functional organization of human epileptic hippocampus. *J Neurophysiol.* (2016) 115:3140–5. doi: 10.1152/jn.00089.2016
19. Zweiphenning WJEM, van't Klooster MA, van Diessen E, van Klink NEC, Huiskamp GJM, Gebbink TA, et al. High frequency oscillations and high frequency functional network characteristics in the intraoperative electrocorticogram in epilepsy. *Neuroimage Clin.* (2016) 12:928–39. doi: 10.1016/j.nicl.2016.09.014
20. Chen D, Wan S, Bao FS. Epileptic focus localization using discrete wavelet transform based on interictal intracranial EEG. *IEEE Trans Neural Syst Rehabil Eng.* (2017) 25:413–25. doi: 10.1109/TNSRE.2016.2604393
21. Varatharajah Y, Berry B, Cimbalnik J, Kremen V, Van Gompel J, Stead M, et al. Integrating artificial intelligence with real-time intracranial EEG monitoring to automate interictal identification of seizure onset zones in focal epilepsy. *J Neural Eng.* (2018) 15:046035. doi: 10.1088/1741-2552/aac960
22. Cimbalnik J, Klimes P, Sladky V, Nejedly P, Jurak P, Pail M, et al. Multi-feature localization of epileptic foci from interictal, intracranial EEG. *Clin Neurophysiol.* (2019) 130:1945–53. doi: 10.1016/j.clinph.2019.07.024
23. Klimes P, Cimbalnik J, Brazdil M, Hall J, Dubeau F, Gotman J, et al. NREM sleep is the state of vigilance that best identifies the epileptogenic zone in the interictal electroencephalogram. *Epilepsia.* (2019) 60:2404–15. doi: 10.1111/epi.16377
24. Polich J. Updating P300: an integrative theory of P3a and P3b. *Clin Neurophysiol.* (2007) 118:2128–48. doi: 10.1016/j.clinph.2007.04.019
25. Albares M, Lio G, Criaud M, Anton JL, Desmurget M, Boulinguez P. The dorsal medial frontal cortex mediates automatic motor inhibition in uncertain contexts: evidence from combined fMRI and EEG studies. *Hum Brain Mapp.* (2014) 35:5517–31. doi: 10.1002/hbm.22567
26. Shaw DJ, Czekóová K, Staněk R, Mareček R, Urbánek T, Špalek J, et al. A dual-fMRI investigation of the iterated Ultimatum Game reveals that reciprocal behaviour is associated with neural alignment. *Sci Rep*. (2018) 8:10896. doi: 10.1038/s41598-018-29233-9
27. Näätänen R, Paavilainen P, Rinne T, Alho K. The mismatch negativity (MMN) in basic research of central auditory processing: a review. *Clin Neurophysiol.* (2007) 118:2544–90. doi: 10.1016/j.clinph.2007.04.026
28. Duncan CC, Barry RJ, Connolly JF, Fischer C, Michie PT, Näätänen R, et al. Event-related potentials in clinical research: guidelines for eliciting, recording, and quantifying mismatch negativity, P300, and N400. *Clin Neurophysiol.* (2009) 120:1883–908. doi: 10.1016/j.clinph.2009.07.045
29. Higuchi Y, Seo T, Miyanishi T, Kawasaki Y, Suzuki M, Sumiyoshi T. Mismatch negativity and p3a/reorienting complex in subjects with schizophrenia or at-risk mental state. *Front Behav Neurosci.* (2014) 8:172. doi: 10.3389/fnbeh.2014.00172
30. Kucewicz MT, Cimbalnik J, Matsumoto JY, Brinkmann BH, Bower MR, Vasoli V, et al. High frequency oscillations are associated with cognitive processing in human recognition memory. *Brain.* (2014) 137:2231–44. doi: 10.1093/brain/awu149
31. Rehulka P, Cimbálník J, Pail M, Chrastina J, Hermanová M, Brázdil M. Hippocampal high frequency oscillations in unilateral and bilateral mesial temporal lobe epilepsy. *Clin Neurophysiol.* (2019) 130:1151–9. doi: 10.1016/j.clinph.2019.03.026
32. Barkmeier DT, Shah AK, Flanagan D, Atkinson MD, Agarwal R, Fuerst DR, et al. High inter-reviewer variability of spike detection on intracranial EEG addressed by an automated multi-channel algorithm. *Clin Neurophysiol.* (2012) 123:1088–95. doi: 10.1016/j.clinph.2011.09.023
33. Urrestarazu E, Chander R, Dubeau F, Gotman J. Interictal high-frequency oscillations (100-500 Hz) in the intracerebral EEG of epileptic patients. *Brain.* (2007) 130:2354–66. doi: 10.1093/brain/awm149
34. Jacobs J, Levan P, Châtillon C-E, Olivier A, Dubeau F, Gotman J. High frequency oscillations in intracranial EEGs mark epileptogenicity rather than lesion type. *Brain.* (2009) 132:1022–37. doi: 10.1093/brain/awn351
35. Nagasawa T, Juhász C, Rothermel R, Hoechstetter K, Sood S, Asano E. Spontaneous and visually driven high-frequency oscillations in the occipital cortex: intracranial recording in epileptic patients. *Hum Brain Mapp.* (2012) 33:569–83. doi: 10.1002/hbm.21233
36. Pail M, Rehulka P, Cimbálník J, DoleŽalová I, Chrastina J, Brázdil M. Frequency-independent characteristics of high-frequency oscillations in epileptic and non-epileptic regions. *Clin Neurophysiol.* (2017) 128:106–14. doi: 10.1016/j.clinph.2016.10.011
37. Binnie CD. Cognitive impairment during epileptiform discharges: is it ever justifiable to treat the EEG? *Lancet Neurol.* (2003) 2:725–30. doi: 10.1016/S1474-4422(03)00584-2
38. Brázdil M, Cimbálník J, Roman R, Shaw DJ, Stead MM, Daniel P, et al. Impact of cognitive stimulation on ripples within human epileptic and non-epileptic hippocampus. *BMC Neurosci.* (2015) 16:47. doi: 10.1186/s12868-015-0184-0
39. Warren CP, Hu S, Stead M, Brinkmann BH, Bower MR, Worrell GA. Synchrony in normal and focal epileptic brain: the seizure onset zone is functionally disconnected. *J Neurophysiol.* (2010) 104:3530–9. doi: 10.1152/jn.00368.2010


**Conflict of Interest:** The authors declare that the research was conducted in the absence of any commercial or financial relationships that could be construed as a potential conflict of interest.

# CHAPTER 9

# Very high-frequency oscillations

The identification of HFOs in epileptogenic tissue is one of the major discoveries in epilepsy research over the last decades, attracting the attention of clinical and experimental epileptologists worldwide. The presence of HFOs between seizures, at seizure onset, and during seizures suggests an inherent relationship between the cellular and network mechanisms of seizures and HFOs (Jiruska et al., 2017). However, the questions of what high these oscillations can reach and which frequency range is clinically important remain unanswered. The published papers showed using HFOs promise for pathological tissue localization, although this approach has been shown successful only in ⅔ of the patients (Jacobs et al., 2018). The reason for the failures might be caused by false-positive detections (Bénar et al., 2010). Another major problem is the considerable overlap of pathological and physiological HFO characteristics (Kucewicz et al., 2014; Brázdil et al., 2015; Matsumoto et al., 2013). Nevertheless, it is proven that fast ripples define the epileptogenic zone more precisely than ripples (Frauscher et al., 2018).

As it was mentioned, the limiting factor for detecting higher frequency activities and oscillations, in particular, is the sampling frequency for EEG recording. The higher sampling frequency is used, the higher activity can be detected in the EEG. To adequately sample the temporal dynamics of HFOs, a reasonable approach is sampling at about 4-5 times the upper frequency of interest because it requires several samples to form the wave shape (Schomer & Lopes da Silva, 2017; Zijlmans et al., 2012). Preferentially, a sampling frequency of 2,000 Hz or above should be used for studying HFOs (Zijlmans et al., 2012). However, the question arises, what if there are HFOs with an even higher frequency? Based on known data, we cannot detect higher oscillations than HFOs if we use a sampling frequency of 2,000 Hz during EEG recording. Usui et al. (2010) was the first researcher who used higher sampling frequency (10 kHz) and surprisingly recorded interictal and ictal very high-frequency oscillations (VHFOs) of 1000–2500 Hz by routinely used subdural electrodes. Such high-frequency EEG activities had never been previously reported. These oscillations were detected in patients with intractable neocortical epilepsy associated with the malformation of cortical development (Usui et al., 2010). Interictal VHFOs and preictal VHFOs had identical characteristics in terms of frequency, amplitude, duration, temporal relationship with spikes, and distribution. The amplitudes of VHFOs were 3.5-29.4 μV, and durations were 2-226 ms (Usui et al., 2010). They appeared intermittently before the start of seizures and were interrupted by spikes.

Several studies investigated the predictive value of HFOs, showing that the resection of areas with high rates of both ictal (Jirsch et al., 2006), as well as interictal HFOs resulted in a favorable surgical outcome (Jacobs et al., 2010; Wu et al., 2010; Pail et al., 2017; Thomschewski et al., 2019). Nevertheless,

better results regarding the outcome prediction were reported for these VHFOs than for ripples and fast ripples (Usui et al., 2015), which was attributed to the possibility that VHFOs might be less prone to being mimicked by physiologic activity or artifacts (Usui et al., 2015).

**Published research**

# Very high-frequency oscillations: Novel biomarkers of the epileptogenic zone

Milan Brázdil

Martin Pail

Josef Halámek

Filip Plešinger

Jan Cimbálník

Robert Roman

Petr Klimeš

Pavel Daniel

Jan Chrastina

Eva Brichtová

Ivan Rektor

Gregory A. Worrell

Pavel Jurák

**Ann Neurol. 2017 Aug;82(2):299-310. doi: 10.1002/ana.25006.**

## Commentary on published paper

High-frequency oscillations (HFOs) in the range of 80-600 Hz (ripples & fast ripples) have been repeatedly observed in intracranial EEG data. Despite the problematic overlaps of pathological and physiological HFO, FR still remain a promising biomarker of tissue epileptogenicity (Zijlmans et al., 2012). However, the occurrence of HFOs having frequencies higher than the conventionally analyzed range in focal epilepsy has attracted attention. As it was mentioned, recently, ictal very high-frequency oscillations (VHFOs; > 1 kHz) were detected using subdural electrodes in a limited cohort of epileptic patients (Usui et al., 2010; 2015). In the first Usui´s study, VHFO were observed in five patients out of six; in the second study, it was six patients out of seven. The results of that studies suggested ictal VHFO to be an even more specific marker than ictal HFOs for identifying the epileptogenic zone that is a crucial target for highly effective epilepsy surgery. Based on these results, we decided to perform a study of VHFOs in our patients as well. In our recently published paper, we focused on interictal oscillations above traditional fast ripple frequency range (> 500 Hz) in depth EEG recordings. Our study is crucial mainly in the size of the observed cohort in comparison with previously published works.

The presented study's primary goal was to investigate the incidence and spatial distribution of spontaneous interictal VHFOs and the reliability of VHFOs as a biomarker of the epileptogenic zone in a group of patients.

We retrospectively analyzed very high-sampled interictal stereo-EEG data in a large cohort of patients with focal drug-resistant epilepsy. Each subject underwent continuous intracerebral EEG recording with clinical video-EEG monitoring equipment. For the very first time, we clearly showed that interictal very high-frequency oscillations (very fast; 600-1000 Hz and ultra-fast ripples; 1-2 kHz) can be recorded using standard depth macro electrode and are relatively frequent events in the epileptic brain.

The results of our study confirmed the previously presented conclusions. There is evidence that ripple generation is influenced by more extensive networks; smaller networks are involved in fast ripples and even less in VFR and UFR generation, which can be observed focally. These phenomena are more spatially restricted and seem to be more specific biomarkers for epileptogenic zone when compared to traditional interictal HFOs. However, it is also noted that VHFOs have not been detected in all subjects, making it only useful for a subgroup of patients. In this context, VHFOs might even more exclusively reflect epilepsy-related activity, making them a very promising candidate for clinical use when present.

These results represent a groundbreaking step into the research of high-frequency oscillatory brain activities and promise to provide important clinical consequences in the future.

# Very High-Frequency Oscillations: Novel Biomarkers of the Epileptogenic Zone

Milan Brázdil, MD, PhD,[1,2] Martin Pail, MD, PhD,[1] Josef Halámek, PhD,[3,4] Filip Plešinger, PhD,[3] Jan Cimbálník,[4] Robert Roman, MD, PhD,[2] Petr Klimeš,[3] Pavel Daniel,[1,2] Jan Chrastina, MD, PhD,[5] Eva Brichtová, MD, PhD,[5] Ivan Rektor, MD, PhD,[1,2] Gregory A. Worrell, MD, PhD,[6] and Pavel Jurák, PhD[3,4]

**Objective:** In the present study, we aimed to investigate depth electroencephalographic (EEG) recordings in a large cohort of patients with drug-resistant epilepsy and to focus on interictal very high-frequency oscillations (VHFOs) between 500Hz and 2kHz. We hypothesized that interictal VHFOs are more specific biomarkers for epileptogenic zone compared to traditional HFOs.

**Methods:** Forty patients with focal epilepsy who underwent presurgical stereo-EEG (SEEG) were included in the study. SEEG data were recorded with a sampling rate of 25kHz, and a 30-minute resting period was analyzed for each patient. Ten patients met selected criteria for analyses of correlations with surgical outcome: detection of interictal ripples (Rs), fast ripples (FRs), and VHFOs; resective surgery; and at least 1 year of postoperative follow-up. Using power envelope computation and visual inspection of power distribution matrixes, electrode contacts with HFOs and VHFOs were detected and analyzed.

**Results:** Interictal very fast ripples (VFRs; 500–1,000Hz) were detected in 23 of 40 patients and ultrafast ripples (UFRs; 1,000–2,000Hz) in almost half of investigated subjects (n = 19). VFRs and UFRs were observed only in patients with temporal lobe epilepsy and were recorded exclusively from mesiotemporal structures. The UFRs were more spatially restricted in the brain than lower-frequency HFOs. When compared to R oscillations, significantly better outcomes were observed in patients with a higher percentage of removed contacts containing FRs, VFRs, and UFRs.

**Interpretation:** Interictal VHFOs are relatively frequent abnormal phenomena in patients with epilepsy, and appear to be more specific biomarkers for epileptogenic zone when compared to traditional HFOs.

ANN NEUROL 2017;82:299–310

Throughout most of the 20th century, there was little clinical interest in electroencephalographic (EEG) frequencies > 100Hz. In 1999, the potential clinical relevance and association of high-frequency oscillations (HFOs; 100 and 500Hz) with epileptogenic human brain were reported.[1–3] HFOs have been observed in both micro- and macroelectrode recordings, between seizures, at seizure onset, and during seizures (reviewed in Zijlmans et al).[4] Interictal ripples (Rs; 80–250Hz) and fast ripples (FRs; 250 and 500Hz) are both increased in the seizure onset zone (SOZ), and removal of tissue generating interictal HFOs correlates with good surgical outcome.[5–9] HFOs have proven to be more specific in indicating the SOZ than interictal epileptiform spikes.[10] A fundamental challenge, however, has been that physiological HFOs associated with normal brain function overlap in frequency with pathological HFOs,[11–13] and how they can be separated remains unclear.[14] Despite this and other challenges, HFOs remain a promising biomarker of tissue epileptogenicity.[15]

Recently ictal very high-frequency oscillations (VHFOs) with frequencies ≥ 1kHz were described in a

View this article online at wileyonlinelibrary.com. DOI: 10.1002/ana.25006

Received Mar 1, 2017, and in revised form Aug 2, 2017. Accepted for publication Aug 2, 2017.

Address correspondence to Dr Brázdil, Brno Epilepsy Center, Department of Neurology, St Anne's University Hospital, Pekařská 53, Brno 65691, Czech Republic. E-mail: mbrazd@med.muni.cz

From the [1]Brno Epilepsy Center, Department of Neurology, St Anne's University Hospital and Medical Faculty of Masaryk University, Brno, Czech Republic; [2]Central European Institute of Technology, Masaryk University, Brno, Czech Republic; [3]Institute of Scientific Instruments, Czech Academy of Sciences, Brno, Czech Republic; [4]International Clinical Research Center, St Anne's University Hospital, Brno, Czech Republic; [5]Brno Epilepsy Center, Department of Neurosurgery, St Anne's University Hospital and Medical Faculty of Masaryk University, Brno, Czech Republic; and [6]Mayo Systems Electrophysiology Laboratory, Departments of Neurology and Physiology & Biomedical Engineering, Mayo Clinic, Rochester, MN



 

cohort of patients with focal epilepsy.[16] In 7 of 13 investigated subjects, the authors detected VHFOs in 1 to 4 subdural electrode contacts per patient. The comparison of postoperative seizure outcome with the presence or absence of ictal VHFOs and ictal HFOs and completeness of resection of the tissue generating HFOs and VHFOs was performed, and ictal VHFOs were a more specific marker than ictal HFOs for identifying the epileptogenic zone.[16] It is notable that for engineering and practical reasons the majority of human intracranial EEG recordings have not explored local field oscillations $> 600$Hz.

The aim of the present study was to investigate penetrating depth EEG recordings in a large cohort of patients with drug-resistant epilepsy and to focus on interictal local field potential (LFP) oscillations between 500Hz and 2kHz. Furthermore, we introduce a technique for visualization, localization, and quantitative description of VHFOs. We hypothesized that interictal VHFOs, by analogy to previously reported very high-frequency ictal activity, are more specific biomarkers for epileptogenic zone compared to Rs or FRs.

## Patients and Methods

Forty patients (n = 40) with focal temporal (n = 28) and extratemporal (n = 12) lobe drug-resistant epilepsy (Commission on Classification and Terminology of the International League against Epilepsy)[17] who underwent presurgical evaluation using intracranial stereo-EEG (SEEG) recordings provided consent and were included in the study. Ten patients (6 females, 4 males) ranging in age from 26 to 57 years (mean age = 40.4 years, standard deviation = 11.1) met the following criteria for analyzing correlations between oscillations and surgical outcomes: detection of interictal HFOs (Rs and FRs) and VHFOs (0.5–2kHz), surgical intervention, and at least 1 year of postoperative follow-up. The main demographic and clinical characteristics of the involved subjects are shown in Table 1.

All 10 patients underwent a comprehensive presurgical evaluation, including a detailed history and neurological examination, magnetic resonance imaging (MRI), neuropsychological testing, and scalp and invasive video-EEG monitoring. Prior to invasive EEG, 1 subject had a vagal nerve stimulation system implanted, with unfavorable seizure frequency outcome (Patient 7). The duration of clinical monitoring and the location and number of implanted electrodes were determined in accordance with clinical considerations. After invasive video-EEG monitoring, all patients underwent surgical intervention, details of which are shown in Table 1. The follow-up interval after epilepsy surgery was at least 12 months. After surgical resection, 7 patients were rated as Engel IA (seizure free), and 3 patients were Engel III (improved but not seizure free). The study was approved by the St Anne's University Hospital Research Ethics Committee and the ethics committee of Masaryk University. All patients signed an informed consent form.

For depth SEEG recordings, standard intracerebral multicontact platinum electrodes (5, 10, and 15 contacts) with a diameter of 0.8mm, a contact length of 2mm, an intercontact distance of 1.5mm, and a contact surface area of $5mm^2$ were used in all patients. Each patient received 5 to 13 orthogonal SEEG electrodes in the temporal and/or frontal, parietal, and occipital lobes using the stereotaxic coordinate system of Talairach.[18] Their position within the brain was verified using MRI with electrodes in situ. In 10 patients, we investigated data from 644 contacts positioned in hippocampus (n = 109), other temporal cortex (n = 413), frontal cortex (n = 69), parietal cortex (n = 36), insular cortex (n = 13), and structural lesion (n = 4). Only contacts localized in gray matter were included in the study.

A 192-channel research EEG acquisition system (M&I; BrainScope, Prague, Czech Republic) was used for recording 30 minutes of awake resting interictal EEG recordings with a sampling rate of 25kHz and dynamic range of $\pm 25$mV with 10nV (24 bits). The EEG acquisition unit was battery powered to eliminate line noise. We used standard epilepsy monitoring unit protocols, but emphasis was given to eliminating power sources of electromagnetic radiation and 50Hz power grid influence. No special shielded environment was used. Thirty minutes of artifact-free continuous interictal SEEG data (recorded during wakefulness) was analyzed for each subject based on the results of previously published papers.[10,19,20] All recordings were acquired using a referential earlobe reference. For analysis, the signals were subtracted from a white matter averaged signal for each contact. All data processing was performed using open platform software SignalPlant and MATLAB software.[21] SignalPlant was used for interactive graphical analysis of large, multichannel data. Custom MATLAB scripts were used for batch processing of data and statistics.

### *Preprocessing*

All data were filtered and downsampled to 5kHz with a 2kHz frequency band. Hilbert transformation of the EEG signal was used to compute power envelopes (PEs) in 4 frequency bands: Rs, 80 to 200Hz; FRs, 200 to 500Hz; very fast ripples (VFRs), 500 to 1,000Hz; and ultrafast ripples (UFRs), 1,000 to 2,000Hz. All PEs were decimated 5 times, to a sampling frequency of 1kHz. UFR PEs were smoothed with the window (10 samples) before decimation.

The results of the PE computation were put into 2-dimensional power distribution matrixes (PDMs), where each row corresponds to 1 recording contact and each column corresponds to time interval (total time = 30 minutes). SignalPlant with the plugin AmpToColor was used for graphical interpretation of PEs. Figure 1 describes in detail the information content of PDMs. Because resolution of created images is significantly lower than the number of samples in data recordings, each point in an image corresponds to a specific data block. Point color intensity represents the maximum of these data blocks in grayscale and is multiplied by a manually adjustable parameter, working as contrast enhancement, intended for the best visual inspection. This type of display provides

**TABLE 1. Patients' Demographic and Clinical Characteristics**

| Subject | Gender | Age at Seizure Onset, yr | Age at SEEG, yr | Seizure Type/No. per mo | MRI Signs | Type/Side of Epilepsy | SOZ | Surgery/ Histopathology | Outcome, Engel Stage (yr) |
|---|---|---|---|---|---|---|---|---|---|
| 3 | F | 19 | 57 | CPS/2 plus, sGTCS/6 | Postischemic lesions within left T-O and H | T/L | B′1–2 | AMTR/gliosis, hemosiderin within T pole | IA (3.5) |
| 7 | F | 16 | 33 | CPS/5 | Bilateral HS | T/bilateral | A1–4, B1–3, C1–2, B′1–2 | Right AMTR/ negative | III (2.5) |
| 13 | F | 17 | 26 | CPS/12 | Normal | T/L | A′5–10 | Left AMTR/ FCD IB | IA (2) |
| 14 | F | 28 | 56 | CPS/8 | Right HS | T/R | B1–2, C1–4 | Right AMTR/ negative | IIIA (2) |
| 15 | M | 1 | 40 | CPS/2 plus | Hypotrophic left H | T/L | B′1–3, C′1–3 | Left AMTR/ negative | IA (2) |
| 21 | M | 33 | 41 | CPS/30 | Focal hyperintensity, right basal T | T/R | B1–4, C1–3, L1–4 | Right AMTR/ FCD IIIB, ganglioglioma | IA (1.5) |
| 31 | M | 31 | 37 | CPS/4 | Normal | T/L | B′1–4, C′1–4, B1–3 | Left AMTR/ negative | IA (1) |
| 32 | F | 9 | 27 | CPS/5 | Left HS | T/L | B′1–3, C′1–4 | Left AMTR/ FCD IIIA | IIIA (1) |
| 33 | M | 2 | 51 | CPS/3 plus | Right H atrophy, slight changes of density | T/R | B1–3, C1–2 | Right AMTR/HS | IA (1) |
| 40 | F | 9 | 36 | CPS/5 | Bilateral H atrophy and malrotation | T/R | Tp, B1–3, C1–3 | Right AMTR/ negative | IA (1) |

′ = left; AMTR = anteromedial temporal resection; CPS = complex partial seizure; F = female; FCD = focal cortical dysplasia; H = hippocampus; HS = hippocampal sclerosis; L = left; M = male; MRI = magnetic resonance imaging; O = occipital; plus = sporadic ictal generalization; R = right; SEEG = stereo-electroencephalography; sGTCS = secondary generalized tonic–clonic seizures; SOZ = seizure onset zone; T = temporal.

overview of the entire 30-minute, multichannel (here up to 192 channels) recording properties in a single image.

### *Artifact Elimination*

Artifact detection is crucial for computation of numerical parameters and statistical evaluation. PDMs provide complete overview, including artificial signals. SignalPlant visualization of raw signal simultaneously with PDMs was used to manually identify noisy contacts or time periods with artifacts. Artifacts were detected in each frequency band in PDM format (Fig 2). The number of detected artifacts was the highest in the VFR and UFR bands. Artificial contacts were removed from further processing. The same set of all deselected contacts were used for the R, FR, VFR, and UFR bands. Figure 1 demonstrates identification of artifact-free regions.

To detect EEG channels with occurrence of HFOs (Rs, FRs) and VHFOs (VFRs, UFRs), we used visual inspection of graphical PDMs. Identification of contacts with HFOs and VHFOs was blind, without any a priori knowledge of the resected areas and positive or negative postsurgical outcome (P.J., F.P.). All detected contacts were subsequently inspected in 5kHz raw data format for the occurrence of visible oscillations.

### *Numerical Parameters*

The relative duration of PE (RPE) was computed for each contact and each frequency range from artifact-free areas. The RPE represents the relative length of signal PEs exceeding the limit. This limit is computed from the mean short-term depression of PEs over all contacts of a given electrode (STDel). After that,

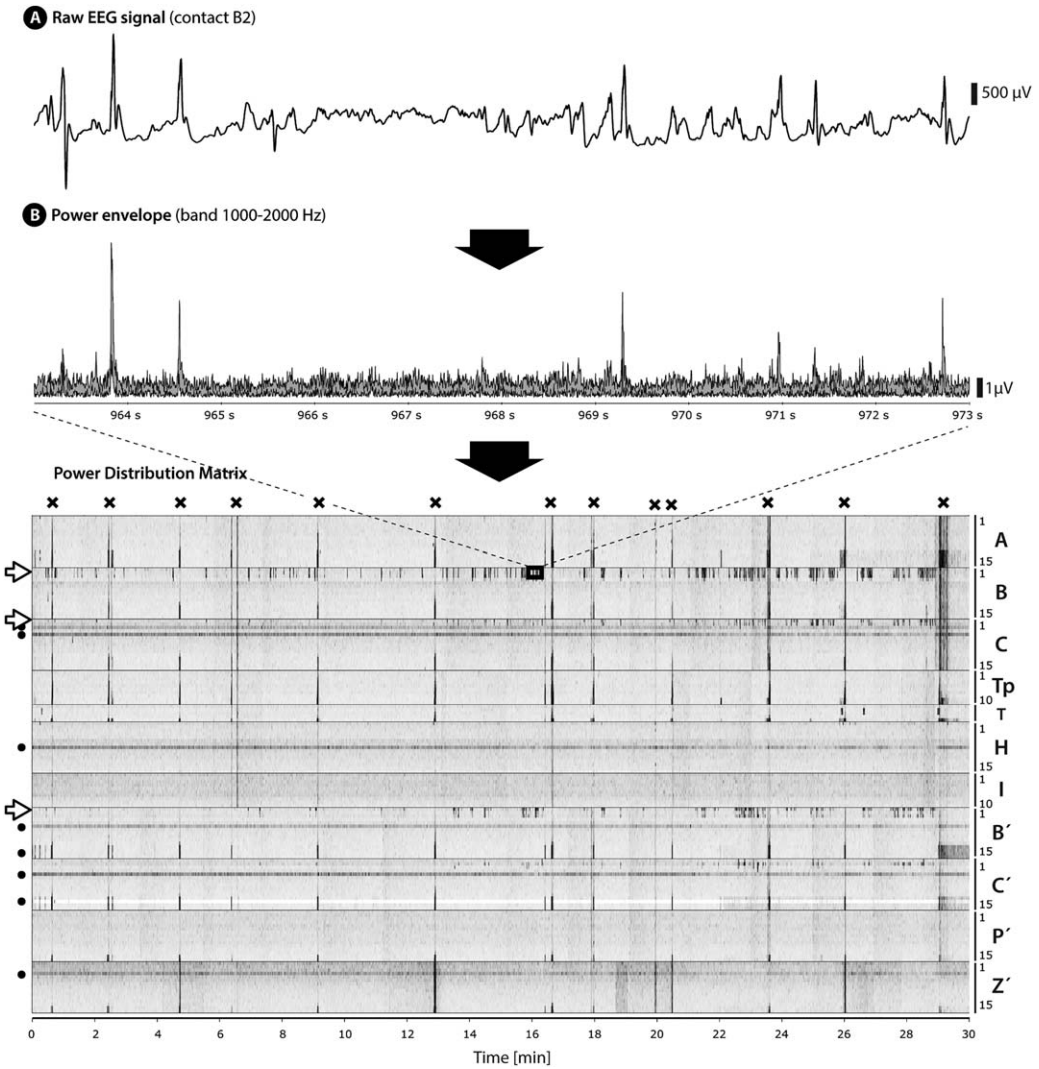


**FIGURE 1: Demonstration of power distribution matrix (PDM) created for the ultrafast ripple (UFR) frequency range. (A, B) Raw electroencephalographic (EEG) signal of recording contact (A) is transformed into power envelope (PE) in a frequency range of 1,000 to 2,000Hz (B). Bottom panel: The PE calculated for each contact is transformed into a high-density image, creating a PDM; 1 row represents the PE of 1 contact. Artifact identification for UFR bandpass is shown. Crosses indicate skipped time regions with artificial signals located in time and widespread over more electrodes and contacts. Dots indicate noise in the selected contact during the whole record. Arrows indicate contacts with unequivocal UFR activity. Identification of artifacts was performed manually on very fast ripple and UFR PDMs and simultaneously verified on raw data using SignalPlant.**

the duration of PEs with amplitude > K multiple of STDel is computed for each contact, and results are presented as a bar graph for each contact. The K is chosen so that low numbers of contacts (maximal = 5) are picked up. The K multiple is mostly 13. The RPE parameter is stored in files, corresponding to 4 analyzed frequency bands.

### *Statistical Analyses*

To investigate correlation between different types of oscillations (Rs, FRs, VFRs, UFRs) and surgical outcomes (ie, the reliability of events for identification of epileptogenic zone), we calculated the ratio between the number of removed and nonremoved contacts showing separately each type of oscillation in the core study patients. We used the identical approach published by Jacobs et al[6]:

$$RatioChanns(ev) = \frac{\#ChannRem_{ev} - \#ChannNonRem_{ev}}{\#ChannRem_{ev} + \#ChannNonRem_{ev}} \quad (1)$$

where *ev* is the type of event (R, FR, VFR, or UFR), *#ChannRem* is the number of removed contacts with events, and *#ChannNonRem* is the number of nonremoved contacts with evaluated events.

Analogous calculations were done for contacts revealing SOZ, defined as the contact(s) with very first ictal SEEG change independently indicated by 2 experienced clinical epileptologists (M.B., M.P.).

In addition, percentage of removed areas with detected oscillations was calculated for each subject and across the core study group as follows:

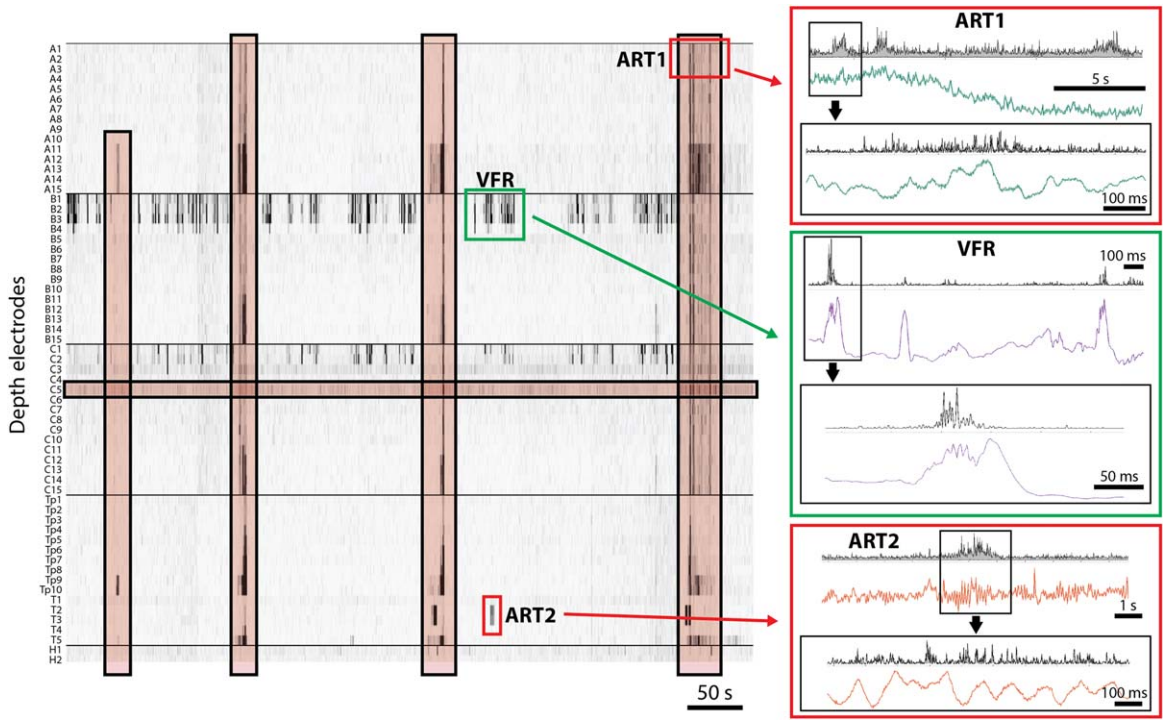


**FIGURE 2: Example of artifact identification in power distribution matrixes (PDMs; left panel). Artifacts are marked by red areas. Frequency range = 500 to 1,000Hz. Red boxes ART1 and ART2 (right panel) display the artifacts in detail. Boxes show power envelopes (top, black) and raw signal (bottom, color) at 2 different time scales. ART1 = artifacts affected most of contacts; ART2 = artifact in only 2 contacts (T2, T3). Green rectangle defines very high-frequency oscillations: a short, sharp, and repetitive power envelope increase only in limited contacts (here B1–B3). VFR = very fast ripple.**

$$PercentageChannel(ev) = 100 \times \frac{\#ChannRem_{ev}}{\#ChannRem_{ev} + \#ChannNonRem_{ev}} \quad (2)$$

The determination of resected and nonresected contacts was done using the fusion of MRI with electrodes in situ and postsurgical MRI (at least 3 months after surgery). Electrode contacts were classified as removed if they were within the surgical cavity on the postsurgical MRI.

Statistical analyses of differences in patients with good (seizure free; Engel class IA) versus poor surgical outcome (persistent seizures; Engel class III) for *RatioChanns, PercentageChanns*, and number of defined or resected contacts was done by analysis of variance. A significant limitation is the number of analyzed subjects (ie, 10).

The data are available on request from the corresponding author.

## Results

HFOs in the frequency range of Rs were detected in 38 of 40 investigated patients. In 32 of 40 patients, we observed FRs. All subjects with FRs also had Rs detected. Analysis of interictal oscillations > 500Hz revealed positive findings in temporal lobe patients only with occurrence of both VFRs and UFRs exclusively in the mesiotemporal structures (hippocampus, amygdala, and entorhinal cortex). VFRs were detected in 23 of 40 patients, and UFRs in about half of investigated subjects (n = 19). Examples of VFRs and UFRs can be seen in Figure 3.

The interictal very high-frequency phenomena occurred mostly in the regions with Rs and FRs and frequently preceded or were embedded in the initial spike slope, less often following the spike (Figs 4 and 5). When compared, the occurrence of Rs, FRs, VFRs, and UFRs typically showing a reduction of involved recording contacts with increasing frequency of analyzed events was observed (Fig 6). The mean number of contacts with Rs was 8.6 (±4.3), FRs 5.4 (±3.5), VFRs 3.8 (±1.8), and UFRs 2.9 (±1.4). Numbers for VFRs and UFRs differed significantly from numbers of contacts with Rs ($p < 0.05$ corrected). In 4 of 10 investigated patients, the contacts with UFRs were less distributed than those with VFRs, and VFRs never exceeded UFRs. Also, there were usually contacts with FRs and especially Rs clearly more widely distributed within mesiotemporal regions than those with VFRs or even UFRs. The same effect was seen in bar graphs of numerical parameters of relative PE duration (Fig 7).

The ratio between the number of removed and nonremoved contacts with FRs, VFRs, and UFRs */RatioChanns(ev)/* significantly differed between patients with good and poor postoperative outcome. The ratio was

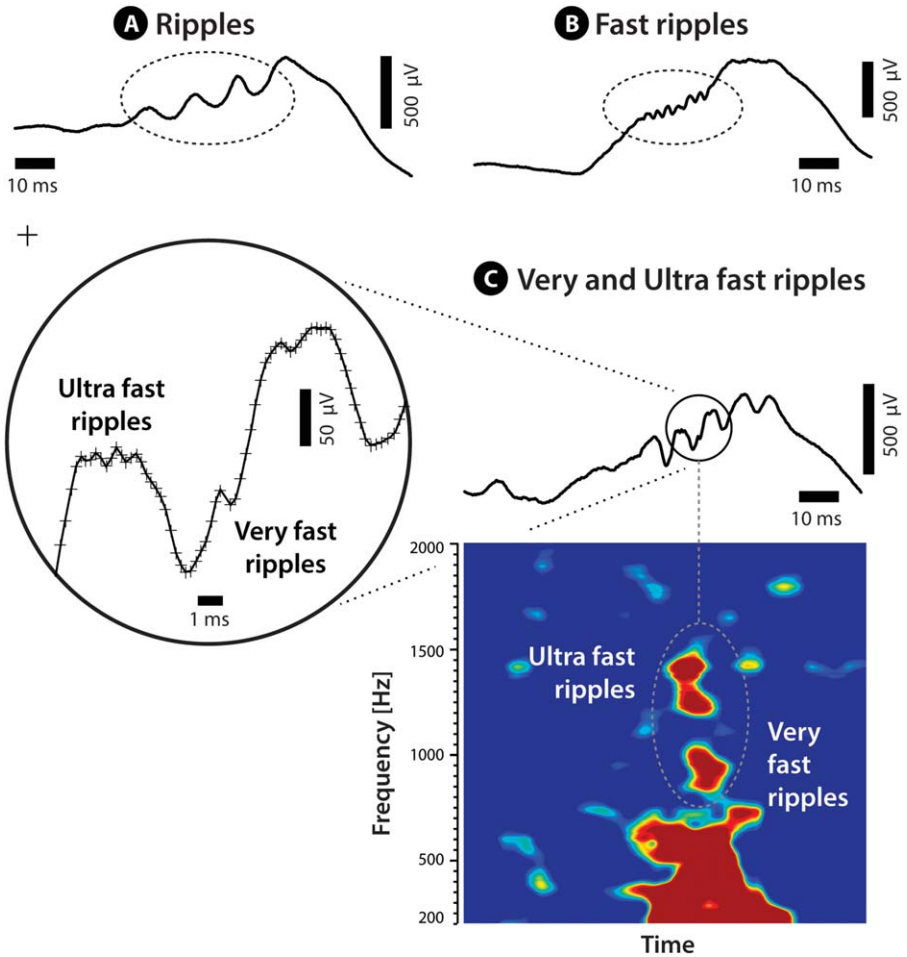


**FIGURE 3: Examples of different types of oscillation recorded at high frequencies with high dynamicity.**

increased for FRs, VFRs, and UFRs in seizure-free patients ($p < 0.01$), but was not significant for ripples in our patients (Table 2). Additional analyses of percentages of removed areas */PercentageChanns(ev)/*showed more understandable differences for UFRs and FRs, which were significant as well. In seizure-free patients, on average 95% of contacts containing UFRs were removed, in contrast to 28% of UFR contacts in patients with persistent seizures. In the FR range, the average percentages for good and poor outcome were 72% and 19%, respectively.

Noteworthy were the calculations of mean numbers of removed contacts and numbers of contacts with detected events in patients with good versus poor postoperative outcomes. In line with our hypothesis, in seizure-free patients mean number of all removed contacts was higher than in subjects with persistent seizures (ie, larger resections): 16.4 (±7.6) versus 9.3 (±4.6). Nevertheless, the difference did not reach statistical significance ($p = 0.188$). The mean numbers of contacts with detected HFOs were slightly different between patients with good and bad outcomes; seizure-free patients revealed a mean number of contacts of 8.6 (±8.7) for Rs, 5.4 (±5.3) for FRs, 3.4 (±4.7) for VFRs, and 2.4 (±4.0) for UFRs. In patients with persistent seizures, mean number of contacts with Rs was 8.7 (±6.4); with FRs, 5.3 (±3.2); with VFRs, 4.7 (±2.1); and with UFRs, 4 (±2). The differences were not statistically significant; nevertheless, a trend was found in the UFR range, with twice as numerous contacts with detected events in patients with poor outcome ($p = 0.096$).

In patients who did not meet criteria for analyzing correlations between HFOs and surgical outcomes (n = 30), there were 13 subjects in whom VHFOs were clearly detected and 17 subjects without VHFOs.

All of 13 patients with VHFOs suffered from suspected temporal lobe epilepsy. In 4 patients, a vagal nerve stimulator (VNS) was implanted after the SEEG as SOZ was not convincingly proven preoperatively in 2 of them and SEEG unequivocally revealed bitemporal epilepsy in the other 2 patients. The decision to implant a VNS system was strictly based on discourse with the patients. Eight patients were operated (anteromedial

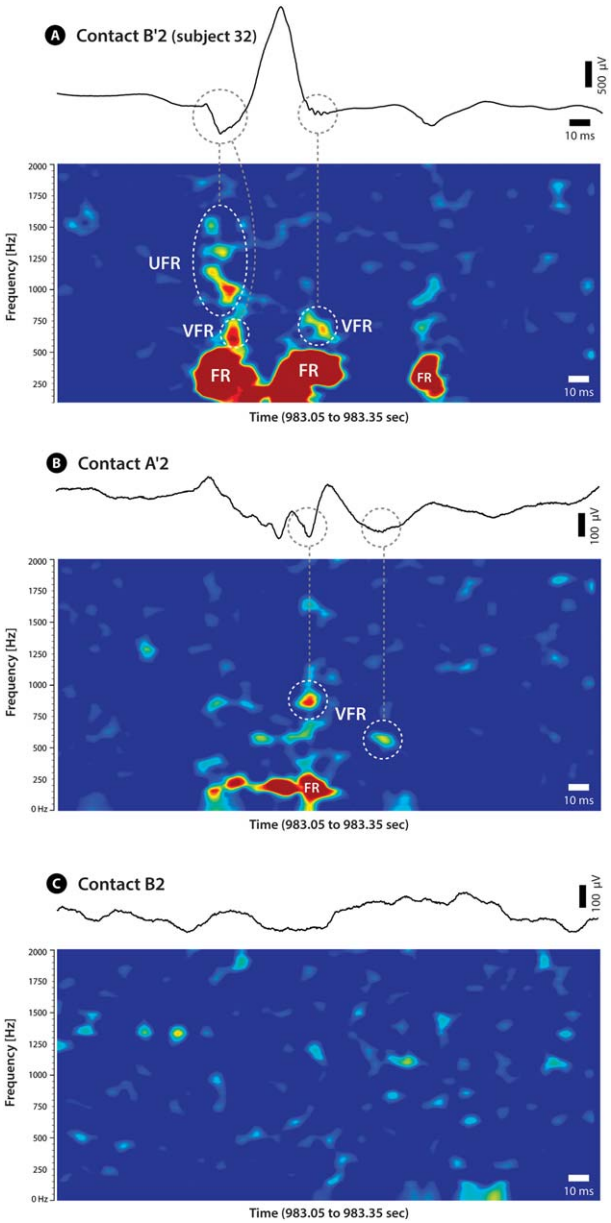


**FIGURE 4: Examples of fast ripple (FR), very fast ripple (VFR), and ultrafast ripple (UFR) distribution in different areas of an individual stereo-electroencephalographic dataset (Patient 32). (A–C) Recordings (raw signals and time-frequency maps) from contact B′2 within left anterior hippocampus (A) and A′2 within left amygdala (B) with detected high-frequency oscillations (HFOs) and very high-frequency oscillations, in contrast to contact B2 within right anterior hippocampus (C), in which HFOs are not presented.**

temporal resection was performed in 6 of them and lateral temporal neocortical resection in 2 of them), but their postoperative follow-up was < 1 year. One patient had not yet been operated. In all 13 patients, VFRs were observed in mesiotemporal structures only. UFRs were seen in 9 of them (also in mesiotemporal structures only).

In 17 patients, we did not detect any VHFOs in their depth EEG data. In this subgroup, there were 12 patients suffering from suspected extratemporal epilepsy and 5 patients with temporal lobe epilepsy. After SEEG, 12 subjects underwent resective surgery (8 of them with at least 1 year of postoperative follow-up), 3 patients were implanted with a VNS device, and 2 patients are scheduled for future operation. Interestingly, within a limited sample of patients with resective procedure and at least 1-year postoperative follow-up, there were 5 patients with temporal lobe epilepsy and 3 patients with suspected extratemporal lobe epilepsy. None of them, except of 1 mesiotemporal epilepsy patient, was seizure free after the surgery.

## Discussion

The presence of high-frequency activities at 2,000Hz in in vivo rat intrahippocampal electrophysiological recordings was recently described by Hsu et al, using a novel pseudowavelet approach for high-resolution time-frequency analysis called the damped-oscillator detector.[22] These activities appeared to be localized in hippocampal layers that were distinct from those of the theta and gamma bands, and increased in prominence with epileptogenesis. In parallel, Usui et al recorded interictal and ictal VHFOs of 1,000 to 2,500Hz in 4 of 5 patients with intractable neocortical epilepsy.[23] These oscillations were detected in highly localized cortical regions and were recorded by 1 to 4 electrodes in each patient. And finally, the VHFOs seemed to be interrupted by spikes in the interictal state.[23] Later, these authors studied the clinical significance of ictal VHFOs, and in 7 patients they detected ictal VHFOs and reported their resection was associated with favorable seizure outcome. Importantly, the percentage of resected HFO-generating areas did not differ significantly between patients with favorable outcome and those with unfavorable outcome.[16]

In our study, we investigated interictal depth SEEG recordings in a large cohort of 40 intractable epilepsy patients and focused on LFP oscillations between 500Hz and 2kHz. By using a high-sampling frequency of 25kHz and visual data analysis, we demonstrated the presence of intermittent oscillations > 1,000Hz (UFRs) in almost half of the patients (47.5%). VHFOs in the frequency range 500 to 1,000 Hz (VFRs) were present in 57.5% of all investigated subjects. The results support the argument that these phenomena are relatively frequent in epileptogenic brain tissue that generates spontaneous seizures. HFOs are more frequent in patients suffering from temporal lobe epilepsies. Interestingly, we never observed both VFRs and UFRs in extratemporal epilepsies, but they were detected in 82% and 68% of temporal lobe epilepsy patients, respectively. This is in contrast to the findings of Usui et al, who observed VHFOs in

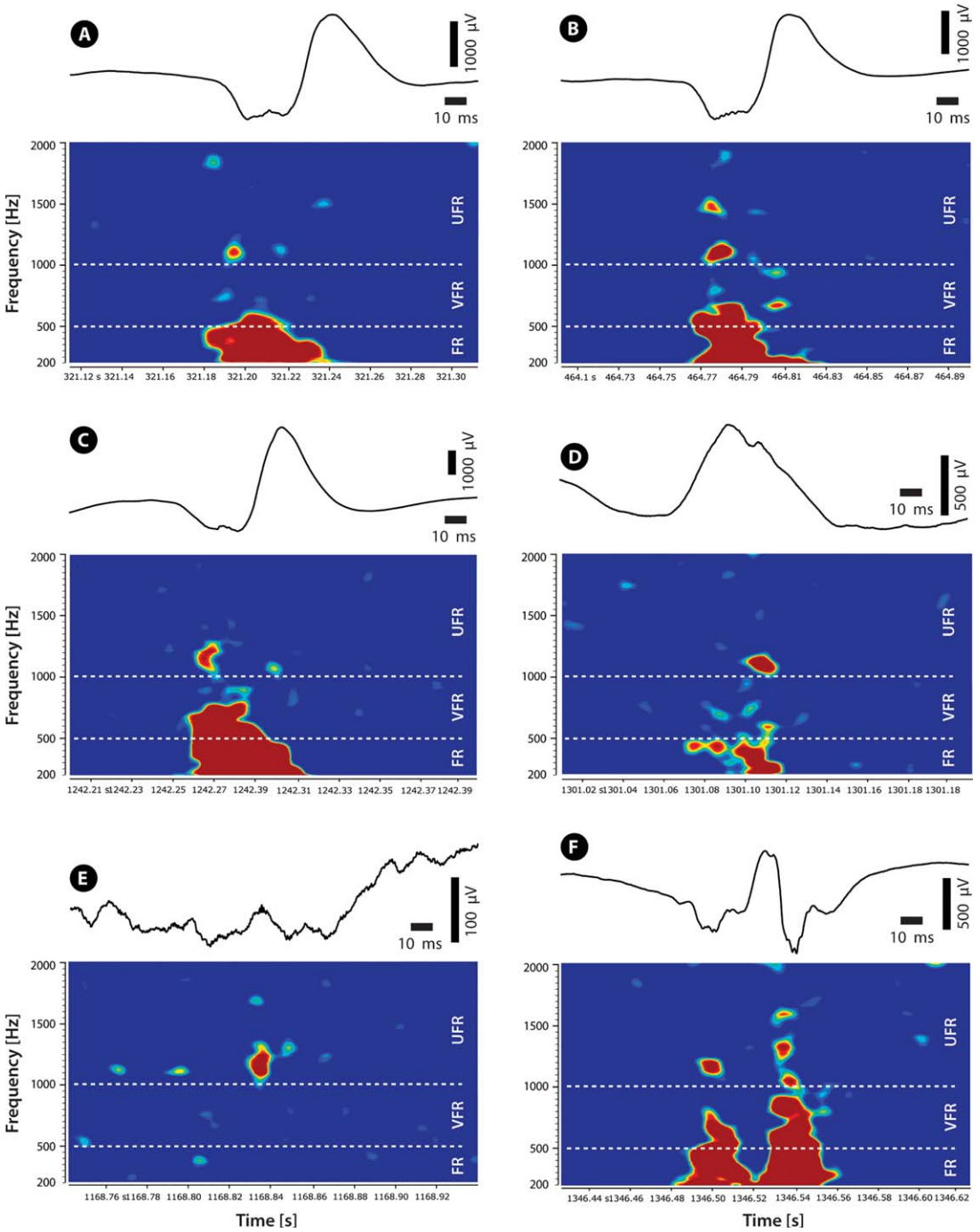


**FIGURE 5: Time-frequency distribution of fast ripples (FRs), very fast ripples (VFRs), and ultrafast ripples (UFRs) in 2 different areas and distinct time periods (Patient 40). (A–F) Recordings from contact B1 within right anterior hippocampus (A–D) and contact C1 within right posterior hippocampus (E, F)**

neocortical extratemporal epilepsies.[16,23] We detected VFRs and UFRs only in hippocampus, amygdala, and entorhinal cortex, which are archicortical areas, and were not investigated by Usui et al.[16,23] Conversely, physiological VHFOs > 1,000Hz were also identified in neocortical regions around primary sensory areas following median nerve stimulation.[24,25] But both pathological and physiological VHFOs were recorded from neocortex using standard subdural electrodes.[16,23–25] Thus, distinct physical properties of subdural and depth electrodes (which were used in our study) might be responsible for the different results found in our study and others.[16,23] An alternative explanation could be bias resulting from a relatively small sample of investigated subjects with presumable nontemporal lobe epilepsies and hypothetical missing SEEG data from the epileptogenic zone in these

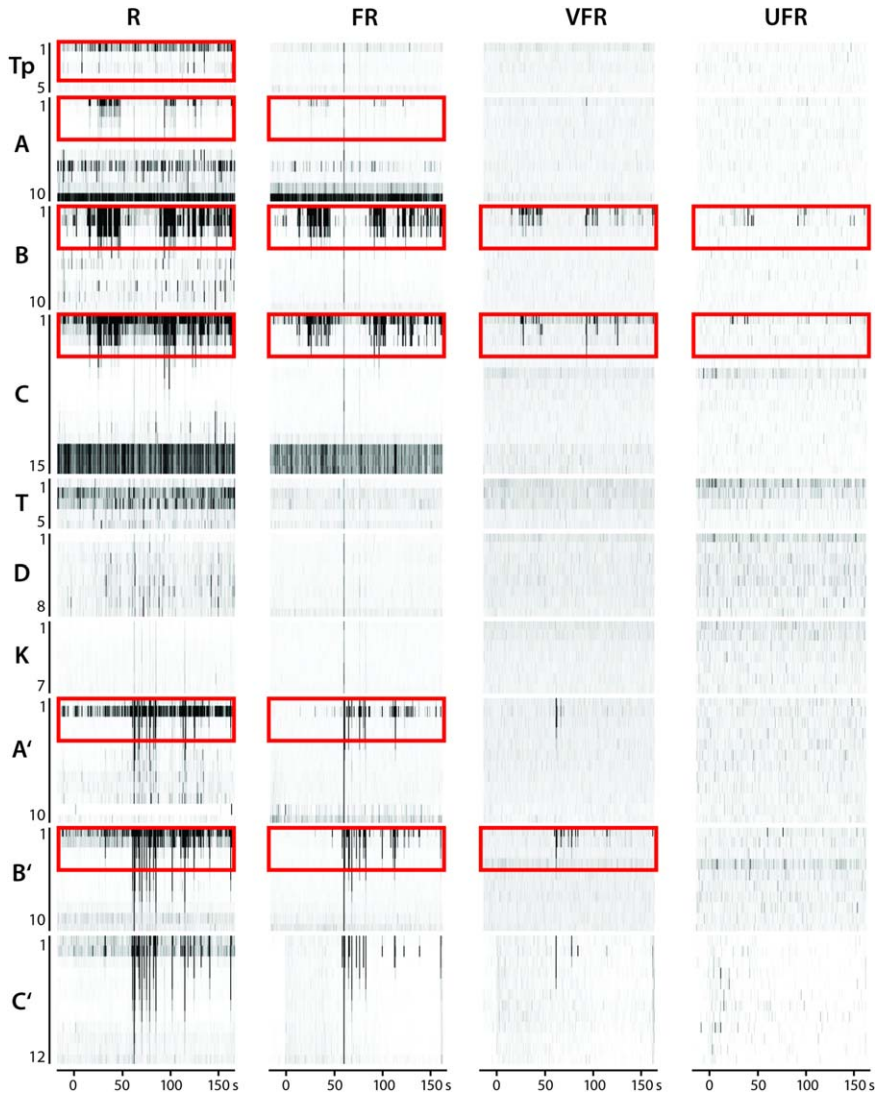


**FIGURE 6: Example of ripple (R), fast ripple (FR), very fast ripple (VFR), and ultrafast ripple (UFR) distribution across all recording contacts in Patient 40 with demonstration of localizing nature of interictal VFR (analysis of 3-minute time window in 20-minute recording is presented). The y-axis of each subplot contains the electrode name and the ordered array of contacts (eg, electrode Tp and contacts 1–5). Each contact is represented by a raster (each hash mark is a detected event), and density of events over time can be quantified to determine average rates. Boxes identify electrodes with R, FR, VFR, and UFR occurrence. In the UFR band, events were identified in B1–2 and C1 contacts only. In the VFR band, events in channels B1–2 dominate, but events were also detected in C1–3 and B′1–2. Events were distributed over 5 electrodes in the FR band and over 7 electrodes in the R band. [Color figure can be viewed at www.annalsofneurology.org]**

patients. Finally, it could be that interictal UFRs recorded from neocortical structures by Usui et al were of significantly higher frequencies (≥2,000Hz), for which our down sampling might be a limiting factor.[23] This issue requires further investigation.

The spectral content of LFP activity reflects both oscillatory activity and high spectral components arising from sharply contoured transients.[26] Here, we have focused our attention on true oscillatory activity present in the raw data. The cellular mechanisms underlying true high-frequency LFP oscillations > ~250Hz have received a great deal of recent interest because the frequency is above what can be generated by synaptic currents, and even above the firing rate of pyramidal neurons (for recent reviews, see Jefferys et al[27] and Menendez de la Prida et al[28]). In vitro slice and in vivo recordings from rodents, as well as simulation studies, support that LFP oscillations > ~300Hz are likely to be an emergent rhythm generated by the in-phase and out-of-phase action potential firing of populations of neuronal clusters, or assemblies. The contribution of synaptic activity to HFOs is limited to approximately 80 to 150Hz.[27] Pathologically interconnected neurons producing hypersynchronous bursts were originally proposed as the origin of FR oscillations,[29] and a population of such clusters could underlie generation of activity > ~500Hz.

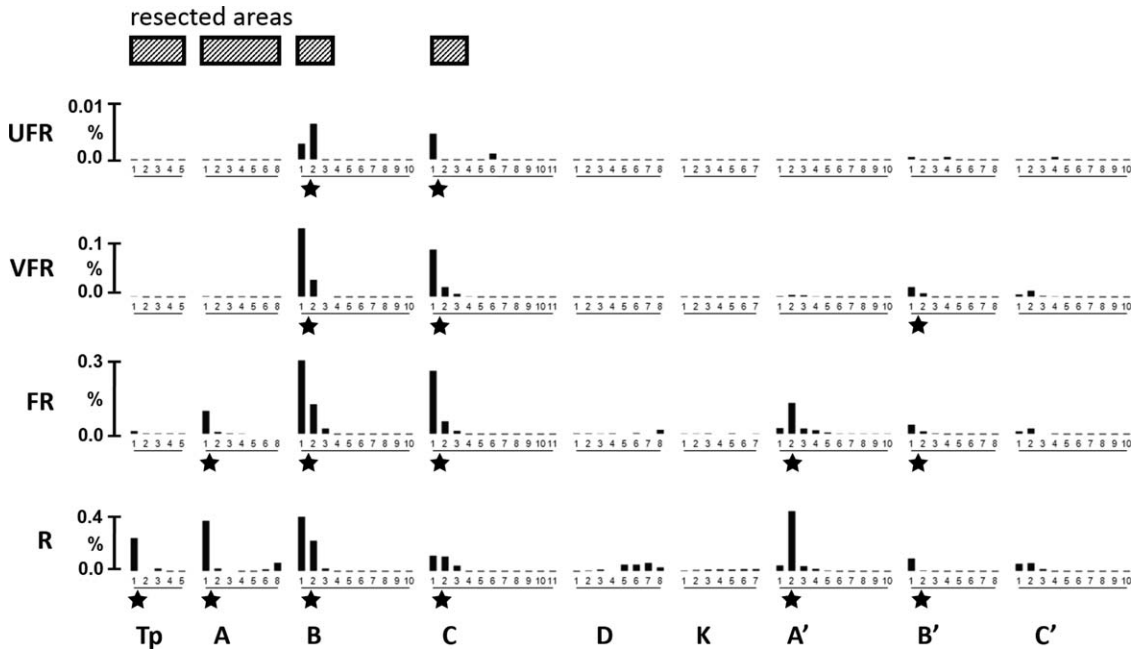


**FIGURE 7: Duration of band power increase for each electrode contact of Patient 40. Subplots of normalized duration of band power increase (y-axis) for each electrode array (x-axis) are shown. Each vertical bar represents the length of signal power envelopes exceeding threshold limit. The amplitude of individual bars is in percentage of total 30-minute record duration. Stars identify regions marked in Figure 5: selected areas with ripples (Rs), fast ripples (FRs), very fast ripples (VFRs), and ultrafast ripples (UFRs). Black rectangles at the top define the resected areas.**

High sampling rate, high dynamic range, and clean electromagnetic environment are crucial for reliable identification of very fast and ultrafast oscillations with period around or $< 1$ millisecond and amplitude declining to 1 μV. High recording quality allows for VHFOs to be seen in raw data with clear oscillatory morphology (see Fig 3). Another important aspect of VHFO studies is an availability of solid, efficient, and practical tools for data analyses. The reason Usui and collaborators did not review VHFOs in their interictal data was "that visual inspection is very time-consuming and labor intensive."[16] In addition, the use of full automatic detection is still under development and challenging. In our study, all data processing was based on interactive graphical analysis (SignalPlant) and on batch processing of partial results (MATLAB). The PDM presentation was very important to assess distorted time areas (vertical clouds) and noisy contacts, and to pick up contacts with probable activity. Exact elimination of artifacts and noisy contacts was based also on simultaneous visual review of PE and raw EEG signals.

The resulting parameters of our analysis do not clearly define the number of events as spikes, Rs, or

**TABLE 2. Correlation between Different Types of Oscillations and Surgical Outcomes**

| Outcome | SOZ | R | FR | VFR | UFR |
|---|---|---|---|---|---|
| RatioChanns(ev) | | | | | |
| Good | 0.54 ± 0.56 | 0.19 ± 0.62 | 0.44 ± 0.54 | 0.70 ± 0.38 | 0.90 ± 0.25 |
| Poor | −0.41 ± 0.55 | −0.63 ± 0.13 | −0.63 ± 0.34 | −0.36 ± 0.67 | −0.44 ± 0.51 |
| *p* | 0.047 | 0.057 | 0.015 | 0.011 | 0.0004 |
| PercentageChanns(ev) | | | | | |
| Good | 77 ± 28 | 60 ± 31 | 72 ± 27 | 84 ± 19 | 95 ± 13 |
| Poor | 29 ± 27 | 18 ± 17 | 19 ± 34 | 32 ± 67 | 28 ± 51 |
| *p* | 0.047 | 0.057 | 0.015 | 0.011 | 0.0004 |

FR = fast ripple; R = ripple; SOZ = seizure onset zone; UFR = ultrafast ripple; VFR = very fast ripple.

UFRs; thus, we do not need the exact definition of events. The presented results define the amplitude properties of single contacts (percentile), occurrence of amplitude level normalized over electrode, and statistical properties in single contacts. The final decision about the activity, however, should be based on visual inspection of defined contact and frequency band. An interactive graphical tool, abovementioned parameters, and batch processing of partial results significantly decreased the time needed for analysis. The introduced methodology represents a reasonable compromise between automatic processing and visual detection.

The findings presented here on different types of HFOs (R, FR, VFR, UFR) and surgical outcomes suggest that a broader spectrum of HFOs be considered as a biomarker of epileptic brain. As expected in mesiotemporal regions, for Rs we did not find significant differences in rate of removed versus nonremoved contacts and postoperative seizure outcome. This finding is consistent with the hypothesis that there is a mixture of pathological and physiological oscillations in the R range. In contrast, significantly better outcomes were observed in patients with bigger percentages of removed contacts containing FRs, VFRs, and UFRs. The percentage was highest for UFRs (95%). These findings suggest a specific pathological character of interictal VHFOs recorded from mesiotemporal structures. Also noteworthy is the observation that UFRs are more spatially restricted in the brain than lower-frequency HFOs. The evidence of spatially highly restricted occurrence of UFRs might explain why some patients probably can exhibit no VHFOs and still can be successfully operated. In this study, we thoroughly investigated a single patient with evident mesial temporal lobe epilepsy and hippocampal sclerosis, in whom no VHFOs were revealed in the depth electrode inserted into the epileptic hippocampus, and still she is seizure free 3.5 years postoperatively. It seems likely that hippocampal tissue investigated here by means of depth electrode was slightly apart from the region producing VHFOs. This finding is, however, very exceptional; negative findings of VHFOs were typically linked to poor postoperative outcomes in both temporal and nontemporal lobe epilepsies.

To conclude, interictal VHFOs (between 500Hz and 2kHz) exist and are frequent in epileptic patients. VFRs and UFRs are abnormal phenomena and seem to be more specific biomarkers for epileptogenic zone when compared to Rs or FRs. For identification of VHFOs, however, high-quality, high-resolution, and low-noise recordings are critical. Another challenge is availability of an efficient and practical tool for analyses of these events. Such a tool (the plugin AmpToColor) was developed and demonstrated in the present study and is now available free as an integral part of SignalPlant software (https://signalplant.codeplex.com/).

## Acknowledgment

The results of this research have been acquired within the CEITEC 2020 (LQ1601) project, with a financial contribution from the Ministry of Education, Youth, and Sports of the Czech Republic (MEYS CR) within special support paid from National Program for Sustainability II funds. Supported by the MEYS CR (LO1212; LH15047, KONTAKT II and CZ.1.05/2.1.00/01.0017), CAS (RVO:68081731), MEYS CR National Program of Sustainability II (LQ1605), and Medical Faculty of Masaryk University (M.P.).

## Author Contributions

M.B., P.J., J.H., M.P., and G.A.W. contributed to study concept and design. M.P., R.R., P.D., P.J., P.K., J.Ci., F.P., E.B., J.Ch., and I.R. contributed to data acquisition and analysis. M.B., M.P., P.J., F.P., and G.A.W. contributed to drafting the manuscript and preparing figures.

## Potential Conflicts of Interest

Nothing to report.

## References

1. Bragin A, Engel J Jr, Wilson CL, et al. Hippocampal and entorhinal cortex high-frequency oscillations (100–500 Hz) in human epileptic brain and in kainic acid–treated rats with chronic seizures. Epilepsia 1999;40:127–137.
2. Bragin A, Mody I, Wilson CL, Engel J Jr. Local generation of fast ripples in epileptic brain. J Neurosci 2002;22:2012–2021.
3. Staba RJ, Wilson CL, Bragin A, et al. Quantitative analysis of high-frequency oscillations (80-500 Hz) recorded in human epileptic hippocampus and entorhinal cortex. J Neurophysiol 2002;88:1743–1752.
4. Zijlmans M, Jiruska P, Zelmann R, et al. High-frequency oscillations as a new biomarker in epilepsy. Ann Neurol 2012;71:169–178.
5. Worrell GA, Gardner AB, Stead SM, et al. High-frequency oscillations in human temporal lobe: simultaneous microwire and clinical macroelectrode recordings. Brain 2008;131:928–937.
6. Jacobs J, Zijlmans M, Zelmann R, et al. High-frequency electroencephalographic oscillations correlate with outcome of epilepsy surgery. Ann Neurol 2010;67:209–220.
7. Wu JY, Sankar R, Lerner JT, et al. Removing interictal fast ripples on electrocorticography linked with seizure freedom in children. Neurology 2010;75:1686–1694.
8. Akiyama T, McCoy B, Go CY, et al. Focal resection of fast ripples on extraoperative intracranial EEG improves seizure outcome in pediatric epilepsy. Epilepsia 2011;52:1802–1811.
9. Höller Y, Kutil R, Klaffenböck L, et al. High-frequency oscillations in epilepsy and surgical outcome. A meta-analysis. Front Hum Neurosci 2015;9:574.
10. Jacobs J, LeVan P, Chander R, et al. Interictal high-frequency oscillations (80–500 Hz) are an indicator of seizure onset areas independent of spikes in the human epileptic brain. Epilepsia 2008;49:1893–1907.

11. Buzsáki G, Silva FL. High frequency oscillations in the intact brain. Prog Neurobiol 2012;98:241–249.
12. Kucewicz MT, Cimbalnik J, Matsumoto JY, et al. High frequency oscillations are associated with cognitive processing in human recognition memory. Brain 2014;137:2231–2244.
13. Brázdil M, Cimbálník J, Roman R, et al. Impact of cognitive stimulation on ripples within human epileptic and non-epileptic hippocampus. BMC Neurosci 2015;16:47.
14. Engel J, Bragin A, Staba R, Mody I. High-frequency oscillations: what is normal and what is not? Epilepsia 2009;50:598–604.
15. Cimbálník J, Kucewicz MT, Worrell GA. Interictal high-frequency oscillations in focal human epilepsy. Curr Opinion Neurol 2016;29: 175–181.
16. Usui N, Terada K, Baba K, et al. Significance of very-high-frequency oscillations (over 1,000Hz) in epilepsy. Ann Neurol 2015;78:295–302.
17. Commission on Classification and Terminology of the International League against Epilepsy. Proposal for revised classification of epilepsies and epileptic syndromes. Epilepsia 1989;30:389–399.
18. Talairach J. Atlas d'anatomie stéréotaxique du télencéphale; études anatomo-radiologiques. Paris, France: Masson, 1967.
19. Zelmann R, Zijlmans M, Jacobs J, et al. Improving the identification of high frequency oscillations. Clin Neurophysiol 2009;120: 1457–1464.
20. Andrade-Valença L, Mari F, Jacobs J, et al. Interictal high frequency oscillations (HFOs) in patients with focal epilepsy and normal MRI. Clin Neurophysiol 2012;123:100–105.
21. Plesinger F, Jurco J, Halamek J, Jurak P. SignalPlant: an open signal processing software platform. Physiol Meas 2016;37:38–48.
22. Hsu D, Hsu M, Grabenstatter HL, et al. Time-frequency analysis using damped-oscillator pseudo- wavelets: application to electrophysiological recording. J Neurosci Methods 2010;194:179–192.
23. Usui N, Terada K, Baba K, et al. Very high frequency oscillations (over 1000 Hz) in human epilepsy. Clin Neurophysiol 2010;121: 1825–1831.
24. Sakura Y, Terada K, Usui K, et al. Very high-frequency oscillations (over 1000 Hz) of somatosensory-evoked potentials directly recorded from the human brain. J Clin Neurophysiol 2009;26: 414–421.
25. Cao D, Terada K, Baba K, et al. Characteristics of very high frequency oscillations of somatosensory evoked potentials in humans with epilepsy. Neurol Asia 2014;19:137–148.
26. Bénar CG, Chauvière L, Bartolomei F, Wendling F. Pitfalls of high-pass filtering for detecting epileptic oscillations: a technical note on "false" ripples. Clin Neurophysiol 2010;121:301–310.
27. Jefferys JG, Menendez de la Prida L, Wendling F, et al. Mechanisms of physiological and epileptic HFO generation. Prog Neurobiol 2012;98:250–264.
28. Menendez de la Prida L, Staba RJ, Dian JA. Conundrums of high-frequency oscillations (80-800 Hz) in the epileptic brain. J Clin Neurophysiol 2015;32:207–219.
29. Bragin A, Staba R, Engel J Jr: The significance of interictal fast ripples in the evaluation of the epileptogenic zone. In: Lüders HO, ed. Textbook of epilepsy surgery. London, UK: Informa Healthcare, 2008:530–536.

# CHAPTER 10

# Conclusion and Future Directions

This habilitation thesis is focused on providing a comprehensive overview of the current state of research on brain high-frequency oscillations in epilepsy and the cognitive sciences and presents our published work on this topic.

High-frequency oscillations (HFOs; 80-600Hz) can be observed in limbic structures and all over the neocortex. Network oscillations are considered instrumental in the synchronization of the activity of anatomically distributed neuron populations (Buzsáki & Chrobak, 1995). HFOs are dependent on both inhibitory and excitatory control, and they can thus be driven by a loss of one or gain of the other (Naggar et al., 2020). HFOs represent a heterogeneous group of both physiologic and pathologic phenomena, including a number of different oscillations that can be classified by many criteria, most often frequency.

Very simplified, pathologic HFOs tend to be of higher frequency than physiologic HFOs (Alkawadri et al., 2014; Brázdil et al., 2017) and are thought to be a feature of the seizure onset zone/epileptogenic zone in patients with epilepsy (Bragin et al., 1999a,b). According to the modern concept, it has been demonstrated that epileptic focus is organized into small neuronal clusters of pathologically interconnected epileptic neurons. Several structural, molecular, and functional changes have been found within epileptic neuronal networks (Jiruska & Bragin, 2011). These small neuronal clusters can generate local activities as pHFOs and microseizures, when the synchrony of discharges between clusters reaches a certain level, but also some global patterns – interictal discharges and seizures (Stead et al., 2010; Jiruska & Bragin, 2011).

The study of HFOs contributed to understanding many aspects of physiological cognitive processes, and especially the pathophysiology of epilepsy and seizures. However, cellular (the complex role of pyramidal cells and especially interneurons) and network mechanisms of these oscillations that could lead to an understanding of the functional network organization, primarily of epileptogenic tissue and the mechanism of epileptic seizures are still not fully explained (Jiruska et al., 2017). It is also important to note that most experimental models describe the genesis of pathological HFOs within mesial temporal lobe epilepsy. Only a few papers deal with HFOs genesis in neocortical epilepsy (Grenier et al., 2003; Timofeev et al., 2002; Schevon et al., 2009). Importantly, results obtained in temporal epilepsy models cannot be automatically transferred to the pathophysiology of neocortical epilepsy. Therefore, further description of spacio-temporal properties of HFOs will provide a much-needed comprehensive insight into the functional organization and dynamics of neuronal populations that play a crucial role in both physiological and pathophysiological processes (Jiruska et al., 2013). When understanding the mentioned aspects of pHFOs, HFOs will offer a unique opportunity to use them as a clinical marker of epileptogenesis (Jiruska et al., 2017). Despite, fast ripples (>250 Hz) are already

now a promising biomarker for the epileptogenic zone, responsible for seizure generation (Frauscher et al., 2017). All our mentioned published studies are in the line with this statement.

Automatic detectors help to minimize the time required for HFO detection and to reduce the human inter-raters bias. A high signal-to-noise ratio and sufficient data sampling are critical when attempting to detect HFOs. We proved that standard automated detection of HFOs, in comparison with visual analysis of HFO, achieves comparable results and enables the evaluation of HFO characteristics (Pail et al., 2013). Nonetheless, the development and implementation of a framework for standardized HFO detection need to be pursued in order to reduce biases and make the analysis of HFOs useful in clinical routine (Zelmann et al., 2012; Worrell et al., 2012; Zijlmans et al., 2017; Cimbalnik et al., 2019). Preprocessing the data with particular emphasis on reducing artifacts or training algorithms to acknowledge artificial HFOs might prove helpful to increase the specificity of detection algorithms (Thomschewski et al., 2020).

For patients with drug-resistant focal epilepsy, there is an increasing body of evidence pointing toward the use of HFOs (especially fast ripples) for delineating the epileptogenic zone with a potential to improve surgical success even without the need to record seizures (Frauscher et al., 2017; Thomschewski et al., 2019). Also, in our epileptic center, in individual patients, we try to use matrices with the rates of HFOs in different frequency bands in individual electrode contacts as part of preoperative diagnostics (Fig.12).

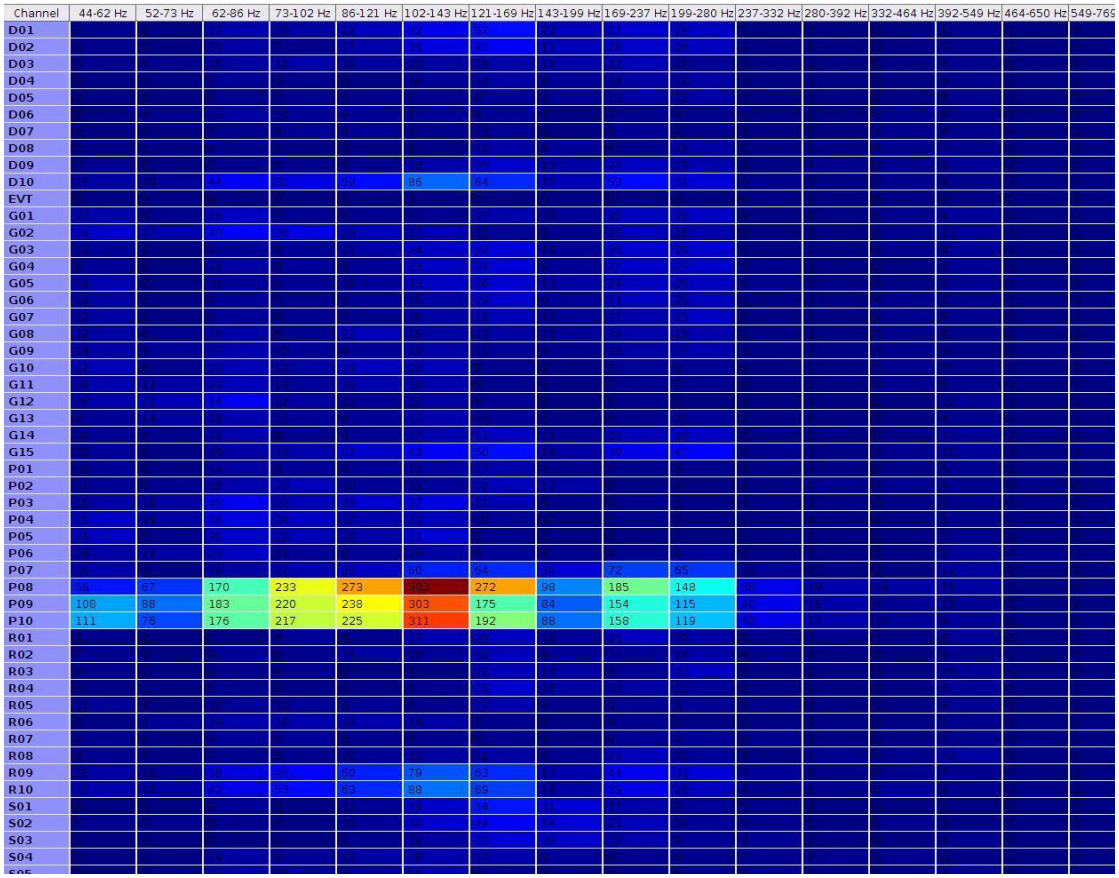


*Figure 12: The matrices with the rates of HFOs in different frequency bands in individual electrode contacts.*

Furthermore, as we showed in our recent study based on HFO rates, it is possible to distinguish between unilateral and bilateral mesial temporal lobe epilepsy (Řehulka et al., 2019). Although there is currently an attempt to extend the clinical use of high-frequency oscillations, there are a number of limitations that prevent their more extensive use. The majority of clinical studies that focused on the use of HFOs in the localization of the epileptogenic zone were retrospective studies, the results of which were often presented in the form of group analysis. It has been repeatedly shown that areas with a high incidence of HFOs should be included in resection to eliminate the seizures. However, the definition of high rates of HFOs is very general, and mean values or median incidence cannot be used prospectively. In addition, a multicentre prospective study has not yet been conducted to validate the used detectors and determine the clinical utility of HFO biomarkers. This step is needed for the translation of HFO electrophysiological biomarkers to clinical practice (Cimbalnik et al., 2016). Therefore, it is indicated that conclusions of findings, especially concerning surgical decision-making, need to be taken with caution. Regarding HFOs, each patient should be assessed individually.

Transient high-frequency oscillations in local field potentials generated by especially human hippocampal but also extrahippocampal areas have been related in nature to both physiological and pathological processes. The existence of physiologic HFOs in multiple brain areas is another obstacle that needs to be tackled. Based on the presented results, there are no unambiguous characteristics of HFOs (clear cut off values) that would distinguish pathological and physiological HFOs in both ripples and fast ripples (Pail et al., 2017, 2020). Nevertheless, based on our studies, it seems pHFOs have higher rate frequencies, amplitude and lower spectral entropy in epileptogenic zone (Pail et al., 2017, 2020). Individual studies show no significant difference in individual characteristics; and in addition to that, some studies contradict each other in the results. Thus, there are currently no established criteria for distinguishing physiological HFOs from pathological ones (Engel et al., 2009; Le Van Quyen et al., 2006). However, a suitable approach was shown: multiple invasive EEG and connectivity features in presurgical evaluation using machine learning tools could improve epileptogenic tissue localization, which is superior to using a single feature (Cimbalnik et al., 2019, 2020). We have also to mention results presented in our recent studies: the differences between epileptic and non-epileptic hippocampus during cognitive processing bring new insight in delineation between pathological and physiological processes, particularly the suppression of pathological HFOs in the epileptic hippocampus during a cognitive task (Cimbalnik et al., 2020; Pail et al., 2020).

Until recently, it has not been possible to differentiate physiological from pathological HFOs. Moreover, baseline rates of HFO occurrence vary substantially across brain regions. Nevertheless, recently presented multicenter atlas provided region-specific normative values for physiological HFO rates and HFA in common stereotactic space. According to this atlas, ripples are frequent in eloquent cortex areas and rare outside these regions. In contrast, physiological fast ripples are very rare, even in eloquent cortical areas, making fast ripples a good candidate for defining the epileptogenic zone, when present (Frauscher et al., 2018). Knowing the physiological rates of HFOs in every brain region allows the definition of rates that are too high to be physiological and should, therefore, statistically be pathological (Frauscher et al., 2018). However, the data were obtained from a small set

of subjects under particular conditions. We still have to count on the possible bias of the data obtained from patients with brain disease. An extended atlas describing normal invasive EEG in different behavioral states would significantly broaden our knowledge of the brain and could serve as a reference for identifying abnormal activity.

An essential contribution in this field was the discovery of very high-frequency oscillations. The phenomena of very high-frequency oscillations are more spatially restricted and seem to be more specific biomarkers for epileptogenic zone when compared to traditional interictal HFOs (Brazdil et al., 2017).

It is likely that considering the results of several studies, differences between them might also be caused by the datasets and subsequent feature selection. This implies that there may be a dependence on the electrodes, reference signals, and acquisition system used. Studies with different datasets are needed to elucidate the impact of these variables on pathologic tissue localization. Future studies with larger datasets should explore their impact on pathological tissue localization in more detail (Cimbalnik et al., 2019). Most clinical invasive EEG studies are restricted to a limited amount of data, mainly due to technical difficulties. The brain's electrophysiological activity is not consistent across time and is affected by different states of vigilance, circadian rhythms, and cognitive processes (Staba et al., 2002; Frauscher et al., 2017; Gliske et al., 2018; Pail et al., 2020). In the future, more multicentric studies using automatic approaches are needed to analyze significantly longer recordings of EEG signal to provide a clearer idea of HFO phenomena and their behavior in physiological and pathological areas of the brain. Moreover, combining multiple features and using machine learning tools might provide a more robust estimation of the epileptogenic zone. The iEEG data in our studies were processed by automated algorithms that were already used in other published studies. The Python codes of these algorithms are part of the ElectroPhYsiology Computation Module (EPYCOM) and can be found online at https://gitlab.com/icrc-bme/epycom.

Research on HFOs represents an important direction in the research of current and future epileptology and has opened the door to improving the diagnosis and treatment of epilepsy. However, there is still a need to continue seeking answers to several questions, as the failure of answering them does not allow the full use of HFOs as a clinical biomarker. Our goal is to continue in participating actively in this research. We would like to contribute significantly to the understanding of epilepsy, HFOs, and especially VHFOs origin, generating and spreading epileptic activity and, therefore, improve the treatment and the quality of life of epileptic patients.

# REFERENCES


Alkawadri R, Gaspard N, Goncharova II, Spencer DD, Gerrard JL, Zaveri H, Duckrow RB, Blumenfeld H, Hirsch LJ. The spatial and signal characteristics of physiologic high frequency oscillations. Epilepsia. 2014; 55(12):1986-95.

Alvarado-Rojas C, Huberfeld G, Baulac M, Clemenceau S, Charpier S, Miles R, de la Prida LM, Le Van Quyen M. Different mechanisms of ripple-like oscillations in the human epileptic subiculum. Ann Neurol. 2015; 77(2):281-90.

Anastassiou CA, Montgomery SM, Barahona M, Buzsáki G, Koch C. The Effect of Spatially Inhomogeneous Extracellular Electric Fields on Neurons. The Journal of Neuroscience. 2010; 30:1925–1936.

Andrade-Valenca LP, Dubeau F, Mari F, Zelmann R, Gotman J. Interictal scalp fast oscillations as a marker of the seizure onset zone. Neurology. 2011; 77(6):524-31.

Ayala M, Cabrerizo M, Jayakar P, Adjouadi M. Subdural EEG classification into seizure and nonseizure files using neural networks in the gamma frequency band. J Clin Neurophysiol. 2011; 28:20-9.

Axmacher N, Elger CE, Fell J. Ripples in the medial temporal lobe are relevant for human memory consolidation. Brain. 2008; 131(Pt 7):1806-17.

Bagshaw AP, Jacobs J, LeVan P, Dubeau F, Gotman J. Effect of sleep stage on interictal high-frequency oscillations recorded from depth macroelectrodes in patients with focal epilespy. Epilepsia. 2009; 50:617–28.

Bénar CG, Chauvière L, Bartolomei F, Wendling F. Pitfalls of high-pass filtering for detecting epileptic oscillations: a technical note on "false" ripples. Clin Neurophysiol. 2010; 121(3):301-10.

Berger H. Über das Elektroenzephalogramm des Menschen: 1. Mitteilung. Arch. Psychiatr. Nervenkr., 87 (1929), pp. 527-528.

Bernard C, Anderson A, Becker A, Poolos NP, Beck H, Johnston D. Acquired dendritic channelopathy in temporal lobe epilepsy. Science. 2004; 305(5683):532-5.

Bernasconi N, Bernasconi A, Caramanos Z, Antel SB, Andermann F, Arnold DL. Mesial temporal damage in temporal lobe epilepsy: a volumetric MRI study of the hippocampus, amygdala and parahippocampal region. Brain. 2003; 126(Pt 2):462-9.

Blanco JA, Stead M, Krieger A, Stacey W, Maus D, Marsh E, Viventi J, Lee KH, Marsh R, Litt B, Worrell GA. Data mining neocortical high-frequency oscillations in epilepsy and controls. Brain. 2011; 134(Pt 10):2948-59.

Bragin A, Engel J Jr, Wilson CL, Fried I, Mathern GW. Hippocampal and entorhinal cortex high-frequency oscillations (100–500 Hz) in human epileptic brain and in kainic acid-treated rats with chronic seizures. Epilepsia. 1999a; 40:127–37.

Bragin A, Engel J Jr, Wilson CL, Fried I, Buzsáki G. High-frequency oscillations in human brain. Hippocampus. 1999b; 9:137–42.

Bragin A, Wilson CL, Engel J Jr. Chronic epileptogenesis requires development of a network of pathologically interconnected neuron clusters: a hypothesis. Epilepsia. 2000; 41 Suppl 6:S144-52.

Bragin A, Mody I, Wilson CL, Engel J Jr. Local generation of fast ripples in epileptic brain. J Neurosci. 2002a; 22(5):2012-21.

Bragin A, Wilson CL, Staba RJ, Reddick M, Fried I, Engel J Jr. Interictal high-frequency oscillations (80-500 Hz) in the human epileptic brain: entorhinal cortex. Ann Neurol. 2002b; 52(4):407-15.

Bragin A, Wilson CL, Engel J. Spatial stability over time of brain areas generating fast ripples in the epileptic rat. Epilepsia. 2003; 44:1233-7.

Bragin A, Wilson CL, Almajano J, Mody I, Engel J Jr. High-frequency oscillations after status epilepticus: epileptogenesis and seizure genesis. Epilepsia. 2004; 45(9):1017-23.

Bragin A, Wilson CL, Engel J Jr. Voltage depth profiles of high-frequency oscillations after kainic acid-induced status epilepticus. Epilepsia. 2007;48 Suppl 5:35-40.

Bragin A, Benassi SK, Kheiri F, Engel J Jr. Further evidence that pathologic high-frequency oscillations are bursts of population spikes derived from recordings of identified cells in dentate gyrus. Epilepsia. 2011; 52(1):45-52.

Brázdil, M. et al. Hippocampal visual P3 potential in lateralization of primary epileptogenic focus and in assessment of hippocampal memory function in temporal lobe epilepsy. Epilepsia. 1999; 40, Suppl.2: 261.

Brázdil M, Halámek J, Jurák P, Daniel P, Kuba R, Chrastina J, et al. Interictal high-frequency oscillations indicate seizure onset zone in patients with focal cortical dysplasia. Epilepsy Res. 2010; 90:28–32.

Brázdil M, Cimbálník J, Roman R, Shaw DJ, Stead MM, Daniel P, Jurák P, Halámek J. Impact of cognitive stimulation on ripples within human epileptic and non-epileptic hippocampus. BMC Neurosci. 2015; 16:47.

Brázdil M, Pail M, Halámek J, Plešinger F, Cimbálník J, Roman R, Klimeš P, Daniel P, Chrastina J, Brichtová E, Rektor I, Worrell GA, Jurák P. Very high-frequency oscillations: Novel biomarkers of the epileptogenic zone. Ann Neurol. 2017; 82:299-310.

Bruder JC, Dümpelmann M, Piza DL, Mader M, Schulze-Bonhage A, Jacobs-Le Van J. Physiological Ripples Associated with Sleep Spindles Differ in Waveform Morphology from Epileptic Ripples. Int J Neural Syst. 2017; 27(7):1750011.

Burke JF, Ramayya AG, Kahana MJ. Human intracranial high-frequency activity during memory processing: neural oscillations or stochastic volatility? Curr Opin Neurobiol. 2015; 31: 104-110.

Burnos S, Frauscher B, Zelmann R, Haegelen C, Sarnthein J, Gotman J. The morphology of high frequency oscillations (HFO) does not improve delineating the epileptogenic zone. Clin Neurophysiol. 2016; 127(4): 2140-8.

Buzsáki G, Leung LW, Vanderwolf CH. Cellular bases of hippocampal EEG in the behaving rat. Brain Res. 1983; 287(2):139-71

Buzsáki G, Horváth Z, Urioste R, Hetke J, Wise K. High frequency network oscillation in the hippocampus. Science 1992; 256(5059):1025–7.

Buzsáki G, Chrobak JJ. Temporal structure in spatially organized neuronal ensembles: a role for interneuronal networks. Curr Opin Neurobiol. 1995; 5(4):504-10.

Buzsaki G, Traub RD, Pedley TA. The cellular basis of EEG activity. In: Ebersole JS, Pedley TA, editors. Current Practice of Clinical Electroencephalography. Lippincott Williams & Wilkins; Philadelphia: 2003.

Buzsaki G. Large-scale recording of neuronal ensembles. Nat Neurosci. 2004; 7:446–451.

Buzsáki G, Wang XJ. Mechanisms of gamma oscillations. Annu Rev Neurosci. 2012; 35:203-25.

Buzsáki G, Silva FL. High frequency oscillations in the intact brain. Prog Neurobiol. 2012 ;98(3):241-9.

Buzsáki G. Hippocampal sharp wave-ripple: A cognitive biomarker for episodic memory and planning. Hippocampus. 2015; 25(10):1073-188.

Canolty RT, Knight RT. The functional role of cross-frequency coupling. Trends Cogn Sci. 2010; 14:506–515.

Carr MF, Jadhav SP, Frank LM. Hippocampal replay in the awake state: a potential substrate for memory consolidation and retrieval. Nat Neurosci. 2011; 14(2):147-53.

Châtillon CÉ, Zelmann R, Bortel A, Avoli M, Gotman J. Contact size does not affect high frequency oscillation detection in intracerebral EEG recordings in a rat epilepsy model. Clin Neurophysiol. 2011; 122(9):1701-5.

Chrobak JJ, Buzsáki G. High-frequency oscillations in the output networks of the hippocampal-entorhinal axis of the freely behaving rat. J Neurosci. 1996; 16(9):3056-66.

Cimbalnik J, Kucewicz MT, Worrell G. Interictal high-frequency oscillations in focal human epilepsy. Curr Opin Neurol. 2016; 29(2):175-81.

Cimbálník J, Hewitt A, Worrell G, Stead M. The CS algorithm: A novel method for high frequency oscillation detection in EEG. J Neurosci Methods. 2018; 293:6-16.

Cimbalnik J, Klimes P, Sladky V, Nejedly P, Jurak P, Pail M, Roman R, Daniel P, Guragain H, Brinkmann B, Brazdil M, Worrell G. Multi-feature localization of epileptic foci from interictal, intracranial EEG. Clin Neurophysiol. 2019; 130(10):1945-1953.

Cimbalnik J, Pail M, Klimes P, Travnicek V, Roman R, Vajcner A, Brazdil M. Cognitive processing impacts high frequency intracranial EEG activity of human hippocampus in patients with pharmacoresistant focal epilepsy. Front. Neurol. 2020; 11:578571.

Cohen I, Navarro V, Clemenceau S, Baulac M, Miles R. On the origin of interictal activity in human temporal lobe epilepsy in vitro. Science. 2002; 298(5597):1418-21.

Crépon B, Navarro V, Hasboun D, Clemenceau S, Martinerie J, Baulac M, et al. Mapping interictal oscillations greater than 200 Hz recorded with intracranial macroelectrodes in human epilepsy. Brain. 2010; 133:33–45.

Csicsvari J, Hirase H, Mamiya A, Buzsáki G. Ensemble patterns of hippocampal CA3-CA1 neurons during sharp wave associated population events. Neuron. 2000; 28:585–594.

Curio G, Mackert BM, Burghoff M, Koetitz R, Abraham-Fuchs K, Härer W. Localization of evoked neuromagnetic 600 Hz activity in the cerebral somatosensory system. Electroencephalogr Clin Neurophysiol. 1994; 91(6):483-7.

Demont-Guignard S, Benquet P, Gerber U, Biraben A, Martin B, Wendling F. Distinct hyperexcitability mechanisms underlie fast ripples and epileptic spikes. Ann Neurol. 2012; 71(3):342-52.

Draguhn A, Traub RD, Schmitz D, Jefferys JGR. Electrical coupling underlies high-frequency oscillations in the hippocampus in vitro. Nature. 1998; 394: 189–192.

Dzhala VI, Staley KJ. Mechanisms of fast ripples in the hippocampus. J Neurosci. 2004; 24(40):8896-906.

Engel J Jr, Bragin A, Staba R, Mody I. High-frequency oscillations: what is normal and what is not? Epilepsia. 2009; 50:598–604.

Ferrari-Marinho T, Perucca P, Mok K, Olivier A, Hall J, Dubeau F, Gotman J. Pathologic substrates of focal epilepsy influence the generation of high-frequency oscillations. Epilepsia. 2015; 56(4):592-8.

Fink CG, Gliske S, Catoni N, Stacey WC. Network Mechanisms Generating Abnormal and Normal Hippocampal High-Frequency Oscillations: A Computational Analysis. eNeuro. 2015; 2(3).

Fisher RS, Webber WR, Lesser RP, Arroyo S, Uematsu S. High-frequency EEG activity at the start of seizures. J Clin Neurophysiol. 1992; 9(3):441-8.

Foffani G, Uzcategui YG, Gal B, Menendez de la Prida L. Reduced spike-timing reliability correlates with the emergence of fast ripples in the rat epileptic hippocampus. Neuron. 2007; 55(6):930-41.

Frauscher B, Bartolomei F, Kobayashi K, Cimbalnik J, van 't Klooster MA, Rampp S, Otsubo H, Höller Y, Wu JY, Asano E, Engel J Jr, Kahane P, Jacobs J, Gotman J. High-frequency oscillations: The state of clinical research. Epilepsia. 2017; 58(8):1316-1329.

Frauscher B, von Ellenrieder N, Zelmann R, Rogers C, Nguyen DK, Kahane P, Dubeau F, Gotman J. High-Frequency Oscillations in the Normal Human Brain. Ann Neurol. 2018; 84(3):374-385.

Fries P, Nikolić D, Singer W. The gamma cycle. Trends Neurosci. 2007; 30(7):309-16.

Gardner AB, Worrell GA, Marsh E, Dlugos D, Litt B. Human and automated detection of high-frequency oscillations in clinical intracranial EEG recordings. Clin Neurophysiol. 2007; 118:1134-43.

Gibbs J. Letter to the Editor, Fourier's series. Nature. 1899:59200

Girardeau G, Zugaro M. Hippocampal ripples and memory consolidation. Curr Opin Neurobiol. 2011; 21(3):452-9.

Gliske SV, Irwin ZT, Chestek C, Hegeman GL, Brinkmann B, Sagher O, Garton HJL, Worrell GA, Stacey WC. Variability in the location of high frequency oscillations during prolonged intracranial EEG recordings. Nat Commun. 2018; 9(1):2155.

Gray CM. Synchronous oscillations in neuronal systems: mechanisms and functions. J Comput Neurosci. 1994; 1(1-2):11-38.

Grenier F, Timofeev I, Steriade M. Neocortical very fast oscillations (ripples, 80–200 Hz) during seizures: intracellular correlates. J Neurophysiol. 2003; 89:841–852.

Haegelen C, Perucca P, Châtillon CE, Andrade-Valença L, Zelmann R, Jacobs J, Collins DL, Dubeau F, Olivier A, Gotman J. High-frequency oscillations, extent of surgical resection, and surgical outcome in drug-resistant focal epilepsy. Epilepsia. 2013; 54(5):848-57.

Hájos N, Paulsen O. Network mechanisms of gamma oscillations in the CA3 region of the hippocampus. Neural Netw. 2009; 22(8):1113-9

Harris KD, Csicsvari J, Hirase H, Dragoi G, Buzsáki G. Organization of cell assemblies in the hippocampus. Nature. 2003; 424(6948):552-6.

Hirsch LJ, Spencer SS, Williamson PD, Spencer DD, Mattson RH. Comparison of bitemporal and unitemporal epilepsy defined by depth electroencephalography. Ann Neurol. 1991; 30(3):340-6.

Ibarz JM, Foffani G, Cid E, Inostroza M, Menendez de la Prida L. Emergent dynamics of fast ripples in the epileptic hippocampus. J Neurosci. 2010; 30(48):16249-61.

Jacobs J, LeVan P, Chander R, Hall J, Dubeau F, Gotman J. Interictal high-frequency oscillations (80–500 Hz) are an indicator of seizure onset areas independent of spikes in the human epileptic brain. Epilepsia. 2008; 49:1893–907.

Jacobs J, LeVan P, Châtillon C-E, Olivier A, Dubeau F, Gotman J. High frequency oscillations in intracranial EEGs mark epileptogenicity rather than lesion type. Brain. 2009; 132:1022–37.

Jacobs J, Zijlmans M, Zelmann R, Chatillon CE, Hall J, Olivier A, Dubeau F, Gotman J. High-frequency electroencephalographic oscillations correlate with outcome of epilepsy surgery. Ann Neurol. 2010; 67(2):209-20.

Jacobs J, Staba R, Asano E, Otsubo H, Wu JY, Zijlmans M, Mohamed I, Kahane P, Dubeau F, Navarro V, Gotman J. High-frequency oscillations (HFOs) in clinical epilepsy. Prog Neurobiol. 2012; 98(3):302-15.

Jacobs J, Vogt C, LeVan P, Zelmann R, Gotman J, Kobayashi K. The identification of distinct high-frequency oscillations during spikes delineates the seizure onset zone better than high-frequency spectral power changes. Clin Neurophysiol. 2016; 127(1):129-142.

Jacobs J, Wu JY, Perucca P, Zelmann R, Mader M, Dubeau F, Mathern GW, Schulze-Bonhage A, Gotman J. Removing high-frequency oscillations: A prospective multicenter study on seizure outcome. Neurology. 2018 ;91(11):e1040-e1052.

Jefferys JG. Nonsynaptic modulation of neuronal activity in the brain: electric currents and extracellular ions. Physiol Rev. 1995; 75(4):689-723.

Jefferys JG, Menendez de la Prida L, Wendling F, Bragin A, Avoli M, Timofeev I, Lopes da Silva FH. Mechanisms of physiological and epileptic HFO generation. Prog Neurobiol. 2012; 98(3):250-64.

Jirsch JD, Urrestarazu E, LeVan P, Olivier A, Dubeau F, Gotman J. High-frequency oscillations during human focal seizures. Brain. 2006; 129(Pt 6):1593-608.

Jiruska P, Csicsvari J, Powell AD, Fox JE, Chang WC, Vreugdenhil M, Li X, Palus M, Bujan AF, Dearden RW, Jefferys JG. High-frequency network activity, global increase in neuronal activity, and synchrony expansion precede epileptic seizures in vitro. J Neurosci. 2010a; 30(16):5690-701.

Jiruska P, Finnerty GT, Powell AD, Lofti N, Cmejla R, Jefferys JG. Epileptic high-frequency network activity in a model of non-lesional temporal lobe epilepsy. Brain. 2010b; 133(Pt 5):1380-90.

Jiruska P, Bragin A. High-frequency activity in experimental and clinical epileptic foci. Epilepsy Res. 2011; 97(3):300-7.

Jiruska P, de Curtis M, Jefferys JG, Schevon CA, Schiff SJ, Schindler K. Synchronization and desynchronization in epilepsy: controversies and hypotheses. J Physiol. 2013; 591(4):787-97.

Jiruška P. Význam vysokofrekvenčních oscilací v patofyziologii epilepsie a jejich klinické využití. Habilitační práce. 2013, 2.Lékařská fakulta Univerzita Karlova.

Jiruska P, Alvarado-Rojas C, Schevon CA, Staba R, Stacey W, Wendling F, Avoli M. Update on the mechanisms and roles of high-frequency oscillations in seizures and epileptic disorders. Epilepsia. 2017; 58(8):1330-1339.

Johnston D, Brown TH. Giant synaptic potential hypothesis for epileptiform activity. Science. 1981; 211(4479):294-7.

Kajikawa Y, Schroeder CE. How local is the local field potential? Neuron. 2011; 72(5):847-58.

Kerber K, LeVan P, Dümpelmann M, Fauser S, Korinthenberg R, Schulze-Bonhage A, Jacobs J. High frequency oscillations mirror disease activity in patients with focal cortical dysplasia. Epilepsia. 2013; 54(8): 1428-36.

Khazipov R, Holmes GL. Synchronization of kainate-induced epileptic activity via GABAergic inhibition in the superfused rat hippocampus in vivo. J Neurosci. 2003; 23:5337–5341.

Klausberger T, Somogyi P. Neuronal diversity and temporal dynamics: the unity of hippocampal circuit operations. Science. 2008; 321(5885):53-7.

Kobayashi K, Watanabe Y, Inoue T, Oka M, Yoshinaga H, Ohtsuka Y. Scalp-recorded high-frequency oscillations in childhood sleep-induced electrical status epilepticus. Epilepsia. 2010; 51(10):2190-4.

Köhling R, Vreugdenhil M, Bracci E, Jefferys JG. Ictal epileptiform activity is facilitated by hippocampal GABAA receptor-mediated oscillations. J Neurosci. 2000; 20:6820–6829.

Kucewicz MT, Cimbalnik J, Matsumoto JY, Brinkmann BH, Bower MR, Vasoli V, Sulc V, Meyer F, Marsh WR, Stead SM, Worrell GA. High frequency oscillations are associated with cognitive processing in human recognition memory. Brain. 2014; 137(Pt 8):2231-44.

Kucewicz MT, Berry BM, Kremen V, Brinkmann BH, Sperling MR, Jobst BC, Gross RE, Lega B, Sheth S, Stein JM, Das SR, Gorniak R, Stead SM, Rizzuto DS, Kahana MJ, Worrell GA. Dissecting gamma frequency activity during human memory processing. Brain. 2017; 140(5):1337-1350.

Lachaux JP, Axmacher N, Mormann F, Halgren E, Crone NE. High-frequency neural activity and human cognition: past, present and possible future of intracranial EEG research. Prog Neurobiol. 2012;98(3):279-301.

Le Van Quyen M, Khalilov I, Ben-Ari Y. The dark side of high-frequency oscillations in the developing brain. Trends Neurosci. 2006; 29(7):419-427.

Le Van Quyen M, Bragin A. Analysis of dynamic brain oscillations: methodological advances. Trends Neurosci. 2007; 30(7):365-73.

Le Van Quyen M, Muller LE, Telenczuk B, Halgren E, Cash S, Hatsopoulos NG, Dehghani N, Destexhe A. High-frequency oscillations in human and monkey neocortex during the wake-sleep cycle. Proc Natl Acad Sci U S A. 2016; 113(33):9363-8.

Lehmann TN, Gabriel S, Kovacs R, Eilers A, Kivi A, Schulze K, Lanksch WR, Meencke HJ, Heinemann U. Alterations of neuronal connectivity in area CA1 of hippocampal slices from temporal lobe epilepsy patients and from pilocarpine-treated epileptic rats. Epilepsia. 2000; 41 Suppl 6:S190-4.

Liu S, Gurses C, Sha Z, Quach MM, Sencer A, Bebek N, Curry DJ, Prabhu S, Tummala S, Henry TR, Ince NF. Stereotyped high-frequency oscillations discriminate seizure onset zones and critical functional cortex in focal epilepsy. Brain. 2018; 141(3):713-730.

Maier N, Nimmrich V, Draguhn A. Cellular and network mechanisms underlying spontaneous sharp wave-ripple complexes in mouse hippocampal slices. J. Physiol. 2003; 550:873–887.

Malinowska U, Bergey GK, Harezlak J, Jouny CC. Identification of seizure onset zone and preictal state based on characteristics of high frequency oscillations. Clin Neurophysiol. 2015; 126(8):1505-13.

Matsumoto A, Brinkmann BH, Matthew Stead S, Matsumoto J, Kucewicz MT, Marsh WR, Meyer F, Worrell G. Pathological and physiological high-frequency oscillations in focal human epilepsy. J Neurophysiol. 2013; 110(8):1958-64.

Meador KJ, Loring DW, King DW, Gallagher BB, Gould MJ, Flanigin HF, Smith JR. Limbic evoked potentials predict site of epileptic focus. Neurology. 1987; 37(3):494-7.

Melani F, Zelmann R, Mari F, Gotman J. Continuous High Frequency Activity: a peculiar SEEG pattern related to specific brain regions. Clin Neurophysiol. 2013; 124(8):1507-16.

Menendez de la Prida L, Staba RJ, Dian JA. Conundrums of high-frequency oscillations (80-800 Hz) in the epileptic brain. J Clin Neurophysiol. 2015; 32(3):207-19.

Nagasawa T, Juhász C, Rothermel R, Hoechstetter K, Sood S, Asano E. Spontaneous and visually driven high-frequency oscillations in the occipital cortex: intracranial recording in epileptic patients. Hum Brain Mapp. 2012; 33(3):569-83.

Naggar I, Stewart M, Orman R. High Frequency Oscillations in Rat Hippocampal Slices: Origin, Frequency Characteristics, and Spread. Front Neurol. 2020; 11:326.

Najm I, Jehi L, Palmini A, Gonzalez-Martinez J, Paglioli E, Bingaman W. Temporal patterns and mechanisms of epilepsy surgery failure. Epilepsia. 2013; 54(5):772-82.

Nikulin VV, Nolte G, Curio G. A novel method for reliable and fast extraction of neuronal EEG/MEG oscillations on the basis of spatio-spectral decomposition. Neuroimage. 2011; 55:1528-35.

O'Neill J, Pleydell-Bouverie B, Dupret D, Csicsvari J. Play it again: reactivation of waking experience and memory. Trends Neurosci. 2010; 33(5):220-9.

Pail M, Halámek J, Daniel P, Kuba R, Tyrlíková I, Chrastina J, Jurák P, Rektor I, Brázdil M. Intracerebrally recorded high frequency oscillations: simple visual assessment versus automated detection. Clin Neurophysiol. 2013; 124(10):1935-42.

Pail M, Řehulka P, Cimbálník J, Doležalová I, Chrastina J, Brázdil M. Frequency-independent characteristics of high-frequency oscillations in epileptic and non-epileptic regions. Clin Neurophysiol. 2017; 128(1):106-114.

Pail M, Cimbálník J, Roman R, Daniel P, Shaw DJ, Chrastina J, Brázdil M. High frequency oscillations in epileptic and non-epileptic human hippocampus during a cognitive task. Sci Rep. 2020; 10(1):18147.

Palva JM, Palva S, Kaila K. Phase synchrony among neuronal oscillations in the human cortex. J Neurosci. 2005; 25:3962–3972.

Pizzo F, Frauscher B, Ferrari-Marinho T, Amiri M, Dubeau F, Gotman J. Detectability of Fast Ripples (>250 Hz) on the Scalp EEG: A Proof-of-Principle Study with Subdermal Electrodes. Brain Topogr. 2016; 29(3):358-67.

Puce A, Kalnins RM, Berkovic SF, Donnan GA, Bladin PF. Limbic P3 potentials, seizure localization, and surgical pathology in temporal lobe epilepsy. Ann Neurol. 1989; 26(3):377-85.

Ray S, Crone NE, Niebur E, Franaszczuk PJ, Hsiao SS. Neural correlates of high-gamma oscillations (60-200 Hz) in macaque local field potentials and their potential implications in electrocorticography. J Neurosci. 2008; 28(45):11526-36.

Roehri N, Pizzo F, Lagarde S, Lambert I, Nica A, McGonigal A, Giusiano B, Bartolomei F, Bénar CG. High-frequency oscillations are not better biomarkers of epileptogenic tissues than spikes. Ann Neurol. 2018; 83(1):84-97.

Rosenow F, Lüders H. Presurgical evaluation of epilepsy. Brain. 2001; 124(Pt 9):1683-700.

Řehulka P, Cimbálník J, Pail M, Chrastina J, Hermanová M, Brázdil M. Hippocampal high frequency oscillations in unilateral and bilateral mesial temporal lobe epilepsy. Clin Neurophysiol. 2019; 130(7):1151-1159.

Schevon CA, Trevelyan AJ, Schroeder CE, Goodman RR, McKhann G Jr, Emerson RG. Spatial characterization of interictal high frequency oscillations in epileptic neocortex. Brain. 2009; 132(Pt 11):3047-59.

Schomburg EW, Anastassiou CA, Buzsáki G, Koch C. The spiking component of oscillatory extracellular potentials in the rat hippocampus. J Neurosci. 2012; 32:11798–11811.

Schomer DL, da Silva FL. Niedermeyer´s Electroencephalography: Basic Principles, Clinical Applications, and Related Fields. 7th edition, Oxford University Press, 2017, ISBN-13: 9780190228484.

Schönberger J, Huber C, Lachner-Piza D, Klotz KA, Dümpelmann M, Schulze-Bonhage A, Jacobs J. Interictal Fast Ripples Are Associated With the Seizure-Generating Lesion in Patients With Dual Pathology. Front Neurol. 2020; 11:573975.

Schroeder CE, Lakatos P. Low-frequency neuronal oscillations as instruments of sensory selection. Trends Neurosci. 2009; 32:9–18.

Skaggs WE, McNaughton BL, Permenter M, Archibeque M, Vogt J, Amaral DG, Barnes CA. EEG sharp waves and sparse ensemble unit activity in the macaque hippocampus. J Neurophysiol. 2007; 98:898–910.

Singer W, Gray CM. Visual feature integration and the temporal correlation hypothesis. Annu Rev Neurosci. 1995; 18:555-86.

Staba RJ, Wilson CL, Bragin A, Fried I, Engel J Jr. Quantitative analysis of high-frequency oscillations (80–500 Hz) recorded in human epileptic hippocampus and entorhinal cortex. J Neurophysiol. 2002; 88:1743–52.

Staba RJ, Wilson CL, Bragin A, Jhung D, Fried I, Engel J Jr. High-frequency oscillations recorded in human medial temporal lobe during sleep. Ann Neurol. 2004; 56(1):108-15.

Staba RJ, Frighetto L, Behnke EJ, Mathern GW, Fields T, Bragin A, Ogren J, Fried I, Wilson CL, Engel J Jr. Increased fast ripple to ripple ratios correlate with reduced hippocampal volumes and neuron loss in temporal lobe epilepsy patients. Epilepsia. 2007; 48(11):2130-8.

Stacey WC, Lazarewicz MT, Litt B. Synaptic Noise and Physiological Coupling Generate High-Frequency Oscillations in a Hippocampal Computational Model. J Neurophys. 2009; 102:2342–2357.

Stead M, Bower M, Brinkmann BH, Lee K, Marsh WR, Meyer FB, Litt B, Van Gompel J, Worrell GA. Microseizures and the spatiotemporal scales of human partial epilepsy. Brain. 2010; 133(9):2789-97.

Tao JX, Ray A, Hawes-Ebersole S, Ebersole JS. Intracranial EEG substrates of scalp EEG interictal spikes. Epilepsia. 2005; 46:669–676.

Telenczuk B, Baker SN, Herz AV, Curio G. High-frequency EEG covaries with spike burst patterns detected in cortical neurons. J Neurophysiol. 2011; 105(6):2951-9.

Thom M, Liagkouras I, Martinian L, Liu J, Catarino CB, Sisodiya SM. Variability of sclerosis along the longitudinal hippocampal axis in epilepsy: a post mortem study. Epilepsy Res. 2012; 102(1-2):45-59.

Thomschewski A, Hincapié AS, Frauscher B. Localization of the Epileptogenic Zone Using High Frequency Oscillations. Front Neurol. 2019; 10:94.

Thomschewski A, Gerner N, Langthaler PB, Trinka E, Bathke AC, Fell J, Höller Y. Automatic vs. Manual Detection of High Frequency Oscillations in Intracranial Recordings From the Human Temporal Lobe. Front Neurol. 2020; 11:563577.

Timofeev I, Grenier F, Steriade M. The role of chloride-dependent inhibition and the activity of fast-spiking neurons during cortical spike-wave electrographic seizures. Neuroscience. 2002; 114(4):1115-32.

Tito M, Cabrerizo M, Ayala M, Jayakar P, Adjouadi M. Seizure detection: an assessment of time- and frequency-based features in a unified two-dimensional decisional space using nonlinear decision functions. J Clin Neurophysiol. 2009; 26:381-91.

Traub RD, Whittington MA, Buhl EH, LeBeau FE, Bibbig A, Boyd S, Cross H, Baldeweg T. A possible role for gap junctions in generation of very fast EEG oscillations preceding the onset of, and perhaps initiating, seizures. Epilepsia. 2001; 42(2):153-70.

Traub RD, Pais I, Bibbig A, LeBeau FE, Buhl EH, Hormuzdi SG, Monyer H, Whittington MA. Contrasting roles of axonal (pyramidal cell) and dendritic (interneuron) electrical coupling in the generation of neuronal network oscillations. Proc Natl Acad Sci U S A. 2003; 100(3):1370-4.

Traub RD, Pais I, Bibbig A, Lebeau FE, Buhl EH, Garner H, Monyer H, Whittington MA. Transient depression of excitatory synapses on interneurons contributes to epileptiform bursts during gamma oscillations in the mouse hippocampal slice. J Neurophysiol. 2005; 94(2):1225-35.

Uhlhaas PJ, Singer W. Neural synchrony in brain disorders: relevance for cognitive dysfunctions and pathophysiology. Neuron. 2006; 52(1):155-68.

Usui N, Terada K, Baba K, Matsuda K, Nakamura F, Usui K, Tottori T, Umeoka S, Fujitani S, Mihara T, Inoue Y. Very high frequency oscillations (over 1000 Hz) in human epilepsy. Clin Neurophysiol. 2010; 121(11):1825-31.

Usui N, Terada K, Baba K, Matsuda K, Usui K, Tottori T, et al. Significance of very-high-frequency oscillations (over 1,000Hz) in epilepsy. Ann Neurol. 2015; 78:295–302.

Urrestarazu E, Chander R, Dubeau F, Gotman J. Interictal high-frequency oscillations (100–500Hz) in the intracerebral EEG of epileptic patients. Brain. 2007; 130:2354–66.

van Klink N, Hillebrand A, Zijlmans M. Identification of epileptic high frequency oscillations in the time domain by using MEG beamformer-based virtual sensors. Clin Neurophysiol. 2016; 127:197–208.

van 't Klooster MA, van Klink NEC, Zweiphenning WJEM, Leijten FSS, Zelmann R, Ferrier CH, van Rijen PC, Otte WM, Braun KPJ, Huiskamp GJM, Zijlmans M. Tailoring epilepsy surgery with fast ripples in the intraoperative electrocorticogram. Ann Neurol. 2017; 81(5):664-676.

von Ellenrieder N, Frauscher B, Dubeau F, Gotman J. Interaction with slow waves during sleep improves discrimination of physiologic and pathologic high-frequency oscillations (80-500 Hz). Epilepsia. 2016; 57(6):869-78.

Waldert S, Lemon RN, Kraskov A. Influence of spiking activity on cortical local field potentials. J Physiol. 2013; 591(21):5291-303.

Wang S, Wang IZ, Bulacio JC, Mosher JC, Gonzalez-Martinez J, Alexopoulos AV, Najm IM, So NK. Ripple classification helps to localize the seizure-onset zone in neocortical epilepsy. Epilepsia. 2013; 54(2):370-6.

Weiss SA, Berry B, Chervoneva I, Waldman Z, Guba J, Bower M, Kucewicz M, Brinkmann 2, Kremen V, Khadjevand F, Varatharajah Y, Guragain H, Sharan A, Wu C, Staba R, Engel J Jr, Sperling M, Worrell G. Visually validated semi-automatic high-frequency oscillation detection aides the delineation of epileptogenic regions during intra-operative electrocorticography. Clin Neurophysiol. 2018; 129(10):2089-2098.

Weiss SA, Song I, Leng M, Pastore T, Slezak D, Waldman Z, Orosz I, Gorniak R, Donmez M, Sharan A, Wu C, Fried I, Sperling MR, Bragin A, Engel J Jr, Nir Y, Staba R. Ripples Have Distinct Spectral Properties and Phase-Amplitude Coupling With Slow Waves, but Indistinct Unit Firing, in Human Epileptogenic Hippocampus. Front Neurol. 2020; 11:174.

Worrell GA, Parish L, Cranstoun SD, Jonas R, Baltuch G, Litt B. High-frequency oscillations and seizure generation in neocortical epilepsy. Brain. 2004; 127:1496–550.

Worrell GA, Gardner AB, Stead SM, Hu S, Goerss S, Cascino GJ, et al. High-frequency oscillations in human temporal lobe: simultaneous microwire and clinical macroelectrode recordings. Brain. 2008; 131:928–37.

Worrell G, Gotman J. High-frequency oscillations and other electrophysiological biomarkers of epilepsy: clinical studies. Biomark Med. 2011; 5(5):557-66.

Worrell GA, Jerbi K, Kobayashi K, Lina JM, Zelmann R, Le Van Quyen M. Recording and analysis techniques for high-frequency oscillations. Prog Neurobiol. 2012; 98(3):265-78.

Wu JY, Sankar R, Lerner JT, Matsumoto JH, Vinters HV, Mathern GW. Removing interictal fast ripples on electrocorticography linked with seizure freedom in children. Neurology. 2010; 75(19):1686-94.

Xiang J, Liu Y, Wang Y, Kirtman EG, Kotecha R, Chen Y, Huo X, Fujiwara H, Hemasilpin N, Lee K, Mangano FT, Leach J, Jones B, DeGrauw T, Rose D. Frequency and spatial characteristics of high-frequency neuromagnetic signals in childhood epilepsy. Epileptic Disord. 2009; 11(2):113-25.

Xiang J, Luo Q, Kotecha R, Korman A, Zhang F, Luo H, Fujiwara H, Hemasilpin N, Rose DF. Accumulated source imaging of brain activity with both low and high-frequency neuromagnetic signals. Front Neuroinform. 2014; 8:57.

Yaari Y, Beck H. "Epileptic neurons" in temporal lobe epilepsy. Brain Pathol. 2002; 12(2):234-9.

Ylinen A, Bragin A, Nádasdy Z, Jandó G, Szabó I, Sik A, Buzsáki G. Sharp wave-associated high-frequency oscillation (200 Hz) in the intact hippocampus: network and intracellular mechanisms. J Neurosci. 1995; 15(1 Pt 1):30-46.

Zelmann R, Mari F, Jacobs J, Zijlmans M, Dubeau F, Gotman J. A comparison between detectors of high frequency oscillations. Clin Neurophysiol. 2012; 123(1):106-16.

Zelmann R, Lina JM, Schulze-Bonhage A, Gotman J, Jacobs J. Scalp EEG is not a blur: it can see high frequency oscillations although their generators are small. Brain Topogr. 2014; 27(5):683-704

Zijlmans M, Jacobs J, Zelmann R, Dubeau F, Gotman J. High frequency oscillations and seizure frequency in patients with focal epilepsy. Epilepsy Res. 2009; 85(2-3):287-92.

Zijlmans M, Jiruska P, Zelmann R, Leijten FS, Jefferys JG, Gotman J. High-frequency oscillations as a new biomarker in epilepsy. Ann Neurol. 2012; 71(2):169-78.

Zijlmans M, Worrell GA, Dümpelmann M, Stieglitz T, Barborica A, Heers M, Ikeda A, Usui N, Le Van Quyen M. How to record high-frequency oscillations in epilepsy: A practical guideline. Epilepsia. 2017; 58(8):1305-1315.